Power Electronic Systems Laboratory

ETH zürich

Fundamentals and Multi-Objective Design of Inductive Power Transfer Systems

Roman Bosshard & Johann W. Kolar

Power Electronic Systems Laboratory
ETH Zurich, Switzerland

**EPE'2015
ECCE Europe
Geneva**

ACKNOWLEDGEMENT

The authors would like to express their sincere appreciation to ABB Switzerland Ltd. for the support of research on IPT that lead to the results presented in this Tutorial

The authors also acknowledge the support of CADFEM (Suisse) AG concerning the ANSYS software

Agenda

Slide Download:
www.pes.ee.ethz.ch → Publications → Tutorials
or http://people.ee.ethz.ch/boroman/EPE_2015_IPT_Tutorial_RB_JWK.pdf

Introduction	14 slides
Fundamentals: Isolated DC/DC → IPT	51 slides
System Components & Design Considerations	63 slides
Multi-Objective Optimization	40 slides
Power Electronics Concept for 50 kW	32 slides
Summary & Conclusions	9 slides

Introduction

Features & Limitations
Potential Applications
Existing Industry Solutions

► Future Electric Vehicle Charging

- **Electric Vehicles – Key Limitations**
  - Driving Range / Battery Capacity
  - Availability of Charging Stations
  - Time for Battery Re-Charging

- **Drivers for Future Development**
  - Battery Technology
  - Infrastructure Development
  - Charging Technology

Nissan Leaf, www.nissan.com

UNIST, www.unist.ac.kr

Charge Point, www.chargepoint.com

Network World, www.networkworld.com

► Wireless Electric Vehicle Battery Charging


Charge Point, www.chargepoint.com

Delphi, www.delphi.com

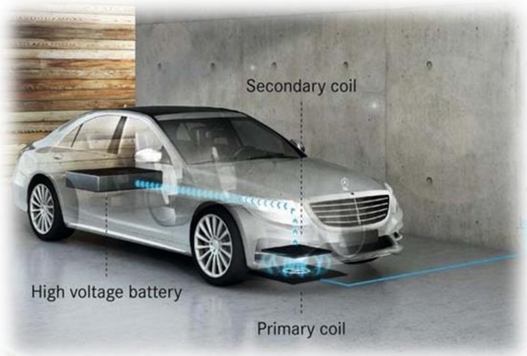

Daimler & BWM, ww.daimler.com, www.bmw.de

- **Higher Convenience & Usability**
  - No Plug Required: Quick Charging at Traffic Lights, Bus Stops, …
- **More Frequent Recharging**
  - Longer Battery Lifetime
  - Smaller Battery Volume & Weight
- **Reduced Fleet in Public Transportation**
  - Shorter Time for Depot Re-Charging

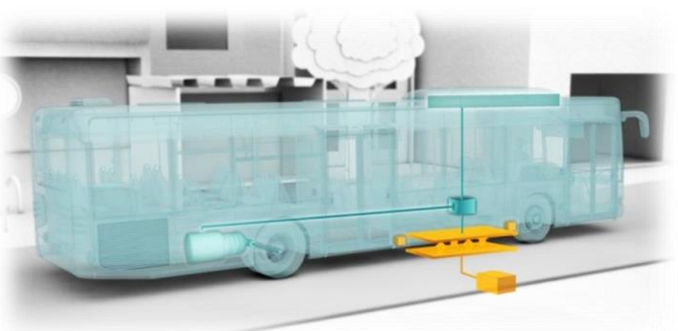
Bombardier PRIMOVE, http://primove.bombardier.com.

▶ EV Charging – Typical AC/DC Power Conversion Chain

- **Conductive EV Charging**

- **Wireless EV Charging**

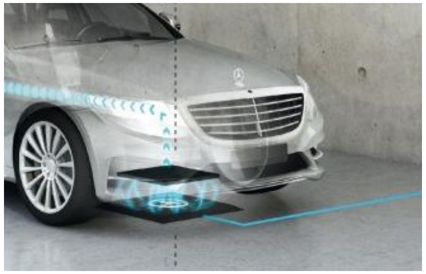

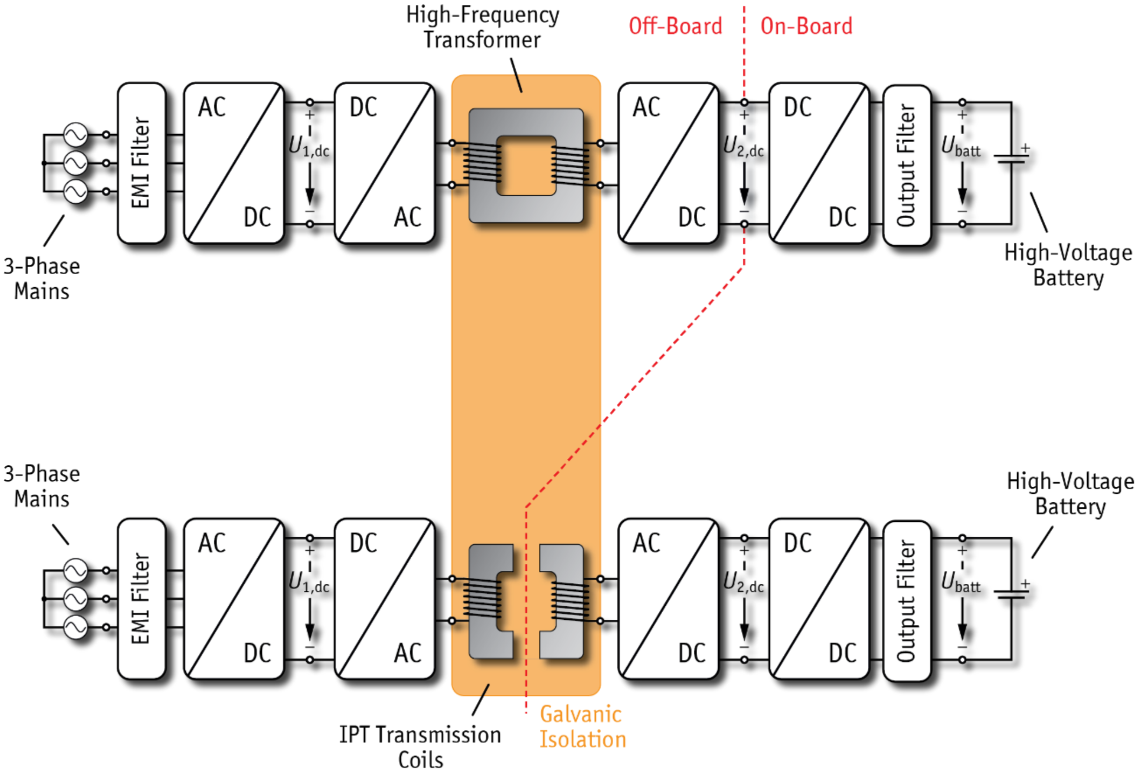

▲ **Structure of a 3-Φ Isolated 2-Stage High-Power Battery Charging System with High-Frequency Transformer or IPT Transmission Coils**

► Electrical Ratings of Conductive EV Chargers

■ **SAE J1772 Definition (USA)**

- AC Level 1: 120 V, 16 A → 1.92 kW
- AC Level 2: 204-240 V, 80 A → 19.2 kW
- AC Level 3: n/a → ≥ 20 kW
- DC Level 1: 200-450 V, 80 A → 36 kW
- DC Level 2: 200-450 V, 200 A → 90 kW
- DC Level 3: 200-600 V, 400 A → 240 kW

■ **IEC 62196 Definition (Europe, Int.)**

- Mode 1: 1x230 V / 3x400 V, 16 A → 7.7 kW
- Mode 2: 1x230 V / 3x400 V, 32 A → 15.4 kW
- Mode 3: 3x400 V, 32-250 A → ≥ 20 kW
- Mode 4: ≤ 1000 V, 400 A (DC) → 240 kW

▲ SAE J1772 Combo Connector for AC or DC (Level 1-2)

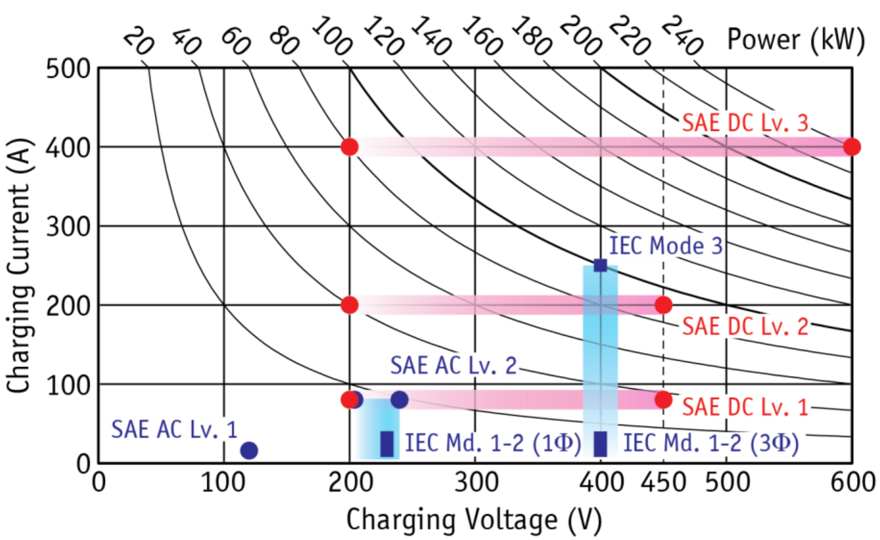

► Regulations & Standards for Inductive EV Charging (1)

■ **SAE J2954 Wireless Charging Standard (under Development, April 2015)**

- Common Operating Frequency 85 kHz
- Minimum Charging Efficiency > 90%

SAE INTERNATIONAL

- Charging Levels: 3.7 kW (WPT1: Private Low Power)
  7.7 kW (WPT2: Private/Publ. Parking)
  22 kW (WPT3: Fast Charging)

- Interoperability: Air Gap, Coil Dimensions, x,y,z-Misalignment Tolerance, Communication & Interfaces
- Safety Features: Foreign Object Detection, Electromagnetic Stray Field
- Validation Methods: Performance, Safety

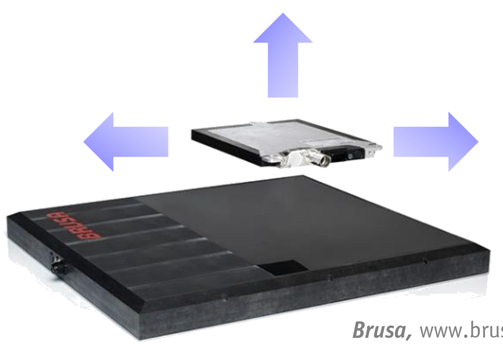

Brusa, www.brusa.eu

Qualcomm Halo, www.qualcommhalo.com

► Regulations & Standards for Inductive EV Charging (2)

■ **ICNIRP 1998/2010: Guidelines for Limiting Exposure to Time-Varying EM Fields**

- Living Tissue affected by Power Dissipation caused by Electromagnetic Fields
- Limitation of Human Body SAR (=Specific Absorption Rate, [W/kg]) by Limiting Electric and Magnetic Fields
- Distinction between "General Public" and "Occupational Exposure"
- Poynting Vector $\vec{S} = \vec{E} \times \vec{H}$ [W/m²] shows H- and E-Field are needed for Power Transfer
  → Minimum Required Area for Power Transfer: $P_2 = \iint (\vec{E} \times \vec{H})\, \mathrm{d}\vec{A}$

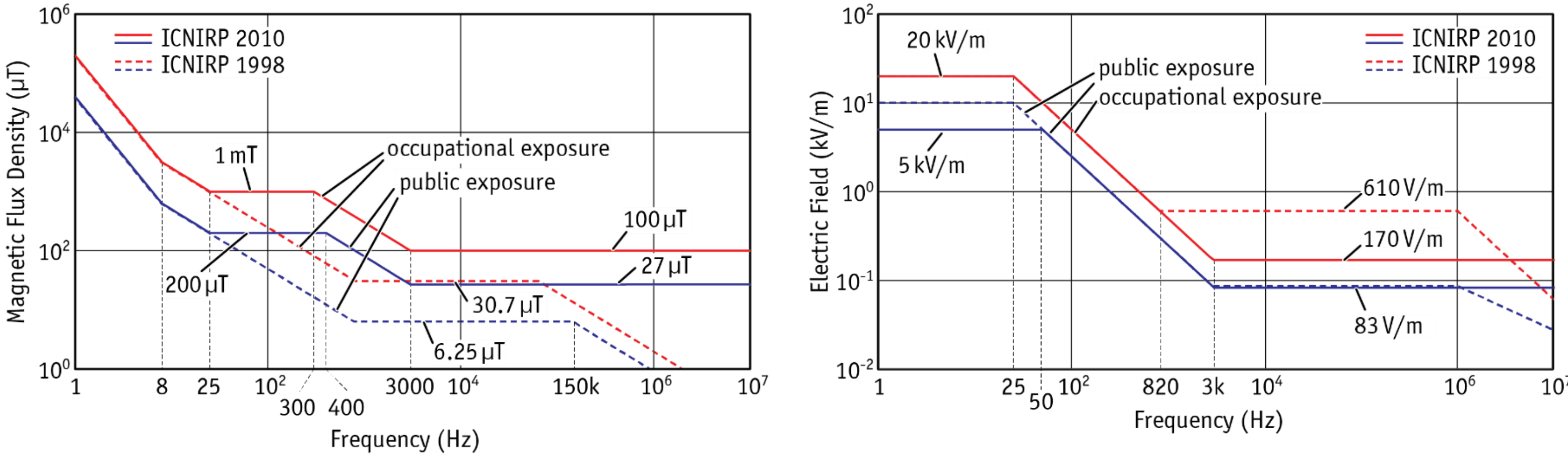

▲ **ICNIRP 1998 and 2010 Reference Values for RMS Magnetic Flux Density and Electric Field**

Realization Examples

► IPT for Industry Automation Applications

■ Industry Automation & Clean-Room Technology

- Automatic Guided & Monorail Transportation Vehicles
- Stationary/Dynamic Charging in Closed Environment
- Key Features: Wireless, Maintenance-Free, Clean & Safe
- Lower Requirements & Less Restrictive Standards than EV Charging

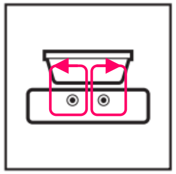
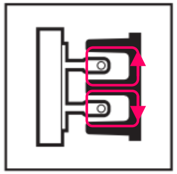


▲ **Wireless Powered Floor Surface Conveyors**

▲ **Ceiling-Mounted Monorail Transportation System**

Conductix-Wampfler, www.conductix.ch (1.11.2014),
«Product Overview: Inductive Power Transfer»

►IPT for EV: Selected Demonstration/Research Activities

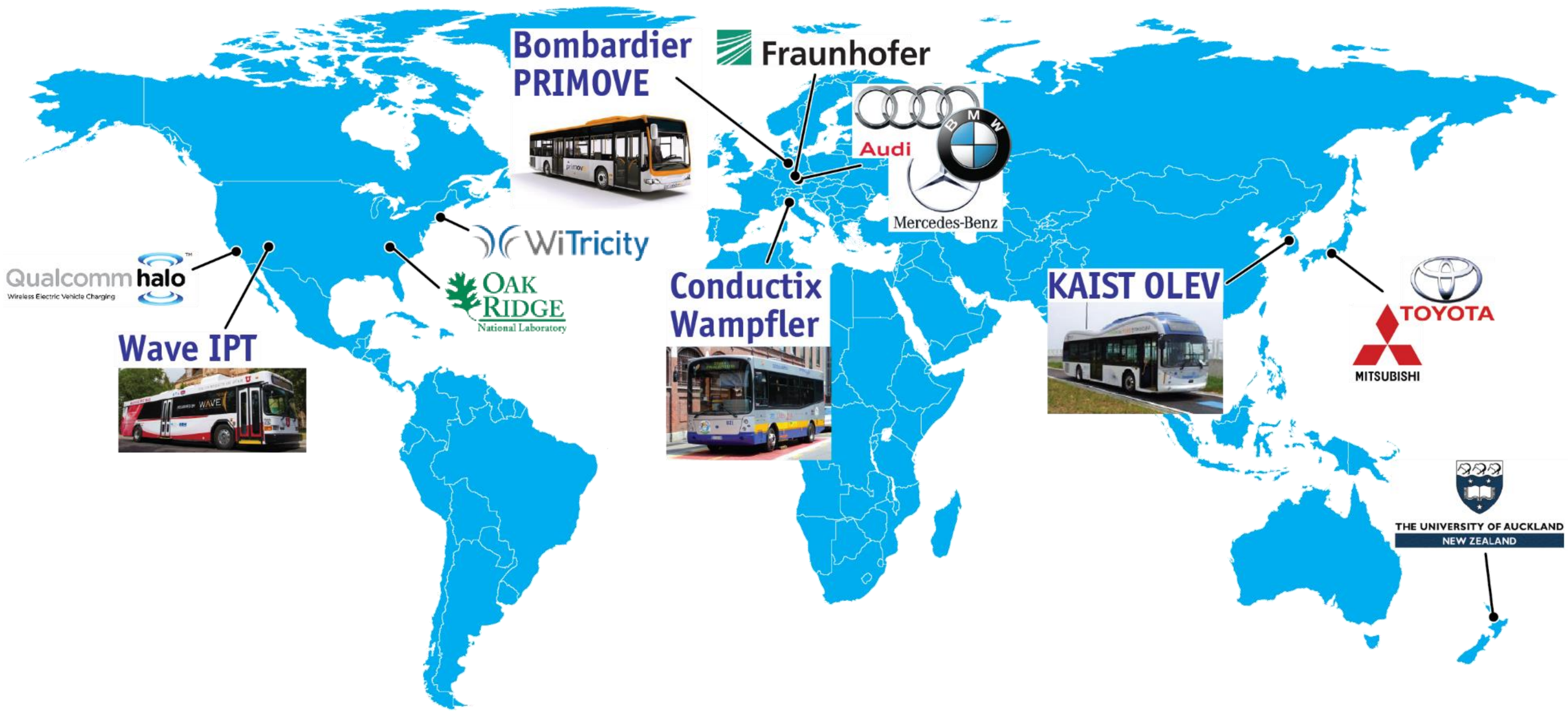

► IPT Public Transportation Systems

	Conductix-Wampfler IPT Charge	Bombardier PRIMOVE	KAIST On-Line EV	Wave IPT
				
Location	Genoa (IT) Hertogenbosch (NL)	Augsburg, Braunschweig, Mannheim (DE) Lommel (BE)	Seoul, Daejeon, Yeosu, Gumi (KR)	Salt Lake City, McAllen Monterey-Salinas, Lancaster (USA)
Year	2002 - 2012	2010 - 2015	2010 - 2015	2014 - 2015
Air Gap	Approx. 4 cm	Approx. 4 cm	Up to 20 cm	Up to 20 cm
Power	Up to 60 kW	150-200 kW	3-100 kW	50 kW
Details	• Coil Lowered to Ground at Bus Stations • Charging Efficiency > 90% • ICNIRP 1998 Compliant • 50% Red. Battery Capacity (240→120 kWh)	• Coil Lowered to Ground at Bus-Stations • Reduced Number of Fleet Vehicles • Extended Battery Life • Lower Total Cost	• Electrified Track for In-Motion Charging • ICNIRP 1998 Compl. • 30% Reduced Battery Weight • Reduced Number of Fleet Vehicles	• Wireless Charging at Bus-Stations without Lowering the Coil • Charging Efficiency > 90% • ICNIRP Compliant

► Historic Background: Medical Applications

O. Knecht, R. Bosshard, and J. W. Kolar, "Optimization of Transcutaneous Energy Transfer Coils for High Power Medical Applications," in *Proc. Workshop on Control and Modeling for Power Electron. (COMPEL)*, **2014**.

■ Electro-Mechanical Heart Assist Devices

- Percutaneous Driveline Major Cause of Lethal Infections
- Transcutaneous Power Supply for Heart Assist Devices
- No Reliable and Medically Certified Solution Exists

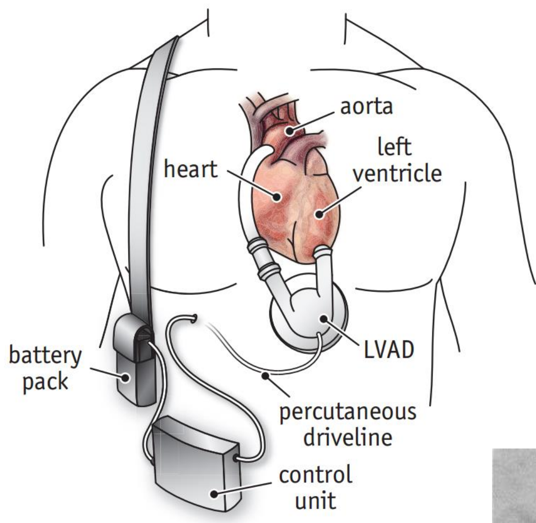

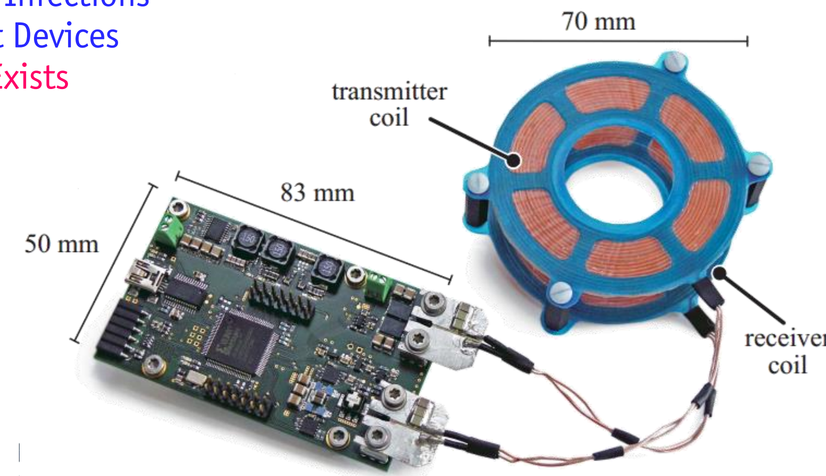

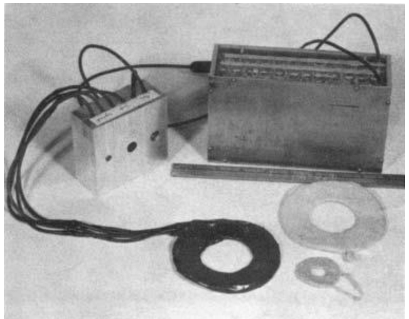

J. C. Schuder, "Powering an artificial heart: birth of the inductively coupled-radio frequency system in **1960**," Artificial Organs, vol. 26, no. 11, pp. 909–915, 2002.

► State-of-the-Art for Conductive EV Charging

B. Whitaker et al. (APEI),
«High-Density, High-Efficiency, Isolated On-Board Vehicle Battery Charger Utilizing SiC Devices,"
IEEE Trans. Power Electron.,
vol. 29, no. 5, 2014.

■ **Best-in-Class Conductive Isolated On-Board EV Battery Chargers Reach up to 5 kW/dm³ with Efficiency > 95%**

■ **Example: B. Whitaker et al. (APEI), 2014**
- Single-Phase Bridgeless Boost-Type PFC & Isolated Phase-Shift DC-DC-Converter
- Switching Frequency 200 kHz with 1.2 kV, 20 A SiC MOSFET Modules
- Power: 6.1 kW
- Volume: 1.2 dm³
- Weight: 1.6 kg
- Power Density 5 kW/dm³
- Spec. Weight 3.8 kW/kg
- Efficiency > 95%

■ **Typical Price for EV Chargers (Frost & Sullivan 2015):**
- Approx. 130 - 230 $/kW (e.g. for 6.6 kW: 860 - 1500 $)

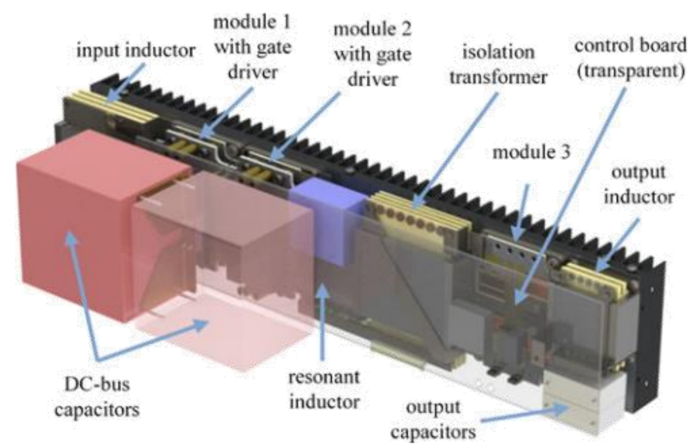

▲ **Best-in-Class 6.1 kW On-Board EV Charger (APEI)**

► Engineering Challenges for Competitive IPT System

- **High Power Density (kW/dm², kW/kg)**
  - High Ratio of Coil Diameter / Air Gap Needed
  - Heavy Shielding & Core Materials Necessary
- **Low Magnetic Stray Field $B_s < B_{lim}$**
  - Limited by Standards (e.g. ICNIRP or Lower)
  - Eddy Current Loss in Surrounding Metals
- **High Efficiency η**
  - Efficiency Limited by Magnetic Coupling k
  - Sensitivity to Coil Misalignment
- **High Reliability of Components**
  - High Mechanical Stress for Transmitter (1-10t)
  - Receiver Fully Exposed to Environment
- **Low Infrastructure & Installation Cost**
  - Material Effort for On-Board Components
  - Installation of Transmitter into Road Surf.

Lexus, www.lexus.com, 2014

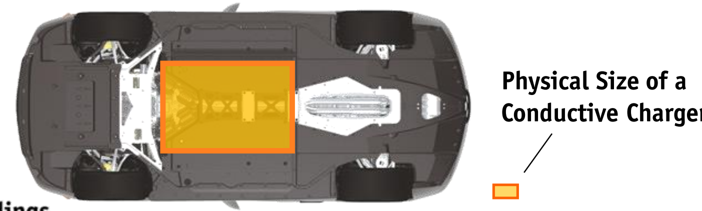

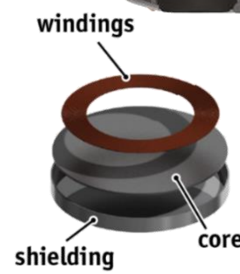

TDK, www.tdk.com, 2015

***Multi-Objective Design Problem* !**

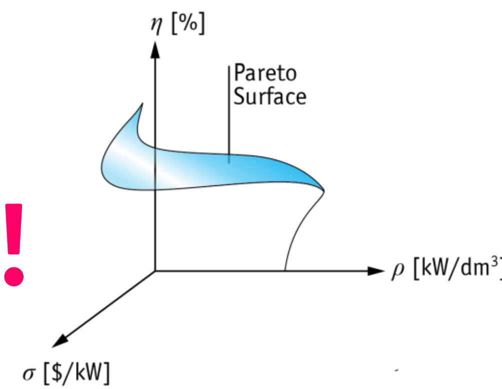

Fundamentals:
Isolated DC/DC → IPT

Transformer Equivalent
Series Resonant Topologies
Zero-Voltage Switching
Inductive Power Transfer

▶ Isolated DC/DC-Converter for Conductive EV Charging

- **Soft-Switching DC/DC-Converter without Output Inductor**
  - Galvanic Isolation
  - Minimum Number of Components
  - Clamped Voltage across Rectifier
- **Constant Switching Frequency of Full-Bridge Inverter on Primary**
  - di/dt given by Voltage Levels & Transformer Stray & Magn. Induct.

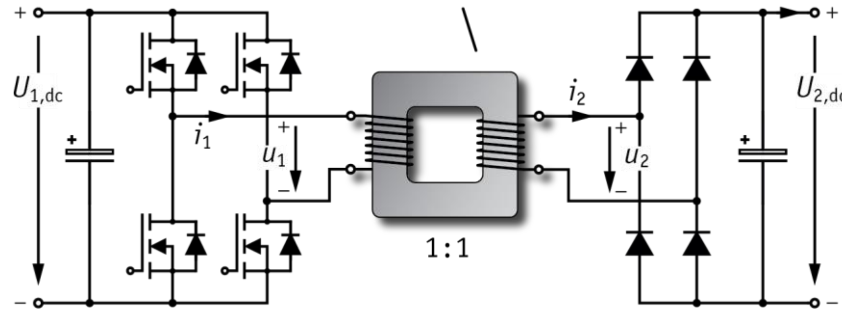

▲ Isolated DC/DC Converter Topology with MF Transformer

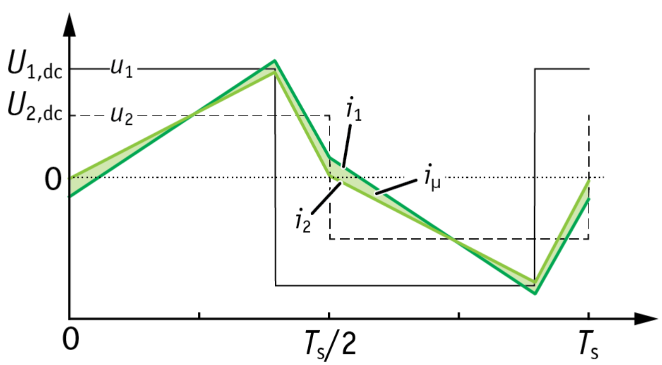

▲ Schematic Converter Waveforms (i_1-i_2 not to Scale)

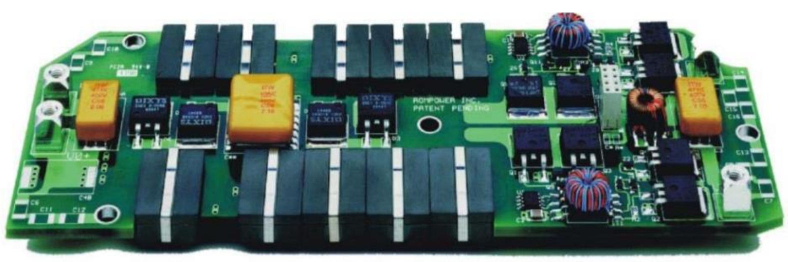

I. D. Jitaru, «A 3 kW Soft-Switching DC-DC Converter," *Proc. IEEE APEC*, pp. 86-92, 2000.

▲ Realization Example (1 kW Module, Rompower)

► Transition to IPT System (1)

■ Airgap in the Magnetic Path

- Reduced Primary & Secondary Induct.
- Higher Magnetizing Current
- Reduced Magnetic Coupling *k*
- Load Dependency of Output Voltage due to Non-Dissip. Inner Impedance

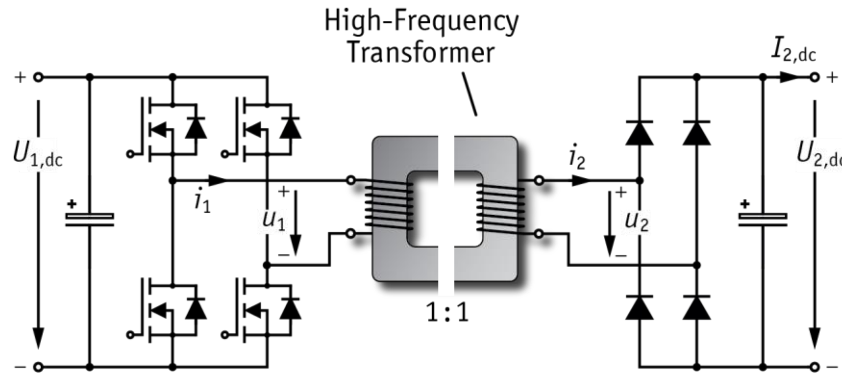

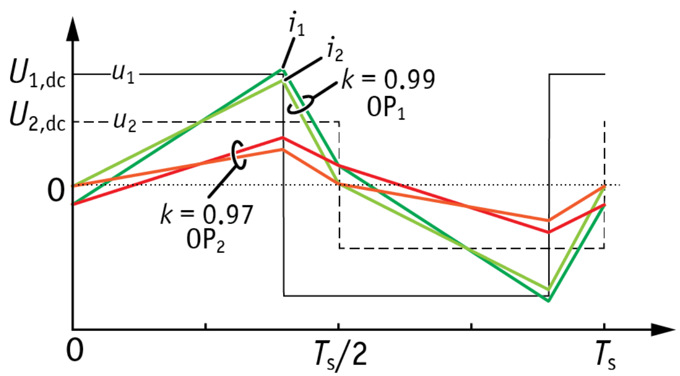

▲ Schematic Converter Waveforms for OP$_1$ and OP$_2$ (i_1-i_2 not to Scale)

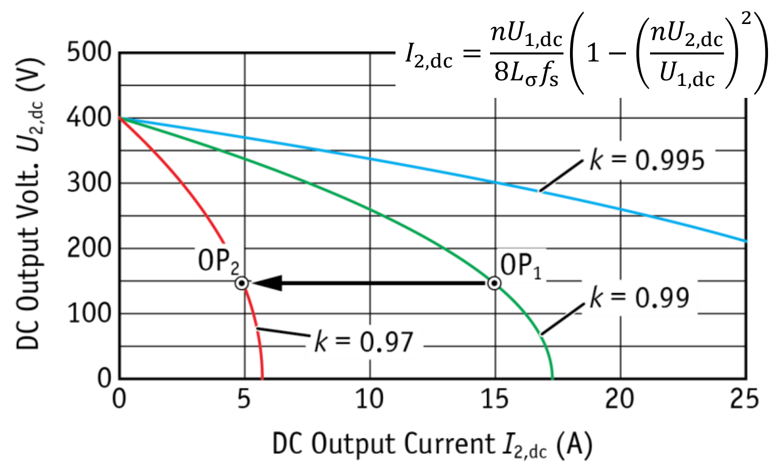

▲ Converter Output Characteristics

Transformer Characterization

▶ Characterization of the Transformer

■ Transformer Differential Equations

$$u_1 = L_1 \frac{\mathrm{d}i_1}{\mathrm{d}t} - M \frac{\mathrm{d}i_2}{\mathrm{d}t}$$
$$u_2 = M \frac{\mathrm{d}i_1}{\mathrm{d}t} - L_2 \frac{\mathrm{d}i_2}{\mathrm{d}t}$$

Note: No Explicit Dependency on N_1, N_2 (Unknown in General Case)

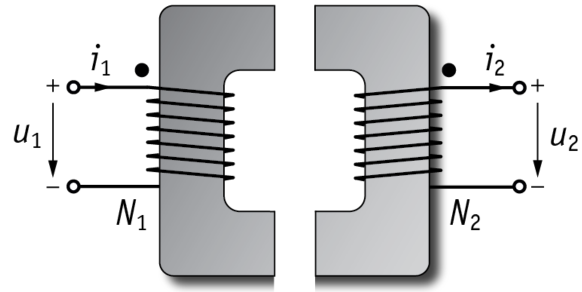

■ Measurement of the Three (!) Parameters L_1, L_2 and M

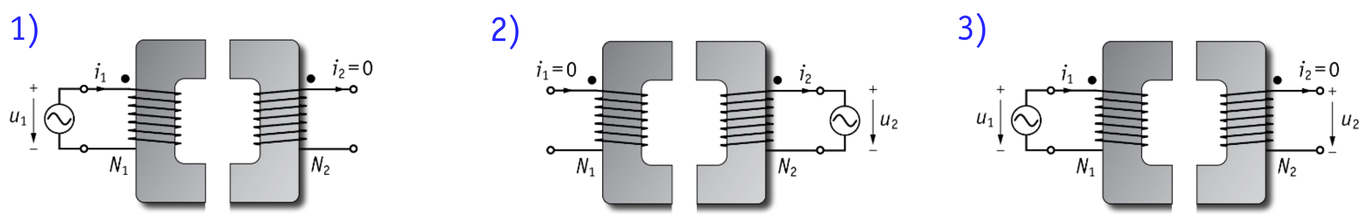

1) $$L_1 = \frac{1}{\omega}\left(\frac{\hat{U}_1}{\hat{I}_1}\right)\bigg|_{i_2=0}$$

2) $$L_2 = \frac{1}{\omega}\left(\frac{\hat{U}_2}{\hat{I}_2}\right)\bigg|_{i_1=0}$$

3) $$M = L_1\left(\frac{\hat{U}_2}{\hat{U}_1}\right)\bigg|_{i_2=0}$$

■ General Equivalent Circuit Diagram

$$u_1(t) = (L_1 - M)\frac{\mathrm{d}i_1}{\mathrm{d}t} + M\frac{\mathrm{d}}{\mathrm{d}t}(i_1 - i_2)$$
$$u_2(t) = M\frac{\mathrm{d}}{\mathrm{d}t}(i_1 - i_2) - (L_2 - M)\frac{\mathrm{d}i_2}{\mathrm{d}t}$$

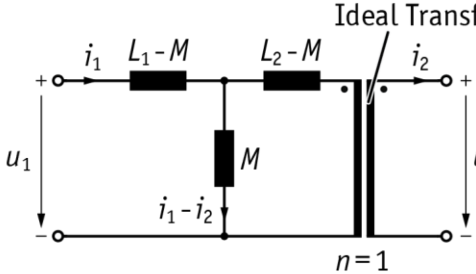

■ Definitions:

Coupling Factor $k = \frac{M}{\sqrt{L_1 L_2}}$, Stray Factor $\sigma = 1 - k^2$ → Ideal: $k = 1$, $\sigma = 0$.

▶ Transformer Equivalent Circuits (1)

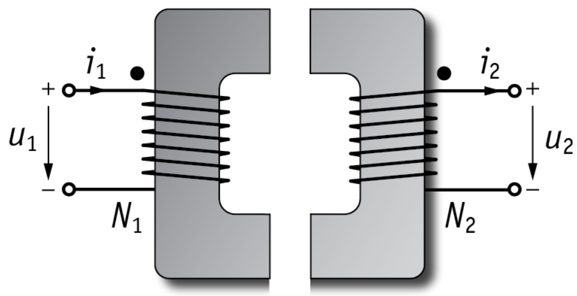

■ Transformer Differential Equations

$$u_1 = L_1 \frac{\mathrm{d}i_1}{\mathrm{d}t} - M \frac{\mathrm{d}i_2}{\mathrm{d}t} \;=\; L_1 \frac{\mathrm{d}i_1}{\mathrm{d}t} + u_{1,\mathrm{ind}}$$
$$u_2 = M \frac{\mathrm{d}i_1}{\mathrm{d}t} - L_2 \frac{\mathrm{d}i_2}{\mathrm{d}t} \;=\; u_{2,\mathrm{ind}} - L_2 \frac{\mathrm{d}i_2}{\mathrm{d}t}$$

- Equivalent Circuit Representation with Induced Voltages as Voltage Sources:

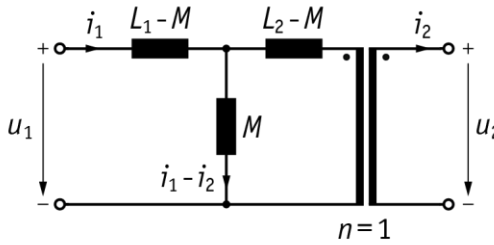

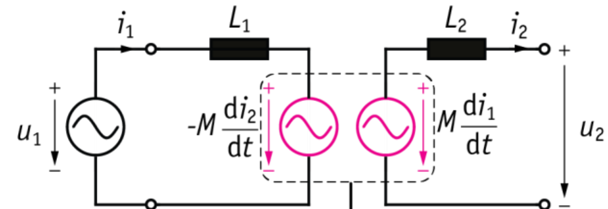

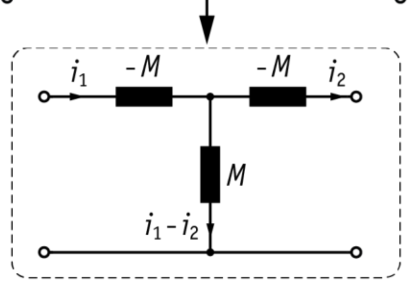

■ Inductive Behavior Partly Hidden in Voltage Sources $u_{1,\mathrm{ind}}$, $u_{2,\mathrm{ind}}$

$$\underline{\hat{u}}_1 = \mathrm{j}\omega L_1 \underline{\hat{i}}_1 - \mathrm{j}\omega M \underline{\hat{i}}_2 = \mathrm{j}\omega L_1 \underline{\hat{i}}_1 + \underline{\hat{u}}_{1,\mathrm{ind}}$$
$$\underline{\hat{u}}_2 = \mathrm{j}\omega M \underline{\hat{i}}_1 - \mathrm{j}\omega L_2 \underline{\hat{i}}_2 = \underline{\hat{u}}_{2,\mathrm{ind}} - \mathrm{j}\omega L_2 \underline{\hat{i}}_2$$

- 90° Phase-Difference between $\underline{\hat{i}}_1$ and $\underline{\hat{u}}_{2,\mathrm{ind}}$ and between $\underline{\hat{i}}_2$ and $\underline{\hat{u}}_{1,\mathrm{ind}}$

▶ Transformer Equivalent Circuits (2)

■ Introduction of a General Transformation Ratio *n*

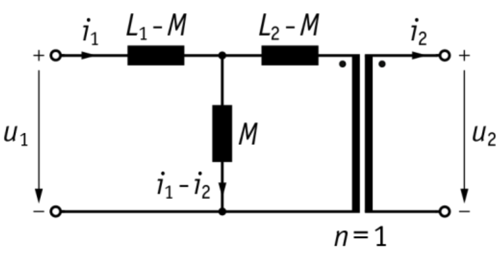

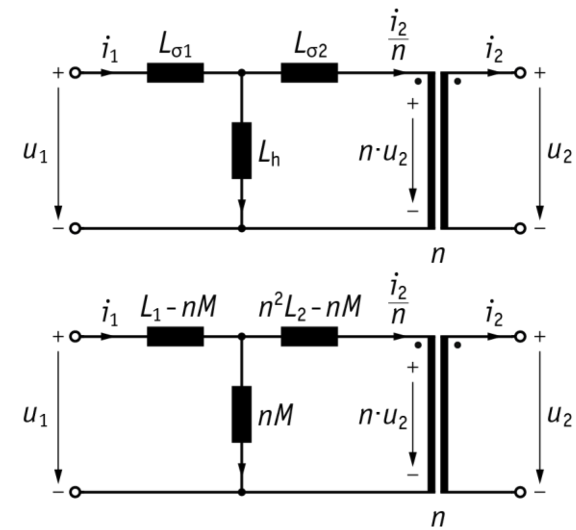

- 4 Degrees of Freedom ($L_{\sigma 1}$, $L_{\sigma 2}$, L_h, n), but only 3 Transformer Parameters (L_1, L_2, M)
- Assume n as given and Calculate Remaining Parameters ($L_{\sigma 1}$, $L_{\sigma 2}$, L_h)

■ Equivalent Circuit Diagrams for Specific Values of *n*

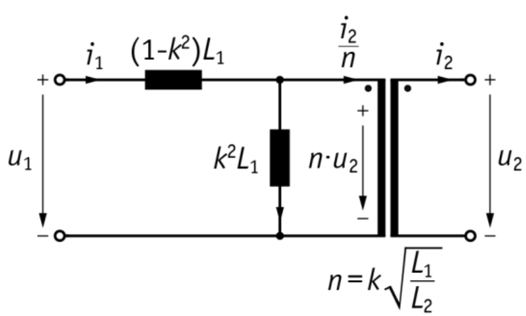

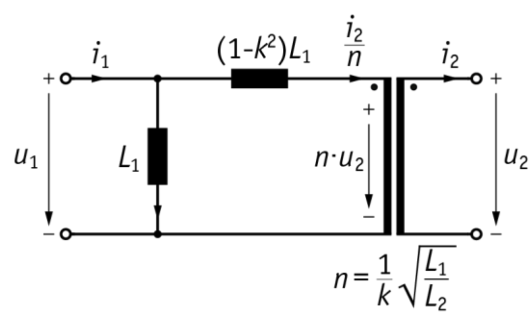

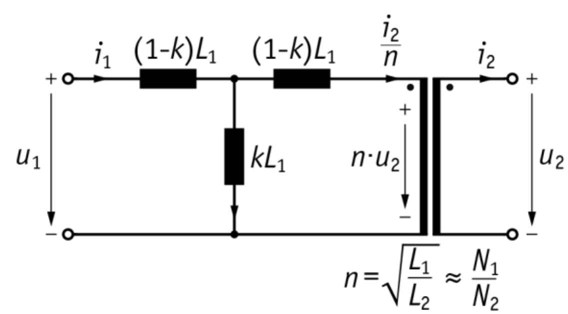

- All Equivalent Circuits Fully Represent the Same Transformer!

▶ Transformer Equivalent Circuits (3)

- **Direct Measurement of Transformer Equivalent Circuit Parameters**

- **Measurement 1:** Secondary-Side Terminals Shorted

$$L_\sigma = \frac{1}{\omega}\left(\frac{\hat{U}_1}{\hat{I}_1}\right)\Bigg|_{u_2=0}$$

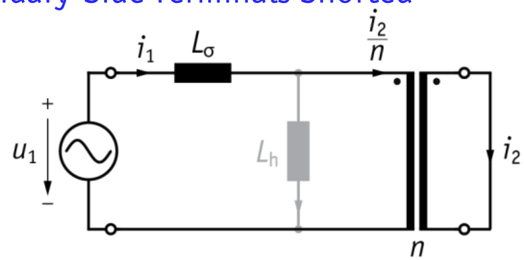

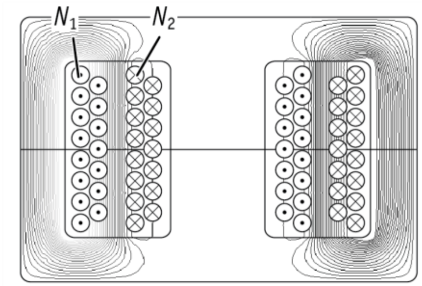

- **Measurement 2:** Secondary-Side Terminals Open

$$L_1 = \frac{1}{\omega}\left(\frac{\hat{U}_1}{\hat{I}_1}\right)\Bigg|_{i_2=0}$$

$$L_h = L_1 - L_\sigma$$

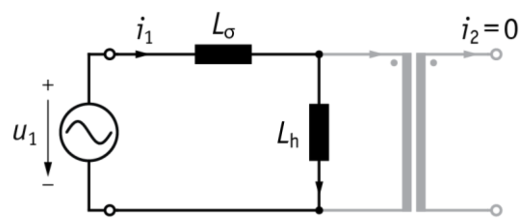

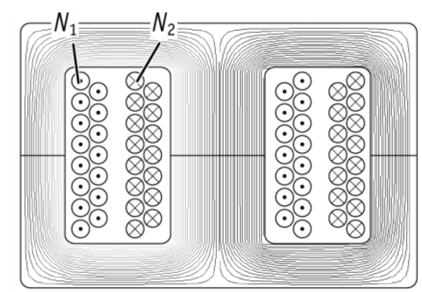

- **Measurement 3:** Primary-Side Terminals Open

$$n = \left(\frac{\hat{U}_1}{\hat{U}_2}\right)\Bigg|_{i_1=0}$$

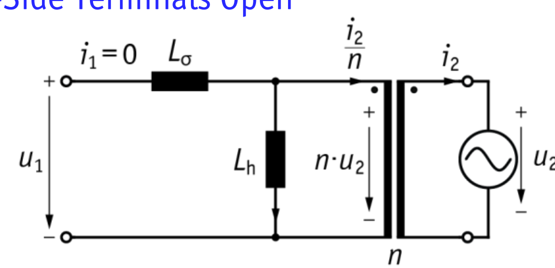

► Field Lines of a Coupled Coil Pair

■ **Mutual and Leakage Inductance is not Immediately Evident from FEM-Field Images**
- Field Distribution Depends on Shown Time Instant and Phase Angle between Winding Currents

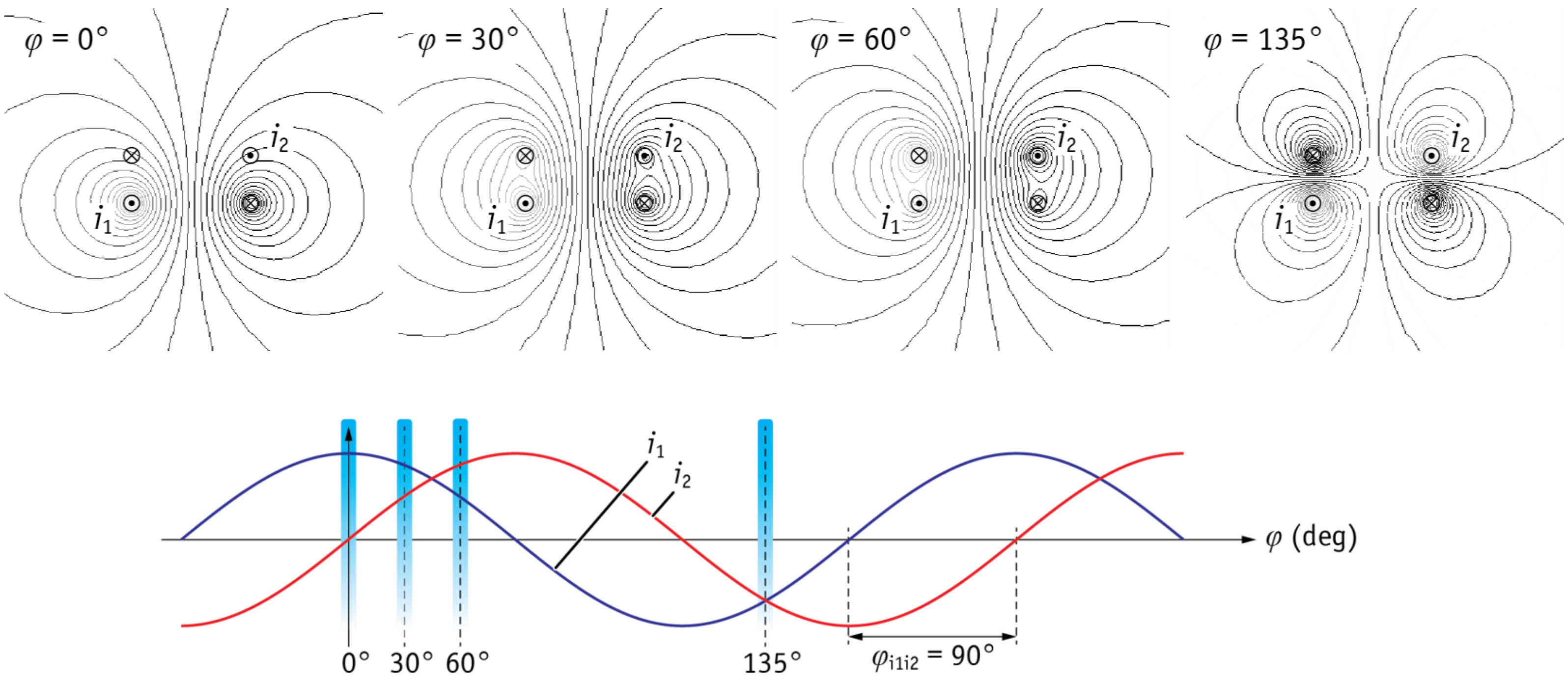

▲ **Sinusoidal Currents in Both Coils, 90° Phase Shift as Typical for IPT Systems**

▶ Transition to IPT System (2)

■ **Airgap in the Magnetic Path**
- Reduced Primary & Secondary Induct.
- Higher Magnetizing Current
- Reduced Magnetic Coupling *k*
- Load Dependency of Output Voltage due to Non-Dissip. Inner Impedance

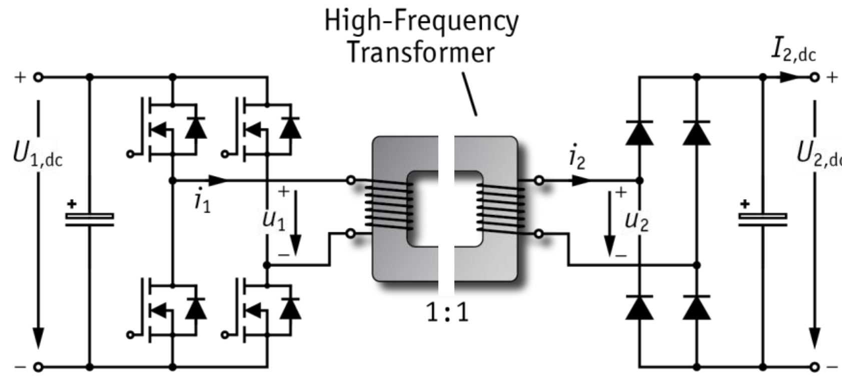

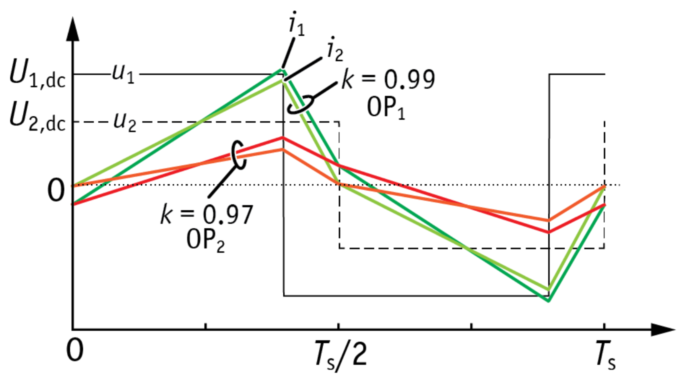

▲ **Schematic Converter Waveforms for OP_1 and OP_2 (i_1-i_2 not to Scale)**

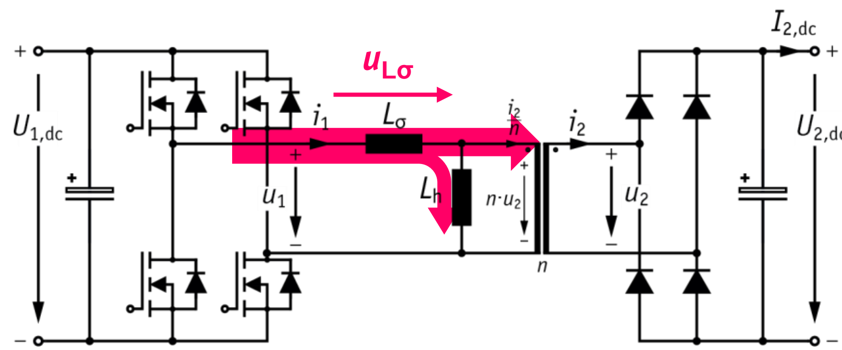

▲ **Effects of an Air Gap in the Transformer**

$$L_\sigma = (1 - k^2)L_1, L_h = k^2 L_1, n = k\sqrt{L_1/L_2}$$

▶ Transition to IPT System (3)

■ **Airgap in the Magnetic Path**
- Reduced Primary & Secondary Induct.
- Higher Magnetizing Current
- Reduced Magnetic Coupling k
- Load Dependency of Output Voltage due to Non-Dissip. Inner Impedance

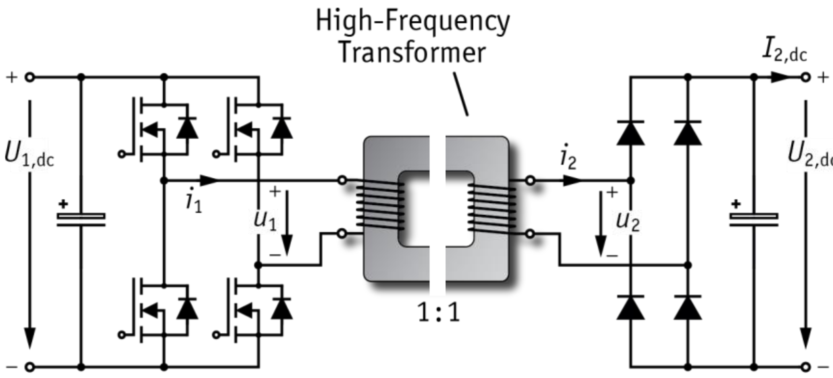

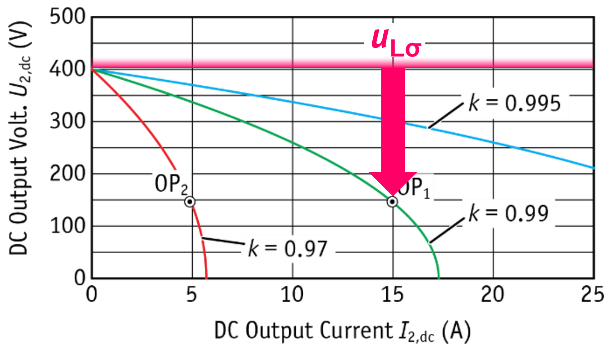

▲ **Converter Output Characteristics**

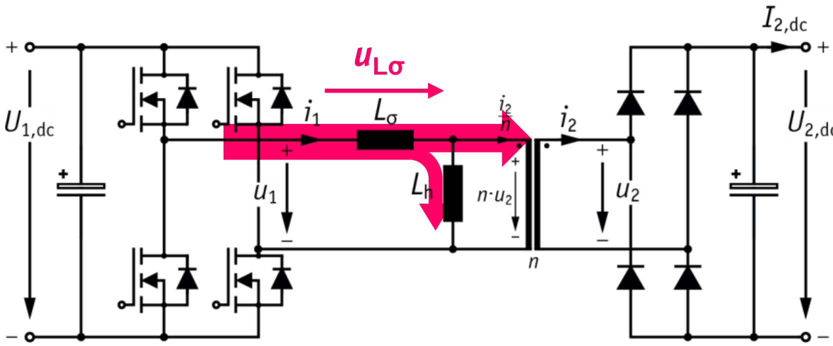

▲ **Effects of an Air Gap in the Transformer**

$$L_\sigma = (1 - k^2)L_1, L_h = k^2 L_1, n = k\sqrt{L_1/L_2}$$

Resonant Compensation of Stray Inductance

▶ Resonant Compensation of Stray Inductance (1)

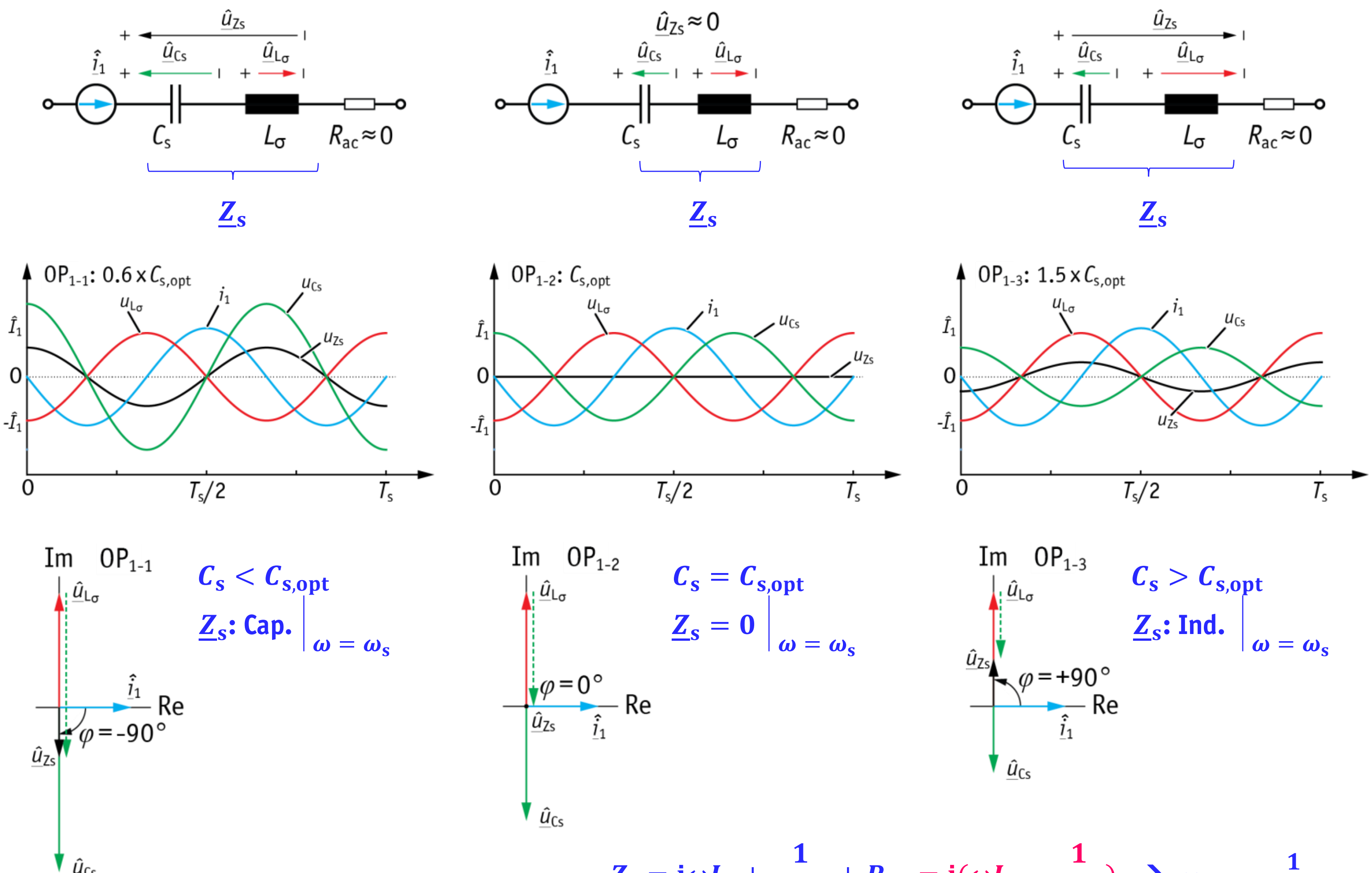

$C_s < C_{s,opt}$

$\underline{Z}_s$: Cap. $\Big|_{\omega=\omega_s}$

$C_s = C_{s,opt}$

$\underline{Z}_s = 0 \Big|_{\omega=\omega_s}$

$C_s > C_{s,opt}$

$\underline{Z}_s$: Ind. $\Big|_{\omega=\omega_s}$

$$\underline{Z}_s = j\omega L_s + \frac{1}{j\omega C_s} + \underbrace{R_{ac}}_{\approx 0} = j\left(\omega L_s - \frac{1}{\omega C_s}\right) \rightarrow \omega_s = \frac{1}{\sqrt{L_s C_s}}$$

► Resonant Compensation of Stray Inductance (2)

- **Insert Capacitor in Series to Transformer Stray Inductance L_σ**
- **Select Capacitance $C_{s,opt} = 1/(\omega_s^2 L_\sigma)$ to Match Resonance and Inverter Switching Frequency**

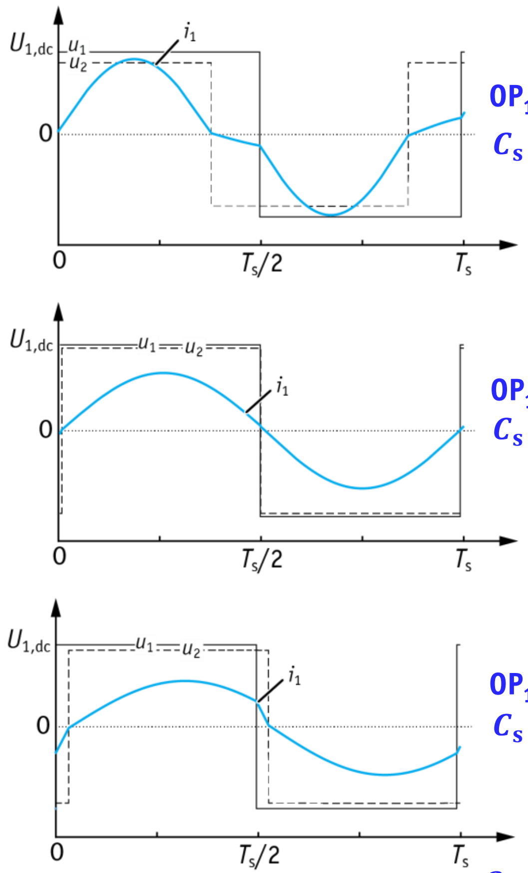

$OP_{1\text{-}1}$: $C_s < C_{s,opt}$

$OP_{1\text{-}2}$: $C_s = C_{s,opt}$

$OP_{1\text{-}3}$: $C_s > C_{s,opt}$

$\omega_s = \dfrac{2\pi}{T_s}$

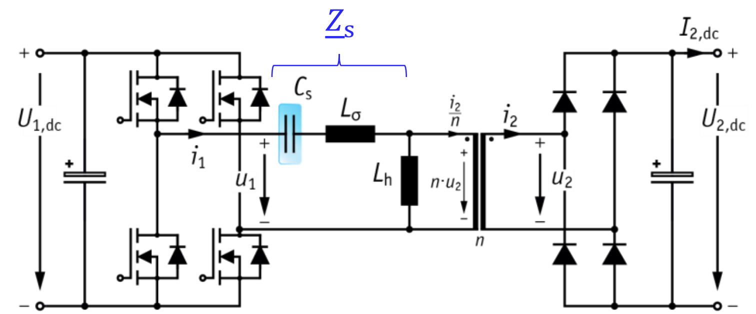

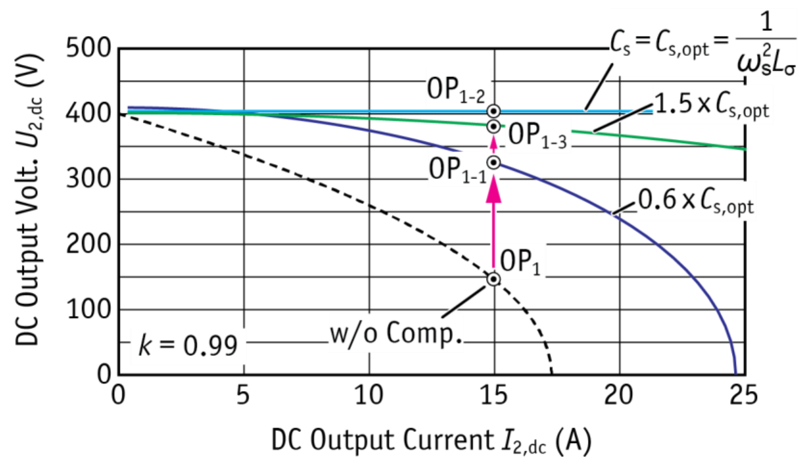

▲ **Converter Output Characteristics**

► Resonant Compensation of Stray Inductance (3)

- Insert Capacitor in Series to Transformer Stray Inductance L_σ
- Select Capacitance $C_{s,opt} = 1/(\omega_s^2 L_\sigma)$ to Match Resonance and Inverter Switching Frequency

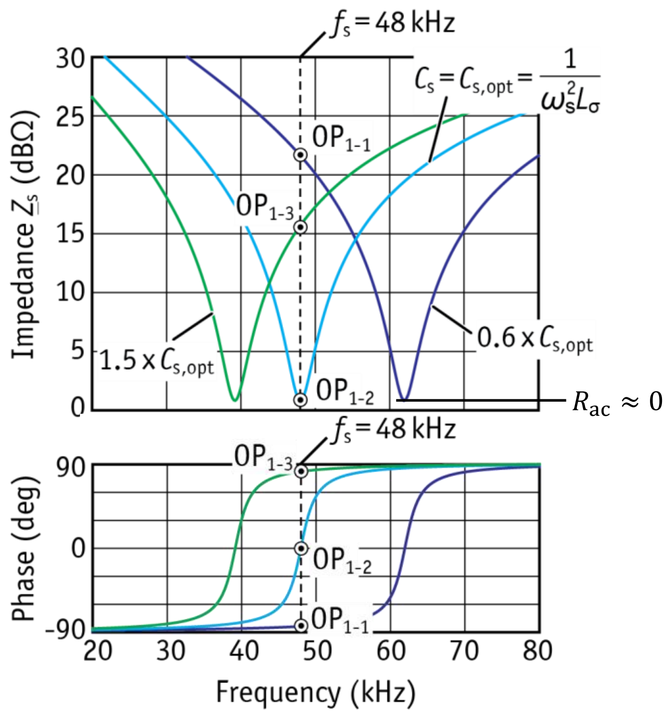

▲ Bode Diagram for Different Selections of the Compensation Capacitance C_s

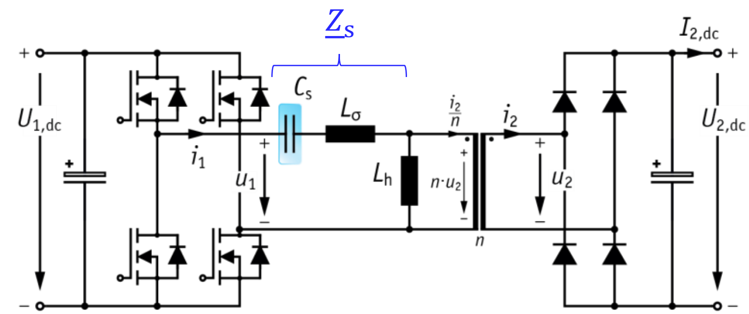

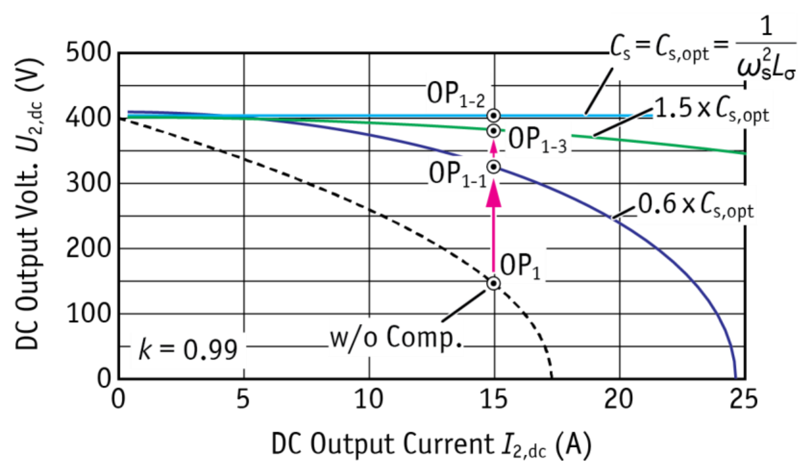

▲ Converter Output Characteristics

► Alternative Compensation Concepts

■ **Limitations of Series-Compensation**
- High Voltages Across Resonant Elements in High-Power Designs
- Limited to Step-Down Conversion
- No Control of Output at No-Load (with Frequency Control)

■ **Alternative Options:**
- Parallel Resonant Converter (LLC)
- Series/Parallel Res. Converter (LCC)
- General Matching Networks

■ **Limitations of Parallel-Compensation**
- Circulating Reactive Current in Parallel Elements also at Low Load
- Potentially Needs Additional Inductors
- Complex Design Process (Selection of Two Capacitor Values for SP-Comp.)

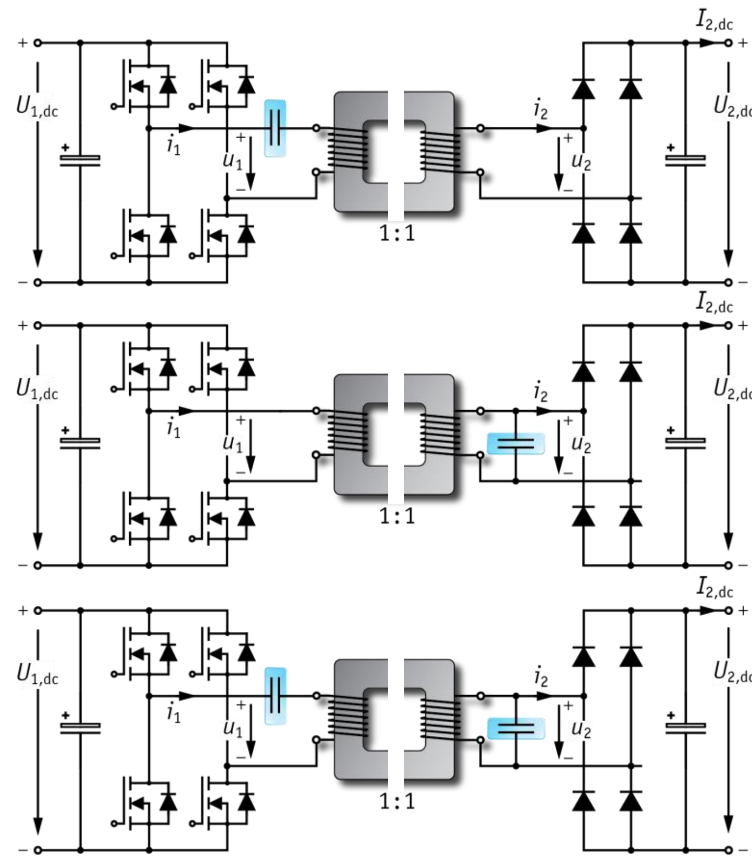

▲ **Alternative Compensation Topologies**

► Fundamental Frequency Approximation (1)

- **Nearly Sinusoidal Current Shape Despite Rectangular Voltage Waveforms**
  - Resonant Circuit Acts as Bandpass-Filter on Inverter Output Voltage Spectrum

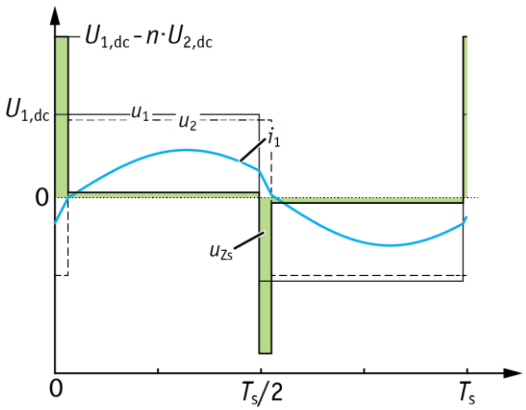

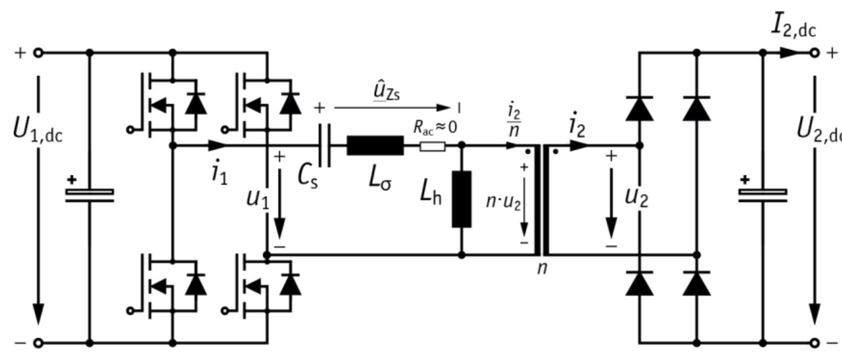

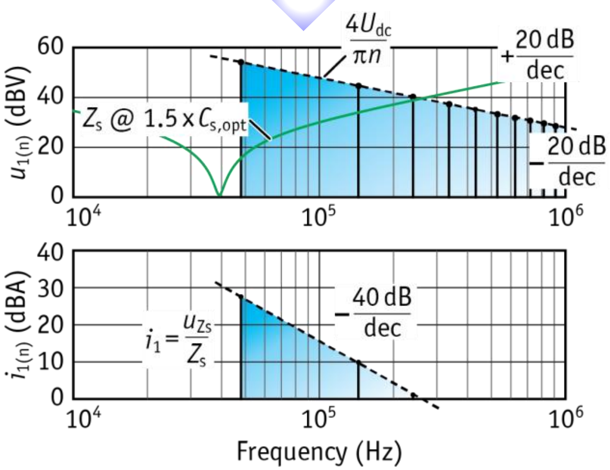

- **Consider only Fundamental Frequency Components:**
  - Fundamentals of u_1, u_2, i_1, i_2
  - Power Transfer Modeled with Good Accuracy as

$$P = \sum_{n=1}^{\infty} U_{1(n)} I_{1(n)} \cos(\phi_n)$$
$$\approx U_{1(1)} I_{1(1)} \cos(\phi_1)$$

→ Fundamental Frequency Model!

► Fundamental Frequency Approximation (2)

R. Steigerwald, "A comparison of half-bridge resonant converter topologies," in IEEE Trans. Power Electron., vol. 3, no. 2, 1988.

■ Replace Rectifier and Load $I_{2,\mathrm{dc}}$ by Power Equivalent Resistance $R_{\mathrm{L,eq}}$

$$\hat{U}_{1(1)} = \frac{4}{\pi} U_{1,\mathrm{dc}}$$

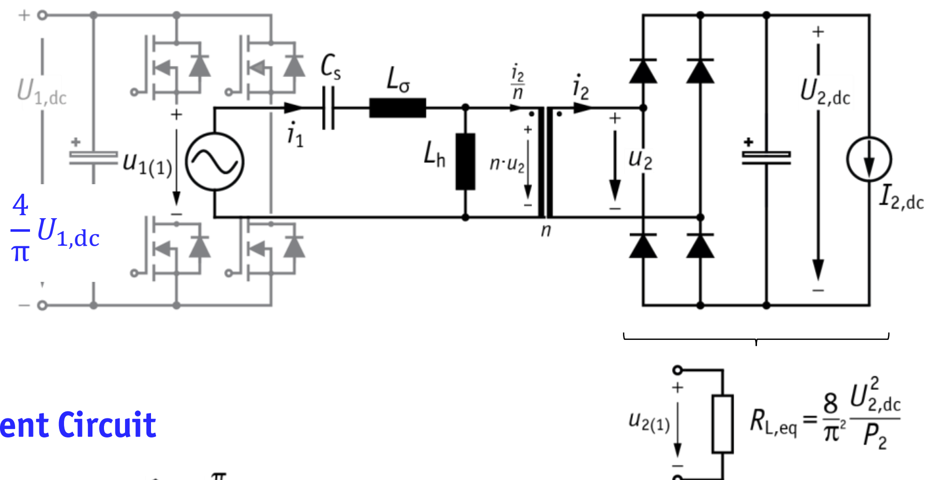

■ Fundamental Frequency Equivalent Circuit

$$R_{\mathrm{L,eq}} = \frac{\hat{U}_{2(1)}}{\hat{I}_{2(1)}} \approx \frac{\frac{4}{\pi} U_{2,\mathrm{dc}}}{\frac{\pi}{2} I_{2,\mathrm{dc}}} = \frac{8}{\pi^2} \frac{U_{2,\mathrm{dc}}^2}{P_2}$$

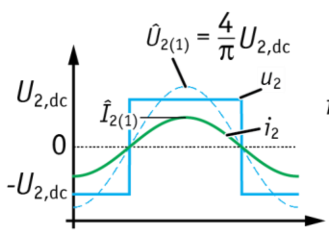

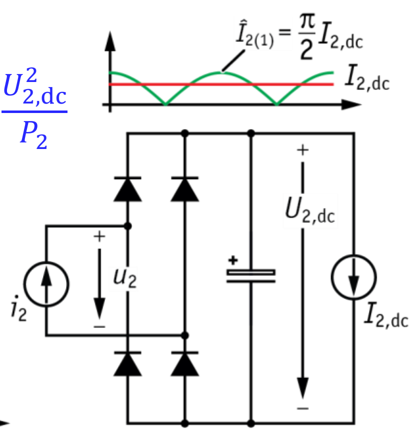

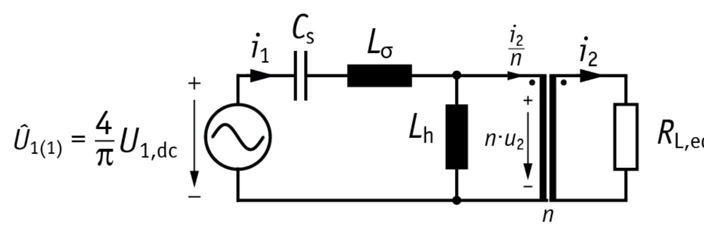

- Simplified Circuit Analysis & Approximate Power Loss Calculations

▶ Resonant Circuit Transfer Characteristics (1)

- **Load-Independent Output Voltage due to Series Resonant Compensation**
  - Except for a (Small) Voltage Drop on Winding Resistances R_1,R_2

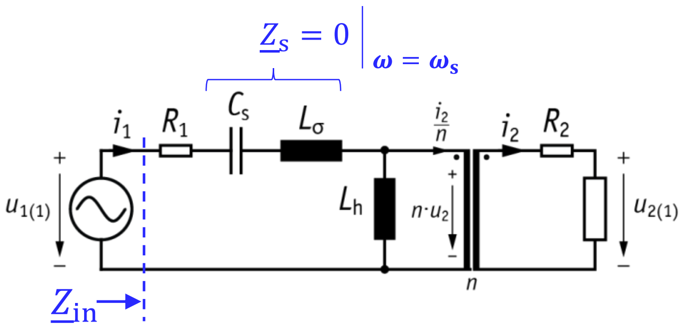

- **Only Small Shift of Resonant Frequency for Different Loads at Constant Coupling**
  - Fixed Frequency Operation Possible

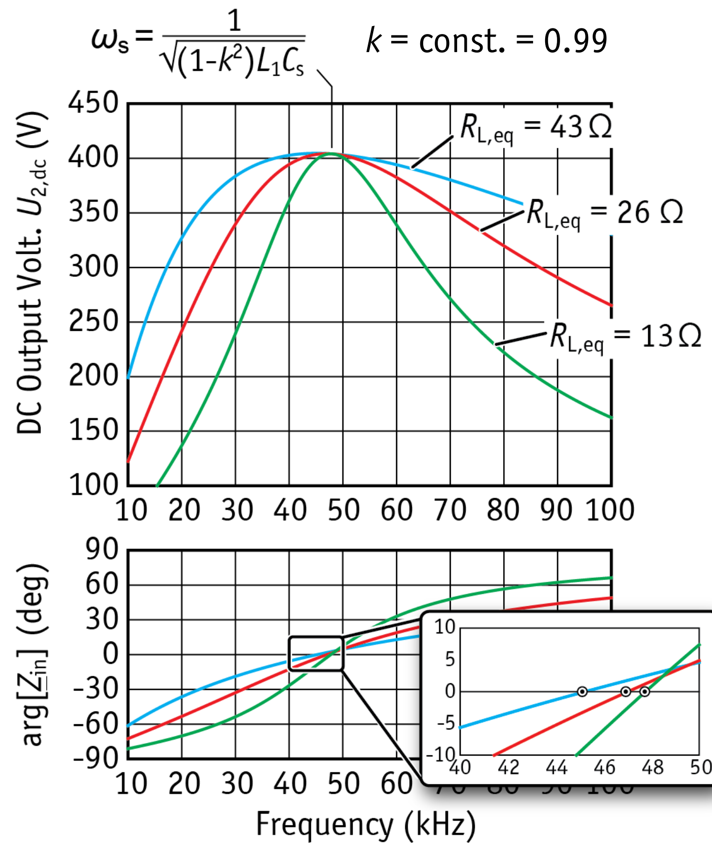

▲ **Voltage Transfer Ratio at k = 0.99**

► Resonant Circuit Transfer Characteristics (2)

■ **Strong Coupling Dependency of Output Voltage due to Variation of Series Impedance**

- Variation of Coupling k Changes L_σ which Leads to Series Voltage Drop on $\underline{Z}_s > 0$

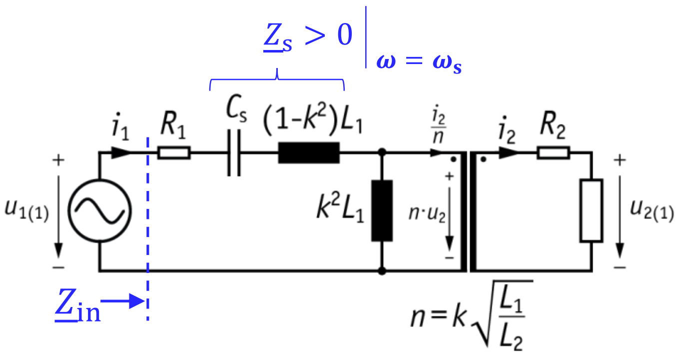

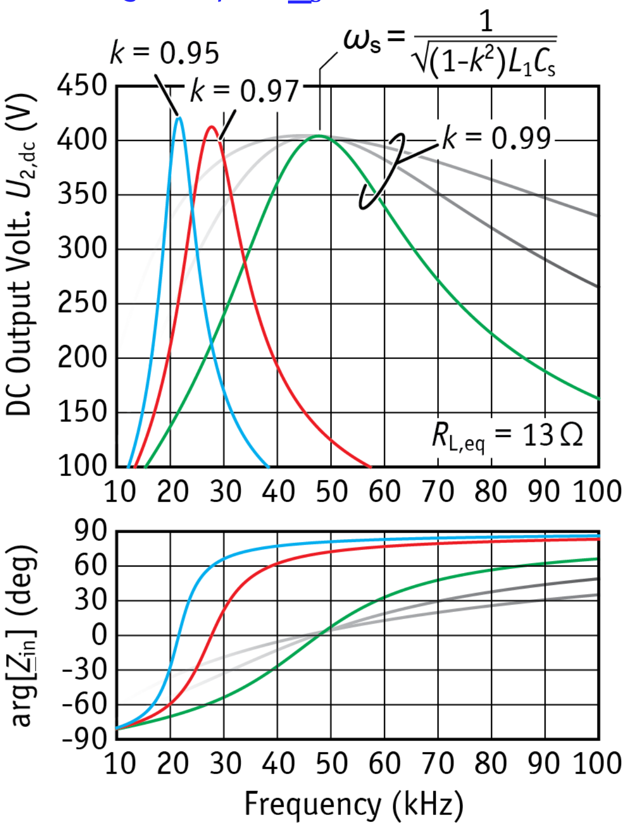

■ **Large Variation of Resonant Frequency with Changing Magnetic Coupling**

- Fixed Frequency Operation Not Possible

■ **Not Practical if Coupling is Variable in the Target Application**

▲ **Transfer Characteristics and Phase Angle of Input Impedance for Different Coupling**

► Series-Series Compensated IPT System (1)

■ **Add Second Series Capacitor to Ensure Fixed Resonant Frequency ($\varphi_{\underline{Z}_{\text{in}}} = 0$) for any Value of the Magnetic Coupling *k***

$$\omega_0 = \frac{1}{\sqrt{L_1 C_1}} = \frac{1}{\sqrt{L_2 C_2}}$$

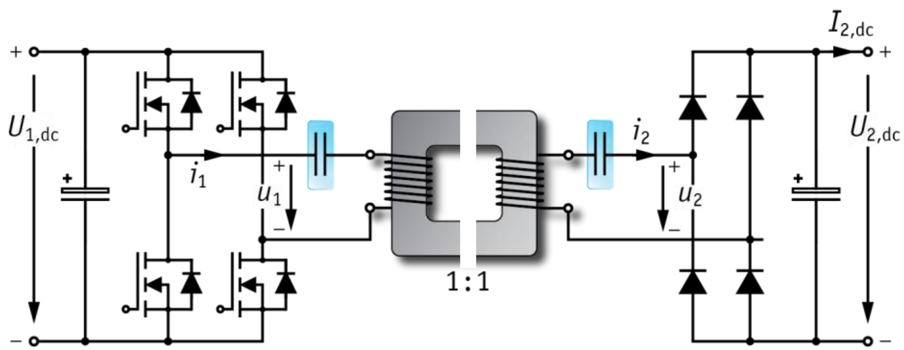

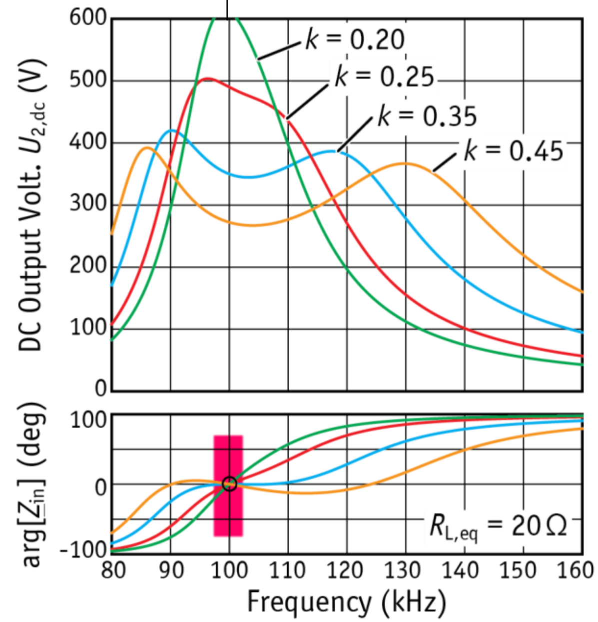

▲ **Transfer Characteristics and Phase Angle of Input Impedance for Different Coupling**

■ **Resulting Equivalent Circuit @ ω_0**

- Cancel Complete Self-Inductance

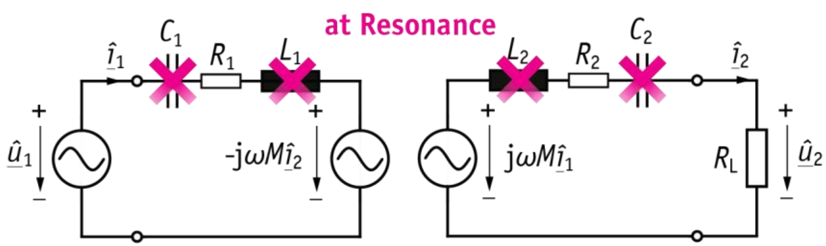

- $\varphi_{\underline{Z}_{\text{in}}} = 0°$ @ ω_s Independent of k, R_L
- But: Voltage Gain @ ω_s Still Coupling & Load Dependent!

► Series-Series Compensated IPT System (2)

■ Resonant Frequency ($\varphi_{\underline{Z}_{\text{in}}} = 0$) is Indepenent of Magnetic Coupling and of Load

- Necessary Condition for Minimum Input Current → Max. Efficiency!

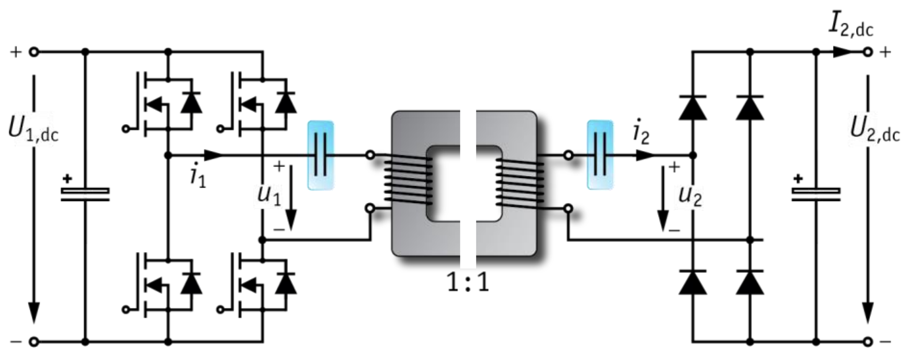

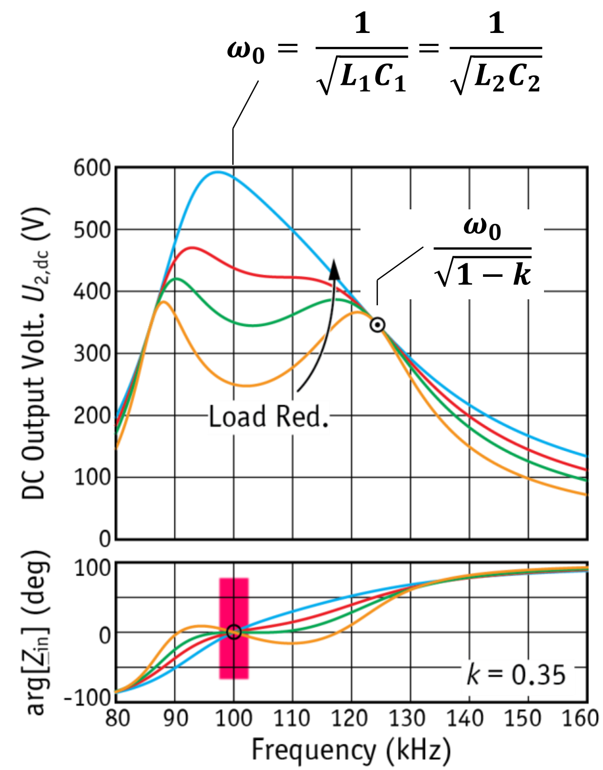

▲ Transfer Characteristics and Phase Angle of Input Impedance for Different Loads

■ Resulting Equivalent Circuit @ ω_0

- Cancel Complete Self-Inductance

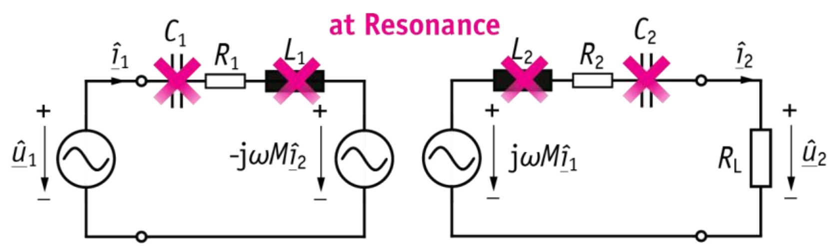

- $\varphi_{\underline{Z}_{\text{in}}} = 0°$ @ ω_s Independent of k, R_L
- But: Voltage Gain @ ω_s Still Coupling & Load Dependent!

▶ Properties of the Series-Series Compensation (1)

■ **Operation at Frequency $\omega_s = \dfrac{\omega_0}{\sqrt{1-k}}$**

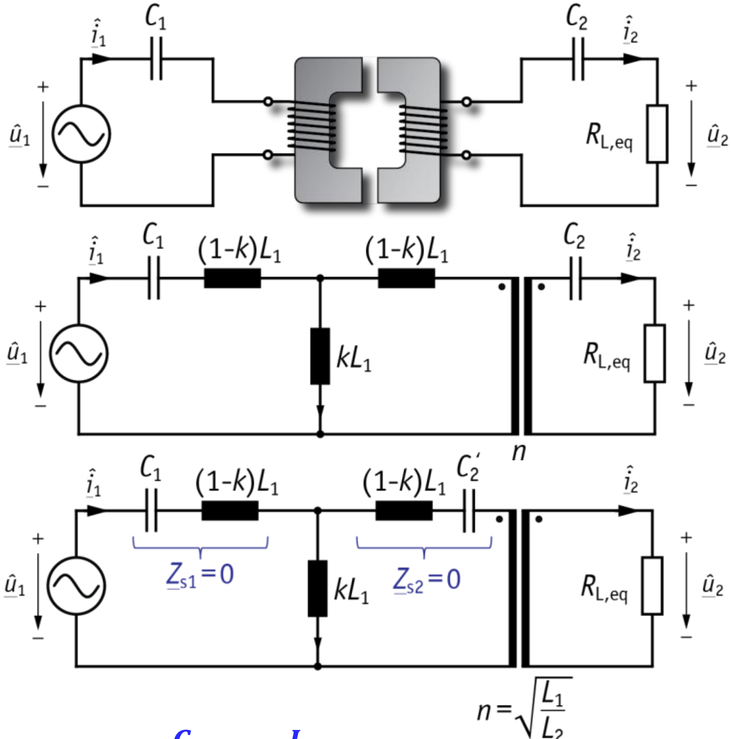

$$C_2' = \frac{C_2}{n^2} = C_s\frac{L_2}{L_1}$$

$$\omega_{s1}^2 = \frac{1}{C_1L_1(1-k)}$$

$$\omega_{s2}^2 = \frac{1}{C_2L_2(1-k)}$$

$$\rightarrow \omega_{s1} = \omega_{s2} = \omega_s = \frac{\omega_0}{\sqrt{1-k}}$$

$$\rightarrow \hat{u}_2 = \hat{u}_1\sqrt{\frac{L_2}{L_1}}$$

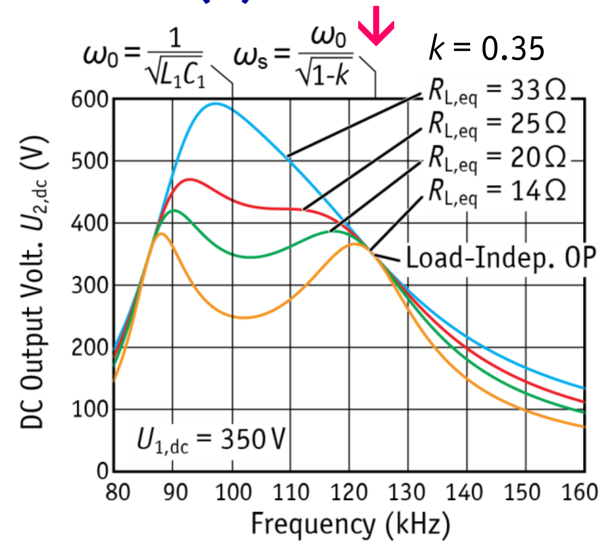

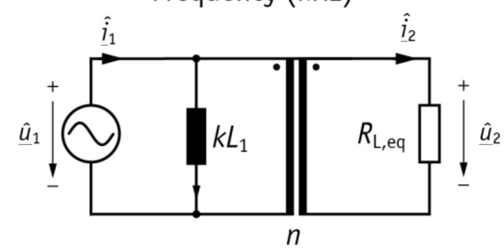

▲ **Output Voltage $\hat{U}_2$ is Indepndent of Load Resistance at ω_s**

■ **Load-Independent Output Voltage**
- ω_s Coupling Dependent
- Inductive Input Impedance @ ω_s

▶ Properties of the Series-Series Compensation (2)

■ **Operation at Resonant Frequency** $\omega_0 = \frac{1}{\sqrt{L_1 C_1}} = \frac{1}{\sqrt{L_2 C_2}}$

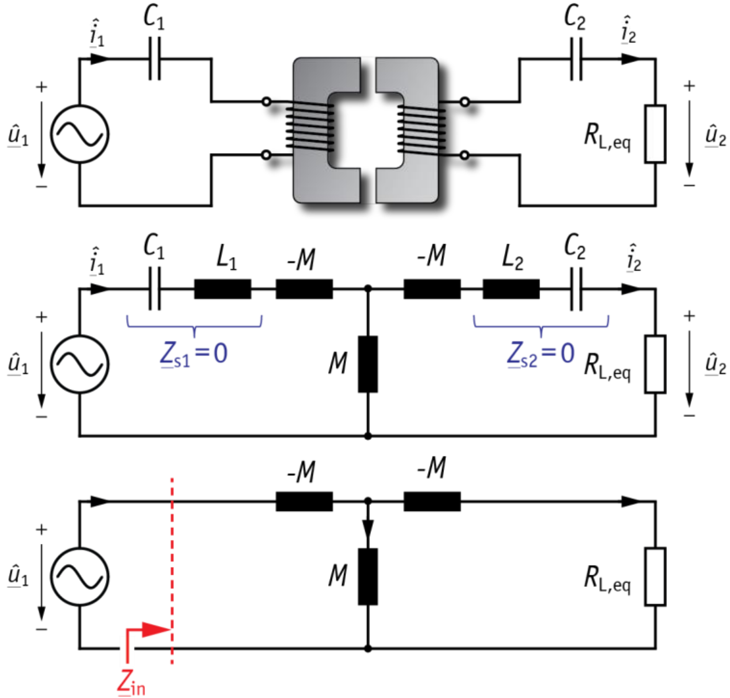

$$\underline{Z}_{in} = -j\omega_0 M + \frac{j\omega_0 M \cdot (R_{L,eq} - j\omega_0 M)}{j\omega_0 M + R_{L,eq} - j\omega_0 M}$$

$$\rightarrow \underline{Z}_{in} = \frac{\omega_0^2 M^2}{R_{L,eq}}$$

$$\rightarrow \arg[\underline{Z}_{in}] = 0$$

$$k = 0 \rightarrow \underline{Z}_{in} = 0$$

$$R_{L,eq} = 0 \rightarrow \underline{Z}_{in} = \infty$$

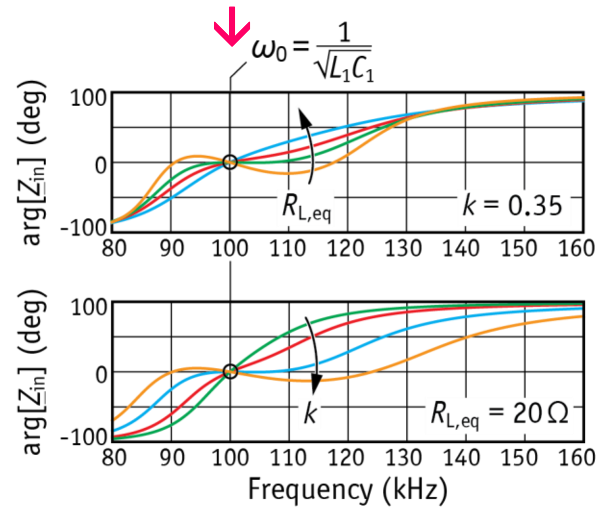

▲ **Phase Angle of Input Impedance for Varying Load (top) and Coupling (bot.)**

■ **Purely Ohmic Input Impedance For any Load & Coupling @ ω_s**

▶ Properties of the Series-Series Compensation (3)

■ **Operation at Resonant Frequency** $\omega_0 = \dfrac{1}{\sqrt{L_1 C_1}} = \dfrac{1}{\sqrt{L_2 C_2}}$

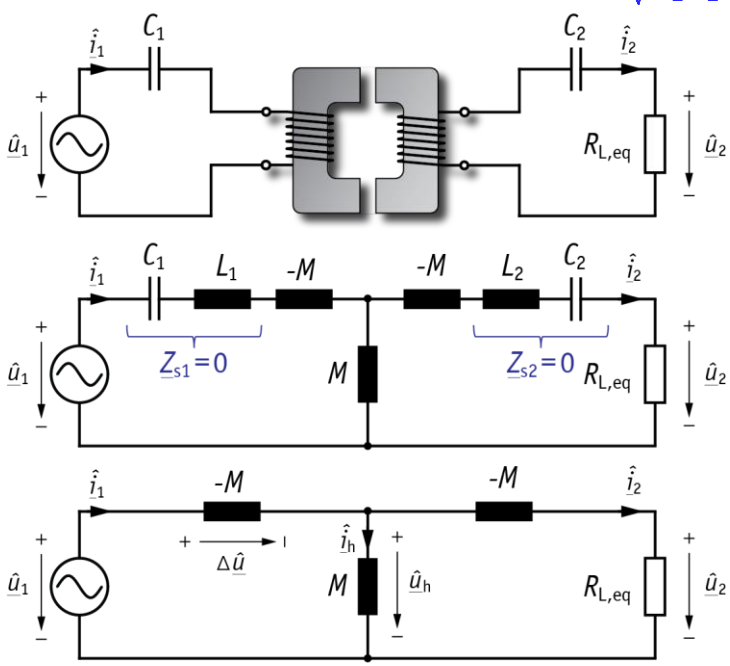

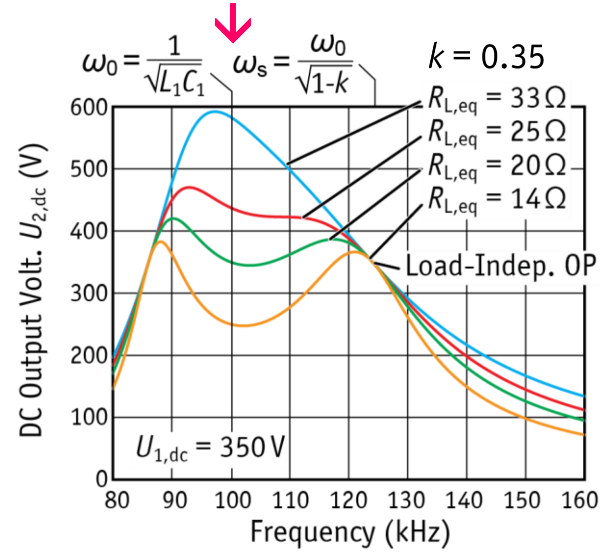

▲ **Output Voltage $\hat{U}_2$ Rises with Load Resistance for Constant $\hat{U}_1$**

$$\underline{\hat{u}}_h = \underline{\hat{\imath}}_2 (R_{\mathrm{L,eq}} - \mathrm{j}\omega_0 M)$$

$$\underline{\hat{\imath}}_h = \frac{\underline{\hat{\imath}}_2}{\mathrm{j}\omega_0 M} (R_{\mathrm{L,eq}} - \mathrm{j}\omega_0 M)$$

$$\Delta\underline{\hat{u}} = -\mathrm{j}\omega_0 M (\underline{\hat{\imath}}_2 + \underline{\hat{\imath}}_h)$$
$$= -\mathrm{j}\omega_0 M \underline{\hat{\imath}}_2 - \underline{\hat{\imath}}_2 (R_{\mathrm{L,eq}} - \mathrm{j}\omega_0 M)$$

■ **Output Current Independent of Load Resistance $R_{\mathrm{L,eq}}$:**

$$\underline{\hat{u}}_1 = \Delta\underline{\hat{u}} + \underline{\hat{u}}_h = -\mathrm{j}\omega_0 M \underline{\hat{\imath}}_2$$

$$\rightarrow \quad \underline{\hat{\imath}}_2 = \mathrm{j}\frac{\underline{\hat{u}}_1}{\omega_0 M}$$

Maximum Efficiency of the Resonant System

▶ Power Losses of the Series-Series Compensation

- **Operation at Resonant Frequency** $\omega_0 = \dfrac{1}{\sqrt{L_1 C_1}} = \dfrac{1}{\sqrt{L_2 C_2}}$

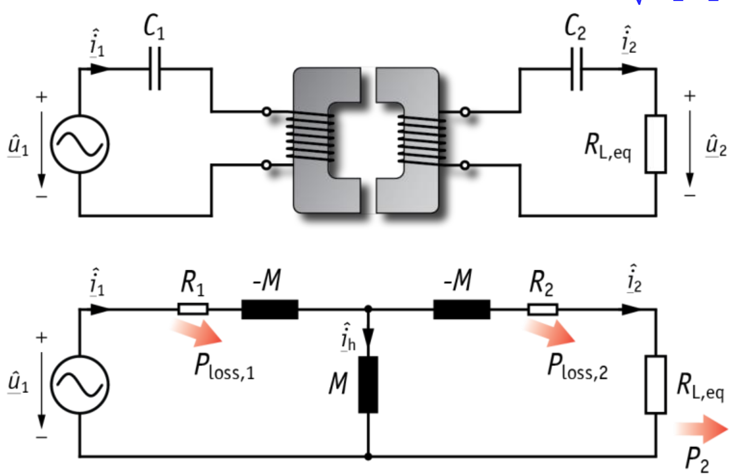

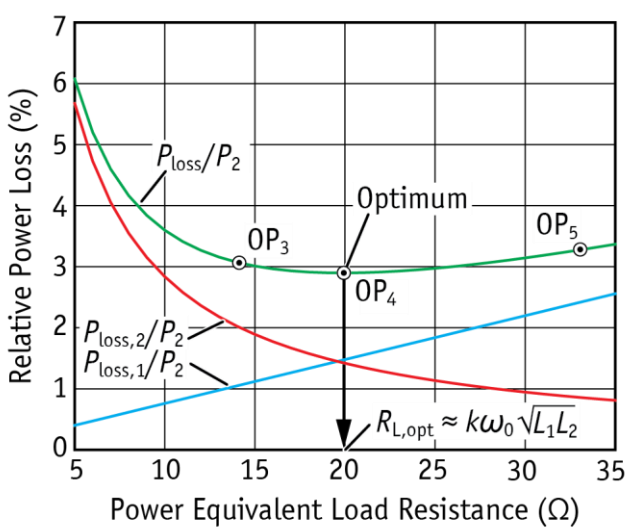

$$P_{\mathrm{loss,1}} = \frac{1}{2}\left|\hat{\underline{i}}_1\right|^2 R_1 \quad P_{\mathrm{loss,2}} = \frac{1}{2}\left|\hat{\underline{i}}_2\right|^2 R_2 \quad P_2 = \frac{1}{2}\left|\hat{\underline{i}}_2\right|^2 R_{\mathrm{L,eq}}$$

- **Total Power Losses**
  - Core Loss Neglected

$$\underbrace{\frac{P_{\mathrm{loss}}}{P_2}}_{\lambda} = \underbrace{\frac{P_{\mathrm{loss,1}}}{P_2}}_{\lambda_1} + \underbrace{\frac{P_{\mathrm{loss,2}}}{P_2}}_{\lambda_2}$$

- **Minimum Relative Losses**
  - Minimize Loss Factor λ

$$\frac{\mathrm{d}}{\mathrm{d}R_{\mathrm{L,eq}}}\underbrace{\left(\frac{P_{\mathrm{loss}}}{P_2}\right)}_{\lambda} = 0 \qquad \rightarrow R_{\mathrm{L,opt}} = \sqrt{\omega_0^2 M^2 + \underbrace{R_{\mathrm{ac}}^2}} \approx k\omega_0\sqrt{L_1 L_2}$$

$$R_1 \approx R_2 = R_{\mathrm{ac}} \ @\ \omega_0$$

Design Condition for Maximum Efficiency!

▶ Efficiency Limit of IPT Systems

K. van Schuylenbergh and R. Puers, *Inductive Powering: Basic Theory and Application to Biomedical Systems*, 1st ed., Springer-Verlag, 2009.

- **Condition for Minimum Total Coil Losses:** $R_{L,opt} \approx k\omega_0\sqrt{L_1 L_2}$

- **Efficiency Limit of IPT Systems**

$$\boxed{\eta_{max} = \frac{k^2 Q_1 Q_2}{\left(1 + \sqrt{1 + k^2 Q_1 Q_2}\right)^2}}$$

→ **Figure-of-Merit** $= k\sqrt{Q_1 Q_2} = kQ$

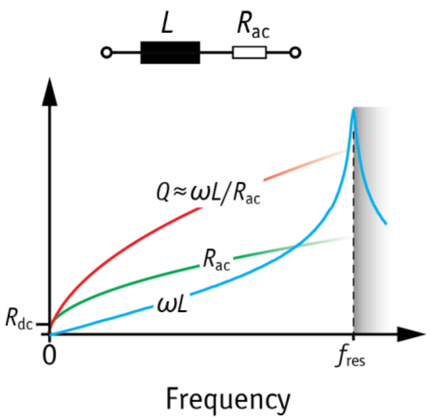

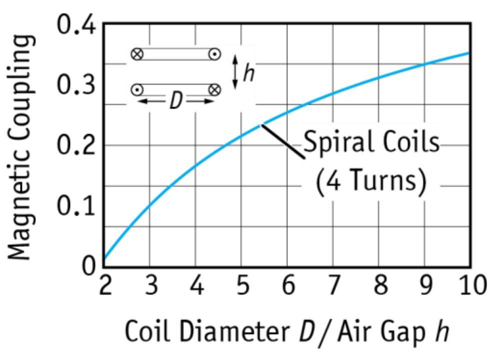

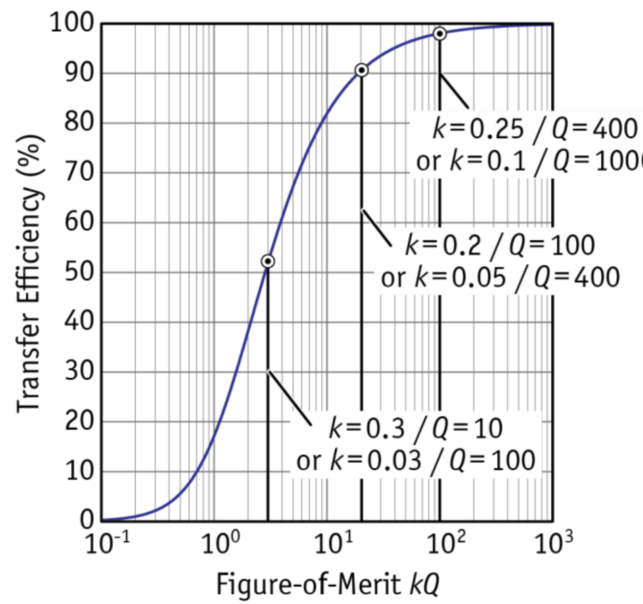

$k = L_h/\sqrt{L_1 L_2}$ .... Magnetic Coupling
$Q = \omega L/R_{ac}$ .... Coil Quality Factor

▲ **Efficiency Limit of IPT Systems (Coil Losses Only, Core Neglected)**

► *FOM* = Quality Factor x Magnetic Coupling

■ «Highly Resonant Wireless Power Transfer»

- Operation of «High-Q Coils» at Self-Resonance
- Compensation of Low k with High Q: High Freedom-of-Position
- High Frequency Operation (kHz ... MHz)

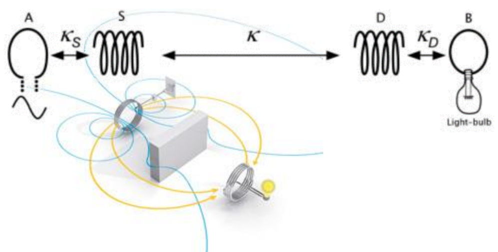

WiTricity, www.witricity.com (13.11.2014).

■ Intelligent Parking Assistants for EV

- Maximize k by Perfect Positioning
- Camera-Assisted Positioning Guide
- Achieve up to 5 cm Parking Accuracy

Toyota, www.toyota.com, (18.11.2014).

Maximum Efficiency Operation of the Inverter

► Zero-Voltage Switching of the Inverter Stage (1)

■ Zero-Voltage Switching of MOSFET Half-Bridge

- Sufficient Load-Current to (Dis-) Charge the Charge-Equivalent MOSFET Capacitances Results in Loss-Free Turn-Off Transition
- Body Diode is Conducting before Loss-Free Turn-On of the MOSFET Channel at U_{dc} = 0 V (= ZVS)

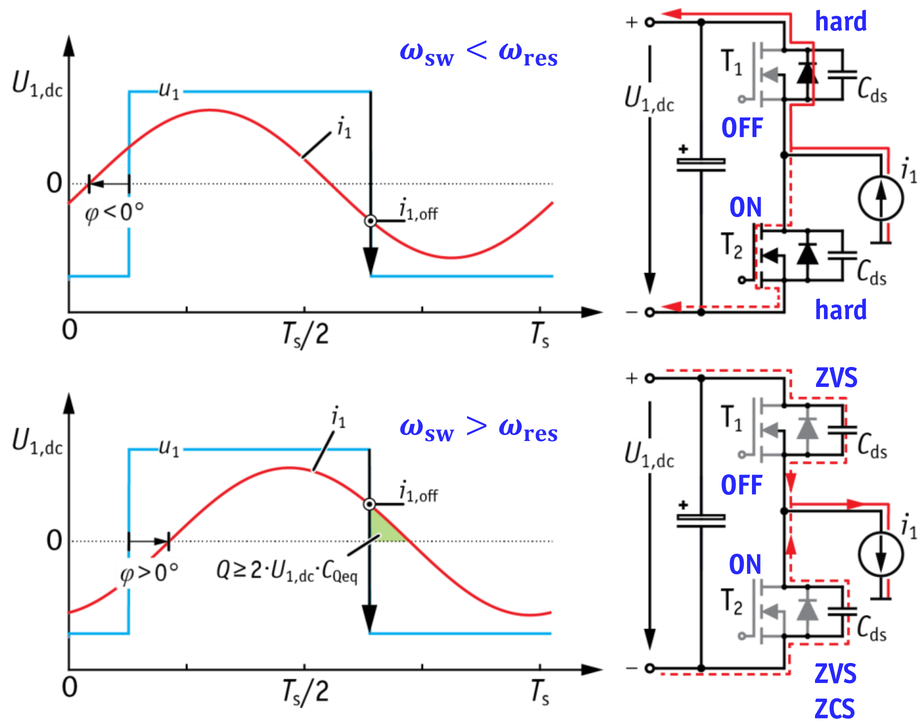

▲ Hard- and Soft-Switching of an Inverter Bridge-Leg

► Zero-Voltage Switching of the Inverter Stage (2)

■ Zero-Voltage Switching

- Sufficient Load-Current to (Dis-) Charge the Charge-Equivalent Capacitance C_{Qeq}
- C_{Qeq} Differs Significantly from Energy-Equivalent Capacitance C_{Eeq}

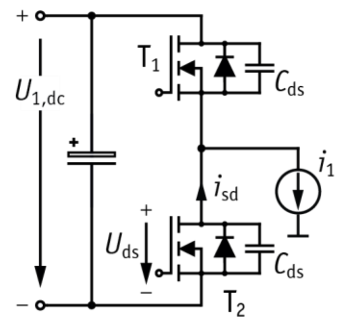

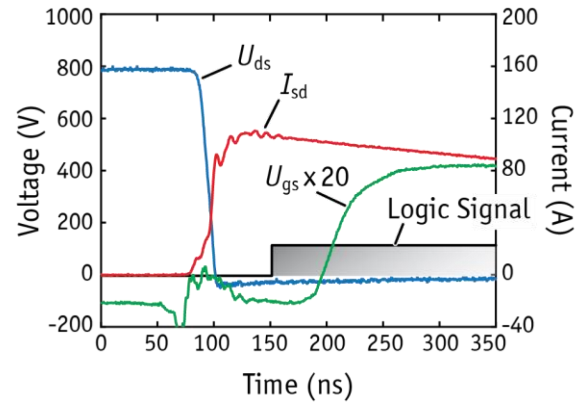

■ Capacitance Definitions:

- Charge-Equivalent Capacitance

$$C_{Qeq} = \frac{Q(U_{1,\mathrm{dc}})}{U_{1,\mathrm{dc}}} = \frac{\int_0^{U_{1,\mathrm{dc}}} C(v)\mathrm{d}v}{U_{1,\mathrm{dc}}},$$

- Energy-Equivalent Capacitance

$$C_{Eeq} = \frac{E(U_{1,\mathrm{dc}})}{\frac{1}{2}U_{1,\mathrm{dc}}^2} = \frac{\int_0^{U_{1,\mathrm{dc}}} v \cdot C(v)dv}{\frac{1}{2}U_{1,\mathrm{dc}}^2}$$

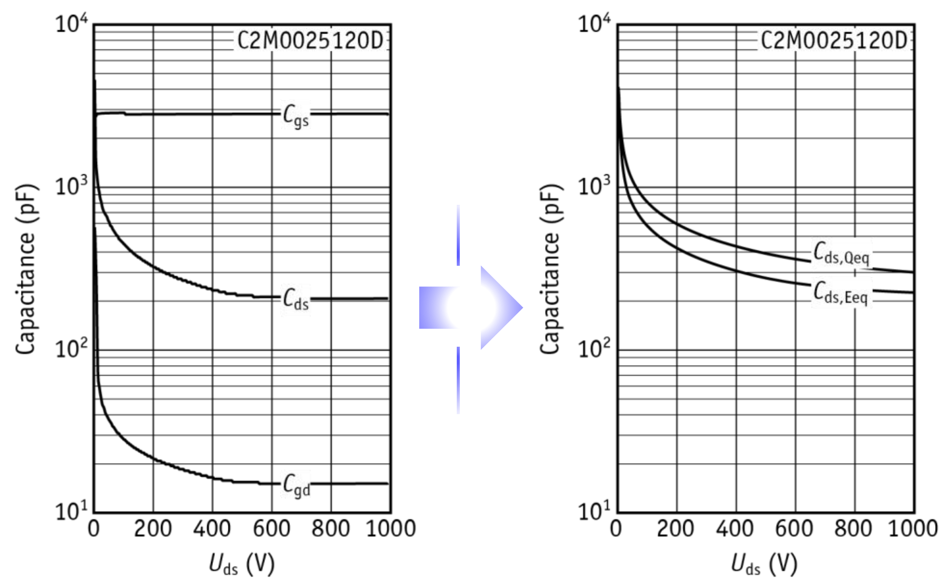

▲ Datasheet Values of a SiC Power MOSFET (C2M0025120D)

► Zero-Voltage Switching of the Inverter Stage (3)

■ Zero-Voltage Switching of Inverter Stage

- Sufficient Inductive Load-Current to (Dis-) Charge Charge-Equivalent MOSFET Capacitance

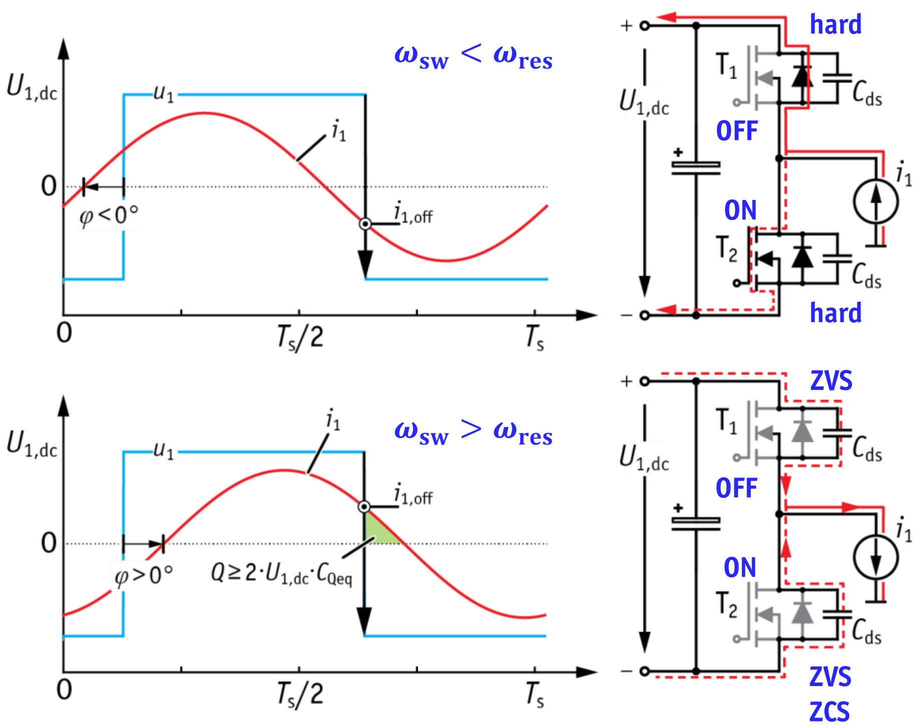

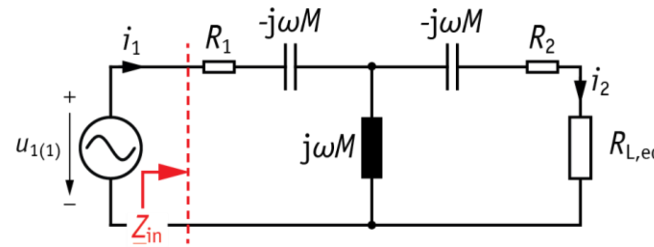

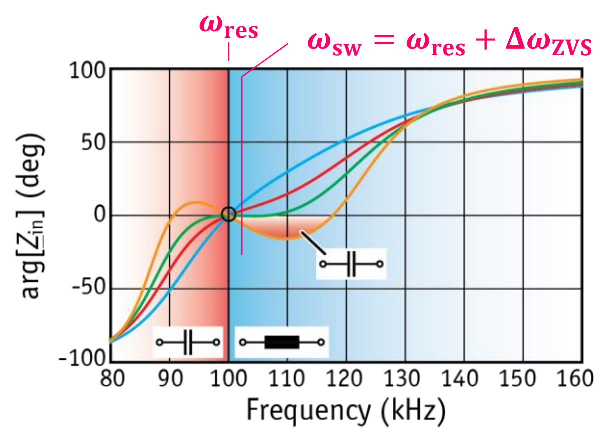

▲ **Phase Angle of Input Impedance for Different Loads**

▶ Frequency Dependency of Voltage Gain (1)

■ Example of SS-Compensated IPT System

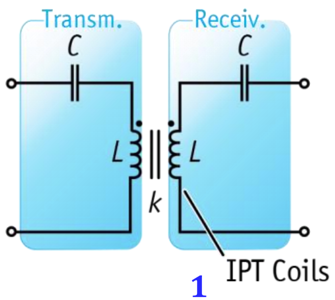

$$\omega_1 = \omega_2 = \frac{1}{\sqrt{LC}} = \omega_0$$

■ Pole Splitting due to Interaction of Transmitter & Receiver Resonant Circuit

- Magnetic Coupling Determines the Strength of Transmitter/Receiver Interaction
- Non-Monotonic Phase Behavior
  → May Lead to Hard-Switching

■ Can be Avoided by Design with Modified Design Rule for Receiver Reactance:

$$\left(\frac{R_\mathrm{L}}{\omega_0\sqrt{L_1 L_2}}\right)_{\mathrm{subopt}} \approx 70..80\% \cdot k_{\max}$$

- Loss-Increase Typically below 5%
- Inductive Behavior Ensured for $\omega_{\mathrm{sw}} > \omega_0$

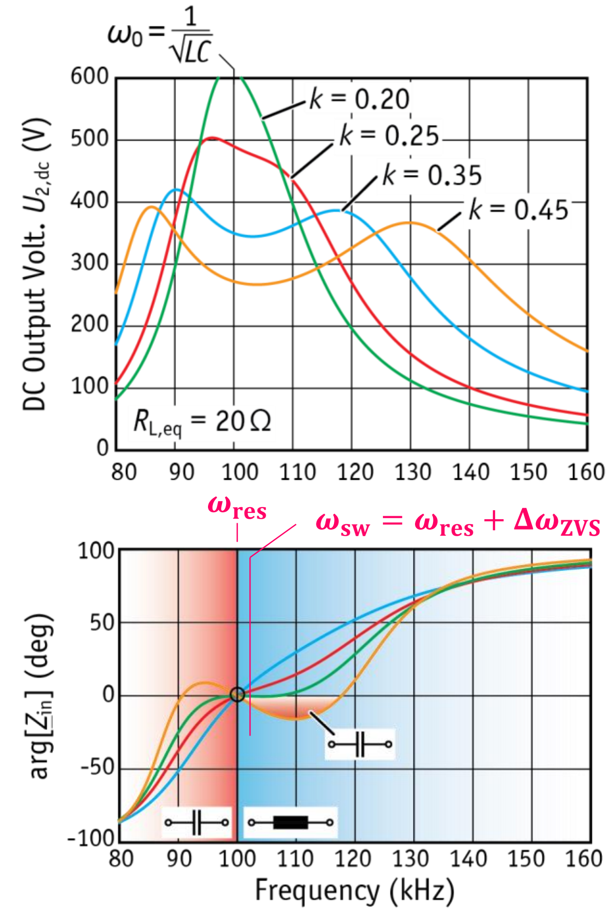

▲ Voltage Transfer Functions and Phase of Input Impedance of an IPT System

► Frequency Dependency of Voltage Gain (2)

- **Explanation of Pole-Splitting: Interaction of Coupled Resonant Circuits Tuned to Same Frequency**

- **Example of a Two-Stage *LC*-Filter**

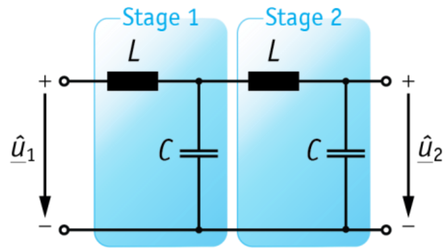

$$\omega_1 = \omega_2 = \frac{1}{\sqrt{LC}} = \omega_0$$

- Both Stages tuned to Same Frequency (100 kHz)
- Pole-Splitting due to Stage-Interaction
- Two Resonant Peaks

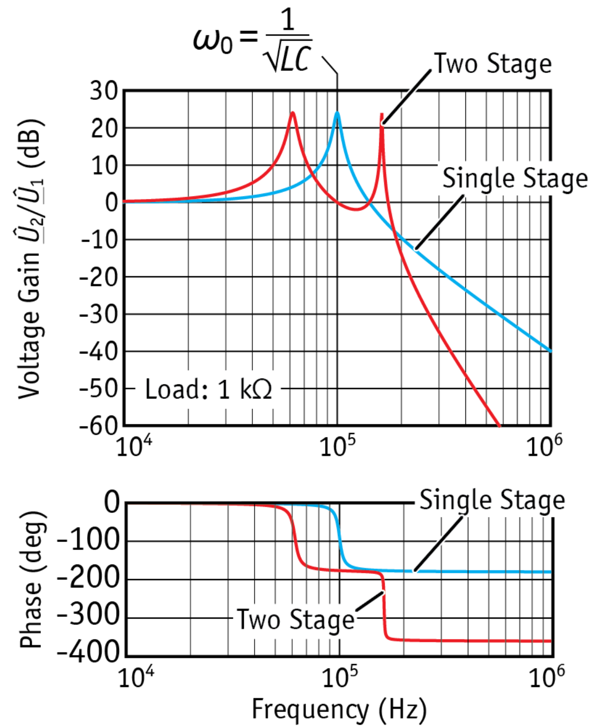

▲ **Transfer Functions of a Single- and a Two-Stage *LC*-Filter**

► Zero-Current Switching of IGBTs

- **Stored Charge in IGBT Drift Region must be Fully Removed at the Device Turn-Off**
  - Phase-Lag between Current and Stored Charge: Residual Charge if Turn-Off at Zero-Current
  - Residual Charge causes Turn-On Losses in the Complimentary Device

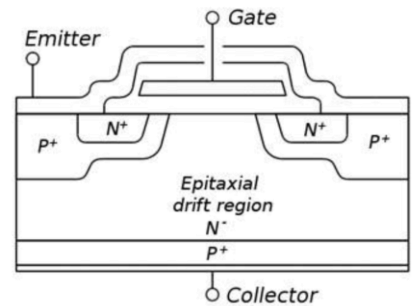

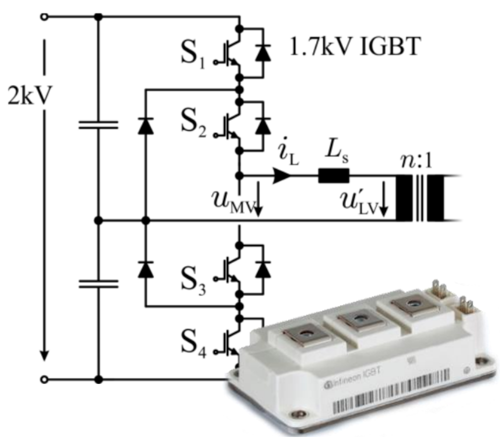

$$\boxed{\frac{dQ(t)}{dt} = -\frac{Q(t)}{\tau} + k_s \cdot i_s(t)}$$

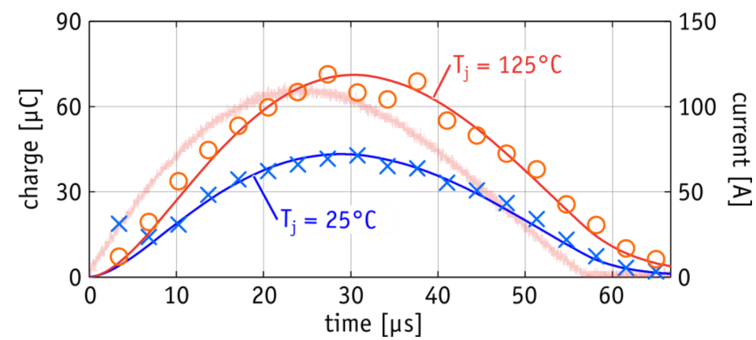

▲ **Experimental Stored Charge Dynamic Analysis on 1.7kV FS IGBT and Resonant Sine Pulse**

P. Ranstad and H.-P. Nee, "On dynamic effects influencing IGBT losses in soft-switching converters," *IEEE Trans. Power Electron.*, vol. 26, no. 1, pp. 260–271, 2011.
G. Ortiz, H. Uemura, D. Bortis, J. W. Kolar, and O. Apeldoorn, "Modeling of soft-switching losses of IGBTs in high-power high-efficiency dual-active-bridge dc/dc converters," *IEEE Trans. Electron Devices*, vol. 60, no. 2, pp. 587–597, 2013.

Efficiency Optimal
IPT System Operation

▶ Efficiency Optimal System Operation (1)

■ **Operation of Series-Series Compensated IPT System in Efficiency Optimum**

- Given Resonant Circuit
- Given Operating Frequency
- Given Magnetic Coupling
- Given Mains & Battery DC-Voltages

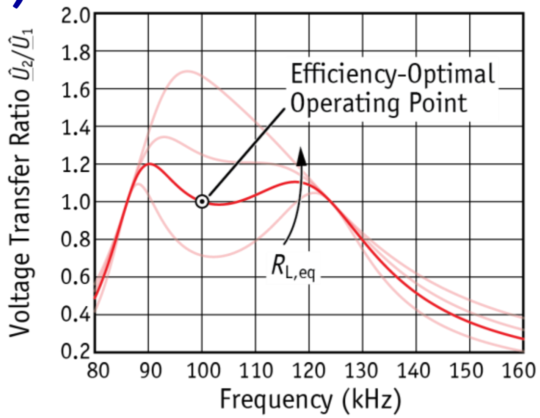

P_2^* ... reference
ω_0 ... selected
U_{batt} ... given
k ... estimated

$$\underbrace{P_2^*,\ \omega_0,\ U_{batt},\ k}_{\text{Controller Input Variables}} \rightarrow \underbrace{R_L^* \approx k\omega_0 L_2 \overset{!}{=} \frac{8}{\pi^2}\frac{U_{2,dc}^2}{P_2^*}}_{\text{Maximum Efficiency Condition}} \rightarrow \underbrace{U_{2,dc}^* = \sqrt{\frac{\pi^2}{8}P_2^* k\omega_0 L_2}}_{\text{Controller Reference}}$$

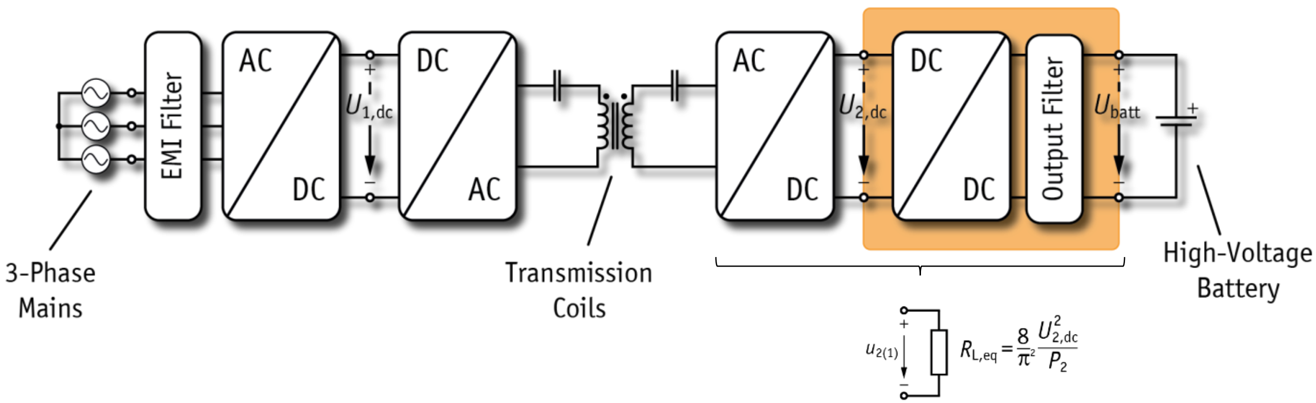

► Control Block Diagram for Efficiency Optimal Operation

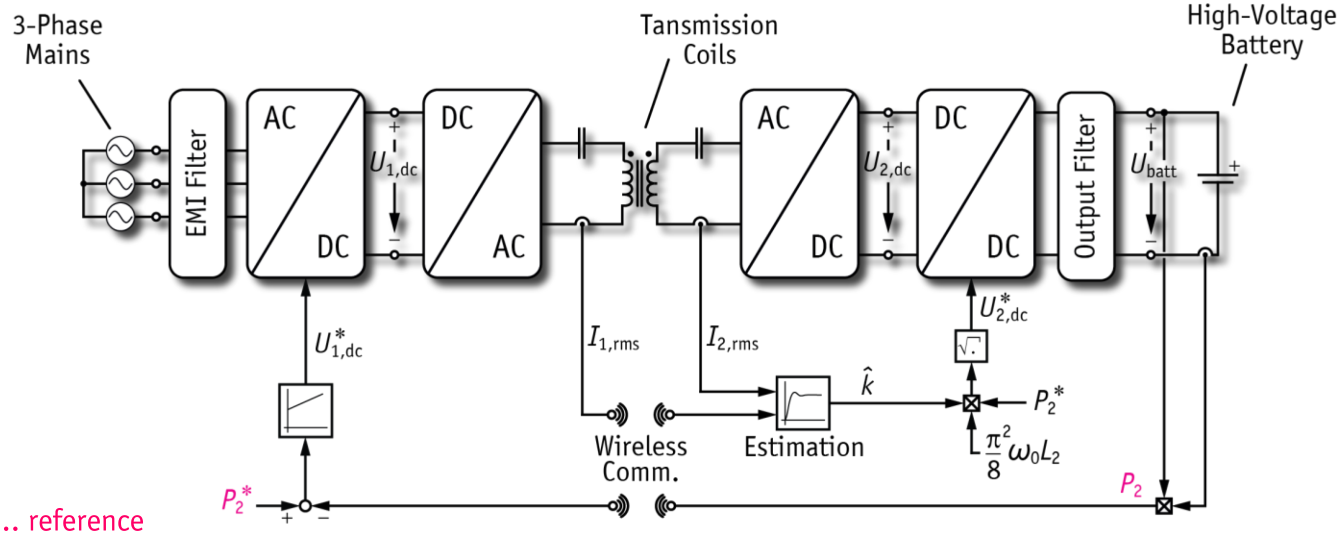

P_2^* ... reference
ω_0 ... selected
U_{batt} ... given
k ... estimated

Controller Input Variables

$$\underbrace{R_L^* \approx k\omega_0 L_2 = \frac{8}{\pi^2}\frac{U_{2,\mathrm{dc}}^2}{P_2^*}}_{\text{Maximum Efficiency Condition}} \rightarrow \underbrace{U_{2,\mathrm{dc}}^* = \sqrt{\frac{\pi^2}{8}P_2^* k\omega_0 L_2}}_{\text{Controller Reference}}$$

Voltage Step-Up or Step-Down

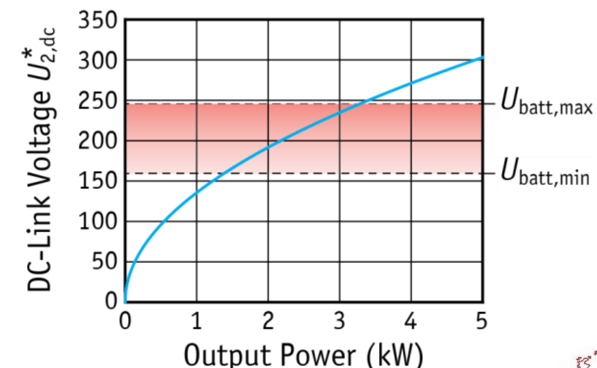

▶ Receiver Electronics – Potential Solutions (1)

■ **Regulation of Receiver-Side DC-Link Voltage with DC/DC Converter**

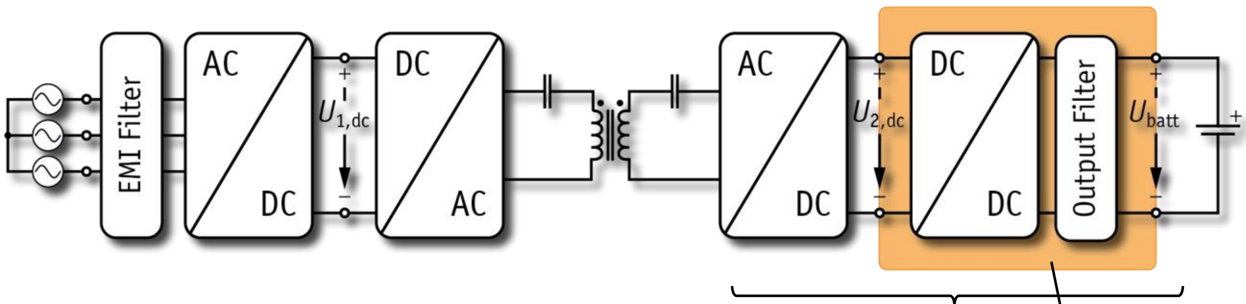

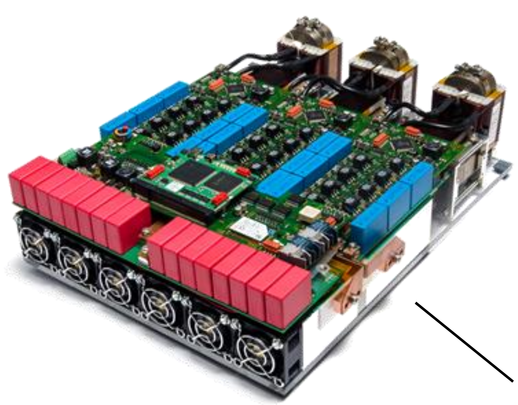

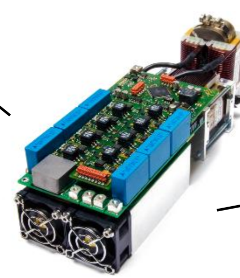

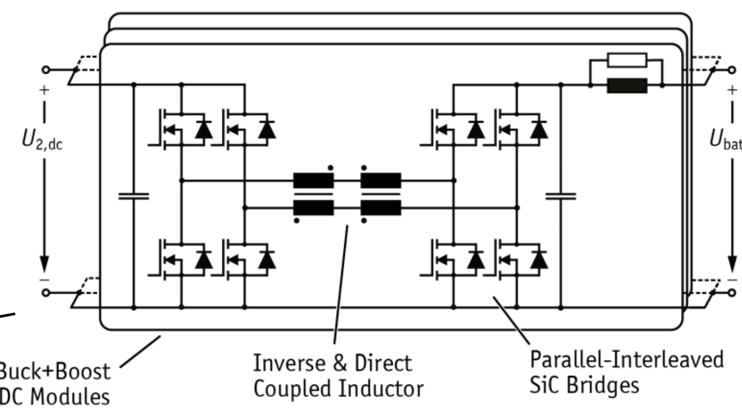

■ **Prototype SiC-Converter for 50 kW IPT (Receiver Side)**
- Efficiency 98%, 9.2 kW/dm^3

▶ Receiver Electronics – Potential Solutions (2)

■ **Integrated Solution: Regulation of Receiver-Side Voltage with AC/DC Converter**

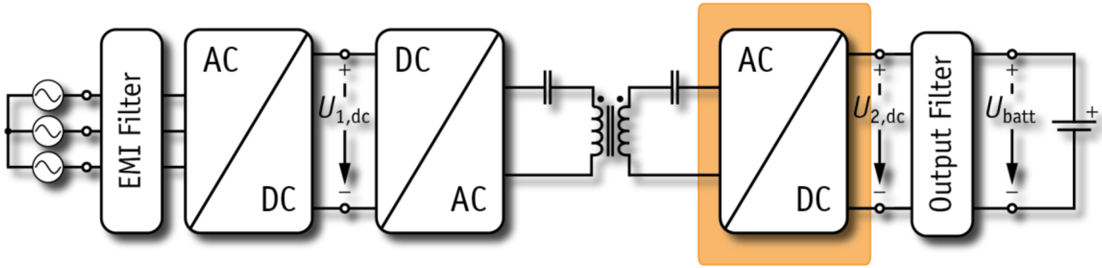

- Utilization of 1-Φ Bridgless-PFC Topology

  T. Diekhans, Rik W. De Donker, "A Dual-Side Controlled Inductive Power Transfer System Optimized for Large Coupling Factor Variations," in *Proc. ECCE USA*, 2014.

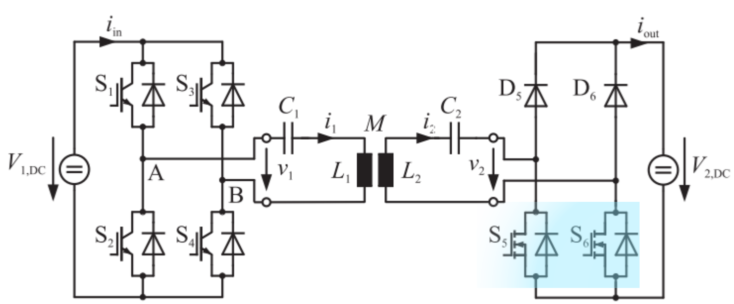

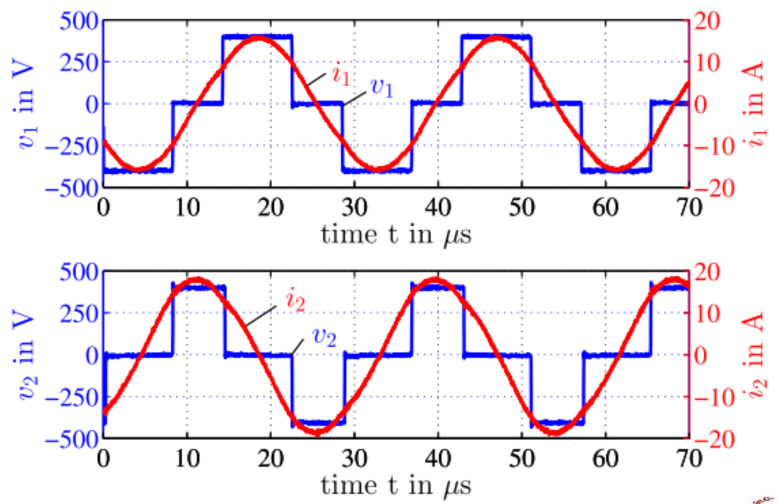

► Transmitter Electronics – Potential Solutions (1)

- **Receiver Voltage $U_{2,dc}$ used for Optimal Load Matching**
  → Power Regulation by Adjustment of $U_{1,dc}$ using Characteristic $P_2 = \frac{8}{\pi^2}\frac{U_{1,dc} \cdot U_{2,dc}}{\omega_0 k \sqrt{L_1 L_2}}$
- **1st Option:** **Cascaded AC/DC, DC/DC Conversion**

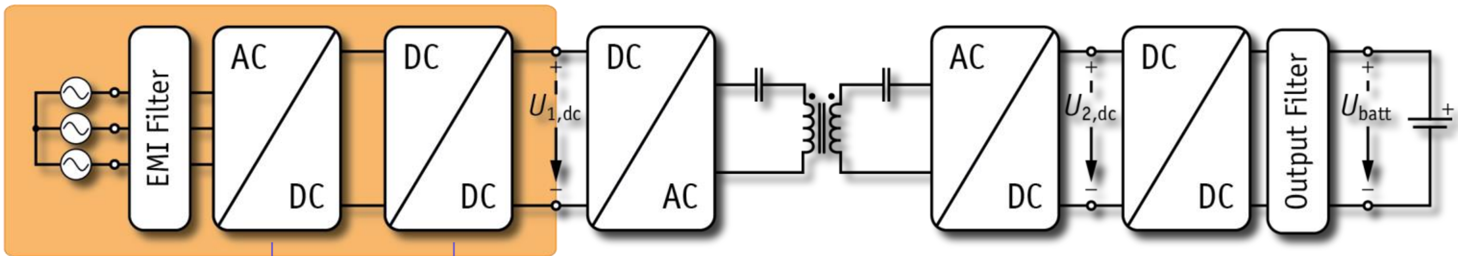

- **Transmitter-Side DC/DC Converter**
  - No Isolation Needed
  - Identical to Receiver-Side?

- **3-Phase Mains Interface (Boost-Type)**
  - Power Factor Correction of Phase Current
  - Standard Solutions Exist in Industry

▶ Transmitter Electronics – Potential Solutions (2)

- **Receiver Voltage $U_{2,dc}$ used for Optimal Load Matching**
  → Power Regulation by Adjustment of $U_{1,dc}$

- **2nd Option:** **Integrated Rectification and Voltage Controller**

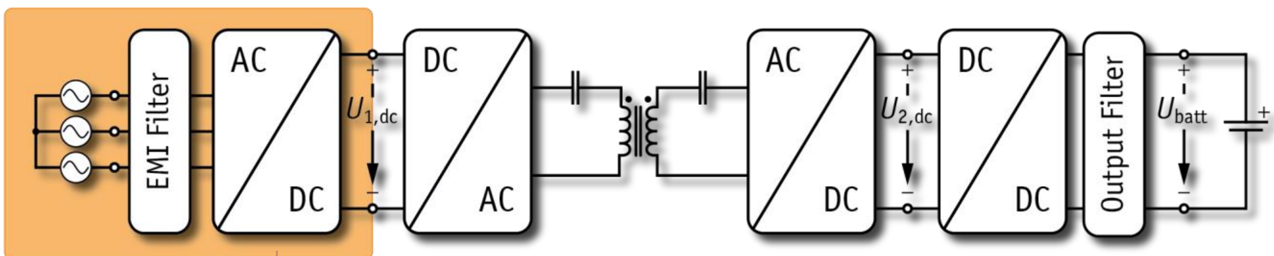

- **3-Phase Buck-Type Mains Interface**
  - Power Factor Correction of Phase Current
  - Regulated Output Voltage below Mains

Example Solution:
SWISS Rectifier

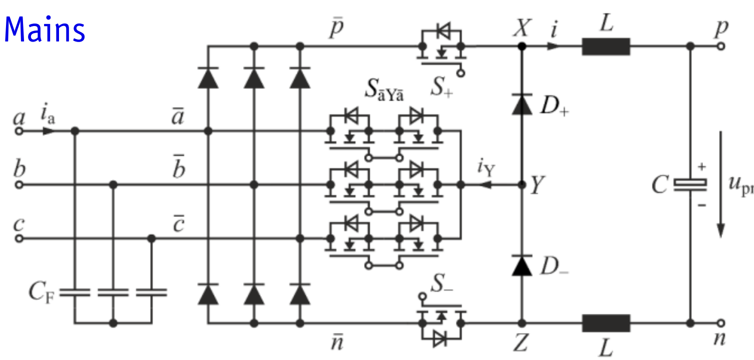

T. B. Soeiro, T. Friedli, J. W. Kolar, "SWISS Rectifier – A Novel 3-Phase Buck-Type PFC Topology for EV Battery Charging," in *Proc. APEC*, 2014.

► Alternative Control Concepts for Series Resonant Converters

■ **Degrees-of-Freedom for the Control**

- Inverter Switching Frequency
- Duty Cycle of Inverter Output Voltage
- DC-Link Voltage (with Front-End DC/DC Conv.)

■ **Common Control Concepts**

- I) Frequency Control @ Fixed Duty Cycle
- II) Duty Cycle Control @ Fixed Frequency
- III) Self-Oscillating/Dual Control
  (Combined Duty Cycle & Frequency Control)

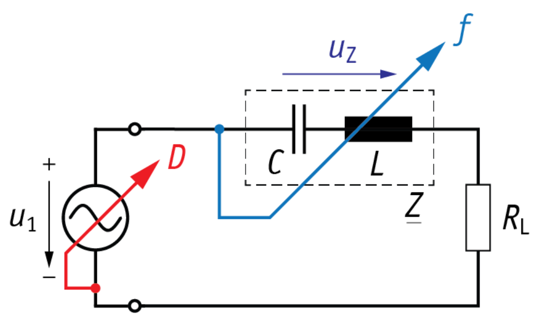

▲ **Switching above Resonance Causes Series Voltage Drop on $\underline{Z}$**

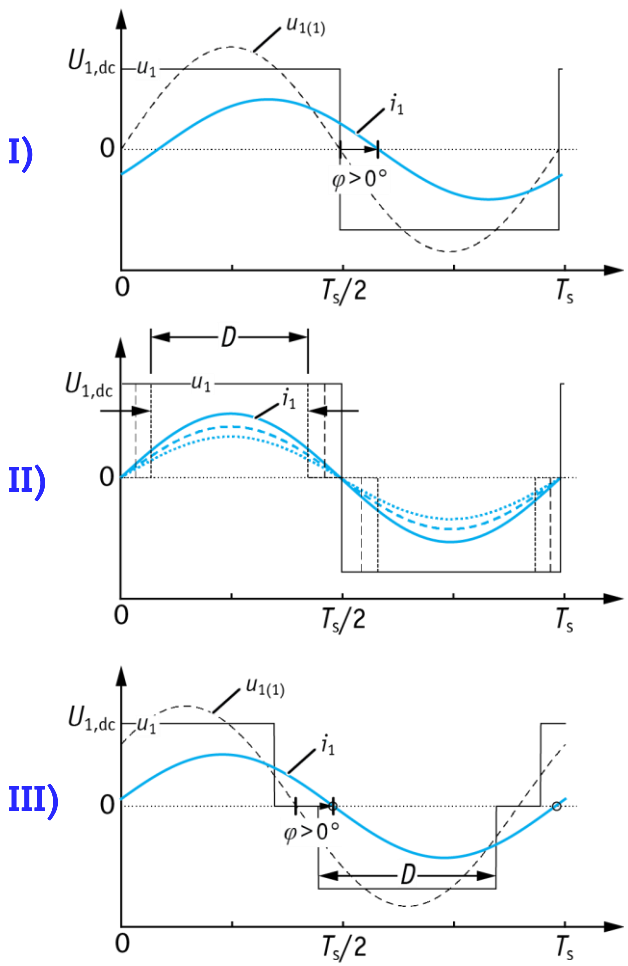

► Frequency Control @ Fixed Duty Cycle

- **Control of Inverter Switching Frequency**
  - Switching above Resonance Causes Voltage Drop on Series Impedance that can be Used to Control Transmitted Power

- **Main Disadvantage:**
  - Requires Additional Reactive Current in Transmitter due to Operation above Resonant Frequency
  - Operation at Efficiency Optimum Only at Maximum Output Power

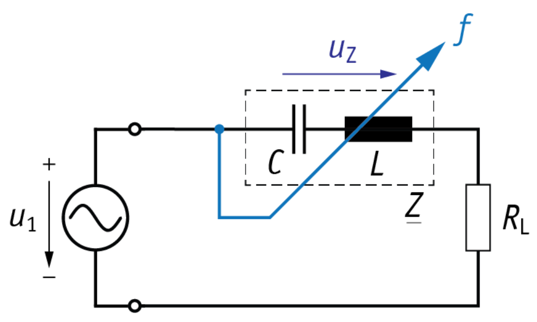

▲ Switching above Resonance Causes Series Voltage Drop on $\underline{Z}$

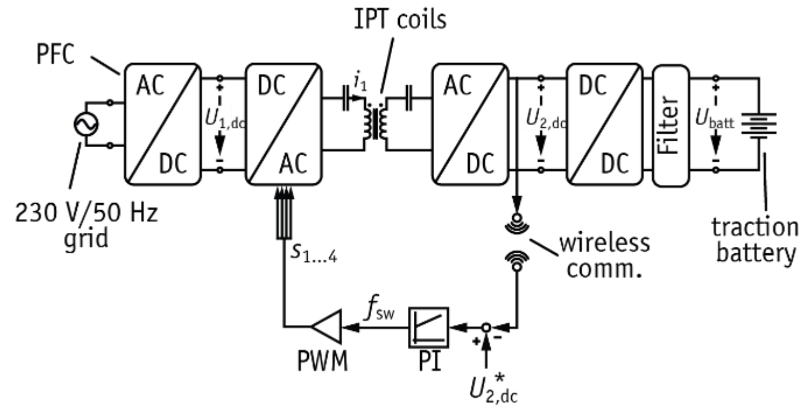

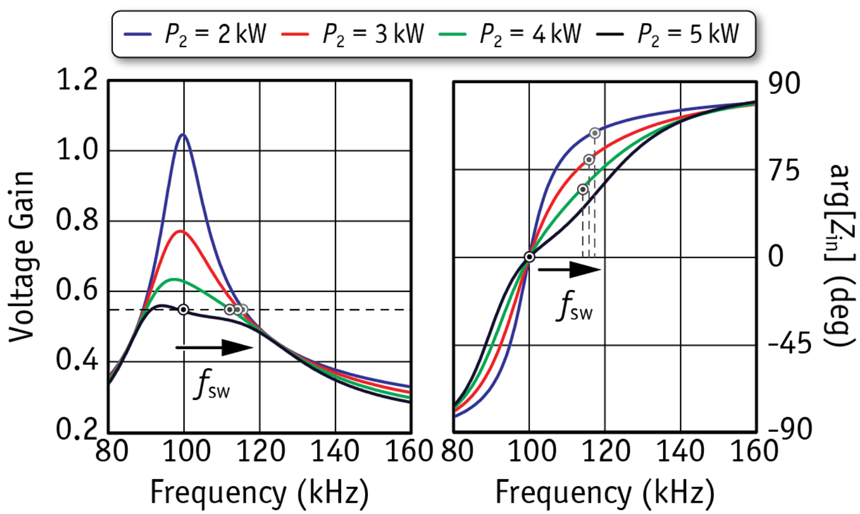

▲ Operating Points shown on Resonant Curves

J. A. Sabate, M. M. Jovanovic, F. C. Lee, and R. T. Gean, "Analysis and design-optimization of LCC resonant inverter for high-frequency AC distributed power system," in *IEEE Trans. Ind. Electron.*, vol. 42, no. 1, pp. 63–71, 1995.

► Self-Oscillating/Dual Control Method

■ Switching at Current Zero-Crossings

- Tracking Resonant Frequency Automatically
- Duty-Cycle is Modulated for Power Control
- Operation with ZVS with Small Phase-Shift α_{ZVS} between Zero-Crossings and Gate Sig.

■ Main Disadvantage:

- Requires Additional Reactive Current in Transmitter due to Operation above Resonant Frequency
- Operation at Efficiency Optimum Only at Maximum Output Power

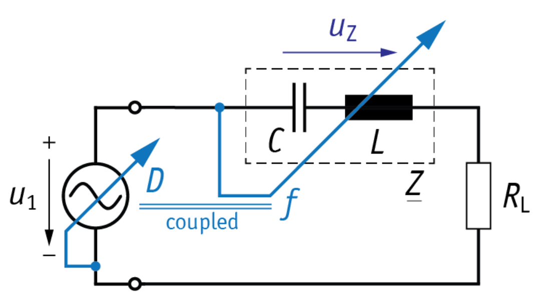

▲ Switching above Resonance Causes Series Voltage Drop on $\underline{Z}$

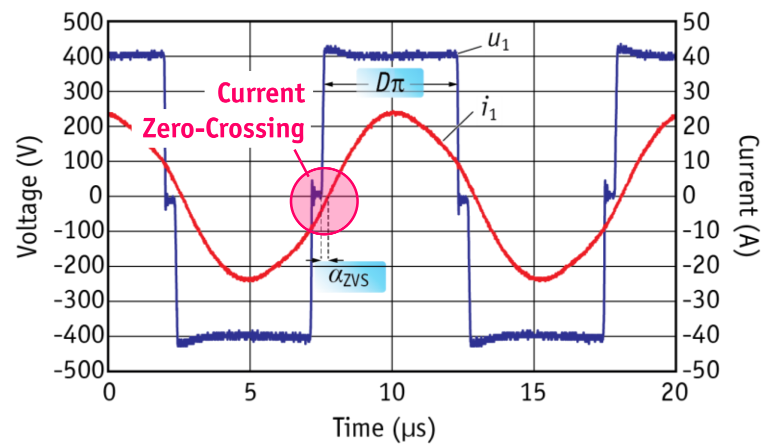

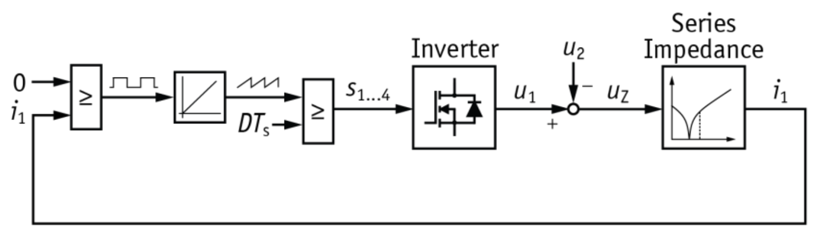

▲ Control Block Diagram and Measure Waveform

R. Bosshard, J. W. Kolar and B. Wunsch, "Control Method for Inductive Power Transfer with High Partial-Load Efficiency and Resonance Tracking," *IEEE IPEC/ECCE Asia*, 2014.

► Comparison of Control Methods (1)

- **Frequency Control Methods have (almost) Load-Independent Transmitter Current**

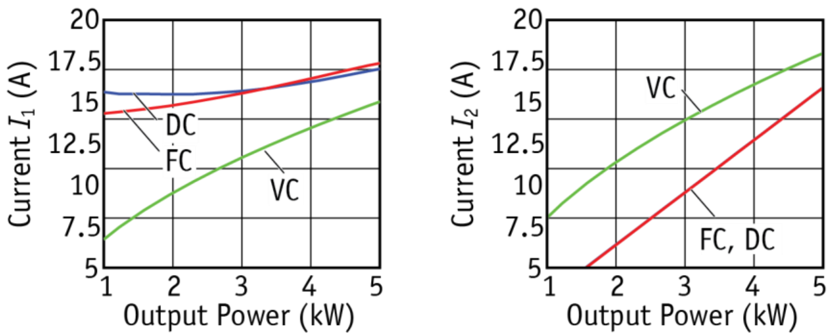

VC ... DC-Link Voltage Control
(Optimal Load Matching)
FC ... Frequency Control
DC ... Dual/Self-Osc. Control

- **Reduction in Transmitter Current I_1 Leads to Over-All Loss Reduction Despite Increased I_2 due to Lower $U_{2,dc}$**

- **Large Reduction of Power Losses in Partial-Load Condition with VC**
  - Reduced Transmitter-Coil RMS-Current
  - Decreasing instead of Constant I^2R Losses in Coils/Caps/Switches

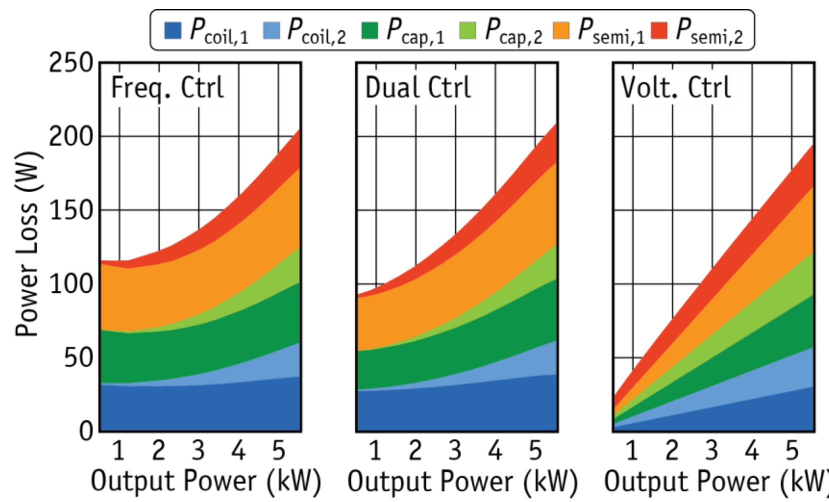

▲ **For 5 kW IPT Prototype Presented Later**

R. Bosshard, J. W. Kolar and B. Wunsch, "Control Method for Inductive Power Transfer with High Partial-Load Efficiency and Resonance Tracking," *IEEE IPEC/ECCE Asia*, 2014.

▶ Measured Efficiency for DC-Link Voltage Control

- **Large Reduction of Power Losses in Partial-Load Condition with Controlled DC-Link Voltages (= Optimal Load Matching)**
  - Reduced Transmitter-Coil RMS-Current:
    Decreasing instead of Constant I^2R Losses in Coils/Caps/Switches

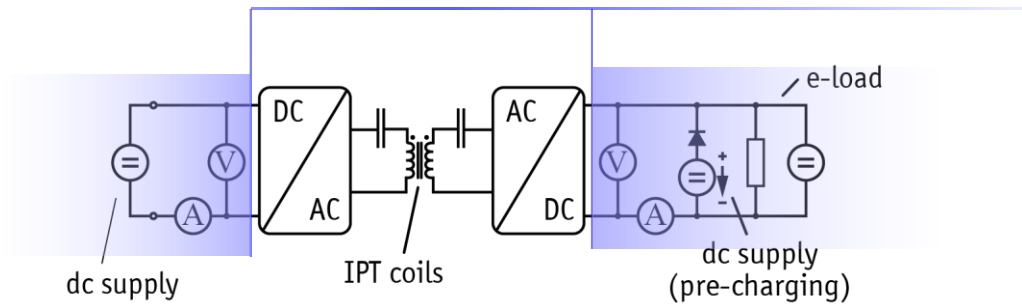

▲ **Efficiency Measurement Setup**

▲ **Yokogawa WT3000**

- **Extremely Flat Efficiency Curve Even at Low Output Power thanks to Operating Constantly at Optimal Conditions**

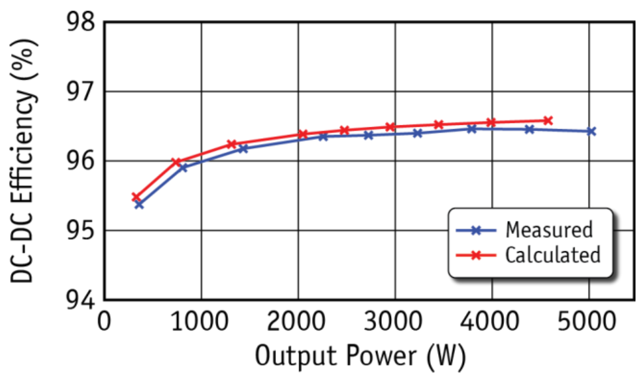

▲ **For 5 kW IPT Prototype (Shown in Later Sect.)**

Components Modeling & Multi-Objective System Optimization

► Multi-Objective System Optimization (1)

■ Mapping of Design Space into System Performance Space
- Requires Accurate Models for the Main System Components
- Allows Sensitivity & Trade-Off Analysis

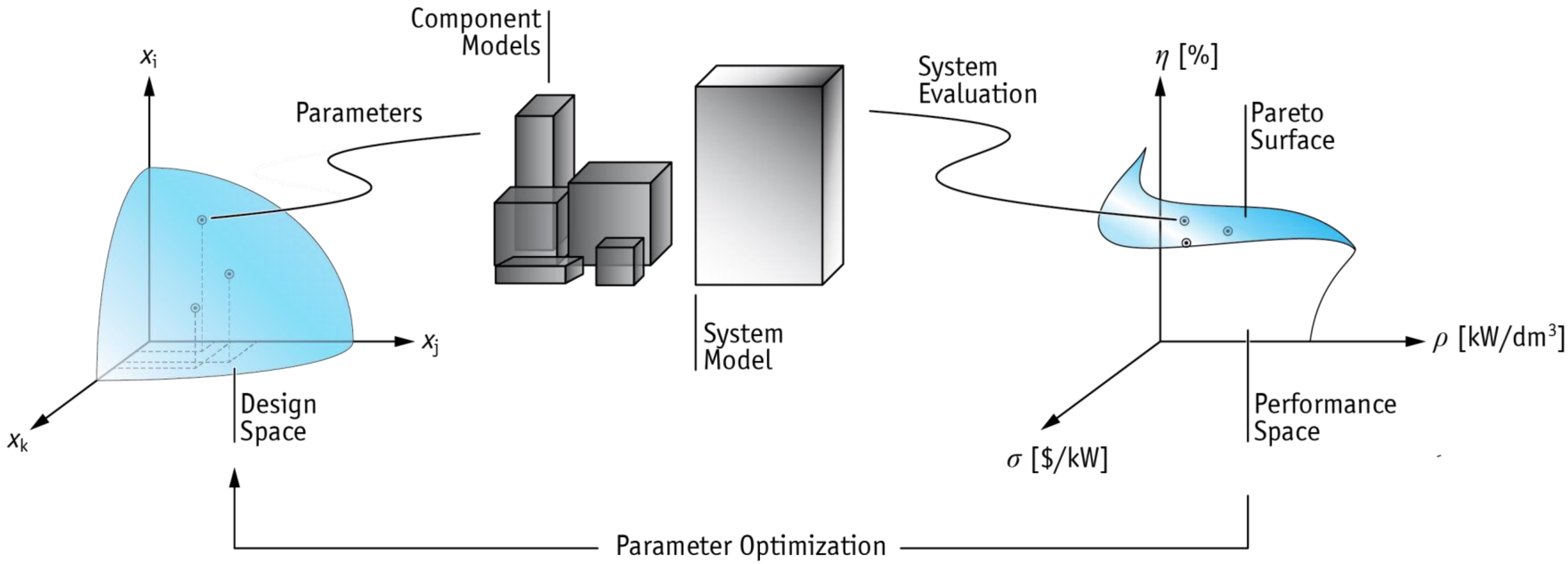

- Coil Dimensions
- Winding Scheme
- Number of Turns
- Litz Wire Design
- Core Design
- Core Material

- AC-Losses
- Magnetic Fields
- Capacitor Losses
- Converter Losses
- Component Cost
- Component Size

- Efficiency $\eta = P_{out}/P_{in}$ [%]
- Power Density $\rho = P_{out}/V_{tot}$ [kW/dm^3]
- Stray Field $\beta = B_{max}/B_{norm}$ [%]
- Pos. Tolerance $\delta = \Delta x/D_{coil}$ [%]
- Specific Cost $\sigma = C_{tot}/P_{out}$ [$/kW]
- Material Effort $\gamma = kg_{Cu/Fe}/P_{out}$ [kg/kW]

► Multi-Objective System Optimization (2)

- **Clarifies Influence of Main Components and Operating Parameters on System Performance**
  - Analysis of Physical Performance Limits → Pareto Front
  - Trade-Off between Efficiency and Power Density

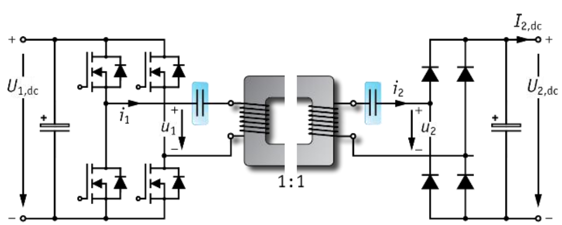

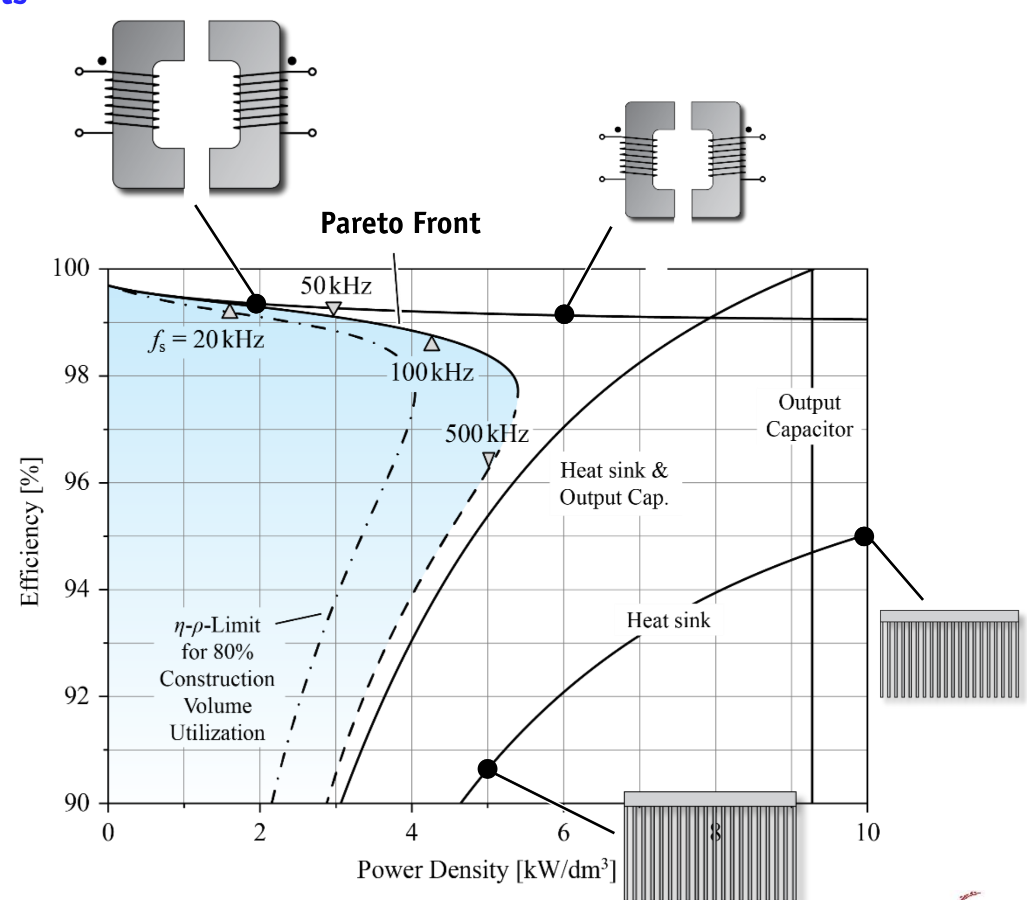

System Components and Design Considerations

Coil Modeling
Resonant Capacitors
Magnetic Shielding

▶ Main System Components (1)

■ **IPT Transmission Coils**
- Magnetic Design using FEM
- Shielding of Stray Field

■ **Receiver-Side Power Electronics**
- Synchronous Rectification
- Battery Current Regulation

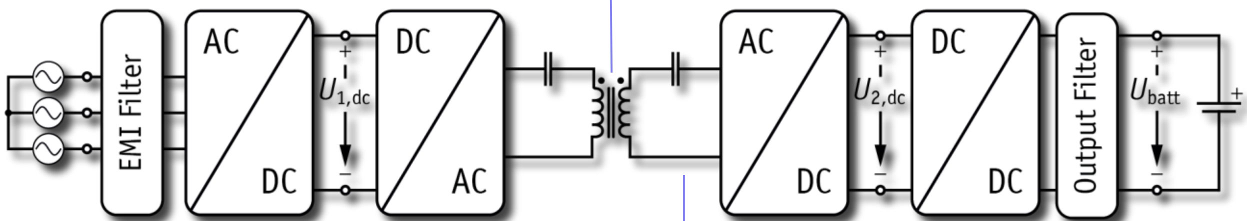

■ **Transmitter-Side Power Electronics**
- 1/3-Φ Mains Interface
- High-Frequency Inverter Stage

■ **Resonant Compensation**
- Requirements for Capacitor
- Optimal Component Selection

▶ Main System Components (2)

■ **IPT Transmission Coils**
- Magnetic Design using FEM
- Shielding of Stray Field

■ **Receiver-Side Power Electronics**
- Synchronous Rectification
- Battery Current Regulation

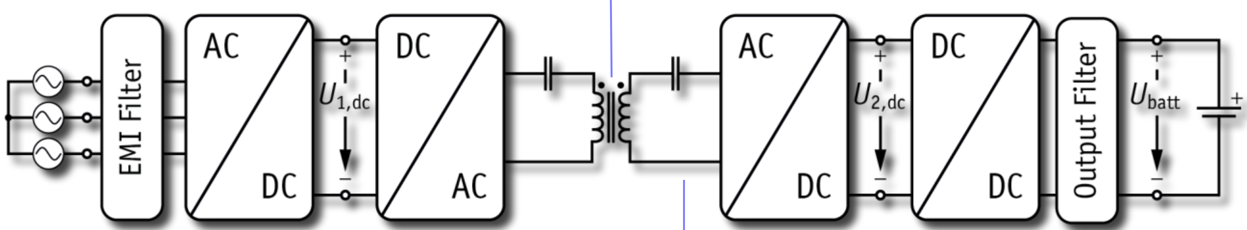

■ **Transmitter-Side Power Electronics**
- 1/3-Φ Mains Interface
- High-Frequency Inverter Stage

■ **Resonant Compensation**
- Requirements for Capacitor
- Optimal Component Selection

Transmission Coil:
Coil Geometry Options

► Structures of Single-Phase Transformers

■ Common Transformer Shapes: E- and U-Type

- One or Two Closed Paths for Core-Flux
- Available Ferrite Parts: E-/U-/Pot-/Toroid-Cores

▲ **Available Ferrite Parts for Power Transformers**
Huigao Megnetics, www.huigao-magnetics.com (18.11.2014).

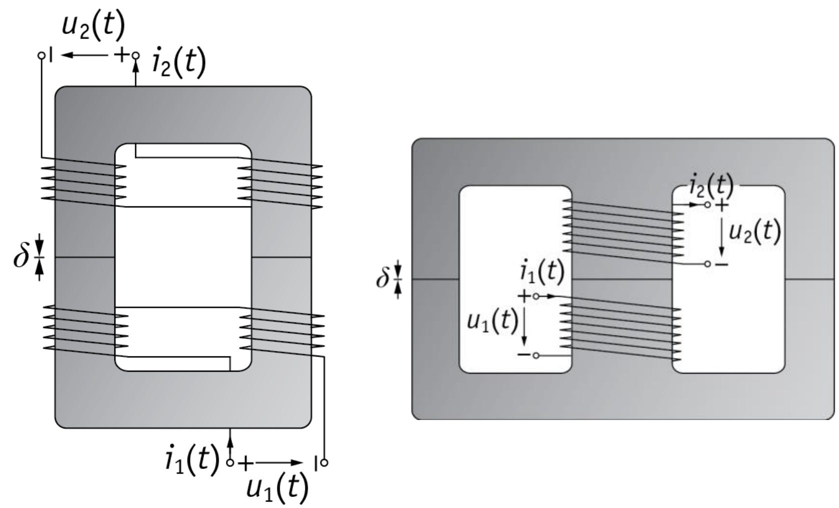

▲ **Common Transformer Structures**

▶ Classification of IPT Coil Geometries (1)

E-Type IPT Coils

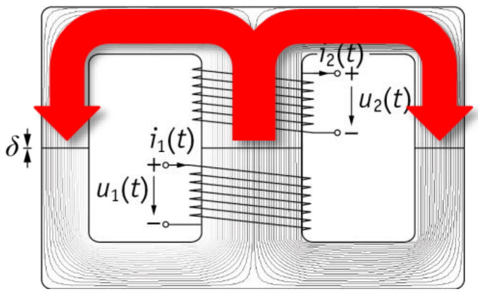

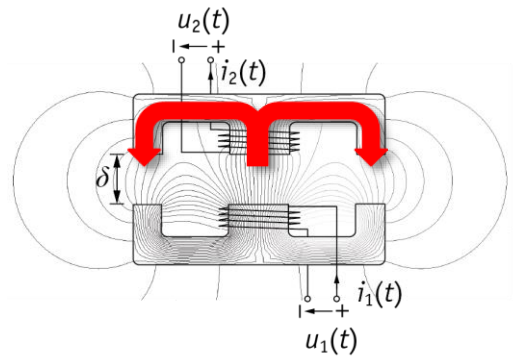

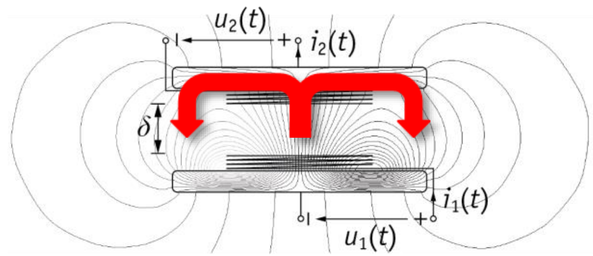

- **E-Core Transformer**
  - Flux Divided to Two Equal Loops
  - 2x Thickness for Central Leg
- **E-Type IPT Coil**
  - Flux Divided to Two Equal Loops
  - Max. Coupling for Certain Ratio of Core Size Compared to Winding Diam.

▶ Classification of IPT Coil Geometries (2)

U-Type IPT Coils

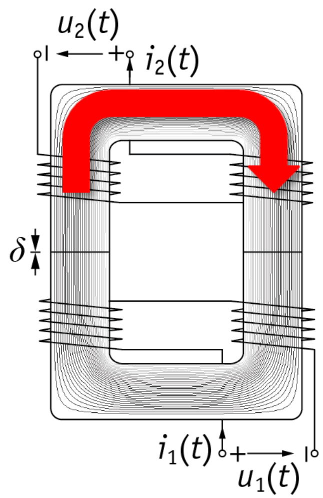

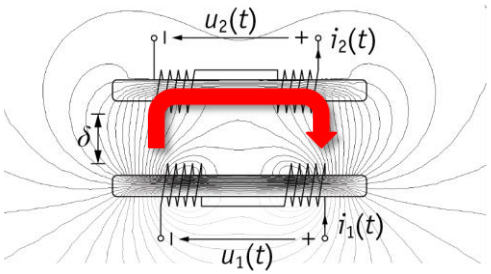

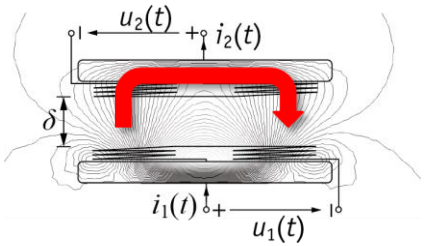

- **U-Core Transformer**
  - Flux on Single Loop
- **U-Type IPT Coil**
  - Single Loop formed by two Windings

► Literature: Realized Example Prototypes

■ E-Type IPT Coils

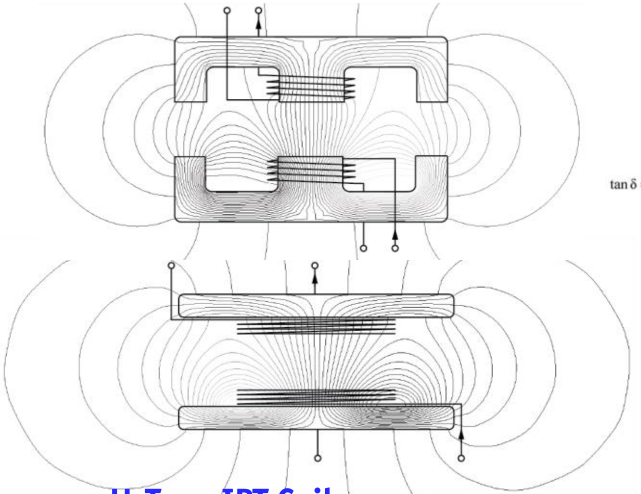

J. Kim et al. (KAIST), 2014.

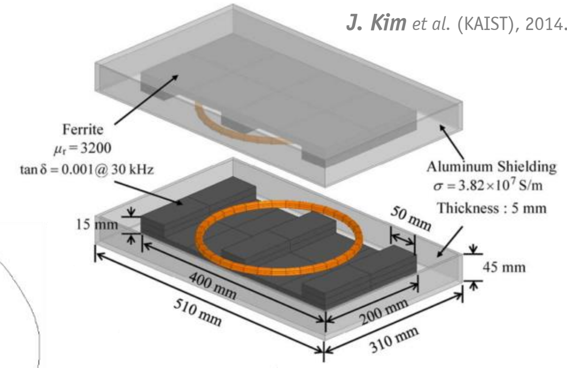

S. Reichert et al. (Fraunhofer ISE), 2013.

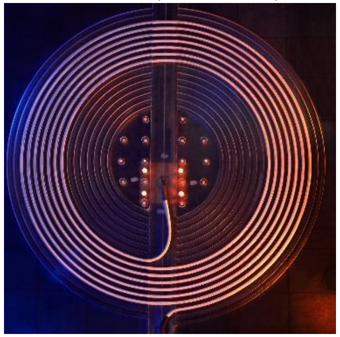

■ U-Type IPT Coils

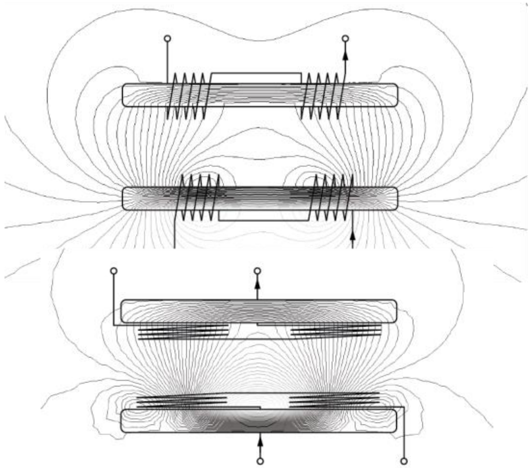

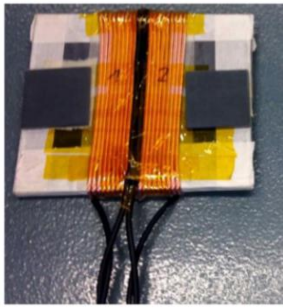

F. Turki et al., PCIM Europe, 2014.

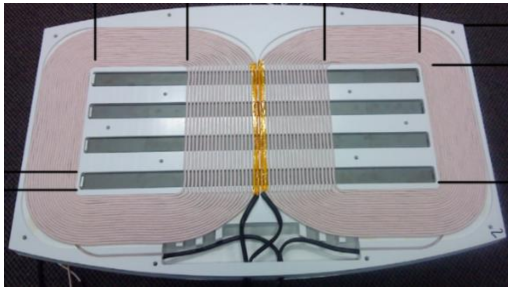

C.-Y. Huang, M. Budhia, G. Covic, T. Boys, 2011-2013.

► Coil Geometry Optimization (1)

■ **Conceptual Analysis with Reluctance Model**

J. Kim et al. (KAIST), 2014.

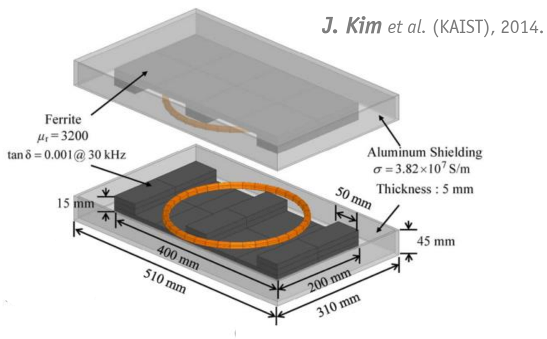

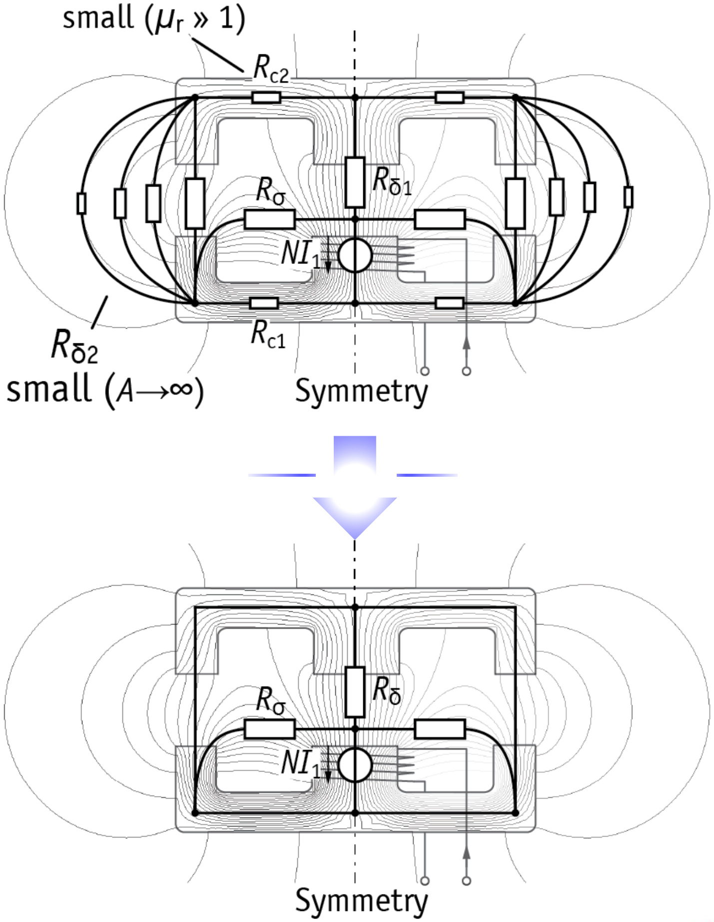

■ **Maximize Figure-of-Merit *kQ*:**

$$k = \frac{\psi_h}{\psi_\sigma + \psi_h} \propto \frac{R_\sigma}{R_\delta + R_\sigma}$$

■ **Approximations:**

- Core Reluctance Small (high Permeability)
- Only Air Gap in Central Leg Considered,
  Side Legs have small Reluctance (large Area)

▶ Coil Geometry Optimization (2)

■ Conceptual Analysis with Reluctance Model

J. Kim et al. (KAIST), 2014.

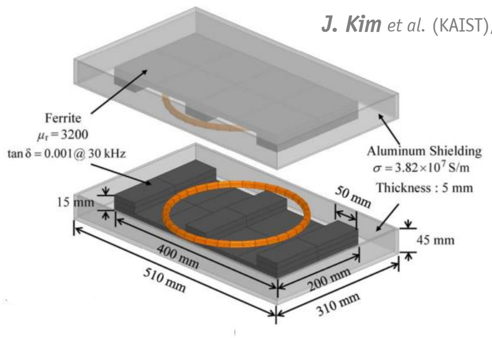

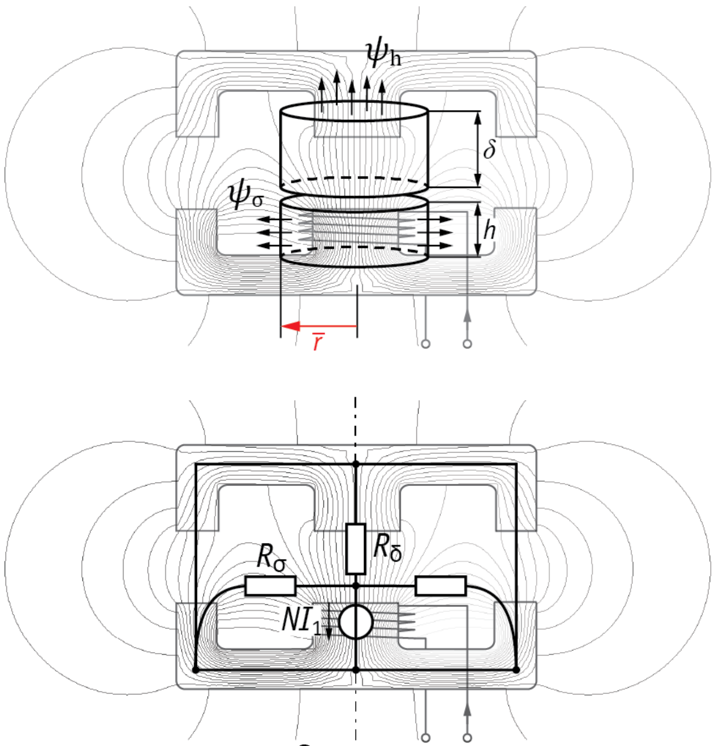

■ Maximize Figure-of-Merit *kQ:*

$$k = \frac{\psi_h}{\psi_\sigma + \psi_h} \propto \frac{R_\sigma}{R_\delta + R_\sigma}$$

■ Reluctance: Approximate Scaling Law

$$R_\sigma \approx \frac{\bar{r}}{\mu_0 \cdot 2\pi\bar{r}h} \approx \text{const.}$$

$$R_\delta \approx \frac{\delta}{\mu_0 A_c} \propto \frac{\delta}{\mu_0 \bar{r}^2}$$

▶ Coil Geometry Optimization (3)

■ **Conceptual Analysis with Reluctance Model**

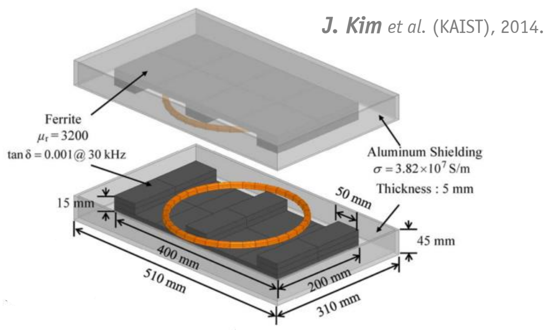

■ **Maximize Figure-of-Merit *kQ*:**

$$k = \frac{\psi_h}{\psi_\sigma + \psi_h} \propto \frac{R_\sigma}{R_\delta + R_\sigma}$$

■ **Reluctance: Approximate Scaling Law**

$$R_\sigma \approx \frac{\bar{r}}{\mu_0 \cdot 2\pi\bar{r}h} \approx \text{const.}$$

$$R_\delta \approx \frac{\delta}{\mu_0 A_c} \propto \frac{\delta}{\mu_0 \bar{r}^2}$$

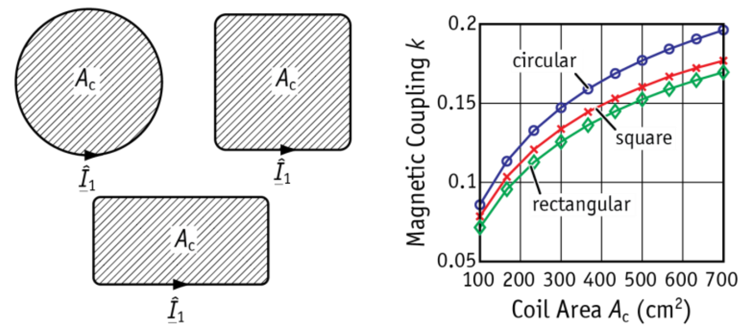

▲ **FEM-Calculated Coupling for Three Exemplary Coil Geometries**

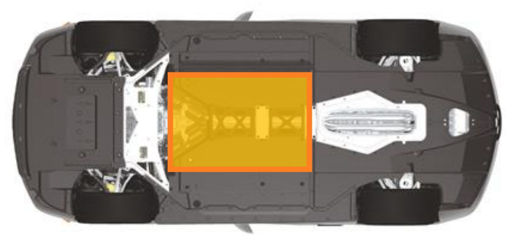

→ **Maximize Coil Area for High Coupling!**
→ Fully Utilize Available Construction Volume
→ Best Choice for Geometry is Application Specific!

► Fair Comparison of IPT Coil Geometries

■ Performance Indicators for IPT Coils

- Efficiency $\eta = P_{out}/P_{in}$ [%]
- Power Density $\alpha = P_{out}/A_{coil}$ [kW/dm²]
- Stray Field $\beta = B_{max}/B_{norm}$ [%]
- Tolerance $\delta = \Delta x/D_{coil}$ [%]
- Specific Cost $\gamma = C_{tot}/P_{out}$ [$/kW]
- Material Effort $\sigma = kg_{Cu/Fe}/P_{out}$ [kg/kW]

Note: Coupling is Indicative for Efficiency, but does not cover all Loss Components, e.g. Core Losses or Eddy Current Losses.

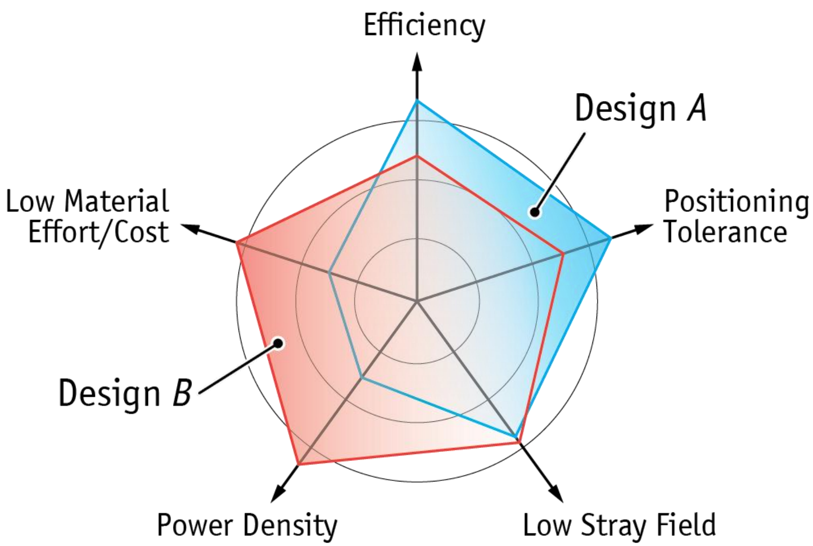

▲ Performance Comparison of two IPT Coil Designs

■ Aspects for a Fair Comparison

- Consider all, not just single Criteria
- Equal Electrical Interfaces
- Designs Optimized for Same Goals with Equal Boundary Conditions

Designed IPT Demonstrator Systems

▶ Demonstrator Systems: 5 and 50 kW Output Power (1)

■ **5 kW System for Model Development**
- Output Power 5 kW @ 400 V, 100 kHz with Forced-Air Cooling
- Lab-Scale Coil and Converter Size (210 mm Diameter / 50 mm Air Gap)
- Basic Geometry for Simplified Modeling
- Verification of Calculation & Optimization

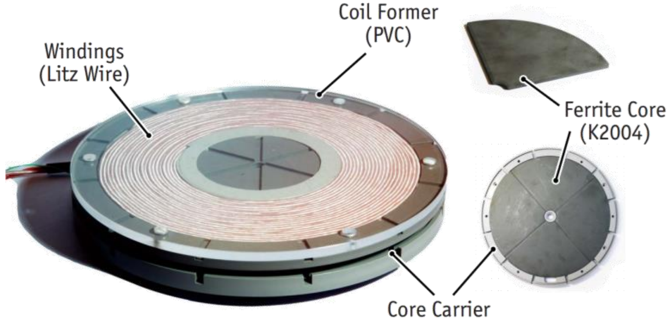

R. Bosshard, J. W. Kolar, J. Mühlethaler, I. Stevanovic, B. Wunsch, F. Canales, "Modeling and η-α-Pareto optimization of inductive power transfer coils for electric vehicles," *IEEE J. Emerg. Sel. Topics Power Electron.*, vol. 3, no. 1., pp.50-64, March 2015.

■ **50 kW Prototype System for EV Specs**
- Output Power 50 kW @ 800 V, 85 kHz with Forced-Air Cooling
- Optimized Geometry for EV Charging (450 x 750 x 60 mm, 25 kg)
- Experimental Verification

▶ Demonstrator Systems: 5 and 50 kW Output Power (2)

■ 5 kW System for Model Development
- Output Power 5 kW @ 400 V, 100 kHz with Forced-Air Cooling
- Lab-Scale Coil and Converter Size (210 mm Diameter / 50 mm Air Gap)
- Basic Geometry for Simplified Modeling
- Verification of Calculation & Optimization

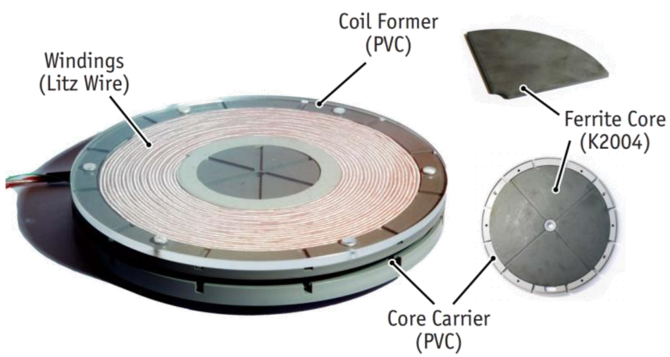

R. Bosshard, J. W. Kolar, J. Mühlethaler, I. Stevanovic, B. Wunsch, F. Canales, "Modeling and η-α-Pareto optimization of inductive power transfer coils for electric vehicles," *IEEE J. Emerg. Sel. Topics Power Electron.*, vol. 3, no. 1., pp.50-64, March 2015.

■ 50 kW Prototype System for EV Specs
- Output Power 50 kW @ 800 V, 85 kHz with Forced-Air Cooling
- Optimized Geometry for EV Charging (450 x 750 x 60 mm, 25 kg)
- Experimental Verification

Coil Modeling: High-Frequency Winding Losses

J. Mühlethaler, "Modeling and multi-objective optimization of inductive power components," Ph.D. dissertation, Swiss Federal Institute of Technology (ETH) Zurich, 2012.

► Winding Loss Calculation – Skin Effect

■ Frequency Dependent Current Distribution in Single Solid Conductor

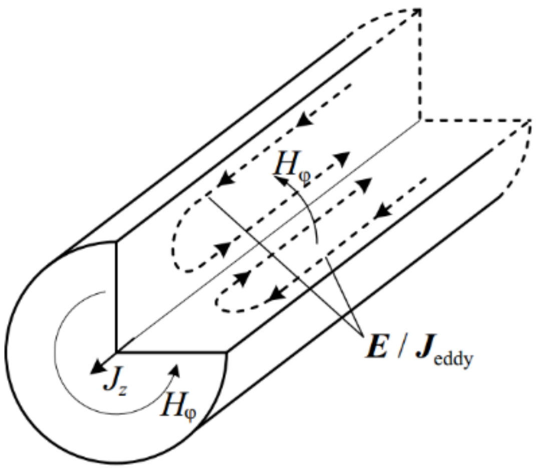

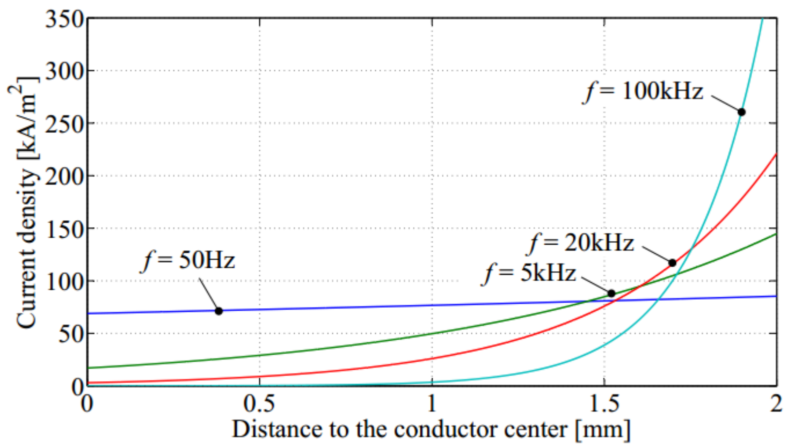

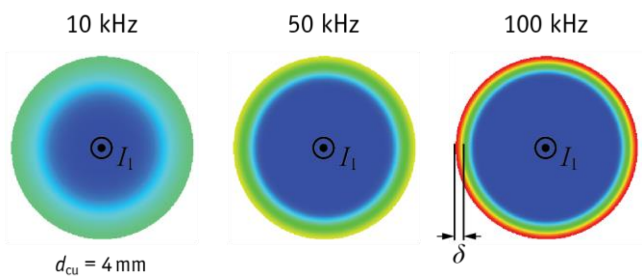

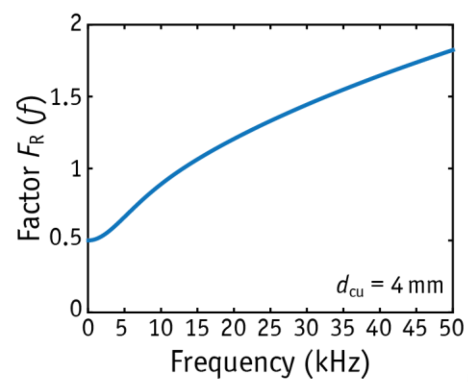

$$P_{\mathrm{skin}} = F_{\mathrm{R}}(f) \cdot R_{\mathrm{DC}} \cdot \hat{I}^2$$

J. **Mühlethaler,** "Modeling and multi-objective optimization of inductive power components," Ph.D. dissertation, Swiss Federal Institute of Technology (ETH) Zurich, 2012.

▶ Winding Loss Calculation – Proximity Effect

■ Frequency Dependent Current Distribution in Neighboring Solid Conductors

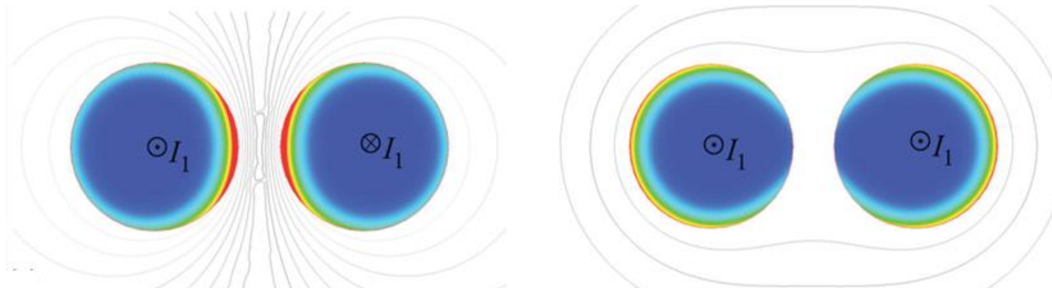

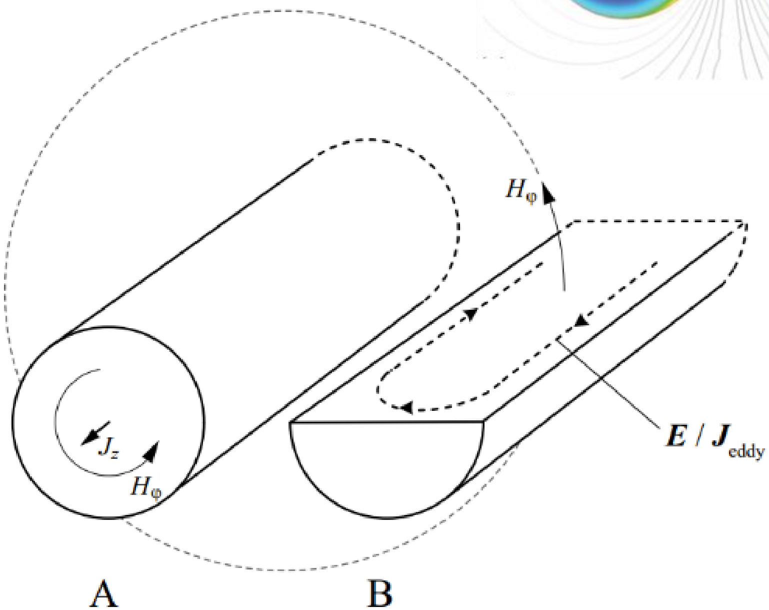

$$P_{\mathrm{prox}} = G_{\mathrm{R}}(f) \cdot R_{\mathrm{DC}} \cdot \hat{H}_e^2$$

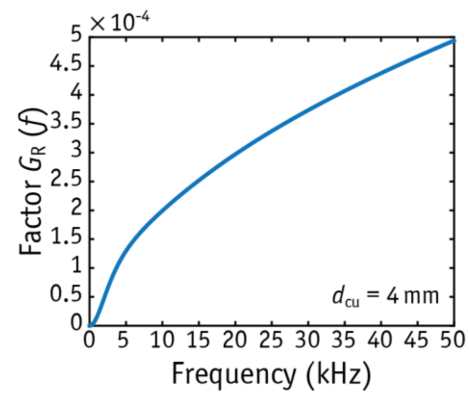

J. Mühlethaler, "Modeling and multi-objective optimization of inductive power components," Ph.D. dissertation, Swiss Federal Institute of Technology (ETH) Zurich, 2012.

▶ Winding Loss Calculation in Litz Wires

- **Calculate Winding Losses in Litz Wire with n Strands, Strand-Diameter d_i & Outer Diameter d_a**
  - Skin-Effect Calculated for each Strand Individually and Summed up

$$P_{\text{skin}} = n \cdot F_R(f) \cdot R_{DC} \cdot \left(\frac{\hat{I}}{n}\right)^2$$

n ... Number of Strands
R_{dc} ... Strand DC-Resistance
d_i ... Strand Diameter
d_a ... Outer Wire Diameter

- **For Proximity-Effect Bundle-Level Effects must be Included**
  - Internal Proximity ... Effect of Currents in other Strands
  - External Proximity ... Effect of External Magnetic Field (e.g. due to Air Gap)

$$P_{\text{prox}} = \underbrace{n \cdot G_R(f) \cdot R_{DC} \cdot \hat{H}_e^2}_{\text{External Proximity}} + \underbrace{n \cdot G_R(f) \cdot R_{DC} \cdot \left(\frac{\hat{I}}{\sqrt{2}\pi d_a}\right)^2}_{\text{Internal Proximity}}$$

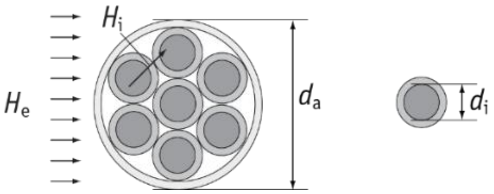

J. Mühlethaler, "Modeling and multi-objective optimization of inductive power components," Ph.D. dissertation, Swiss Federal Institute of Technology (ETH) Zurich, 2012.

► Comparison: Solid Wire vs. Litz Wire

- **Power Loss per 1 m of Solid or Litz Wire at $\hat{I}$ = 1 A with H_{ext} = 0 A/m**
  - Only Internal Proximity Effect (no External Field)

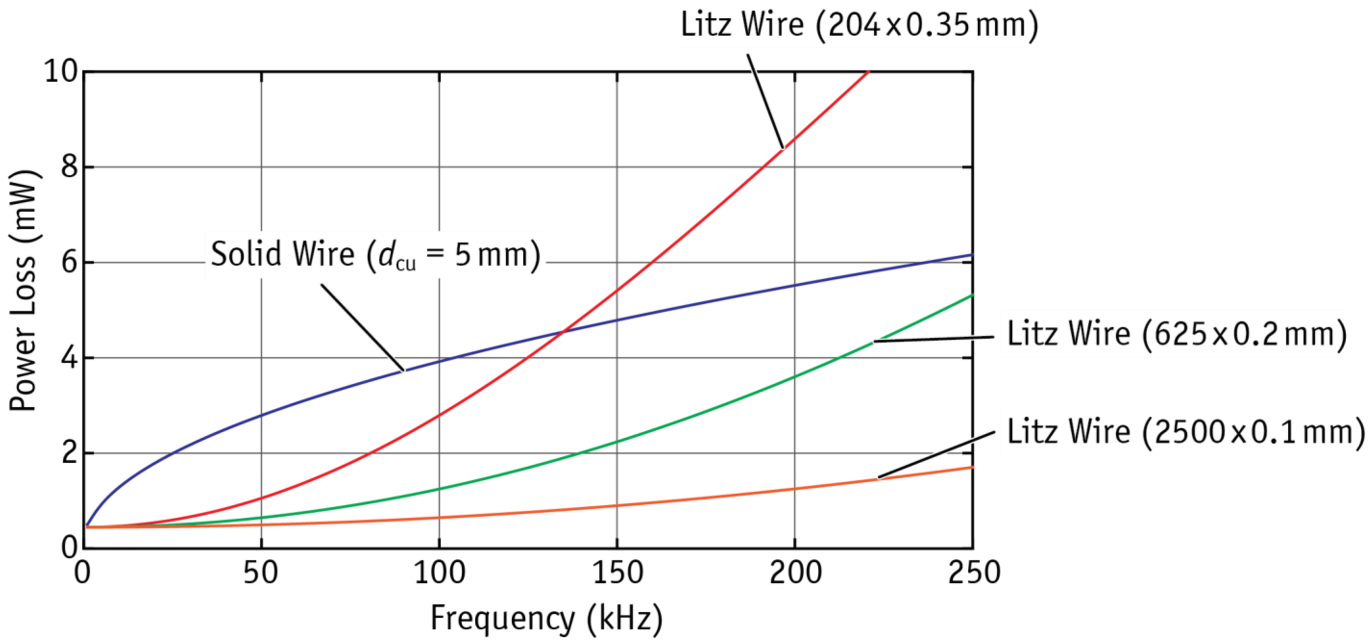

- **If Litz Wire is Operated far from "intended" Operating Frequency, Solid Wire can become Better Option due to Internal Proximity Effect in Litz Wire Bundles**

▶ Example 1: Standard Transformer Winding Losses

■ Power Loss Calculation for Transformer with Litz Wire Windings

- External Magnetic Field (Simplified):

$$|H_{\mathrm{e,RMS}}| \approx \begin{cases} \dfrac{N_\mathrm{p} I_\mathrm{p,RMS}}{b_\mathrm{c}} \cdot \dfrac{k_\mathrm{p} - 1/2}{k_\mathrm{p,max}} & \ldots \text{ primary side: } k_\mathrm{p} = 1, 2, 3 \\ \dfrac{N_\mathrm{s} I_\mathrm{s,RMS}}{b_\mathrm{c}} \cdot \dfrac{k_\mathrm{s} - 1/2}{k_\mathrm{s,max}} & \ldots \text{ secondary side: } k_\mathrm{s} = 1, 2 \end{cases}$$

$$\oint H_e \mathrm{d}l = NI$$

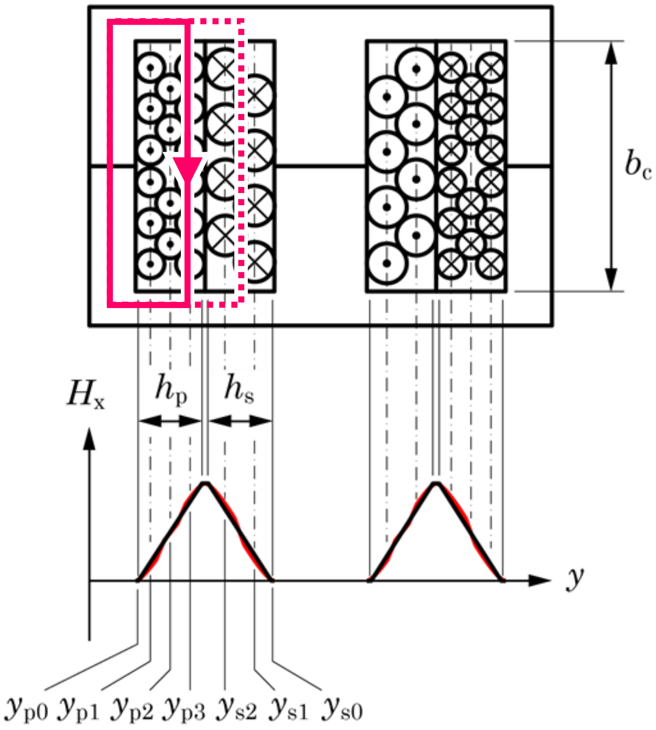

- AC-Resistance of Single Turn of Primary Winding:

$$R_{\mathrm{AC,turn}}(k) = \frac{R_\mathrm{DC}}{N} \cdot \left[2F_\mathrm{R} + 2G_\mathrm{R} \cdot \left(\frac{N}{b_\mathrm{c}} \cdot \frac{2k-1}{2k_\mathrm{max}} \right)^2 \right]$$

$$R_\mathrm{DC} \approx \frac{4Nl_\mathrm{avg}}{\sigma \pi d_\mathrm{Cu}^2}$$

- Equations for F_R and G_R from Literature, e.g.:

  J. Mühlethaler, "Modeling and multi-objective optimization of inductive power components," Ph.D. dissertation, Swiss Federal Institute of Technology (ETH) Zurich, 2012.

► Example 2: FEM-Based Loss Model of *5 kW* Prototype

- **Analytical Field-Calculation not Possible**
  - Core Material / (Asymmetric Geometry)
- **Calculation with Finite Element Method**
  - Extraction of *H*-Fields for Proximity Loss Calculation in Litz Wire

▲ **5 kW Prototype IPT Coil**

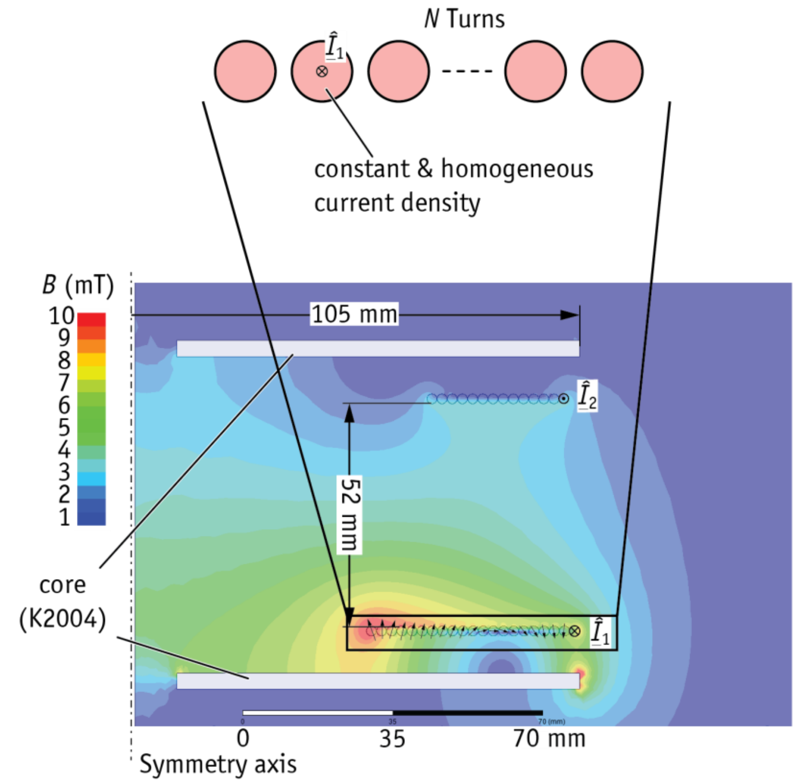

R. Bosshard, J. W. Kolar, J. Mühlethaler, I. Stevanovic, B. Wunsch, F. Canales, "Modeling and η-α-Pareto optimization of inductive power transfer coils for electric vehicles," *IEEE J. Emerg. Sel. Topics Power Electron.*, vol. 3, no. 1., pp.50-64, March 2015.

- **2D-Finite Element Solvers:**
  - FEMM (free, www.femm.info)
  - Ansys Maxwell, COMSOL, …

▶ Fundamental Frequency Model

- **Resonant Tank: Highly Selective Bandpass Characteristic**
  - Filtering Effect on Rectangular Switched Voltage
  - Almost Sinusoidal Currents in Transmission Coils

- **Fundamental Frequency Model Sufficient**
  - Frequency Domain FEM
  - Simplified Analytical Calculations

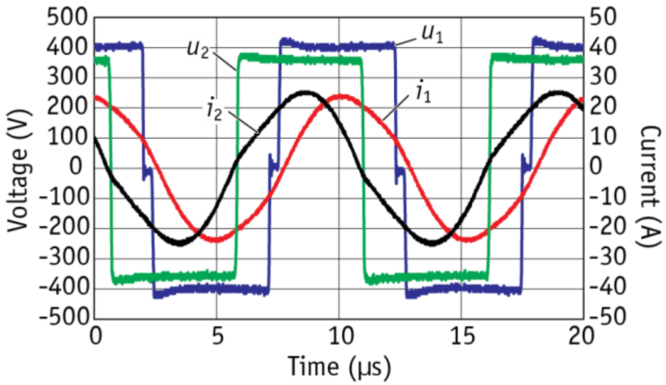

▲ Measured voltage and current waveforms at 5 kW

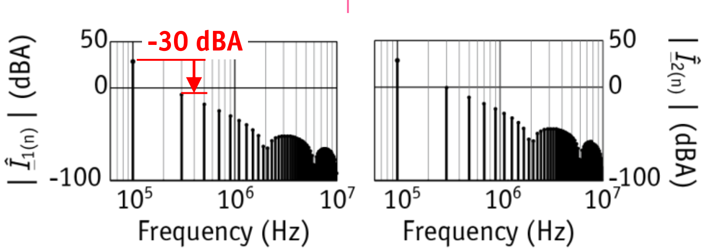

▲ Calculated spectra of the coil currents

▶ High-Frequency Copper Losses in Litz Wire

■ Skin-Effect Calculated Analytically (as for Transformer)

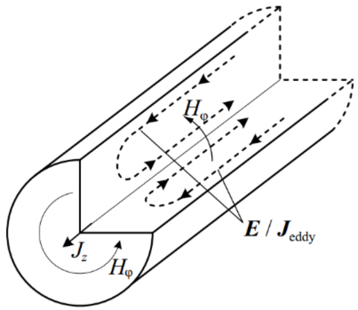

$$P_{\text{skin}} = n \cdot F_{\mathrm{R}}(f) \cdot R_{\mathrm{DC}} \cdot \left(\frac{\hat{I}}{n}\right)^2$$

n ... Number of Strands
R_{dc} ... Strand DC-Resistance
d_{i} ... Strand Diameter
d_{a} ... Outer Wire Diameter

■ Proximity-Effect Calculation with External Magnetic Field from FEM Results

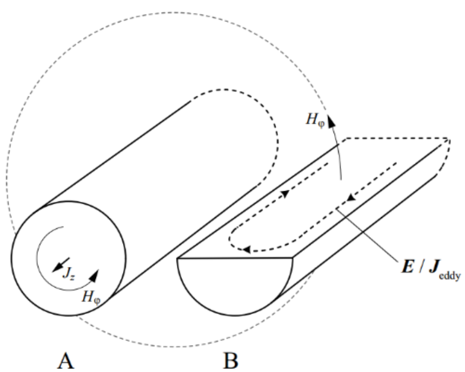

■ **Extracted from FEM Results**
- Evaluation in Center-Point of Each Turn to Isolate External Field

$$P_{\text{prox}} = \underbrace{n \cdot G_{\mathrm{R}}(f) \cdot R_{\mathrm{DC}} \cdot \hat{H}_{\mathrm{e}}^2}_{\text{External Proximity}} + \underbrace{n \cdot G_{\mathrm{R}}(f) \cdot R_{\mathrm{DC}} \cdot \left(\frac{\hat{I}}{\sqrt{2}\pi d_{\mathrm{a}}}\right)^2}_{\text{Internal Proximity}}$$

► Example 3: Analytical Loss Model of *50 kW* Prototype

- **3D Coil Design w/o Symmetry**
  - Resolution of Winding Details not Possible due to Long Simulation Time of 3D-FEM
  - Winding Modeled as Rectangular Box to Reduce Complexity of Geometry

- ***H*-Field Inside Conductors is Not Available Anymore!**

$$P_{\mathrm{prox,ext}} = n \cdot G_{\mathrm{R}}(f) \cdot R_{\mathrm{DC}} \cdot \hat{H}_{\mathrm{e}}^{2}$$

Unknown!

- **Field Calculations Outside Box Still Accurate for Core Loss & Stray Field**

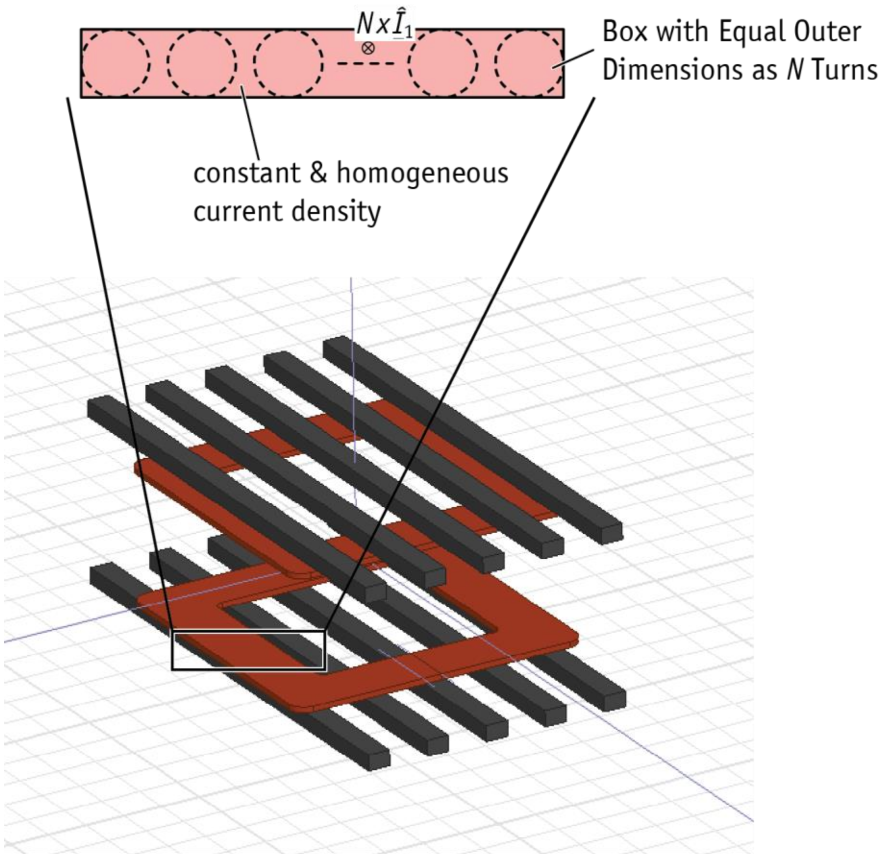

▲ **3D-FEM Model of Tx and Rx Coil**

► Measurement of Inductance & Coupling

- **Verification of Inductance Calculation**
  - Excitation with Linear Amplifier (6 A_{pk}, 85 kHz)
  - Inductance Measured with Power Analyzer and with Impedance Analyzer
  - Induced Voltage Measured with Diff. Probe

- **Measured: L_1 = 66.3 uH, k = 0.230**
- **Calculated: L_1 = 67.6 uH, k = 0.233**

→ High Accuracy Despite Simplifications!

▲ **Yokogawa WT3000**

▲ **50 kW Prototype IPT Coil**

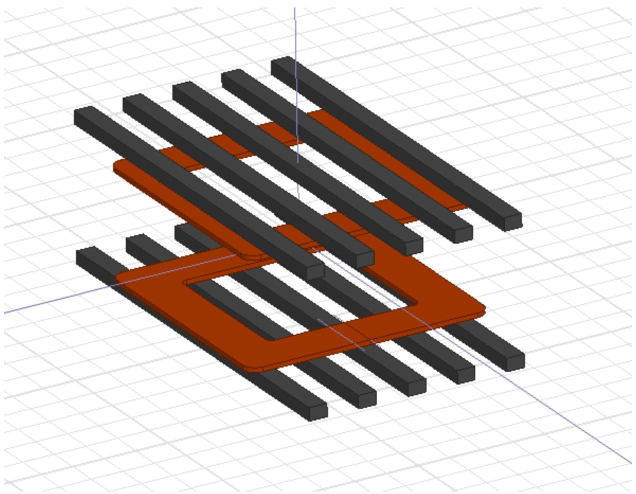

▲ **3D-FEM Model of Tx and Rx Coil**

▶ Estimation of Proximity Effect (1)

■ ***H*-Field Inside Conductors is Needed to Estimate Proximity Effect**
- Not Available if Winding Modeled as "Box" instead of Individual Wires

$$P_{\mathrm{prox,ext}} = n \cdot G_{\mathrm{R}}(f) \cdot R_{\mathrm{DC}} \cdot \hat{H}_{\mathrm{e}}^{2}$$

Unknown!

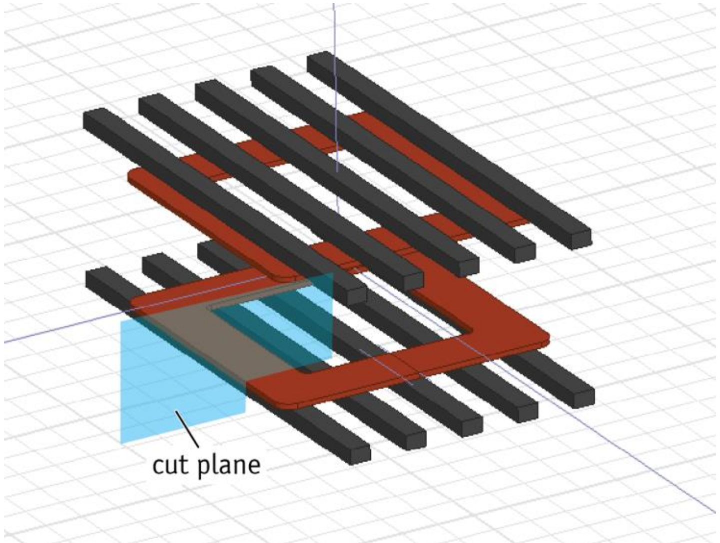

■ **Approximation with 2D-Cut Plane**

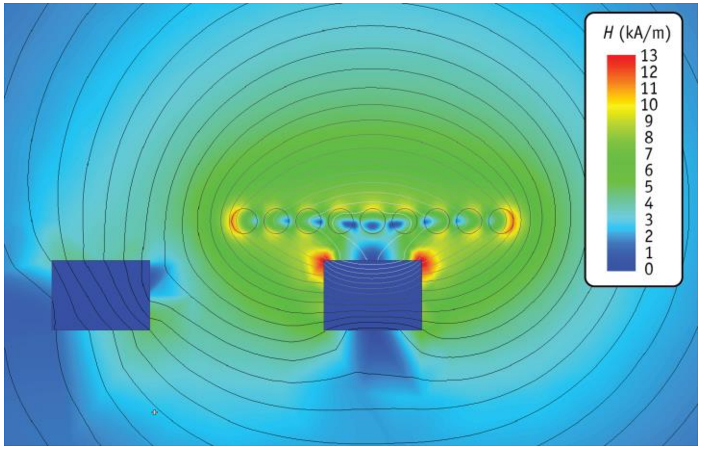

▲ **2D-FE Simulation of Field in Cut Plane**

▶ Estimation of Proximity Effect (2)

■ **Approximation: Analytical Calculation of *H*-Field in Conductors**

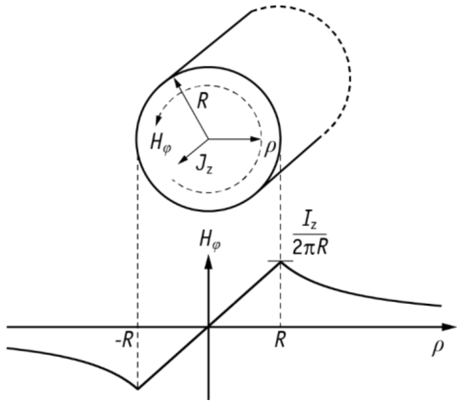

$$H_\varphi(\rho) = \begin{cases} \dfrac{I}{2\pi R^2}\rho, & \text{if } |\rho| \le R \\ \dfrac{I}{2\pi \rho}, & \text{if } |\rho| > R \end{cases}$$

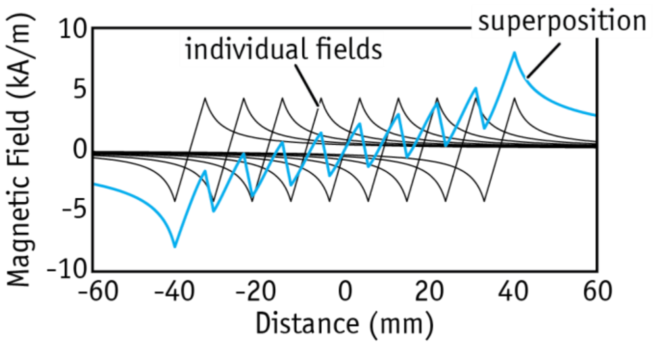

▲ **Analytically calculation for 9 conductors**

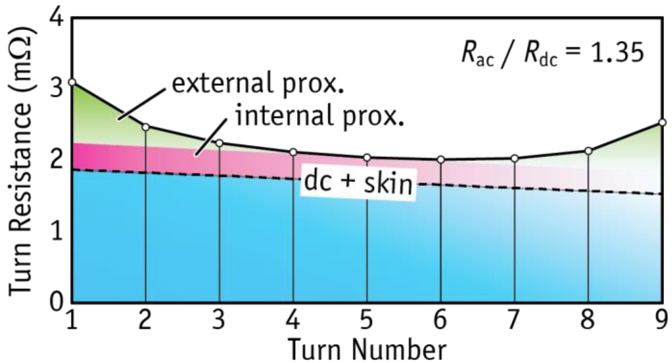

▲ **Calculated AC resistance for each turn**

■ **Assumptions:**
- Ferrite Cores are Neglected
- No Losses due to Receiver Coil
- Corner-Effects Neglected
- Ideally Twisted Litz Wire
- DC-Current Distribution only if $R << \delta$

► Estimation of Proximity Effect (3)

■ Comparison to 2D-FEM Simulation Including Core

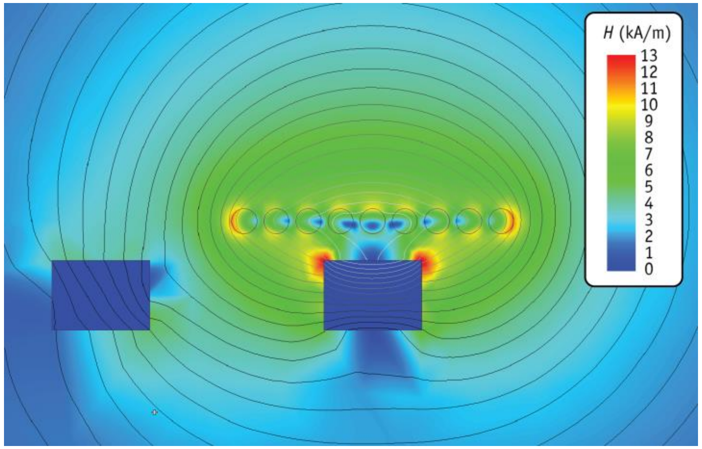

▲ 2D-FE Simulation with Core Rods for Comparison

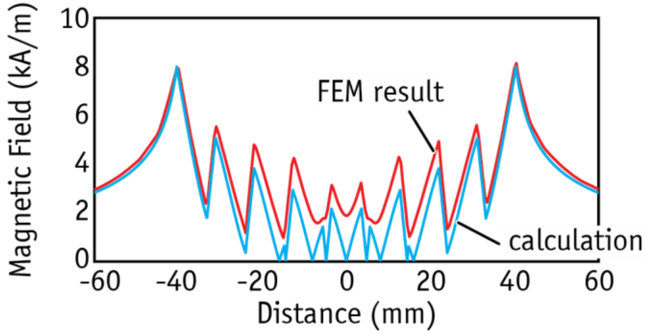

▲ Comparison of analytical calculation and FEM Simulation

■ Core has only Minor Effect on Fields
■ Approximation with 2D-Calculation to Estimate External Field

$$P_{\mathrm{prox,ext}} = n \cdot G_{\mathrm{R}}(f) \cdot R_{\mathrm{DC}} \cdot \hat{H}_{\mathrm{e}}^2$$

Calculated!

► Verification of FEM Field Calculations (1)

R. Bosshard, J. W. Kolar, B. Wunsch "Accurate Finite-Element Modeling and Experimental Verification of Inductive Power Transfer Coil Design," Proc. 29th APEC, 2014.

▲ **Field probe ELT-400**

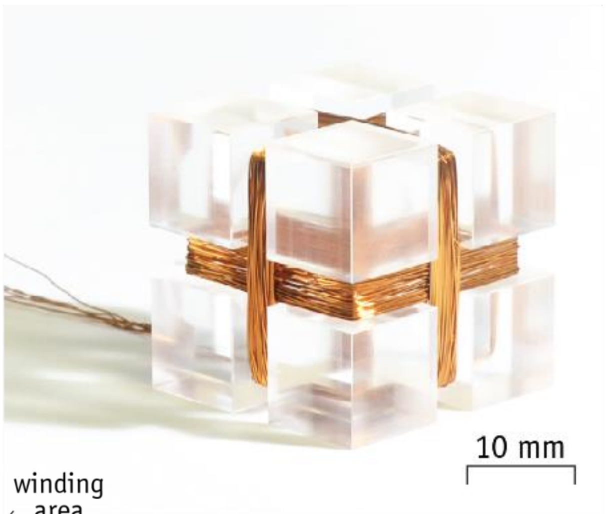

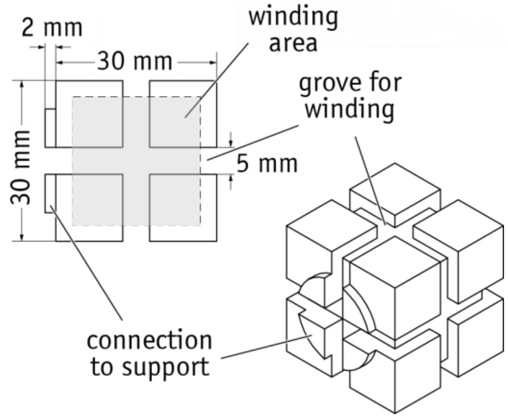

Number of Turns ... 40
Number of Layers ... 2
Wire Diameter ... 0.2 mm
Design Freq. ... 100 kHz
Sensitivity ... 15 mV/uT

► Verification of FEM Field Calculations (2)

R. Bosshard, J. W. Kolar, B. Wunsch "Accurate Finite-Element Modeling and Experimental Verification of Inductive Power Transfer Coil Design," Proc. 29th APEC, 2014.

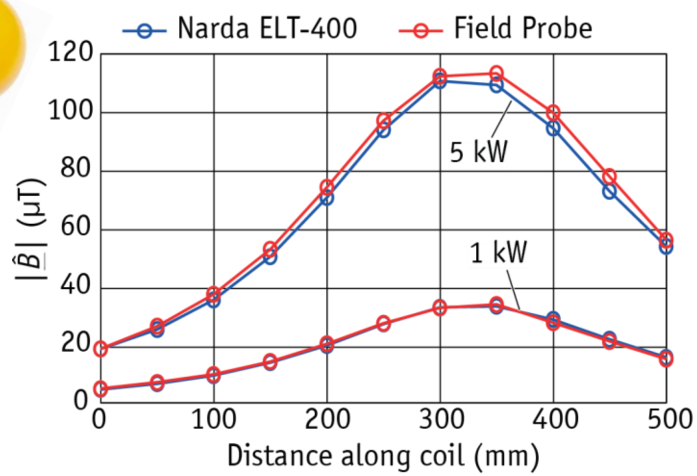

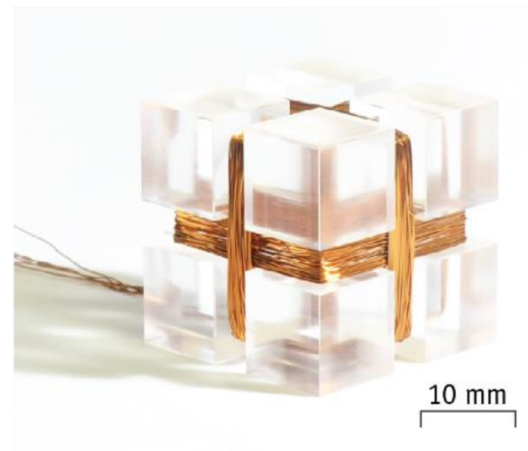

▲ **Comparison to Commercial Product**

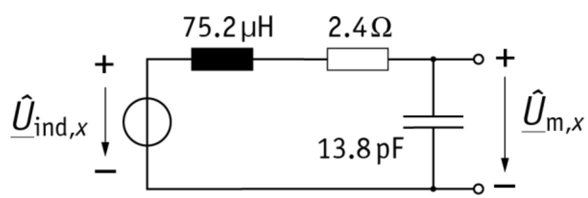

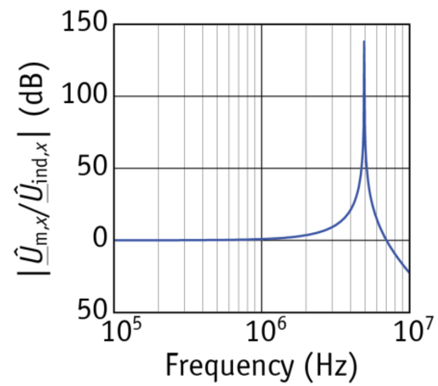

▲ **Equivalent Circuit and Transfer-Function with Measured Parameters**

R. Bosshard, J. W. Kolar, B. Wunsch "Accurate Finite-Element Modeling and Experimental Verification of Inductive Power Transfer Coil Design," Proc. 29th APEC, 2014.

► Verification of FEM Field Calculations (3)

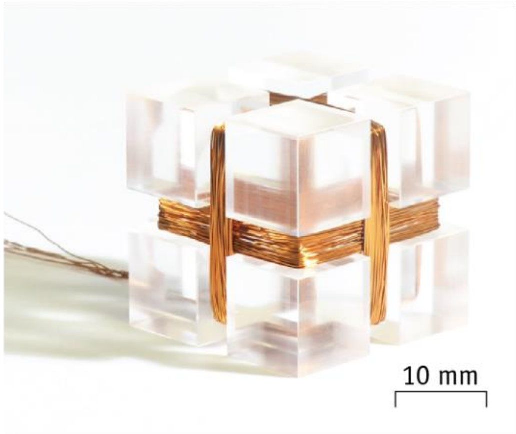

▲ Custom field probe for verification

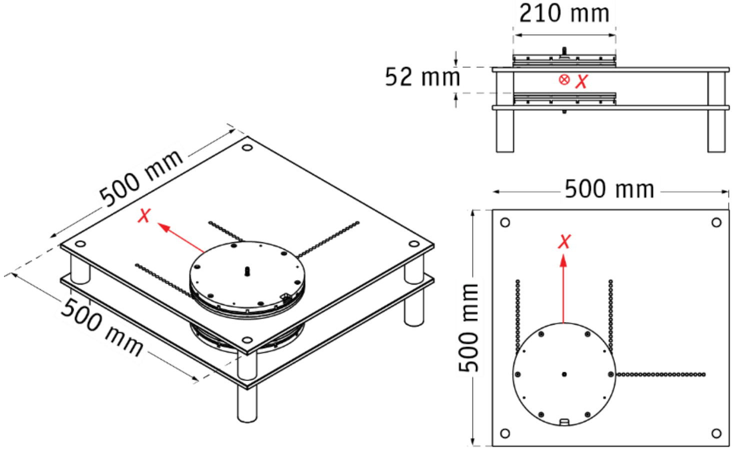

■ **Probe for Magnetic Field Measurements**
- Optimized for 100 kHz, High Accuracy
- Sensitivity: 14.5 mV/µT @ 100 kHz
- Accuracy: < 5% Error (Comp. to ELT-400)
- Size: 30x30x30 mm

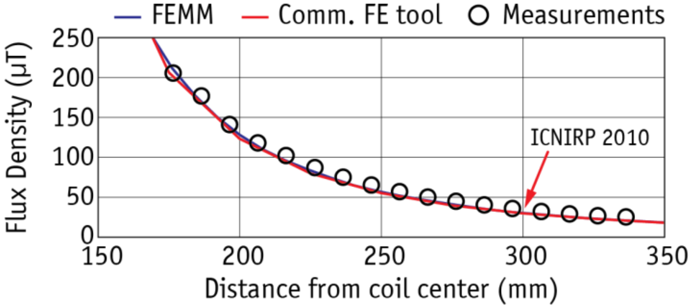

▲ Measured stray field @ 5 kW

Frequency Effects in Non-Ideal Litz Wire

► Copper Losses in Litz Wire – Asymmetric Twisting (1)

- Case study: Litz wire (tot. 9500 strands of 71µm each) with 10 sub-bundles
- Current distribution in internal litz wire bundles depends strongly on interchanging strategy

G. Ortiz, M. Leibl, J. W. Kolar,
"Medium Frequency Transformers for Solid-State Transformer Applications — Design and Experimental Verification", 2013.

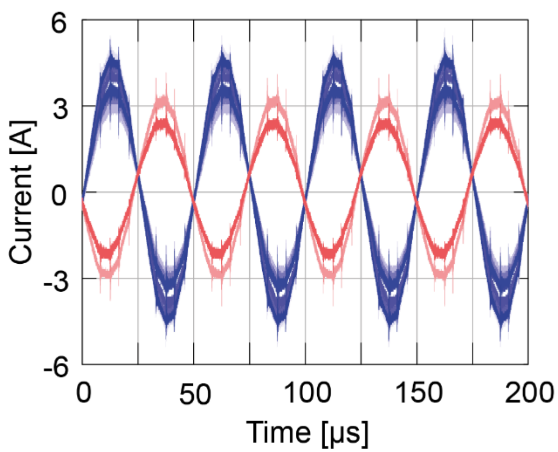

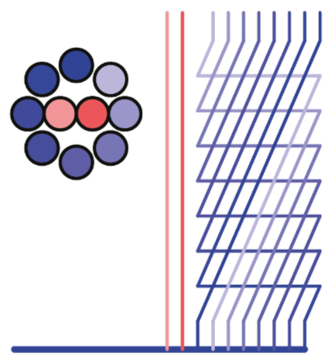

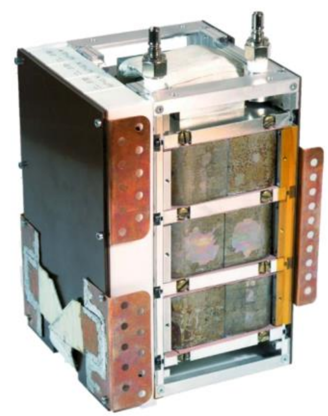

- Total copper losses for 10 bundles: 438W

▲ 166 kW/20 kHz Transformer

► Copper Losses in Litz Wire – Asymmetric Twisting (2)

- Case study: Litz wire (tot. 9500 strands of 71µm each) with 10 sub-bundles
- Current distribution in internal litz wire bundles depends strongly on interchanging strategy

G. Ortiz, M. Leibl, J. W. Kolar, "Medium Frequency Transformers for Solid-State Transformer Applications — Design and Experimental Verification", 2013.

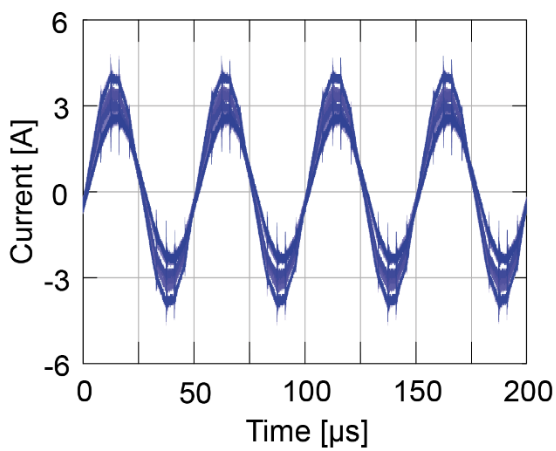

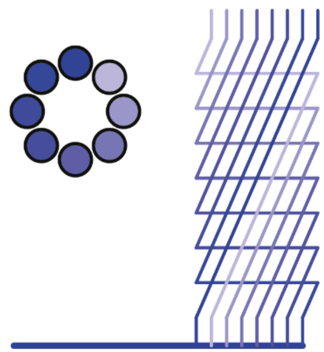

- Total copper losses for 10 bundles: 438W
- Total copper losses for 8 bundles: 353W

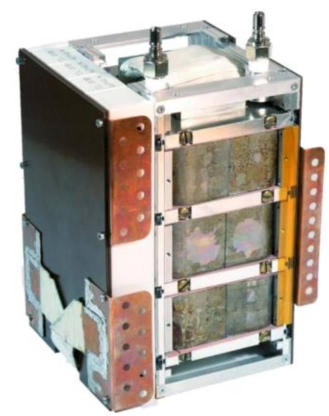

▲ 166 kW/20 kHz Transformer

▶ Copper Losses in Litz Wire – Termination

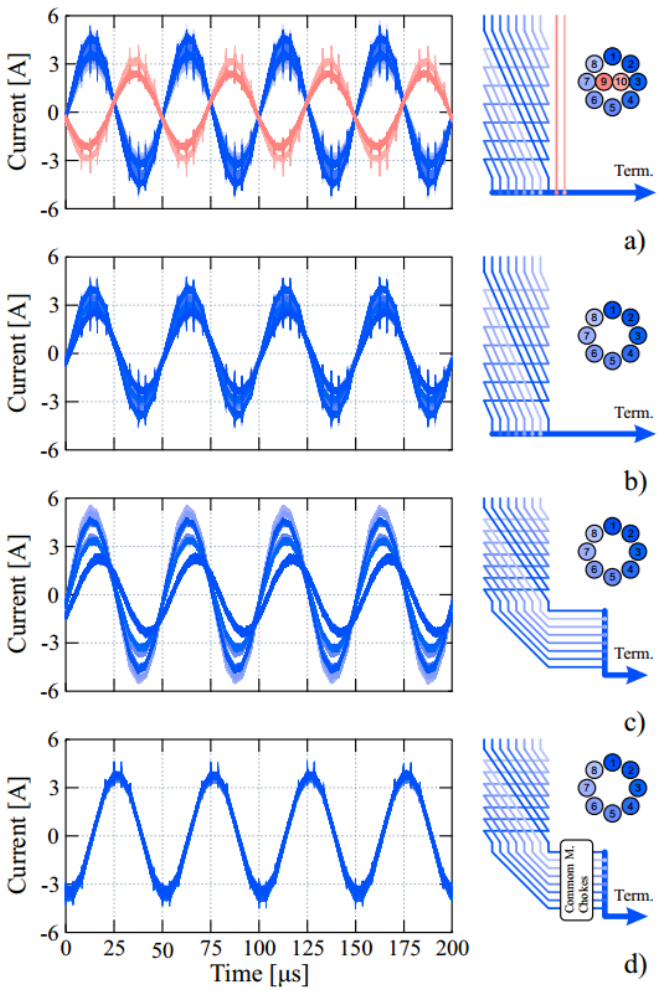

Best Option

G. Ortiz, M. Leibl, J. W. Kolar,
"Medium Frequency Transformers for Solid-State Transformer Applications — Design and Experimental Verification", 2013.

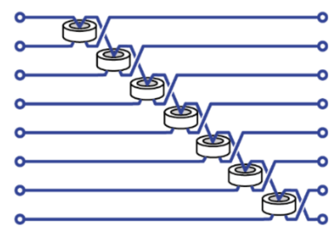

▲ Termination of Litz Wire Bundels with Common-Mode Chokes

► Copper Losses in Litz Wire – Symmetric Twisting

■ **2nd Example: Measurement of 2500 x 0.1 mm Litz Wire at 85 kHz**
- Stranding: 5x5x4x25 Strands of 0.1 mm
- No Common Mode-Chokes are Needed with Symmetric Twisting
- Termination: Standard Cable Shoe (Soldered)

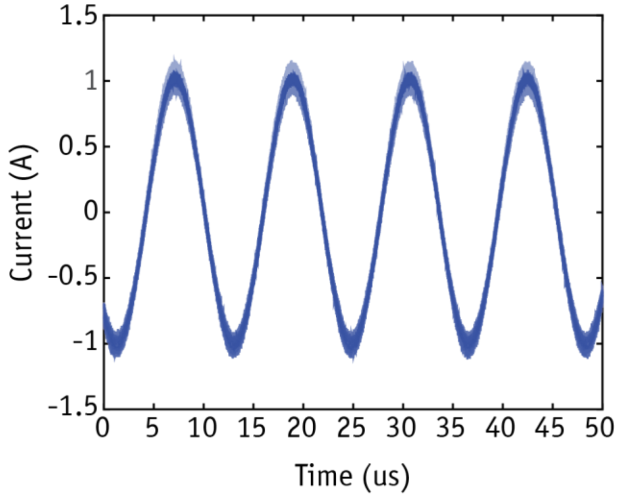

▲ **Equal Current Distribution at 85 kHz Measured in Actual Coil Arrangement**

Coil Modeling:
High-Frequency Core Losses

► Core Materials for IPT Coils (1)

■ **Power Ferrites (e.g. Manganese-Zinc)**
- Lowest Core Losses at High-Frequency (20 … 150 kHz)
- Saturation Typically not Limiting Factor
- Low Specific Weight: 4-5 g/cm^3
- Sintering / Tooling: Arbitrary Shape
- Isotropic Material: Flux in any Direction

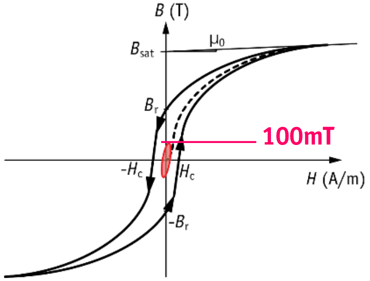

▲ **Schematic drawing of BH-loop**

CMI Ferrite, www.cmi-ferrite.com, (6.11.2014).

► Core Materials for IPT Coils (2)

■ **Tape Wound Cores**
- Custom Shapes with Tape Winding
- High Losses at Frequency > 20..50 kHz
- Higher Specific Weight: 7-8 g/cm^3
- Anisotropic: Orthogonal Flux Causes High Eddy Current Losses in Tapes
- Same Problem would also Occur for Foil instead of Litz Wire Windings

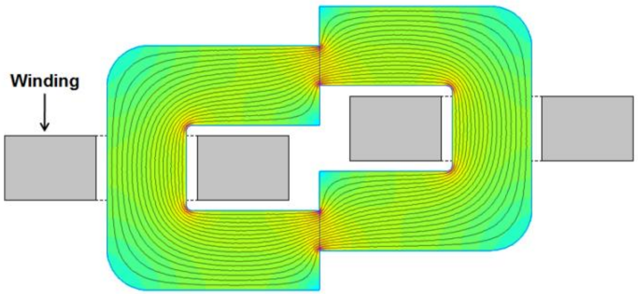

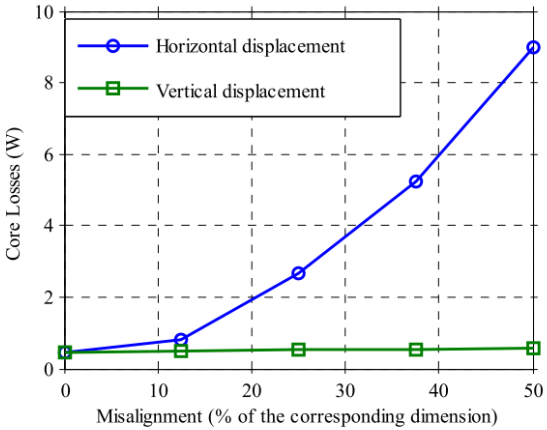

Tape wound core

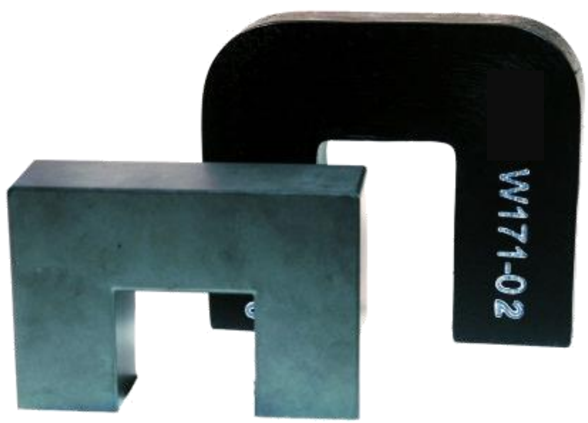

Ferrite core

B. Cougo, J. Mühlethaler, J. W. Kolar, "Increase of Tape Wound Core Losses due to Interlamination Short Circuits and Orthogonal Flux Components", 2011.

► Core Segments for Circular Spiral Coil

■ 5 kW Prototype IPT Coil – Core Construction

- MnZn Power Ferrite (K2004: 300 mW/cm^3, B_{sat} = 455 mT, 4.8 g/cm^3)
- Off-the-Shelf 90°-Ferrite Segments
- Typical Application: Induction Cooking

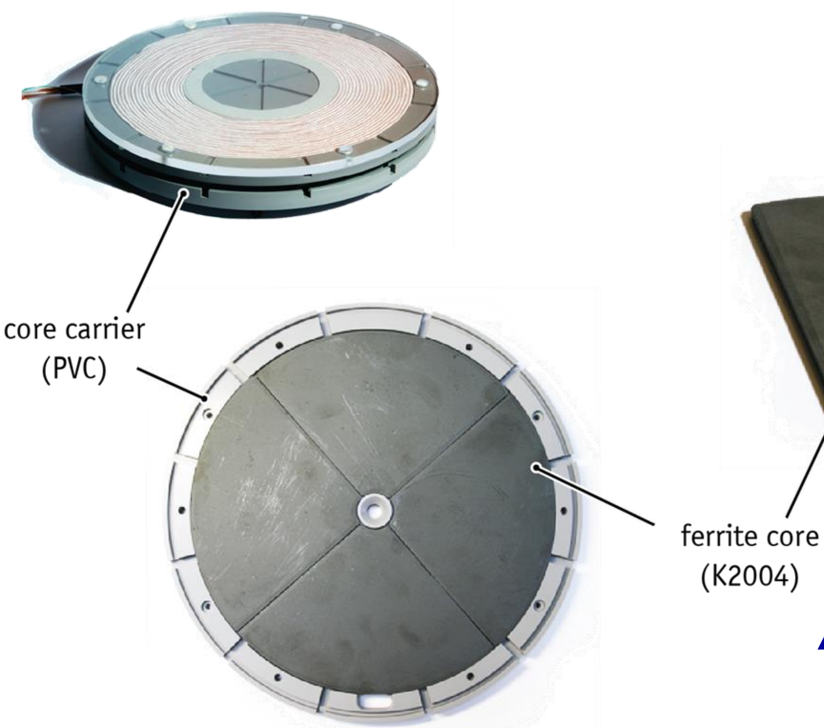

▲ **Ferrite Core Segment used in the 5 kW Prototype System**

J. Mühlethaler, "Modeling and multi-objective optimization of inductive power components," Ph.D. dissertation, Swiss Federal Institute of Technology (ETH) Zurich, 2012.

► Core Loss Calculation – General

■ Calculation of Core-Loss Density According to Current Waveform

Sinusoidal Current

Steinmetz Equation
→ Sinusoidal w/o DC-Offset

DC Current + HF Ripple

Non-Sinusoidal AC Current

Generalized Versions of the Steinmetz Equation (iGSE, i²GSE)
→ Arbitrary Waveform & DC-Offset
→ Relaxation Effects

Sinusoidal Current + HF Ripple

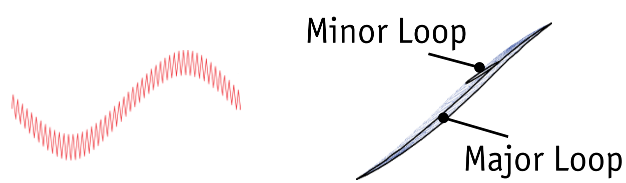

Superposition of Losses due to Minor and Major Loops

► Core Loss Calculation for Sinusoidal Excitation

■ Core Loss Calculation with FEM & Steinmetz Equation

- Integration of Steinmetz Equation over Core Volume Directly within FEM Tool
- Steinmetz Parameters Must be Iteratively Extracted for Flux Density, Frequency and Temperature Points Similar to those Occuring in the Final Design!

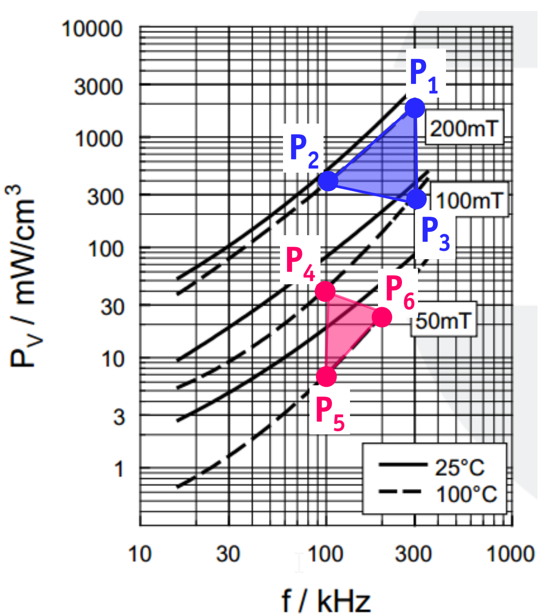

▲ Typical Core Loss Data from Ferrite Manufacturer Datasheet

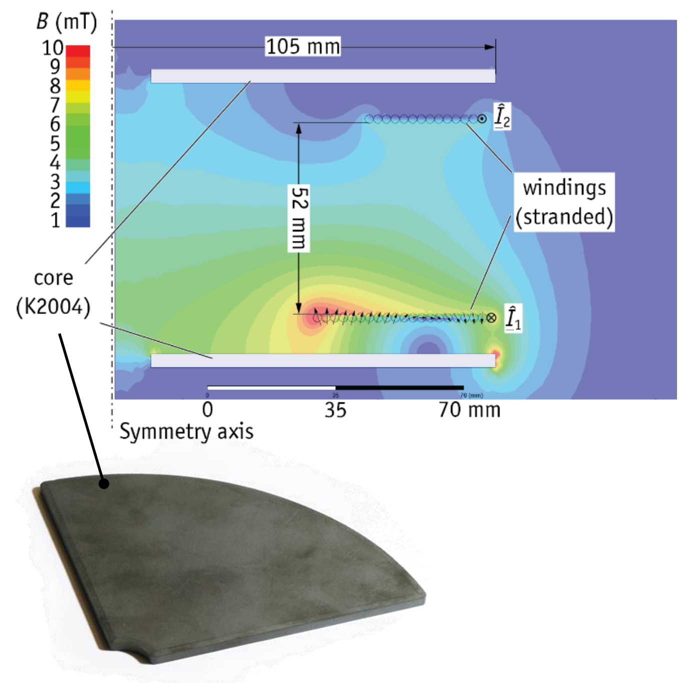

Thermal Modeling

VDI, *Heat Atlas*.,
Springer, Berlin, 2010.

▶ Heat Transfer Mechanisms

■ Heat Conduction

- Calculation Analog to Electric Networks:

  $I \rightarrow P$ … Heat Flux
  $U \rightarrow \Delta T$ … Temperature
  $R \rightarrow R_{\mathrm{th}}$ … Thermal Resistance

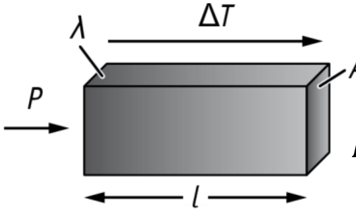

$$R_{\mathrm{th}} = \frac{\Delta T}{P} = \frac{l}{\lambda A}$$

■ Natural/Forced Convection

- Modeling of Fluid Dynamic Effects Required

$$R_{\mathrm{th}} = \frac{\Delta T}{P} = \frac{1}{hA}$$

- Heat Transfer Coefficient h is Influenced by Absolute Temperatures, Fluid Properties, Fluid Flow Rate, Surface Dim., Orientation & Texture
- Empirical Models Exist for Some Typical Situations: Vertical Wall, Top/Bottom Surface

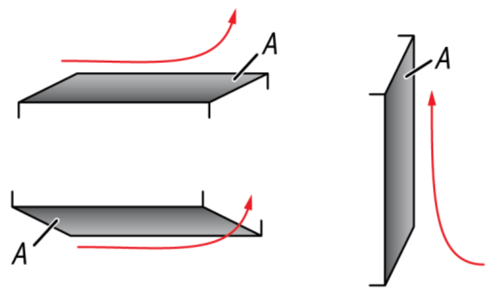

■ Thermal Radiation

- Non-Linear Mechanisms Must be Modeled

$$P_{\mathrm{rad}} = \epsilon_{\mathrm{eff}} A \sigma (T_{\mathrm{b}}^4 - T_{\mathrm{a}}^4)$$

- Which Surfaces are Radiation Sources/Sinks?
- Often Neglected at Low Temperatures (<100°C)

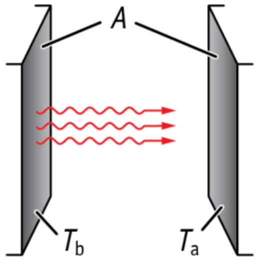

▶ Detailed Thermal Modeling of IPT Coils

- Derivation of Detailed Thermal Network incl. Heat Conduction, Convection at Surfaces is Complex and Might not Lead to a Generally Valid Solution
- Iterative Power Loss Calculation with Thermal Feedback Requires Long Calculation Time due to FEM Calculations in Power Loss Models

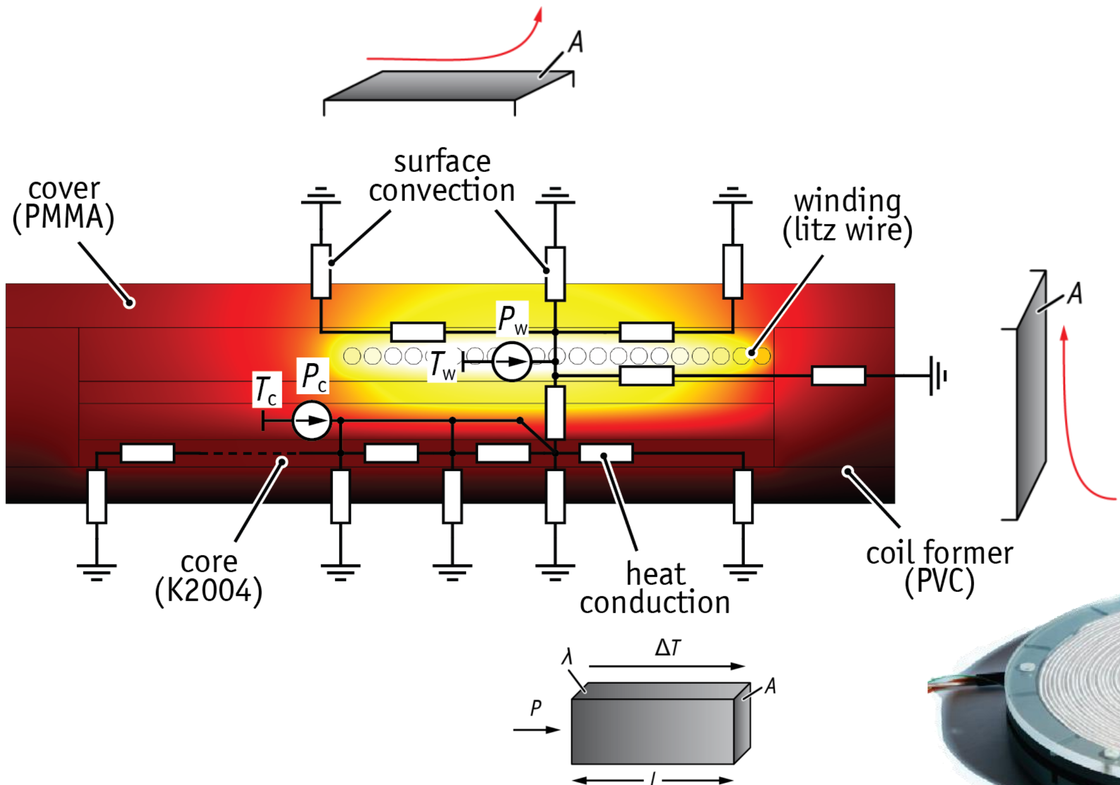

J. Biela, J. W. Kolar, "Cooling Concepts for High Power-Density Magnetic Devices", *Proc. IEEE Power Conversion Conf.*, 2007.

► Simplified Thermal Modeling

- **No Thermal Feedback Included in Calculation of Power Losses, but Elevated Temperature (80-100°C) is Assumed during Calculation and Verified Afterwards**

- **Assumption of Uniform Loss Distribution over Coil Volume**
- **Typical Values for Convective Heat Transfer via Coil Surface**
  - Forced-Air Cooling: 30-60 W/(K·m^2) → $T_{surf,max}$ = 40°C: 200 mW/cm^2 at 50 W/(K·m^2)
  - Natural Convection Cooling: 5-15 W/(K·m^2) → $T_{surf,max}$ = 40°C: 40 mW/cm^2 at 10 W/(K·m^2)

Considered as Thermal Limit in Coil Optimization Loop

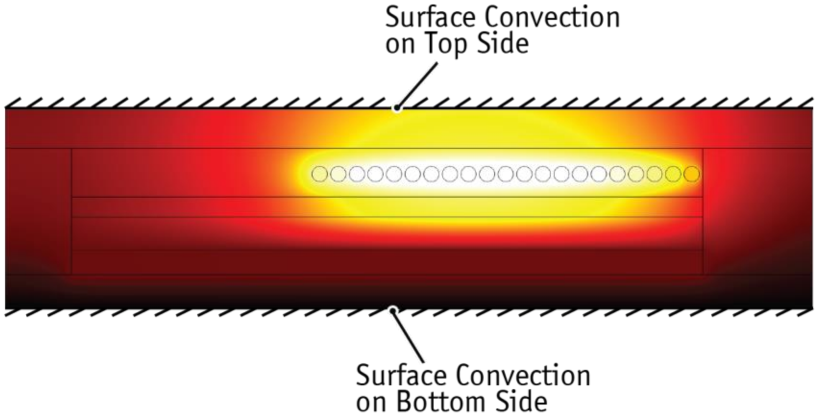

- **Before Building Final Design Double-Check Thermal Feasibility with FEM Model!**

▶ Thermal Simulation & Experimental Verification

■ **Before Building Final Design Double-Check Thermal Feasibility with FEM Model!**

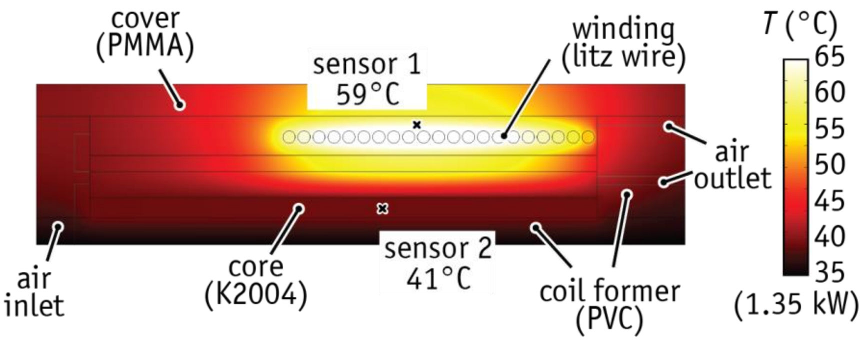

▲ **Thermal Simulation of 5 kW Prototype Coil**

www.fluke.com

■ **Temperature Measurements and Verification of Thermal FEM Results**

- Accuracy: < 5% Error of Steady-State Temperature
- Surface-Related Power Losses of up to 0.2 W/cm² with Forced Air Cooling is Useful Assumption in Design Phase

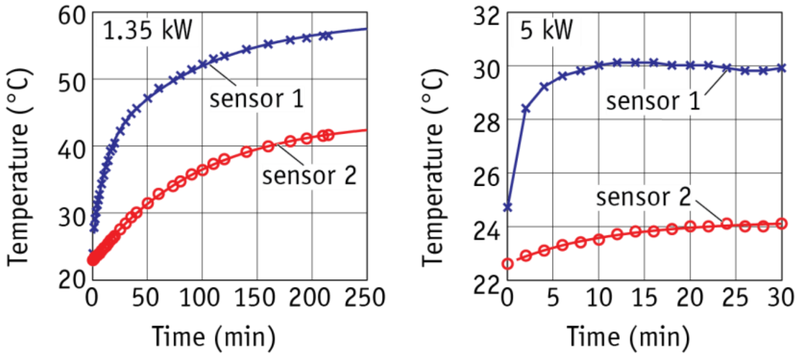

▲ **Thermal Measurements with Thermocouples (with/without Forced Air Cooling)**

► Forced Air Cooling System of the *50 kW* Prototype

- **Forced-Air Cooling is Needed to Reach Power Density 1.6 kW/dm^2 for the 50 kW Prototype**
  - Plastic Components with Low Temperature Rating have to be used to Avoid Eddy Currents

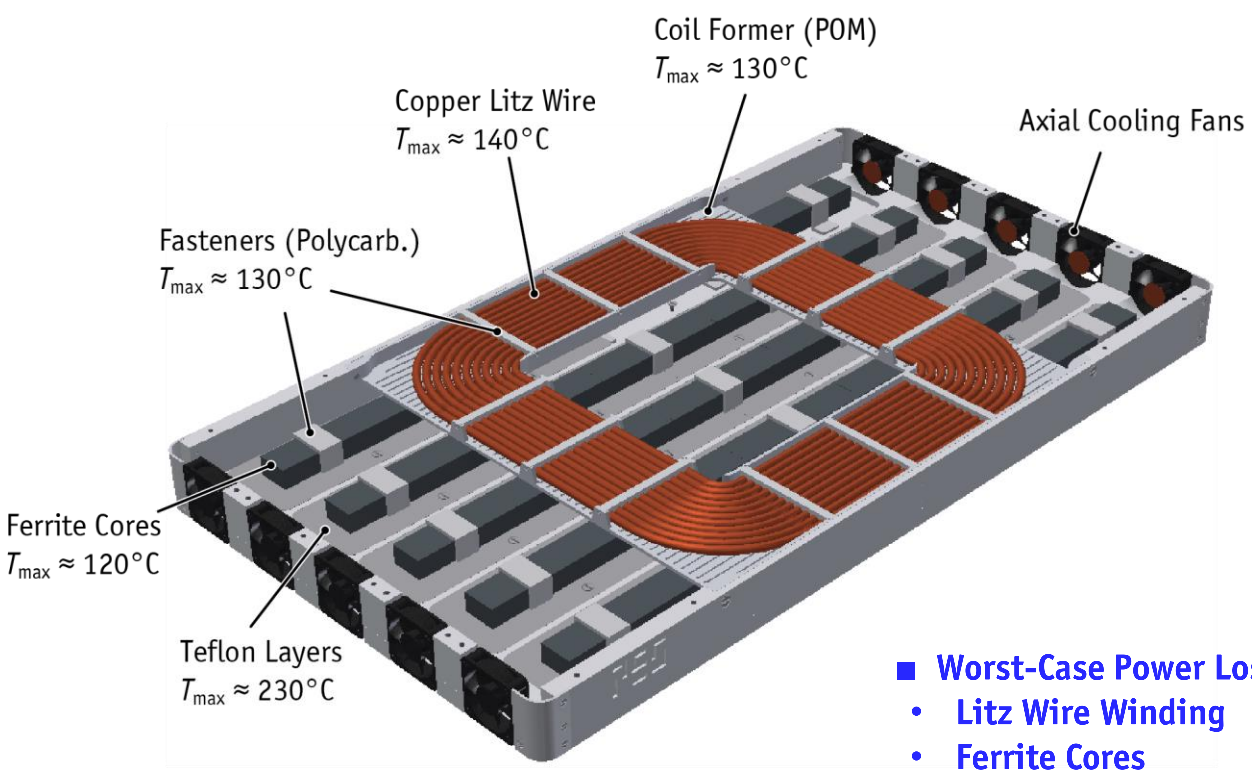

- **Worst-Case Power Losses**
  - **Litz Wire Winding 269 W**
  - **Ferrite Cores 202 W**
  - **Eddy Current Shield 40 W**

A. Van den Bossche and V. C. Valchev, *Inductors and transformers for power electronics*. New York: Taylor & Francis, 2005.

► Estimation of Heat Transfer Coefficient

10x

▲ Axial cooling fan for active cooling of the windings and core elements

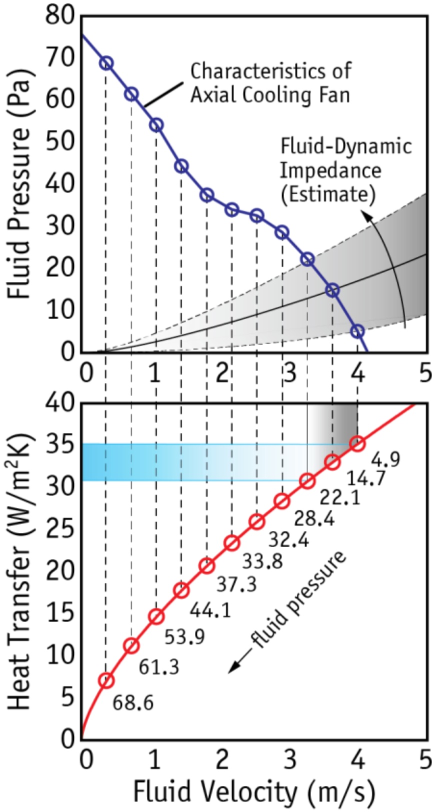

▲ Heat Transfer Coefficient Estimated from Fan Characteristics of AUB0524VHD

■ **Emprical Equation for Surface Heat Transfer Coefficient:**

$$h_v \approx C\frac{\lambda_\mathrm{f}}{d}\left(\frac{u_\infty d}{v_\mathrm{f}}\right)^n Pr_\mathrm{f}^{1/3}$$

$\lambda_\mathrm{f}, v_\mathrm{f}, Pr_\mathrm{f}$ ... conductivity, viscosity, Prantl number
u_∞ ... fluid velocity
d ... component height
C, n ... empirical geometry parameters (C = 0.102, n = 0.675)

► Thermal Design Verification with 3D-FEM

■ **Heat Transfer in Solids with Estimated Coeff.**
- 30 W/m²K … active cooled surfaces
- 7.5 W/m²K … convective cooled surfaces

■ **Parameter Sweep in FEM Tool**
- Heat Transfer Coefficient
- Loss Safety Factor: $P_{sim} = m_{safety} \cdot P_{calc}$

→ **Design is Feasible at Surface-Related Power Loss 0.2 W/cm² with Active Cooling**

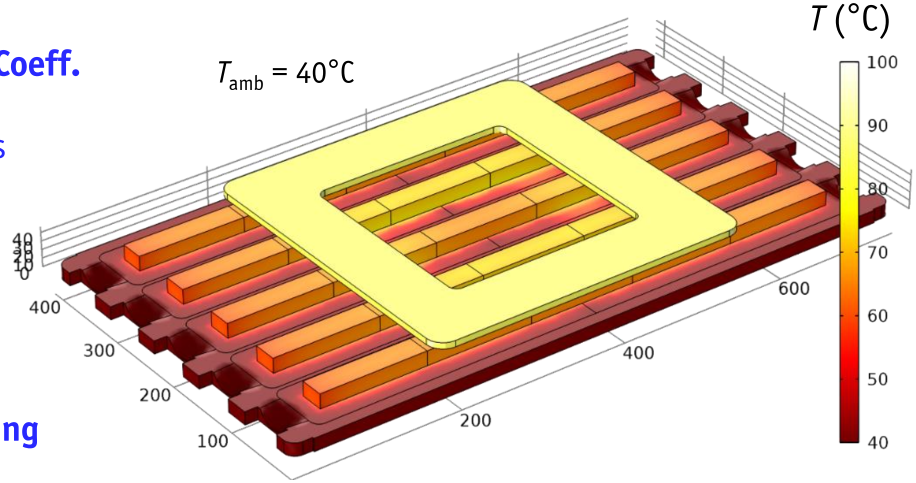

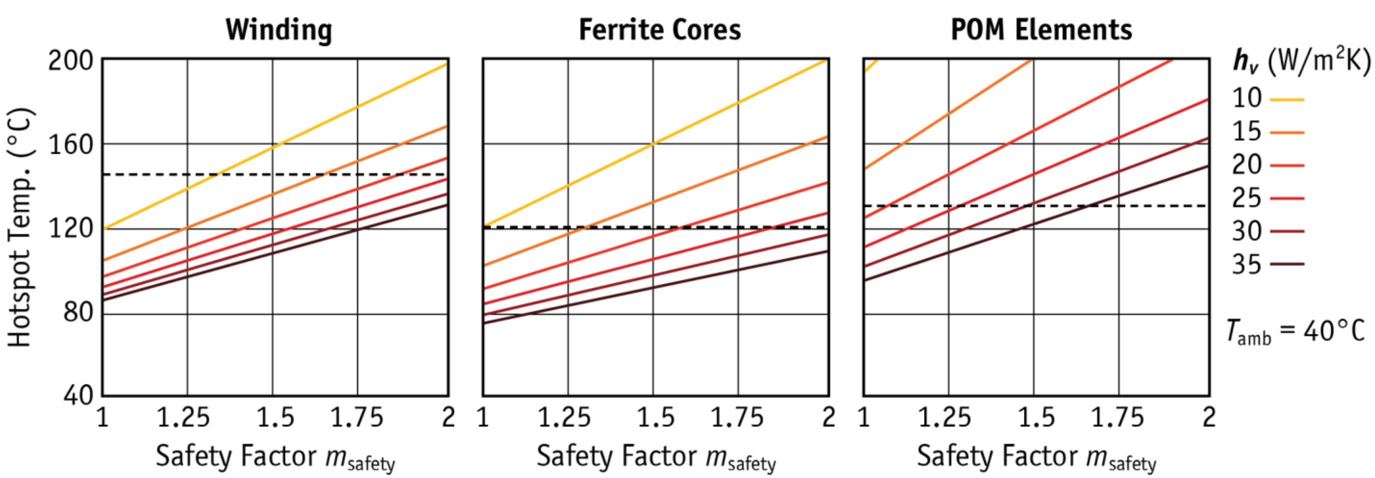

▲ **3D-FEM Thermal Simulation: Results of Parameter Sweep**

Resonant Capacitors

▶ Resonant Capacitors: Component Selection (1)

■ **Polypropylene Film Capacitors for Resonant Applications**
- Low tan(δ) → Low High-Frequency Losses
- Low Parasitic Inductance and *ESR*
- Least Affected by Temperature/Frequency/Humidity (Could Lead to Changing Resonant Frequency)

*MK/F ** … Metallized Plastic Film / Metal Foil
***T* … Polyester
***P* … Polypropylene
***N* … Polyethylene Naphthalate

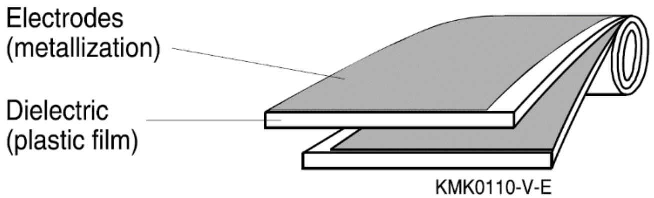

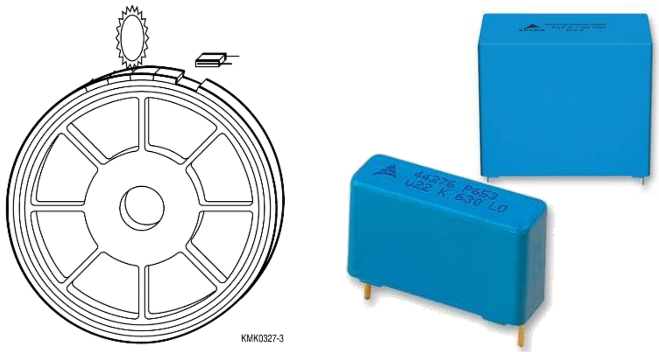

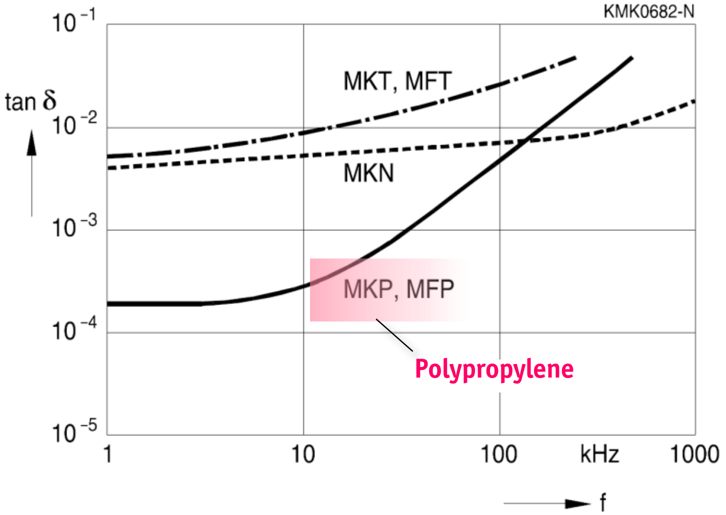

▲ **Datasheet Values of tan(δ) in Funciton of Frequency for EPCOS Film Capacitors**

EPCOS, Film Capacitors
Data Handbook, 2009.

► Resonant Capacitors: Component Selection (2)

- **Polypropylene Film Capacitors for Resonant Applications**
  - Low tan(δ) → Low High-Frequency Losses
  - Low Parasitic Inductance and *ESR*
  - Least Affected by Temperature/Frequency/Humidity (Could Lead to Changing Resonant Frequency)

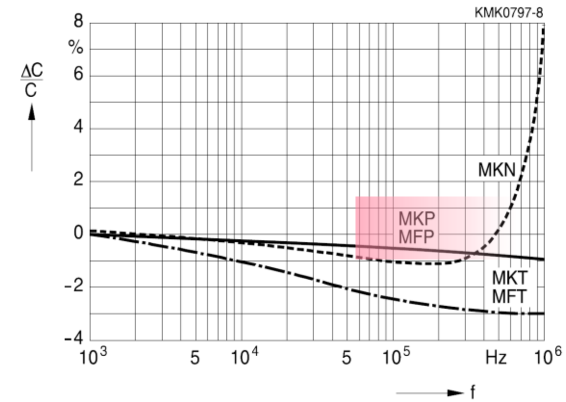

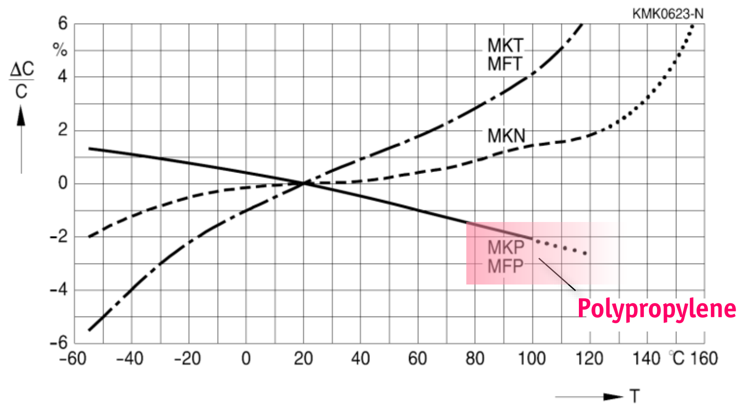

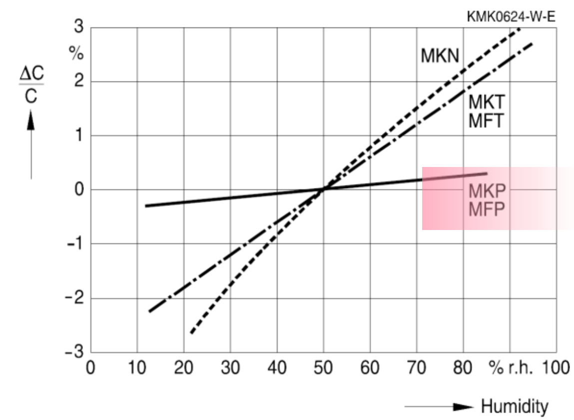

▲ **Typical Material Characteristics for Film Capacitors (EPCOS)**

EPCOS, Film Capacitors
Data Handbook, 2009.

► Capacitor Service Life vs. Temperature & Voltage

■ **Service-Life of Film Capacitors Strongly Depends on Operating Temperature and Voltage Utilization**

$$t_{\text{life}}(T,V) = t_{\text{life,0}} \cdot \frac{1}{\pi_T} \cdot \frac{1}{\pi_V}$$

T (°C)	π_T
≤ 40	1
50	1.8
55	2.3
60	3.1
70	5.2
80	9
85	12
90	16
100	33
105	50

V / V_R	π_V
10%	0.26
25%	0.42
50%	1.00
60%	1.42
70%	2.04
80%	2.93
90%	4.22
100%	6.09
110%	9.00
120%	13.00

▲ Arrhenius Law (Exponential Func.)

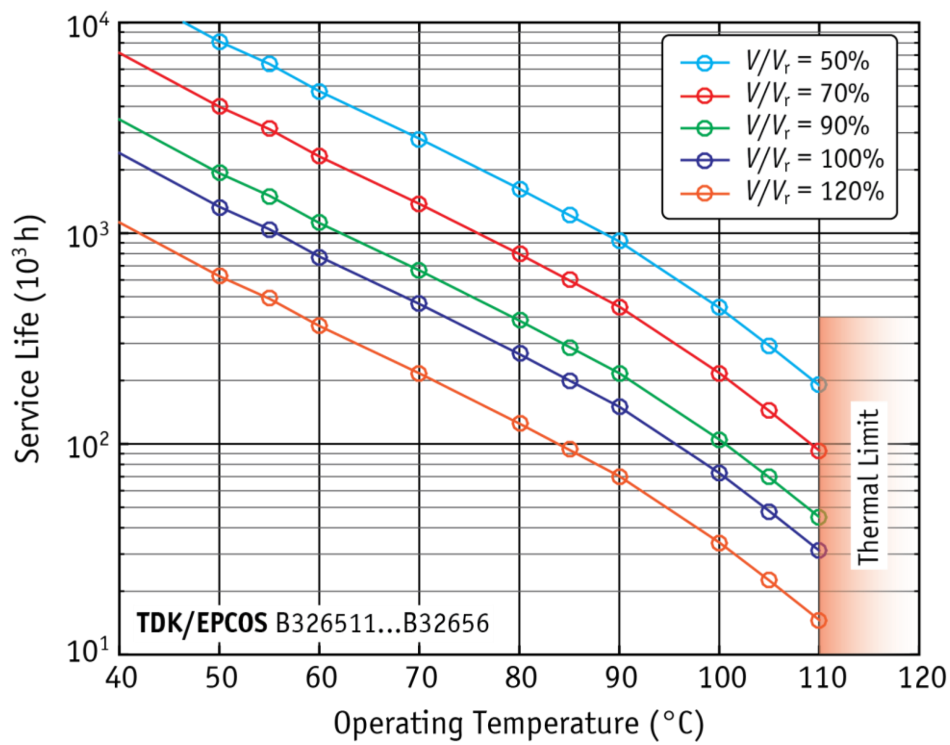

▲ Service Life vs. Operating Temperature for Different Levels of Voltage Utilization

TDK/EPCOS Product Profile,
Film Capacitors for Industrial Applications, 2012.

► High-Power Polypropylene Film Capacitors

■ **50 kW IPT – Capacitor Requirements**
- $> 100\,A_{rms}$ / $3..4\,kV_{rms}$ / $20..150\,kHz$

▲ **CSP 120-200 Polypropylene Film Capacitor ($1.1\,kV_{pk}$ / $100\,A_{rms}$ / 1 MHz @ full power)**

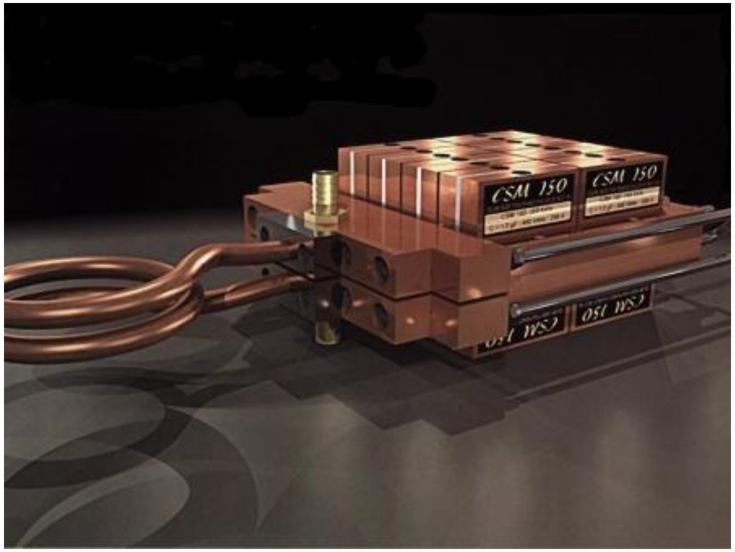

▲ **Induction Heating System** (www.celem.com)

- **Tangent-Delta:** 1/1000 - 1/700
- **High Power Density:** 5.95 kVAr/cm^3
- **Active Cooling:** Water / Air @ 35% Power
- **Typical Application:** Induction Heating

► Capacitor Module with Forced-Air Cooling System

- **Forced-Air Cooling Required for Resonant Capacitors at 50 kW Operation**
  - Aluminum Extrudend Fin Heatsink Mounted to Capacitor Terminals

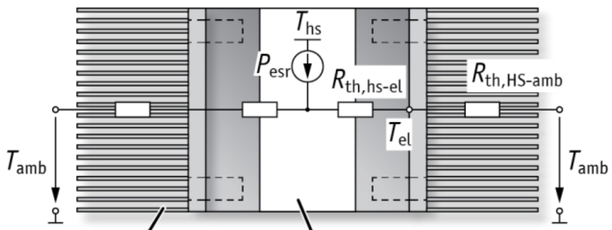

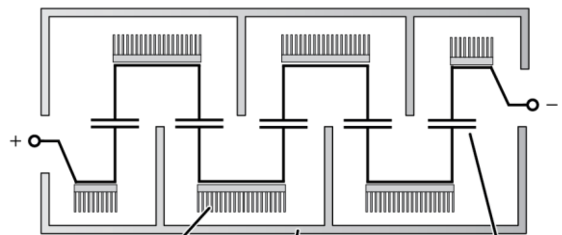

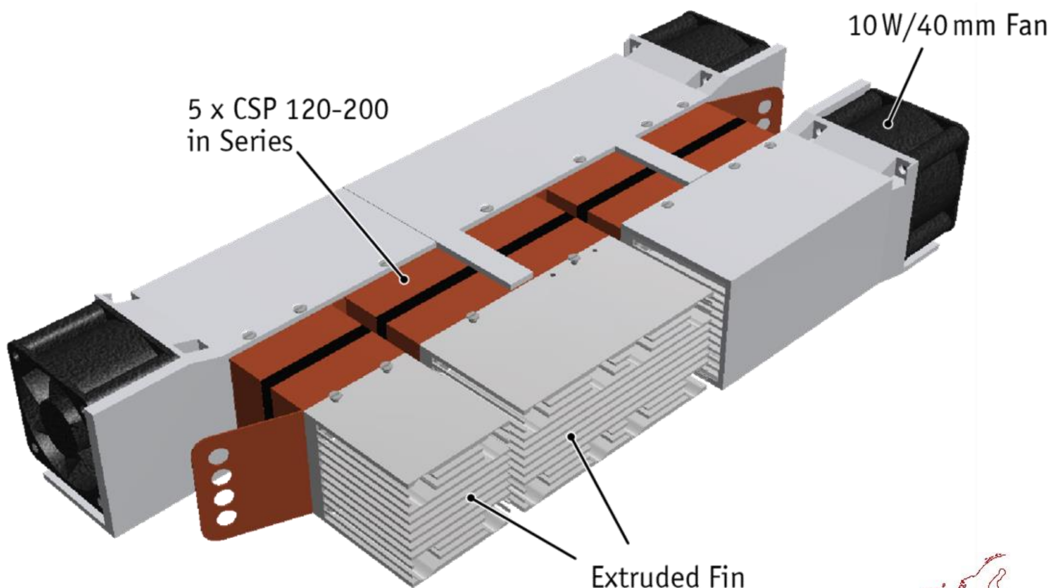

Rated Current	**100 A_{rms}**
Tangent-Delta	**1.5‰**
Power Losses	**314 W**
Cooling System	**Forced-Air**

► Resonant Capacitor Module for 50 kW

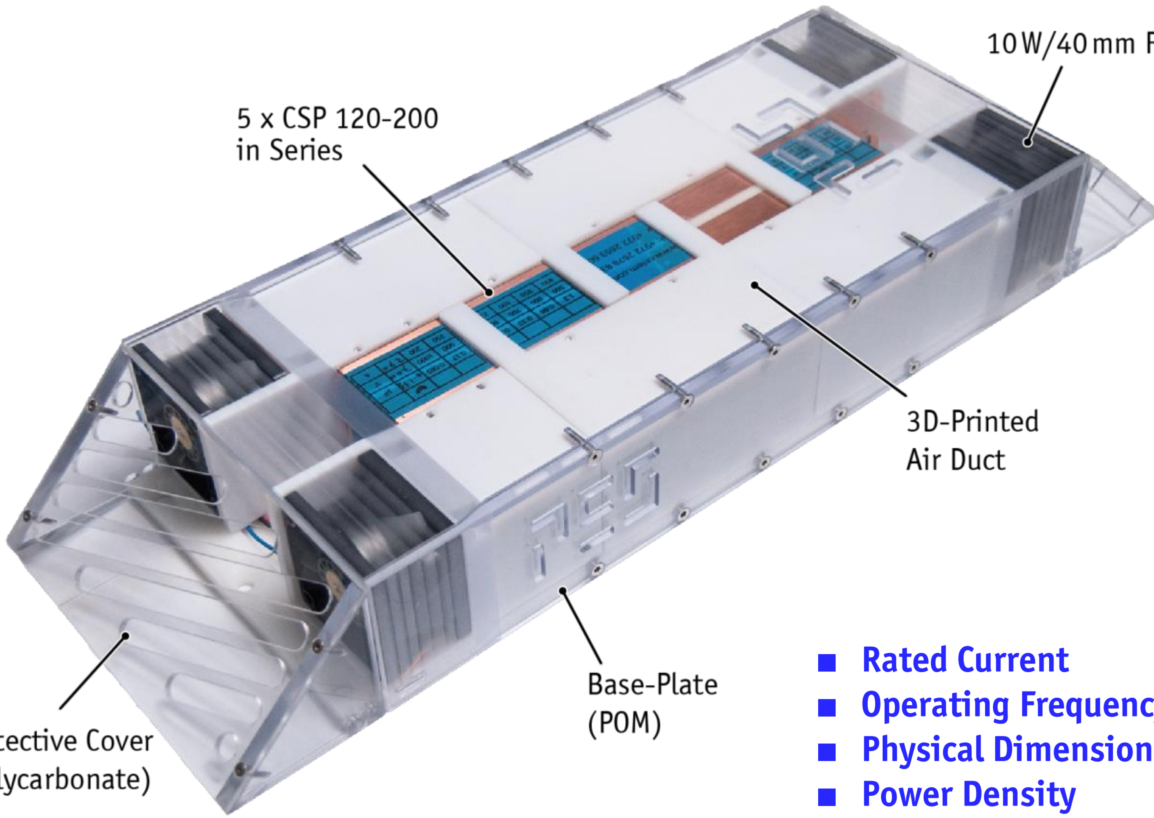

◄ **Capacitor Module: 5 Devices in Series, Forced-Air Cooling System**

- **Rated Current** — **100 A_{rms}**
- **Operating Frequency** — **85 kHz**
- **Physical Dimensions** — **5x12x38 cm, 2.6 kg**
- **Power Density** — **22 kW/l, 19 kW/kg**
- **Efficiency @ 50 kW** — **98.9%**

► Splitting of the Resonant Capacitor

- **Single Resonant Capacitor: Large Common-Mode Voltage $u_{L,cm}$ Applied to IPT Coil**
  - Increased *Electric Stray Field* May Violate ICNIRP and/or Cause Interference with Radio Comm. Systems

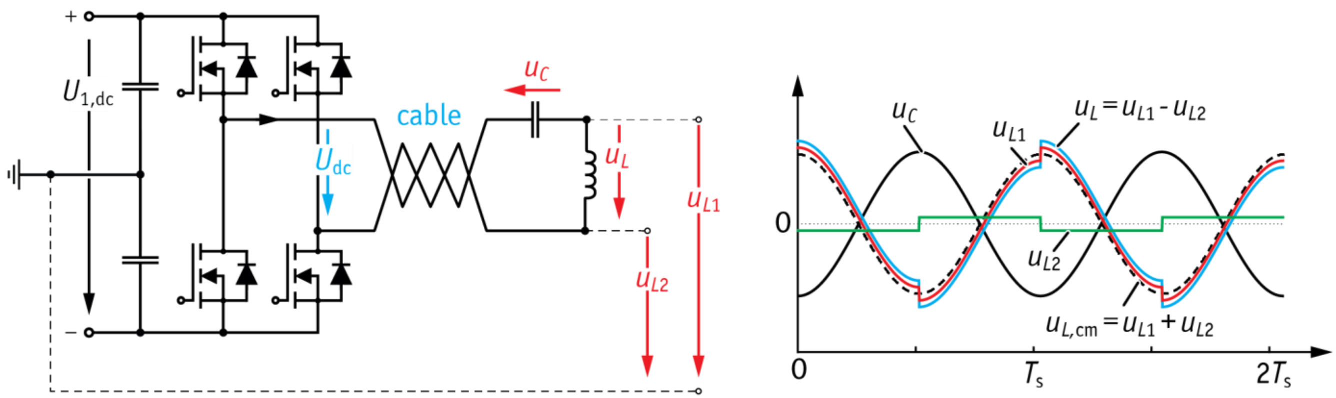

- **Symmetrical Splitting of Resonant Capacitor Eliminates Common-Mode Voltage $u_{L,cm}$**
  - Splitting into >2 Elements Reduces Voltage Stress at Cost of Higher R_{ac} due to Contact Resistances

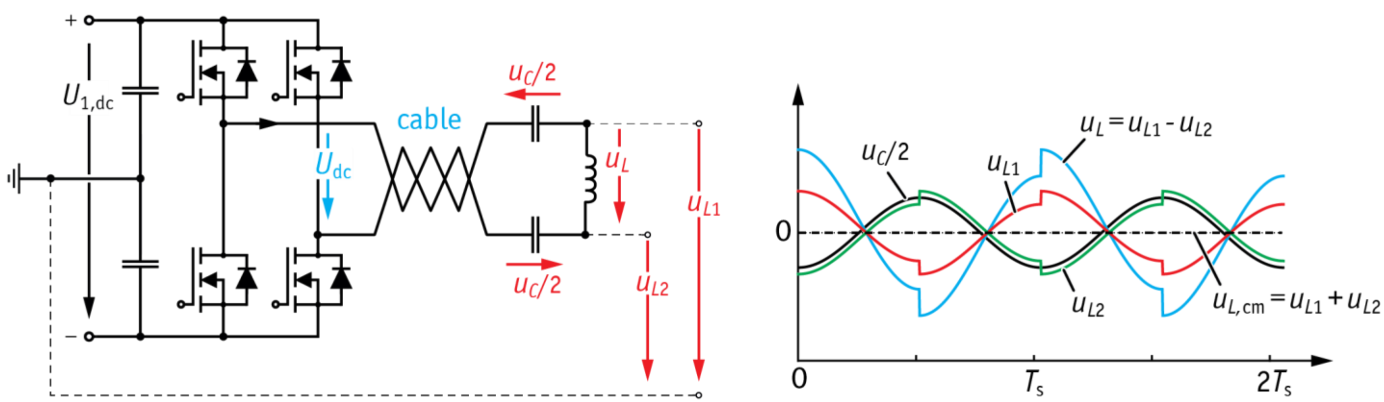

C. Paul, "Shielding," in *Introduction to Electromagnetic Compatibility*, 2nd ed., Jon Wiley & Sons, Hoboken, 2006, ch. 10, sec. 4, pp. 742-749.

► Mounting of Capacitor Module on IPT Coil

■ **Compact Realization as Integrated IPT Coil & Capacitor Module for EV Integration**
- Close Placement of Resonant Components to Limit Electric Stray Field
- Reduction of Eddy Currents in Capacitor Module with Conductive Eddy Current Shield

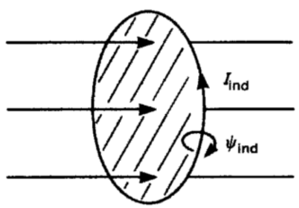

◄ **Current in Conductor Produces Opposing Magnetic Field**

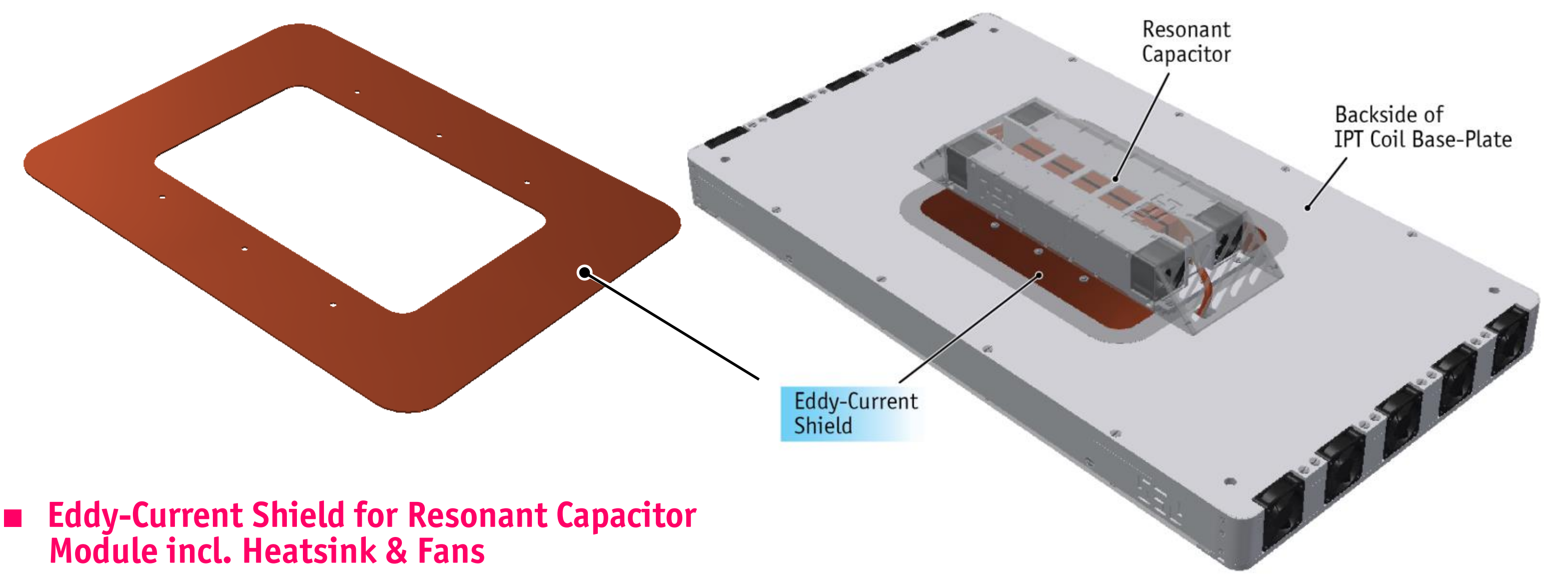

■ **Eddy-Current Shield for Resonant Capacitor Module incl. Heatsink & Fans**

► Magnetic Shielding with *Conductive* Materials

■ **Magnetic Flux Diversion with Eddy Current Shield**
- Create a Field-Free Space Around Capacitor Module

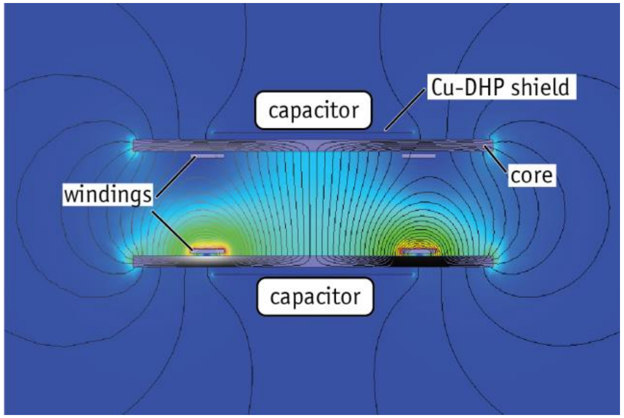

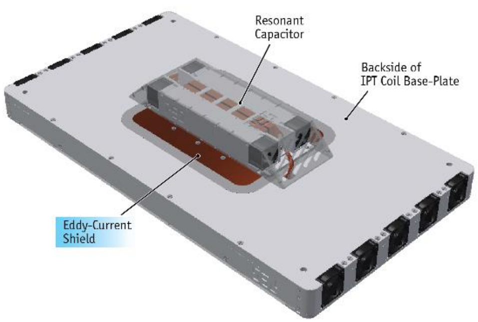

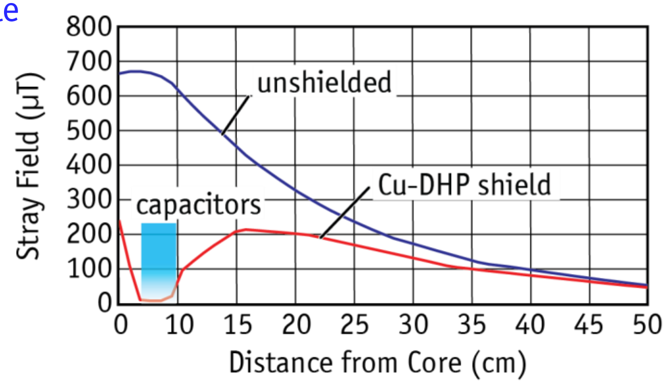

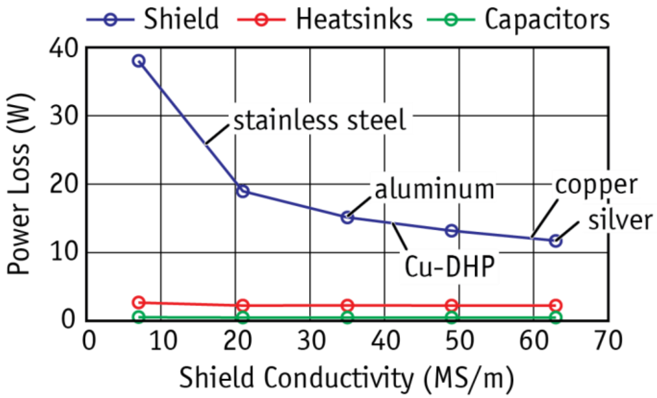

▲ **FE-Calculated Field and Power Loss at 50 kW**

► Magnetic Shielding with *Magnetic* Materials (1)

- **Low Reluctance Path (=Core) Allows Guiding Magnetic Flux**
  - Some Stray Field Remains due to Low Air Gap Reluctance, even at the Backside of the Coil
  - "Complete" Shielding Requires kg's of Core Material

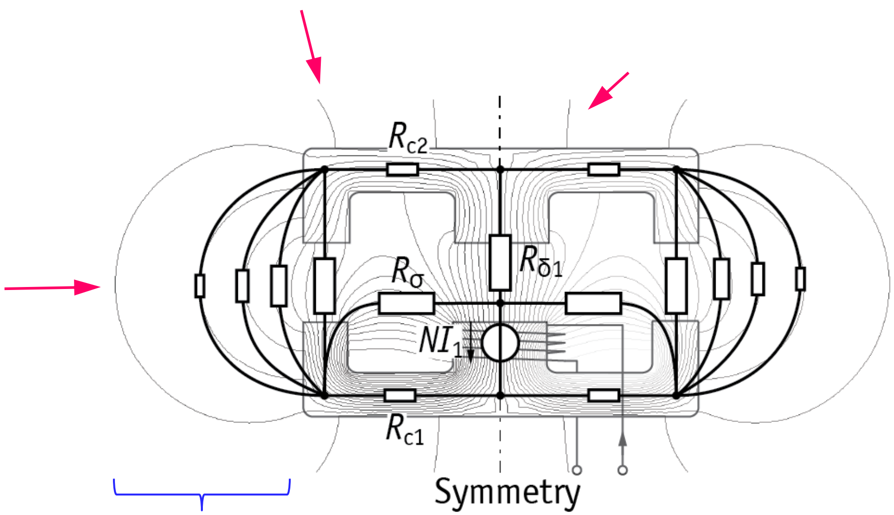

Magnetic Flux Follows
Low Reluctance Path:

$$R_{\delta 2} = \frac{l}{\mu_0 A}$$

- **MMF Across Air Gap is not influenced by the core**

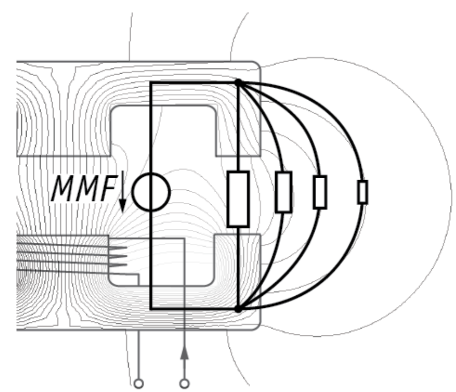

→ Core has no Effect on Stray Field Horizontally Outside the Coil Area

► Magnetic Shielding with *Magnetic* Materials (2)

■ **Save Weight, Use High Permeability Material (μ_r > 10'000)?**
- Machine Steel & Amorphous Iron: High Frequency Losses
- Permalloy: Strong Frequency Dependency and Low Saturation

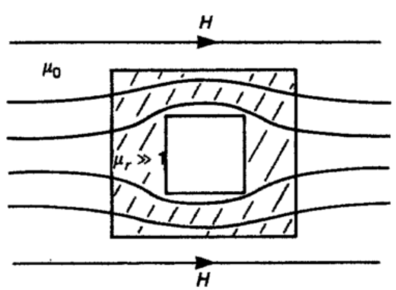

▲ **High-Permeability Material Attracts Magnetic Field**

C. Paul, "Shielding," in *Introduction to Electromagnetic Compatibility*, 2nd ed., Jon Wiley & Sons, Hoboken, 2006, ch. 10, sec. 4, pp. 742-749.

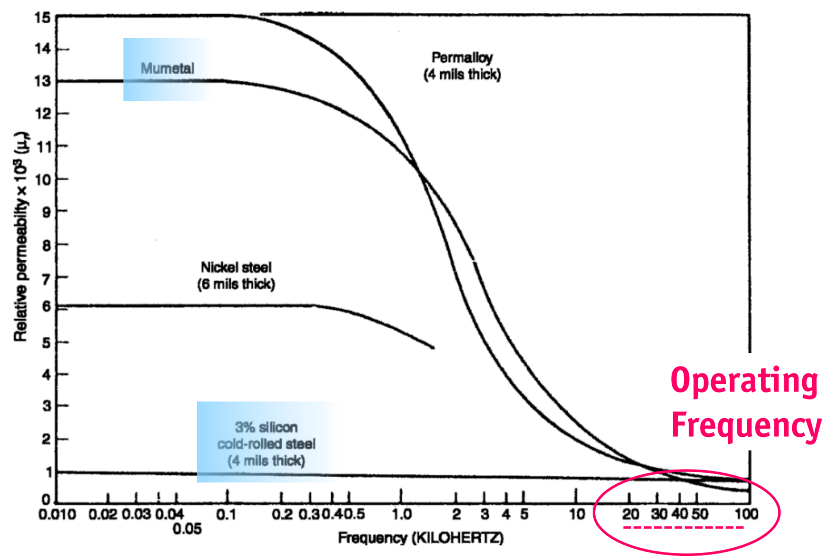

▲ **Frequency dependency of ferromagnetic materials**

H. W. Ott, Noise Reduction Techniques in Electronic Systems, 2nd ed., Wiley- Interscience, New York, 1988.

Multi-Objective Optimization of High-Power IPT Systems

Requirements & Limits
Optimization Method
Trade-Off Analysis

► Multi-Objective Optimization of 5 kW Prototype (1)

■ Design of a 5 kW Prototype System with Maximum Possible Performance

- Use Component Models to Analyze Mapping from Design Space into Performance Space

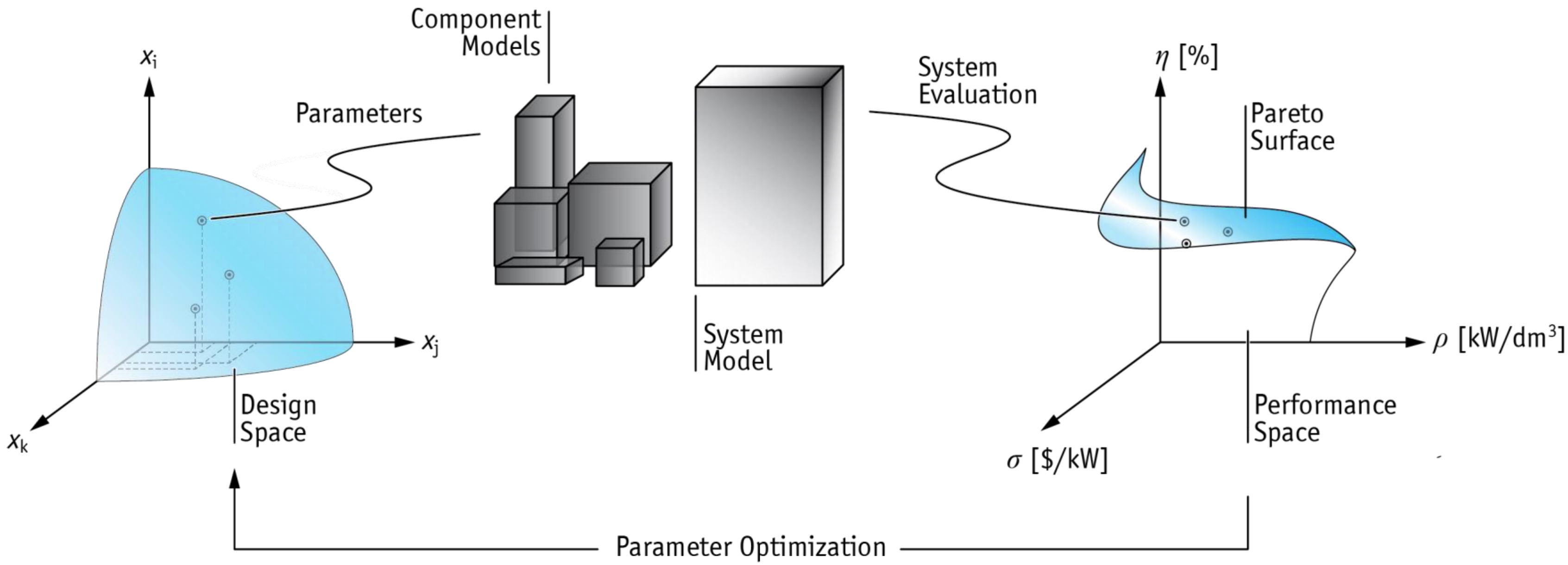

- Coil Dimensions
- Winding Scheme
- Number of Turns
- Litz Wire Design
- Core Design
- Core Material

- AC-Losses
- Magnetic Fields
- Capacitor Losses
- Converter Losses
- Component Cost
- Component Size

- Efficiency $\eta = P_{out}/P_{in}$ [%]
- Power Density $\rho = P_{out}/V_{tot}$ [kW/dm^3]
- Stray Field $\beta = B_{max}/B_{norm}$ [%]
- Tolerance $\delta = \Delta x/D_{coil}$ [%]
- Specific Cost $\gamma = C_{tot}/P_{out}$ [$/kW]
- Material Effort $\sigma = kg_{Cu/Fe}/P_{out}$ [kg/kW]

▶ Multi-Objective Optimization of 5 kW Prototype (2)

■ Design Process Taking All Performance Aspects into Account

■ System Specification

- Input Voltage 400 V
- Battery Voltage 350 V
- Output Power 5 kW
- Air Gap 50 mm

■ Constraints / Side Conditions

- Thermal Limitations [°C]
- Stray Field Limitations [μT]
- Max. Construction Vol. [m^3]
- Switching Frequency [kHz]

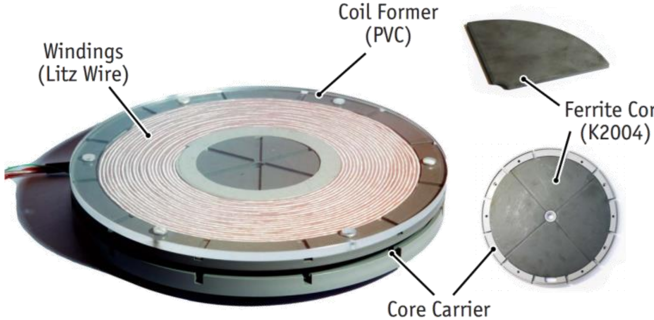

■ System Performance

- Efficiency $\eta = P_{out}/P_{in}$ [%]
- Power Density $\alpha = P_{out}/A_{coil}$ [kW/dm^2]
- Stray Field $\beta = B_{max}/B_{norm}$ [%]

R. Bosshard, J. W. Kolar, J. Mühlethaler, I. Stevanovic, B. Wunsch, F. Canales, "Modeling and η-α-Pareto optimization of inductive power transfer coils for electric vehicles," *IEEE J. Emerg. Sel. Topics Power Electron.*, vol. 3, no. 1., pp.50-64, March 2015.

η-α-Pareto Coil Optimization

► η-α-Pareto Coil Optimization (1)

- **Determine Physical Performance Limits and Study Design Trade-Offs**
  - Analysis of the η-α-Pareto Front

- **Evaluation of Design Options in an Iterative Optimization Procedure**
  - Evaluation of Component Models for Power Losses, Thermal Feasibility, Stray Field Limits, etc.

- **Degrees-of-Freedom:**
  - Coil Dimensions
  - Litz Wire Dimensions
  - Number of Turns
  - Operating Frequency

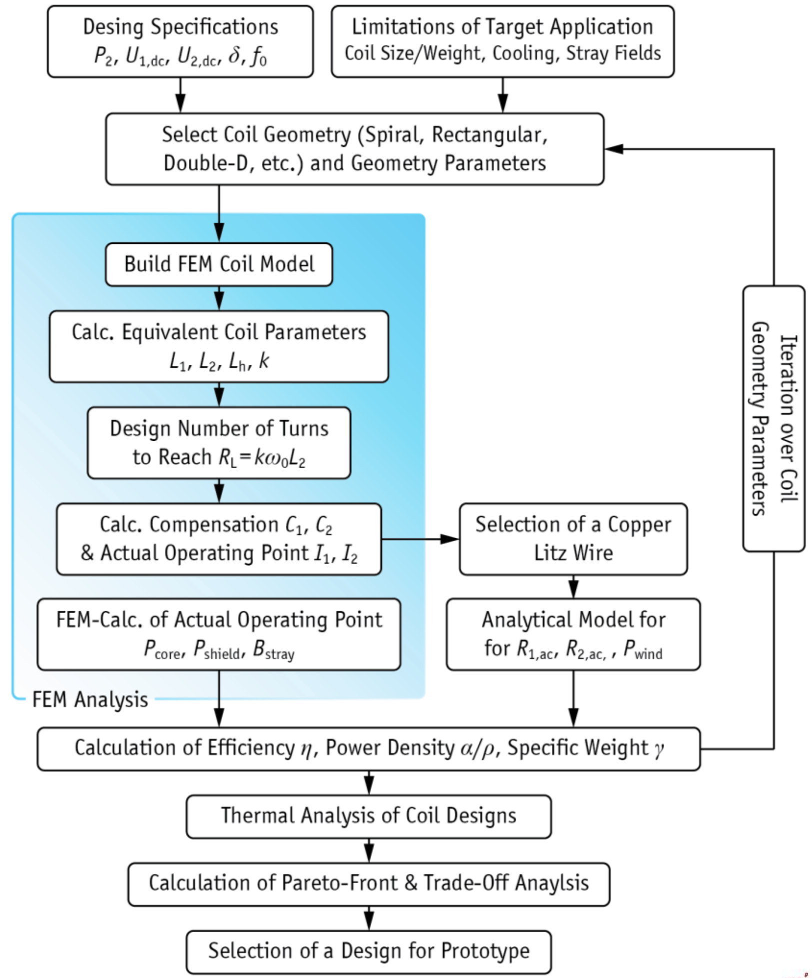

► η-α-Pareto Coil Optimization (2)

■ **Degrees-of-Freedom:**

- Coil Dimensions
- Litz Wire Dimensions
- Number of Turns
- Operating Frequency

Design Space

Component Models

System Model

Performance

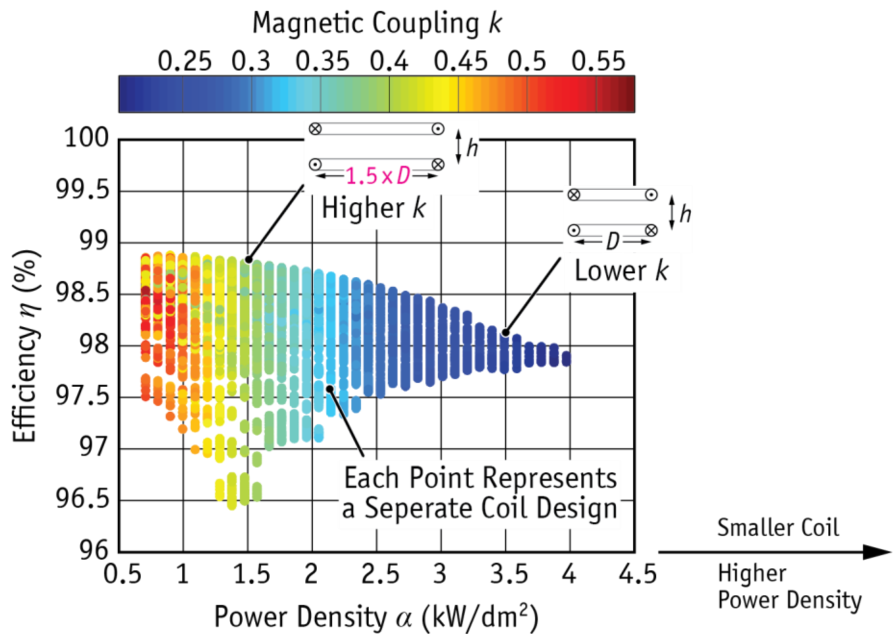

▲ **Efficiency vs. Power Density of >12k IPT Coils with 5 kW Output Power**

► η-α-Pareto Coil Optimization: Pareto Front

■ **Degrees-of-Freedom:**
- Coil Dimensions
- Litz Wire Dimensions
- Number of Turns
- Operating Frequency

■ ***η-α*-Pareto Front**
- Physical Performance Limit
- Trade-Off: Coil Size vs. Efficiency

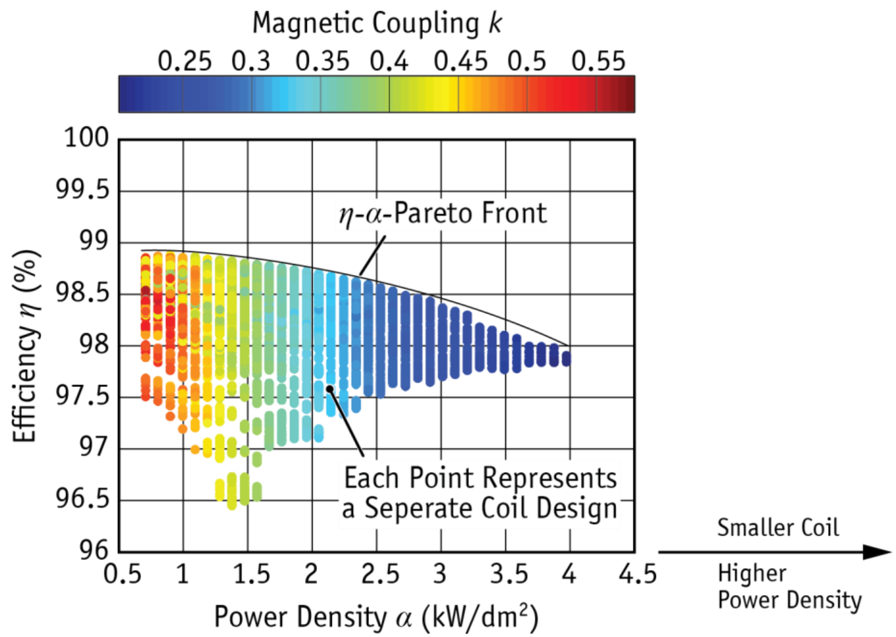

▲ **Efficiency vs. Power Density of >12k IPT Coils with 5 kW Output Power**

► η-α-Pareto Coil Optimization: Thermal Limit

- **Degrees-of-Freedom:**
  - Coil Dimensions
  - Litz Wire Dimensions
  - Number of Turns
  - Operating Frequency

- **η-α-Pareto Front**
  - Physical Performance Limit
  - Trade-Off: Coil Size vs. Efficiency

- **Thermal Limit**
  - Limited Thermal Power Dissipation Capability for Given Coil Size
  - Lower Limit on Efficiency

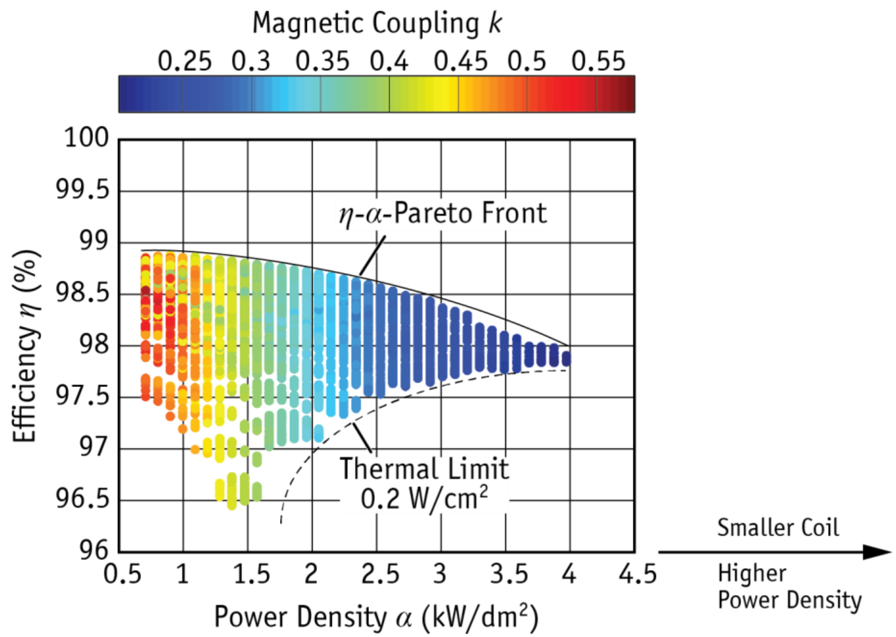

▲ **Efficiency vs. Power Density of >12k IPT Coils with 5 kW Output Power**

► η-α-Pareto Coil Optimization: Key Results (1)

■ **Analysis of Result Data to Understand Relevant Design Trade-Offs**
- Confirm Predictions of Analytical Models and Estimations → *FOM = kQ*
- Identify Key-Parameters that Impact System Performance → High Frequency

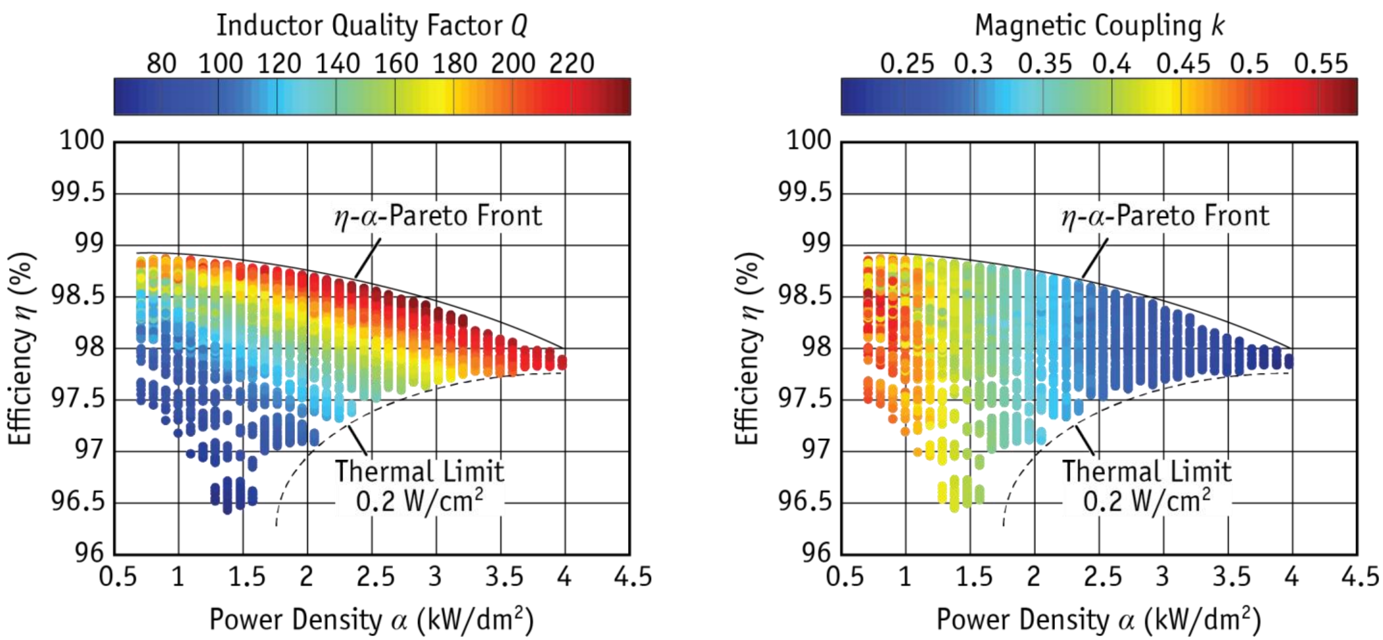

▲ **Trade-Off Analysis with Result Data: Effect of Quality Factor and Magnetic Coupling**

→ **Efficiency depends on *FOM = kQ*: Can be High even if *k* is Low, if instead *Q* is!**

► η-α-Pareto Coil Optimization: Key Results (2)

- **Analysis of Result Data to Understand Relevant Design Trade-Offs**
  - Confirm Predictions of Analytical Models and Estimations → *FOM = kQ*
  - Identify Key-Parameters that Impact System Performance → High Frequency

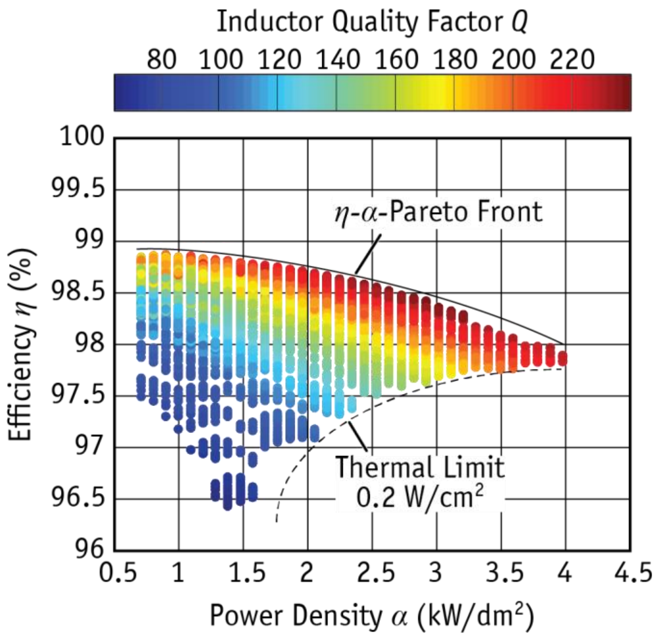

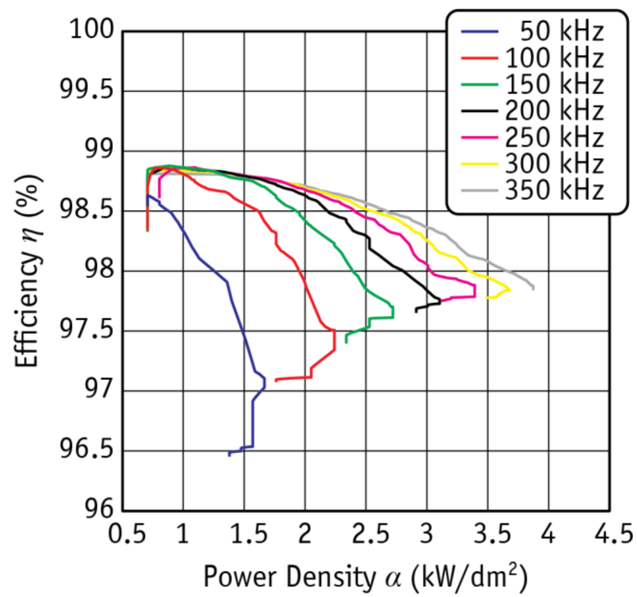

- **High *Q* Results from High Transmission Frequency of IPT System**

▲ **Calculated Efficiency vs. Power Density, divided by Transmission Frequency**

▶ Efficiency at High-Frequency Transmission

■ **Reduced Winding Losses due to Lower Number of Turns in Transmission Coils**

- Design Condition $R_{\mathrm{L,opt}} \approx k\omega_0\sqrt{L_1 L_2}$ allows Lower L_1, L_2 at Higher ω_0
- Reduction of Flux leads to Slow Increase of Core Losses
- Core & Capacitor Losses are Limiting Factors for High Frequency Operation

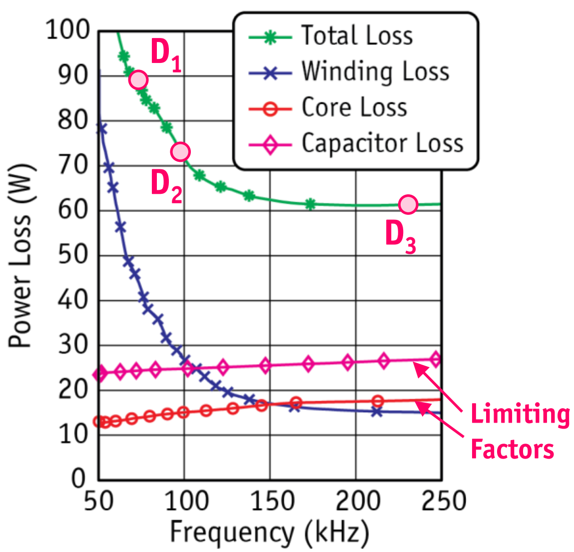

▲ **Power Loss Breakdown at 1.47 kW/dm²**
(Power Density of 5 kW Prototype)

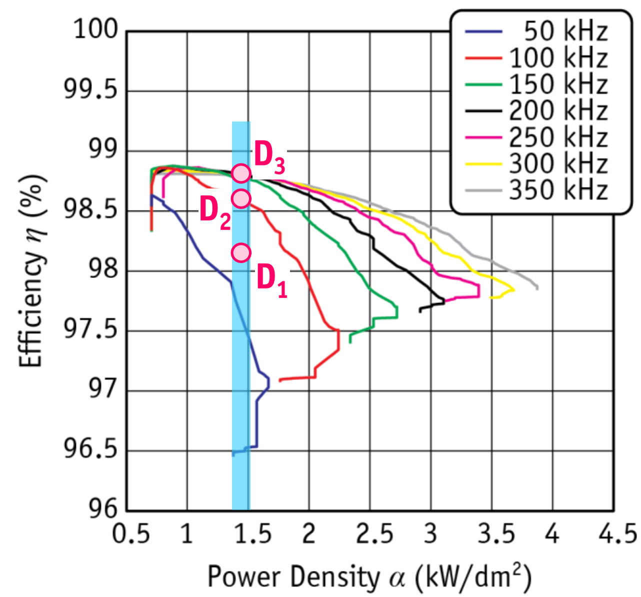

▲ **Calculated Efficiency vs. Power Density, divided by Transmission Frequency**

▶ High-Frequency Transmission & Stray Field

■ Effects of Higher Transmission Frequency

- Scaling Law: $U_L = N\frac{d\phi}{dt} = N\omega\hat{\phi} \propto \omega\hat{B}A_{coil}$
- Smaller Coil Area Possible for Same Voltage U_L
- Lower Flux Density Possible for Same Voltage U_L

■ Encountered Design Trade-Offs:

- Coil Size vs. Efficiency
- Coil Size vs. Stray Field
- Frequency vs. Stray Field

→ Take all Aspects into Account when Selecting Coil Design!

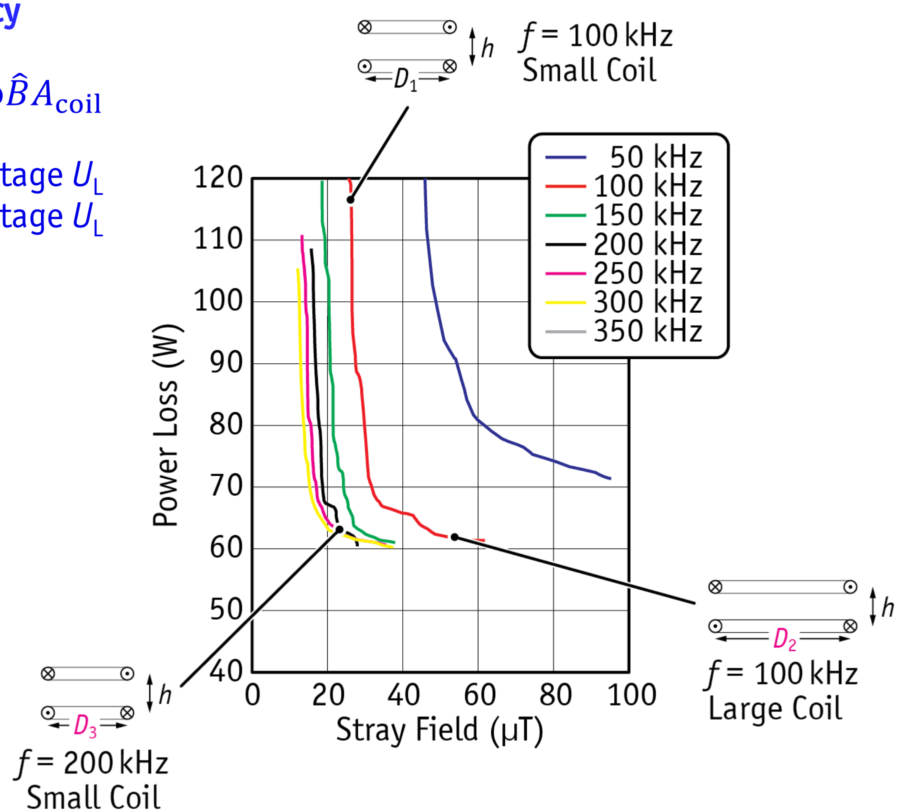

▲ Calculated Losses vs. Stray Field at 30 cm Distance from Coil Center

► Selected Design for 5 kW Prototype System

■ Selection of Transmission Frequency for Prototype System

- Significant Improvements up to 100 kHz, then Slower Loss Reduction
- Power Electronics Design with Standard Products, e.g. Litz Wire (630 x 71 μm)

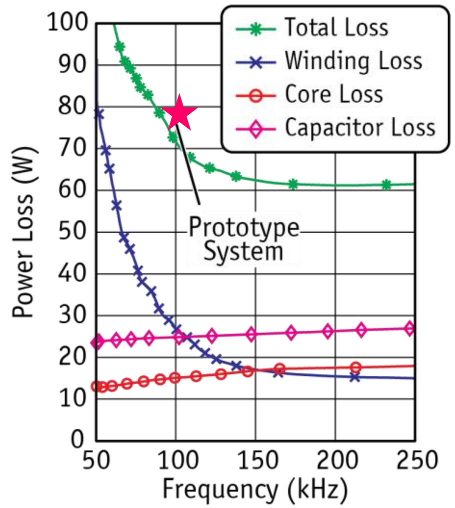

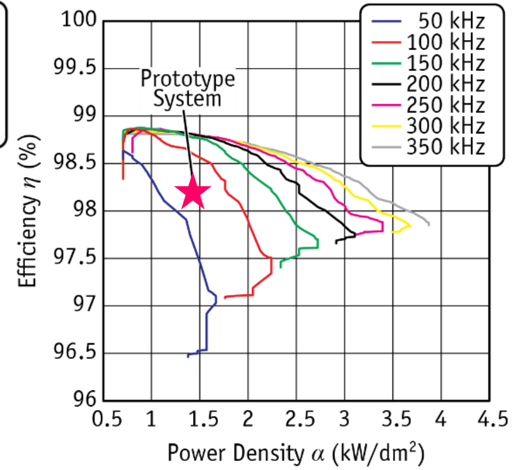

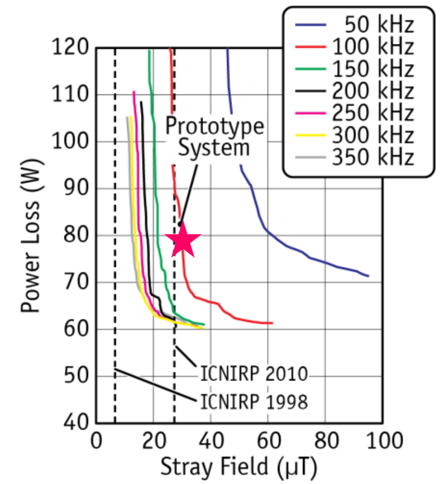

■ 5 kW Prototype IPT System

- **Coil Diameter** **210 mm**
- **Trans. Frequency** **100 kHz**
- **Trans. Efficiency** **98.25% @ 52 mm Air Gap**
- **Power Density** **1.47 kW/dm²**
- **Stray Field** **26.16 μT**
- **Cooling System** **Forced-Air**

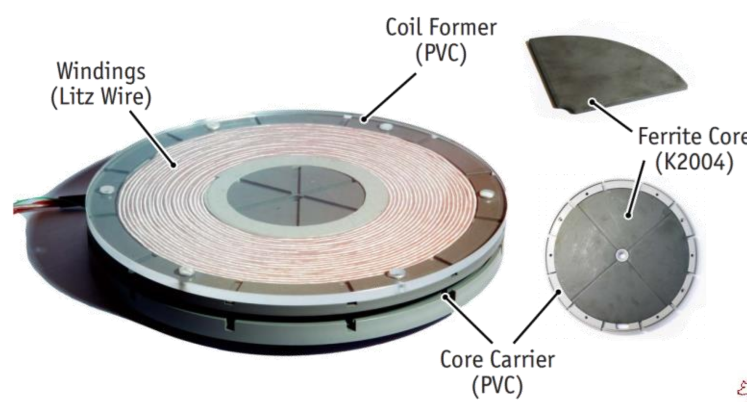

► Resonant Converter for 5 kW Testing

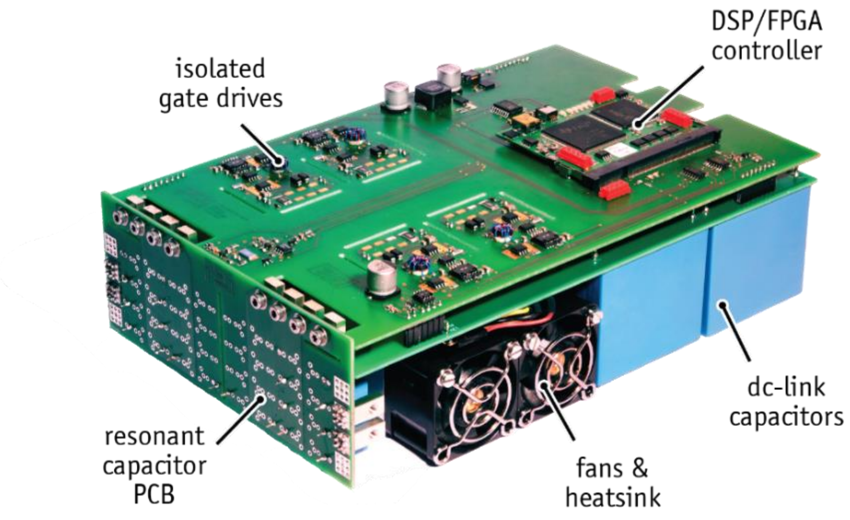

▲ 5 kW Prototype Power Converter

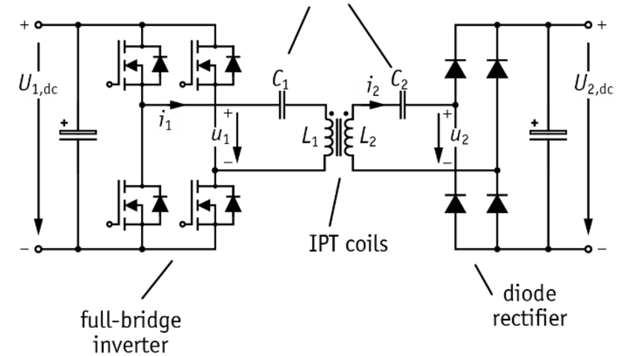

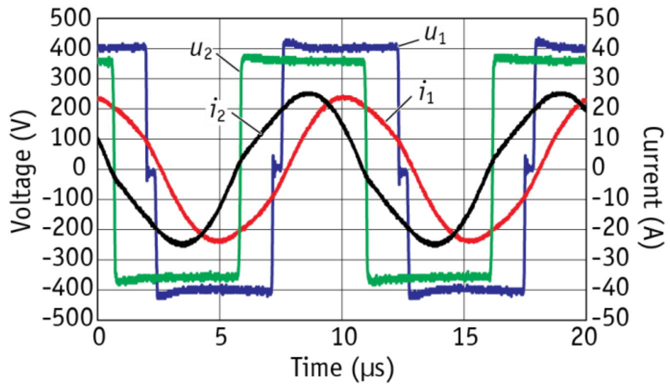

▲ Measured Waveforms at 5 kW / 400 V

■ **Full-Bridge Test-Inverter 5 kW @ 400-800 V**
- Cree 1.2 kV SiC MOSFETs (42 A, 100 kHz)
- DSP/FPGA-Based Control
- Film Capacitors for DC-Link

▶ DC-to-DC Power Loss Measurement

■ Difficult to Measure V/I-Phase Shift at High Frequency (100 kHz)

- Indirect Measurement of DC Input and Output Power

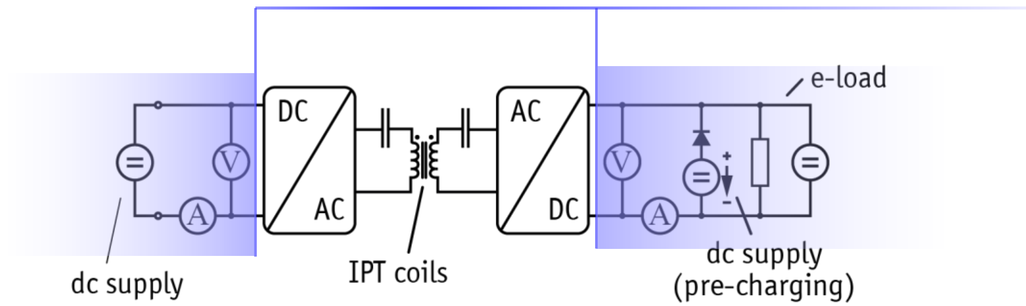

▲ Efficiency Measurement Setup

▲ Yokogawa WT3000

■ Efficiency Measurement

- Maximum Efficiency of 96.5%
- Higher than 96% down to 1 kW
- Flat Efficiency-Curve because of DC-Link Voltage Control

- 30% Winding & Core Losses
- 30% Capacitor Losses
- 30% Semiconductor Losses

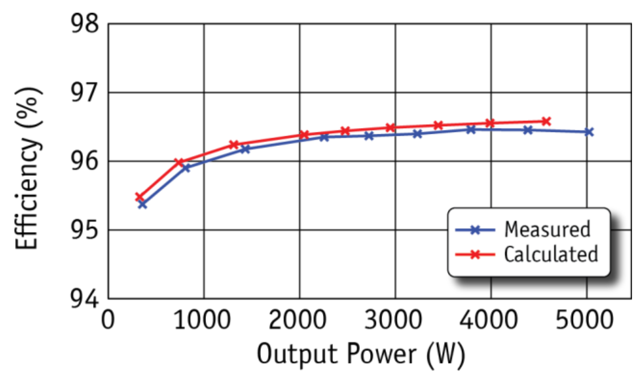

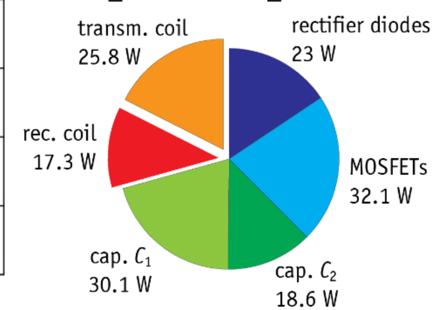

Application to Design of 50 kW Prototype System

► Demonstrator Systems: 5 and 50 kW Output Power

■ 5 kW System for Model Development
- Output Power 5 kW @ 400 V, 100 kHz with Forced-Air Cooling
- Lab-Scale Coil and Converter Size (210 mm Diameter / 50 mm Air Gap)
- Basic Geometry for Simplified Modeling
- Verification of Calculation & Optimization

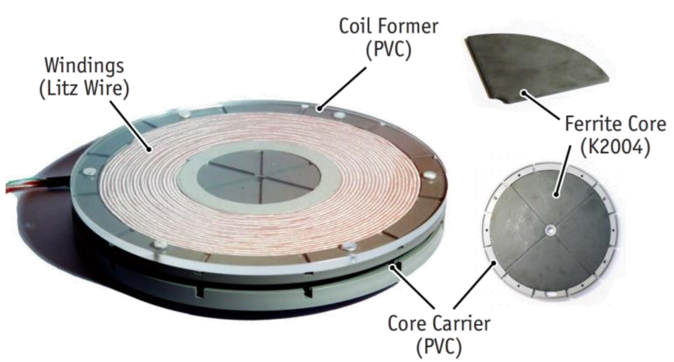

R. Bosshard, J. W. Kolar, J. Mühlethaler, I. Stevanovic, B. Wunsch, F. Canales, "Modeling and η-α-Pareto optimization of inductive power transfer coils for electric vehicles," *IEEE J. Emerg. Sel. Topics Power Electron.*, vol. 3, no. 1., pp.50-64, March 2015.

■ 50 kW Prototype System for EV Specs
- Output Power 50 kW @ 800 V, 85 kHz with Forced-Air Cooling
- Optimized Geometry for EV Charging (450 x 750 x 60 mm, 25 kg)
- Experimental Verification

► Pareto Optimization of the 50 kW Prototype System (1)

■ **Fixed Parameters:**
- Resonant Frequency 85 kHz (Upcoming Standard SAE J2954)
- Litz Wire Parameters (2500 x 0.1mm)
- Core Material (Ferrite K2004)

■ **Degrees of Freedom:**
- Number of Core Rods N_{cores}
- Breath of Copper Winding w_{cu}
- Overlap of Core rods d_{core}
- Outer Coil Dimensions (w_{coil}, l_{coil})

■ **Simplifications:**
- Identical Transmitter & Receiver Coils
- Vehicle Chassis Not Considered

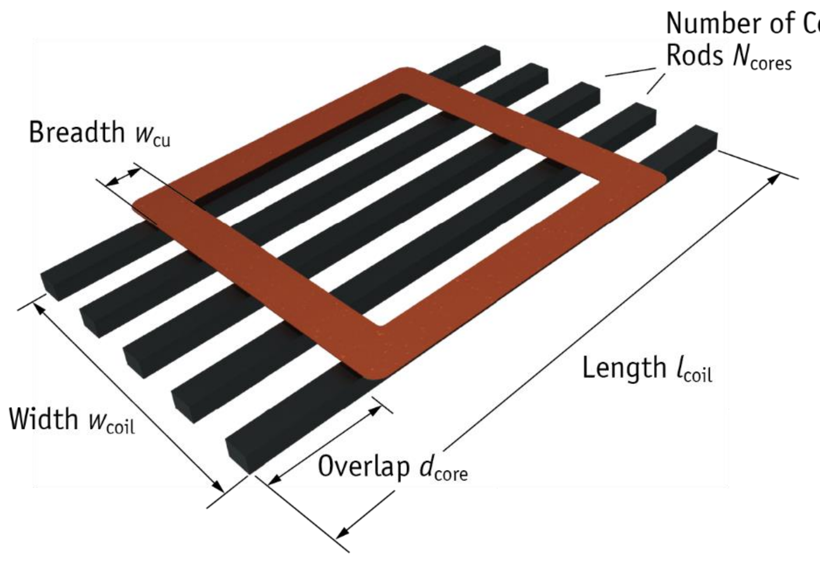

▶ Pareto Optimization of the 50 kW Prototype System (2)

Fixed Parameters:
- Resonant Frequency 85 kHz (Upcoming Standard SAE J2954)
- Litz Wire Parameters (2500 x 0.1mm)
- Core Material (Ferrite K2004)

Degrees of Freedom:
- Number of Core Rods N_{cores}
- Breath of Copper Winding w_{cu}
- Overlap of Core rods d_{core}
- Outer Coil Dimensions (w_{coil}, l_{coil})

Simplifications:
- Identical Transmitter & Receiver Coils
- Vehicle Chassis Not Considered

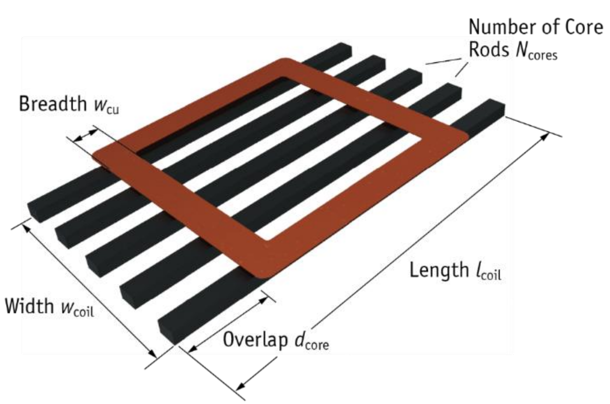

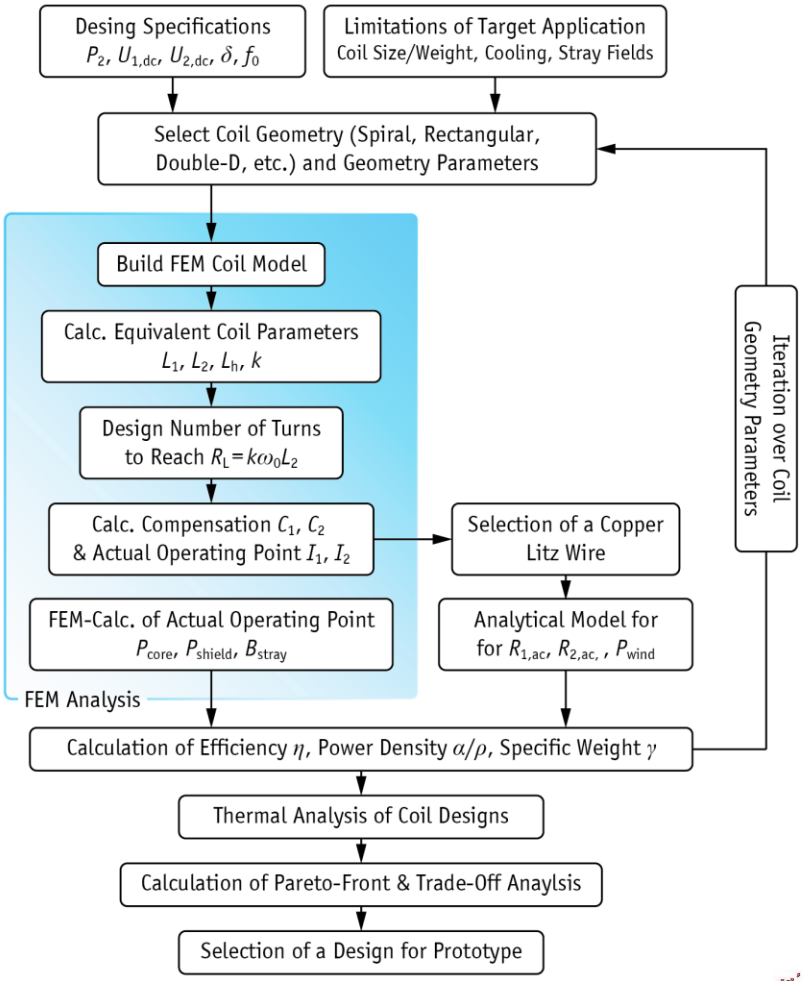

► Pareto Optimization of the 50 kW Prototype System (3)

■ Fixed Parameters:
- Resonant Frequency 85 kHz (Upcoming Standard SAE J2954)
- Litz Wire Parameters (2500 x 0.1mm)
- Core Material (Ferrite K2004)

■ Degrees of Freedom:
- Number of Core Rods N_{cores}
- Breath of Copper Winding w_{cu}
- Overlap of Core rods d_{core}
- Outer Coil Dimensions (w_{coil}, l_{coil})

■ Simplifications:
- Identical Transmitter & Receiver Coils
- Vehicle Chassis Not Considered

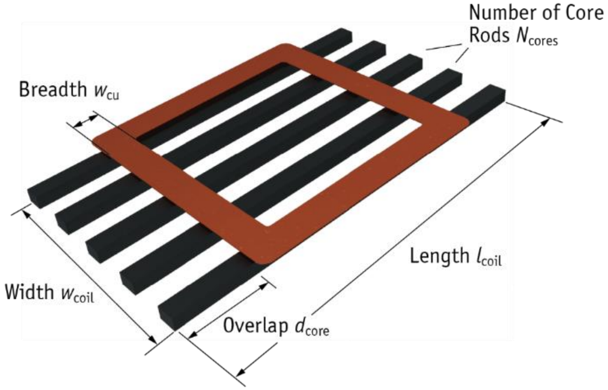

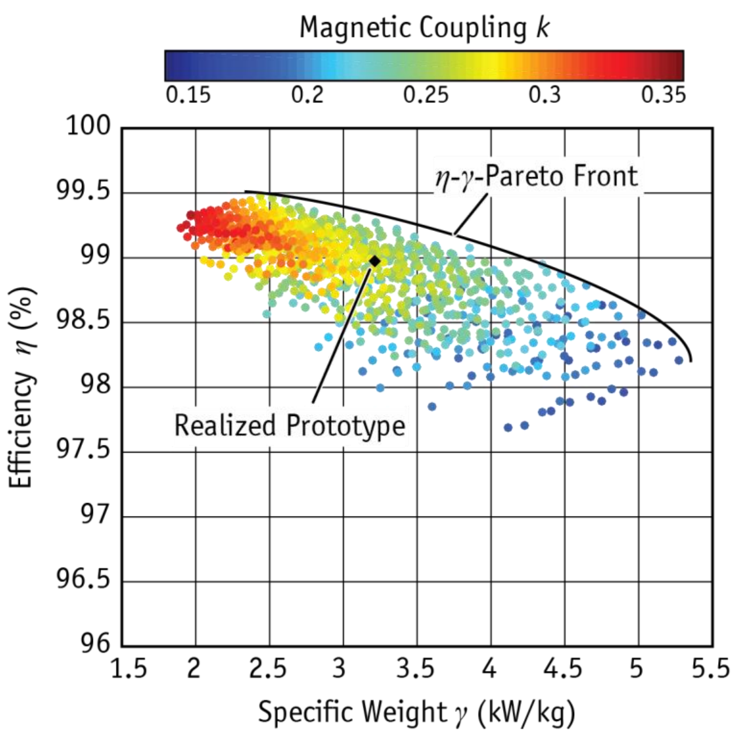

▲ **Results of 3D-FEM Simulations**

► Analysis of Design Parameters (1)

■ Fixed Parameters:

- Resonant Frequency 85 kHz (Upcoming Standard SAE J2954)
- Litz Wire Parameters (2500 x 0.1mm)
- Core Material (Ferrite K2004)

■ Degrees of Freedom:

- Number of Core Rods N_{cores}
- Breath of Copper Winding w_{cu}
- Overlap of Core rods d_{core}
- Outer Coil Dimensions (w_{coil}, l_{coil})

■ Simplifications:

- Identical Transmitter & Receiver Coils
- Vehicle Chassis Not Considered

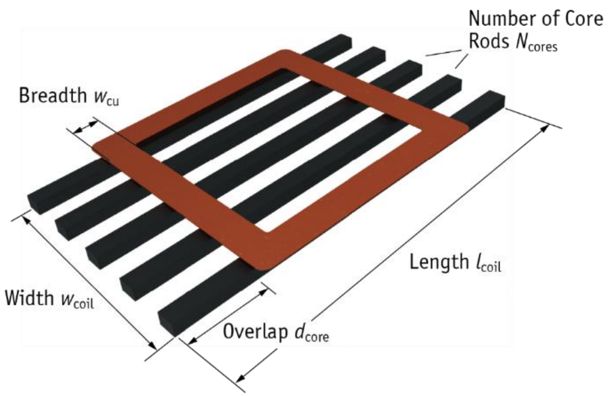

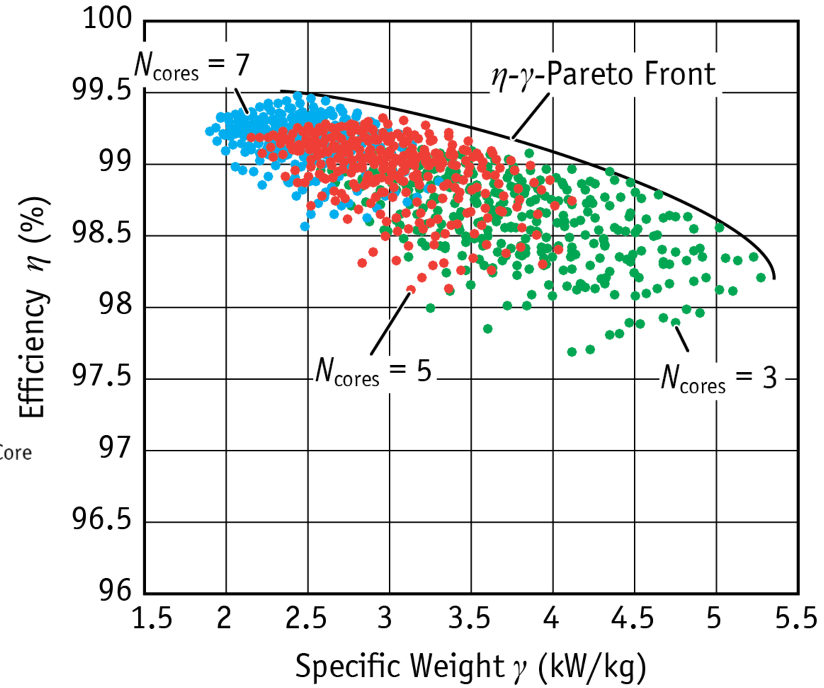

▲ **Results of 3D-FEM Simulations**

► Analysis of Design Parameters (2)

■ **Fixed Parameters:**
- Resonant Frequency 85 kHz (Upcoming Standard SAE J2954)
- Litz Wire Parameters (2500 x 0.1mm)
- Core Material (Ferrite K2004)

■ **Degrees of Freedom:**
- Number of Core Rods N_{cores}
- Breath of Copper Winding w_{cu}
- Overlap of Core rods d_{core}
- Outer Coil Dimensions (w_{coil}, l_{coil})

■ **Simplifications:**
- Identical Transmitter & Receiver Coils
- Vehicle Chassis Not Considered

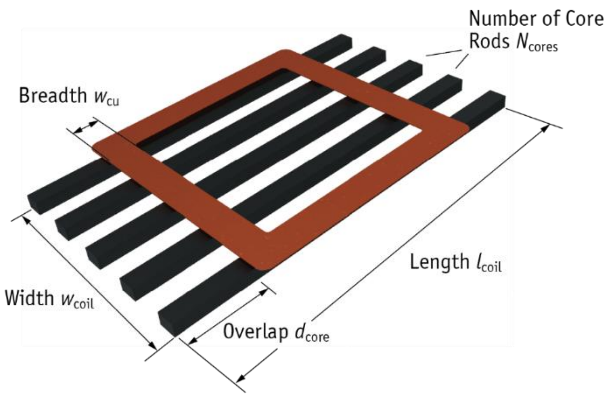

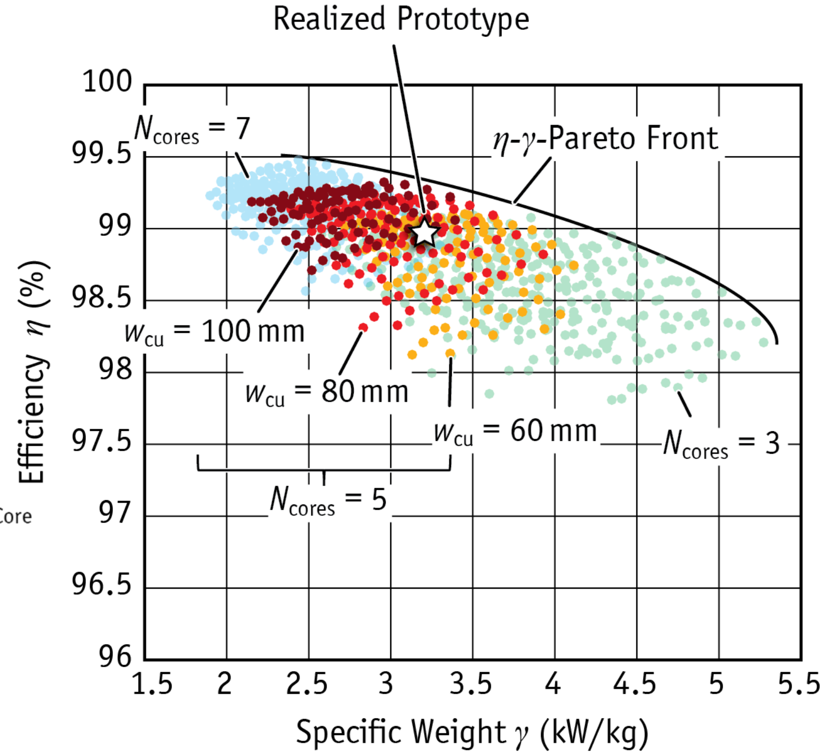

▲ **Results of 3D-FEM Simulations**

► Effect of the Transmission Frequency (1)

- **Resonant Frequency 85 kHz in Upcoming Standard SAE J2954**
  - Analyze Benefit from of Lower (50 kHz) or Higher (120 kHz) Transmission Frequency

- **η-γ-Pareto Front for 50 kHz Slightly below Pareto Front for 85 kHz**

- **Very Similar η-γ-Pareto Front for 85 kHz 120 kHz**

→ **Further Increase Above 85 kHz Shows Only Small Improvement**

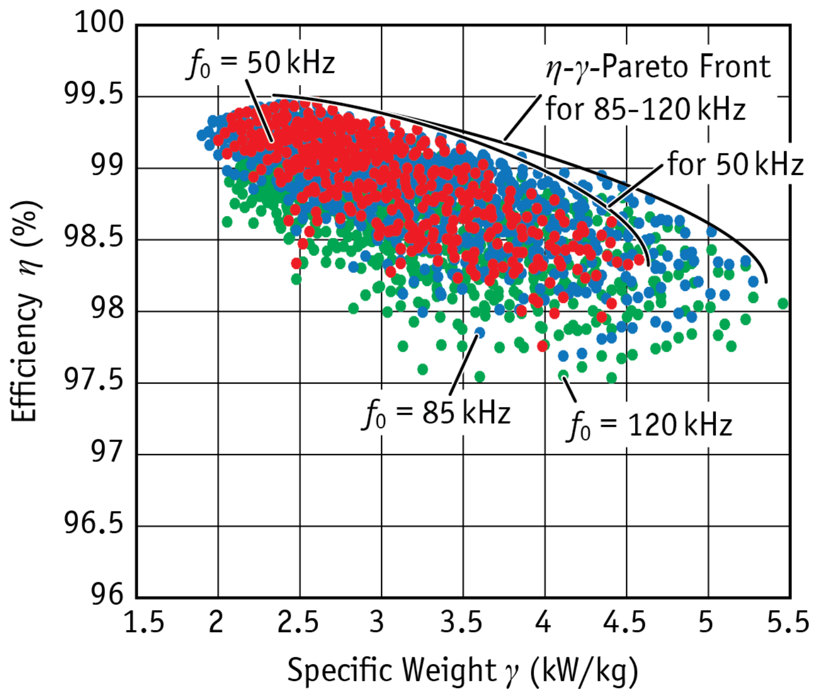

▲ **Results of 3D-FEM Simulations**

► Effect of the Transmission Frequency (2)

■ Sweep Over Transmission Frequency for Prototype Design

- Decreasing Power Losses in the Transmission Coils
- Reasons: Lower Inductance & Flux, Fewer Turns/Shorter Wires
- Significant Improvements Only Up to Approx. 50 kHz

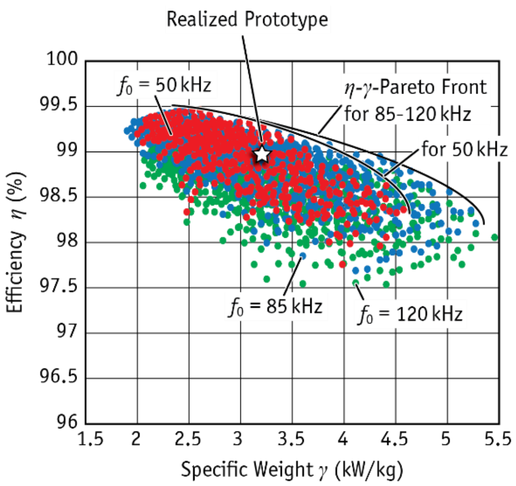

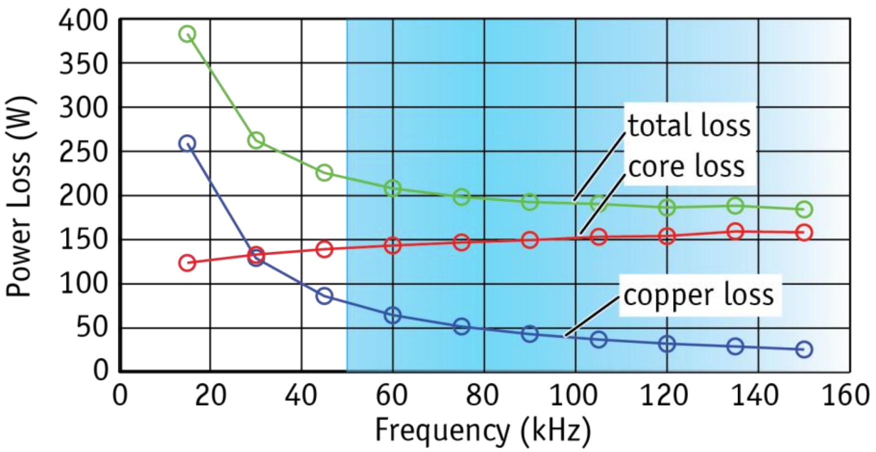

▲ **Calculated Coil Losses in Function of the Transmission Frequency of the Designs**

► Effect of the Transmission Frequency (3)

■ **Sweep Over Transmission Frequency for Prototype Design**
- Decreasing Stray Field at Higher Frequency
- Reasons: Reduced Flux for Equal Output Power
- Stray Field Norm @ 1 m from Coil Center above 70 kHz

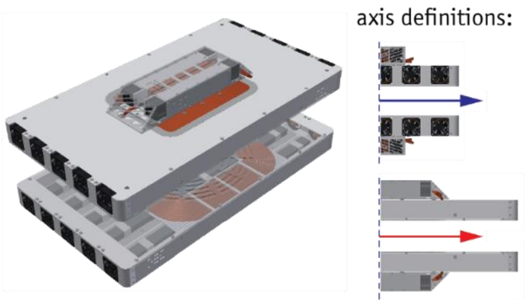

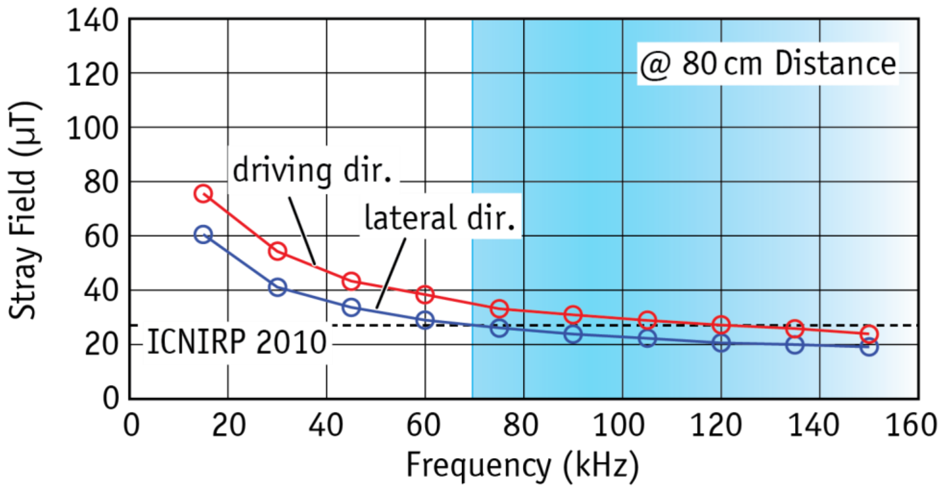

▲ **Calculated Stray Field in Function of the Transmission Frequency of the Designs**

► 50 kW IPT: Prototype Hardware

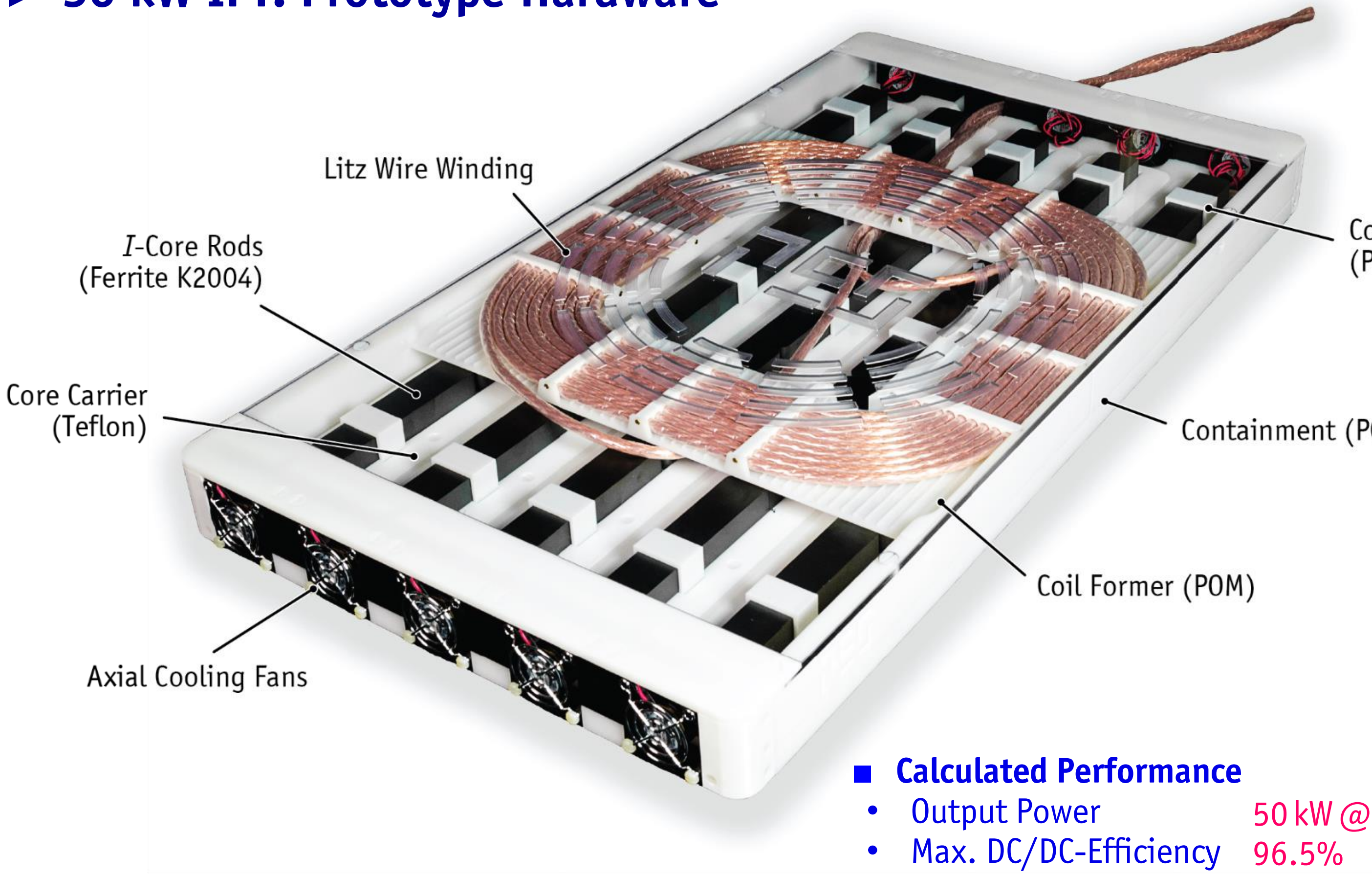

■ **Calculated Performance**

Output Power	50 kW @ 800 V, 85 kHz
Max. DC/DC-Efficiency	96.5%
Coil Dimensions	41 x 76 x 6 cm
Coil + Cap. Weight	24.6 kg

▶ Estimated DC-to-DC Performance

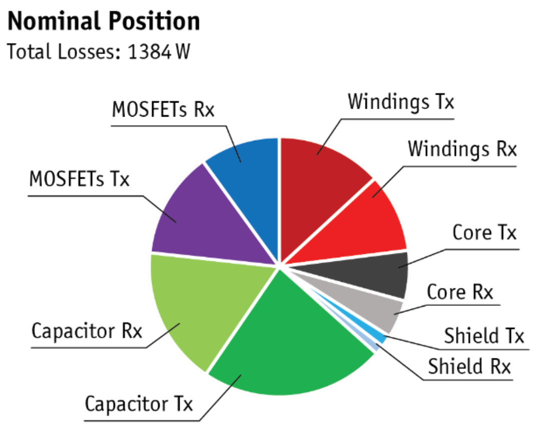

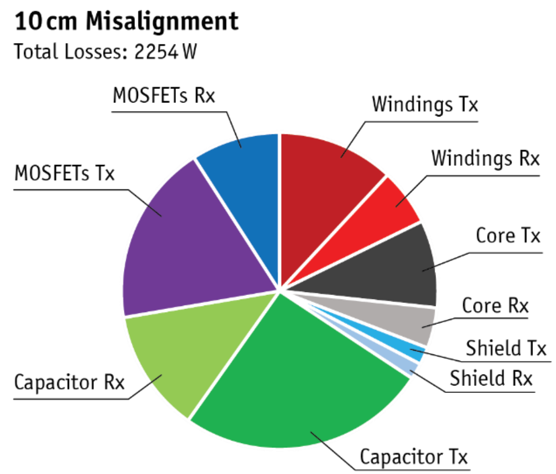

- **Calculated Performance**
  - Output Power 50 kW
  - Maximum Efficiency 95.2% ... 96.5 %
  - Coil Dimensions 41x76x6 cm
  - Weight (Coil + Cap) 25.7 kg
  - Power Density 2.7 kW/l, 1.9 kW/kg

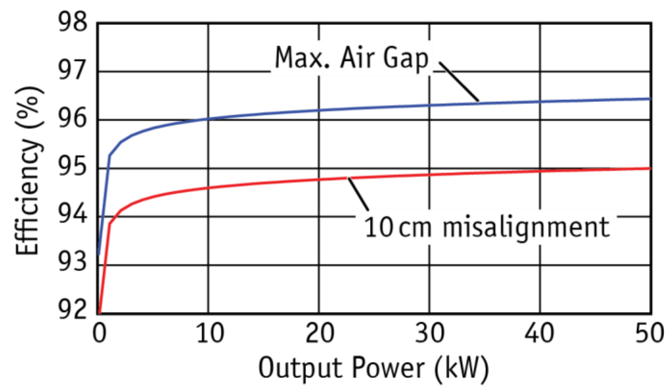

▲ **Calculated efficiency over output power for control with variable DC-link voltage**

Comparison to Double-D Coil

► Comparison: Rectangular Prototype vs. Double-D Coil

Lexus, www.lexus.com

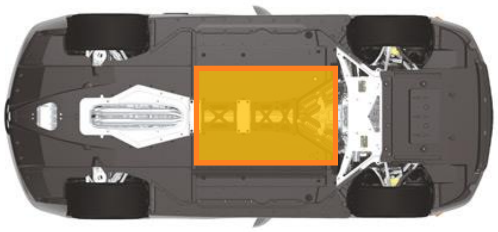

■ **Which Performance is Achieved within Same Footprint?**
- DD Coil Designed to Fit into Housing of Existing Rectangular 50 kW Prototype
- Equal Electrical Interface and Transmission at 85 kHz
- Optimized for Maximum Efficiency

▲ **Realized 50 kW Prototype IPT Coil**

vs.

▲ **50 kW DD-Prototype Optimized for same Footprint**

► Magnetic Coupling for Equal Footprint

- **Evaluation of Magnetic Coupling for Ideal and Misaligned Coil Positions**
  - 3D-FEM Simulation Results in Frequency Domain

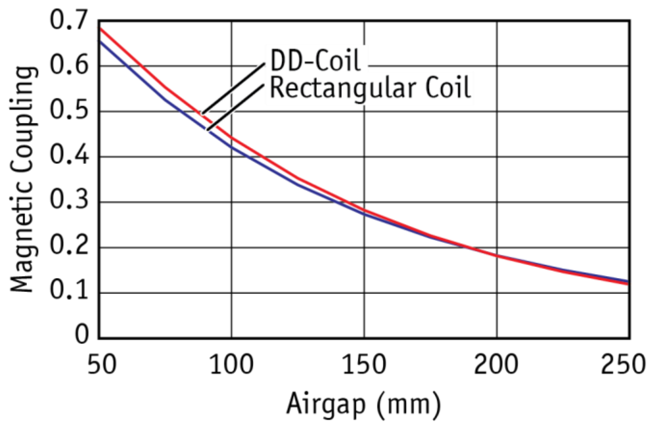

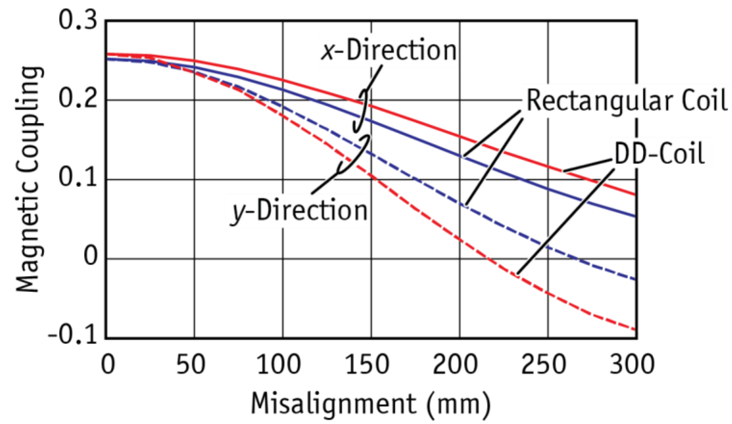

- **Rectangular and Double-D Coil Achieve Equal Coupling at Ideal Positioning**

- **Coil Positioning Tolerance:**
  - DD-Coil Better in *x*-Direction
  - Rect.-Coil Better in *y*-Direction

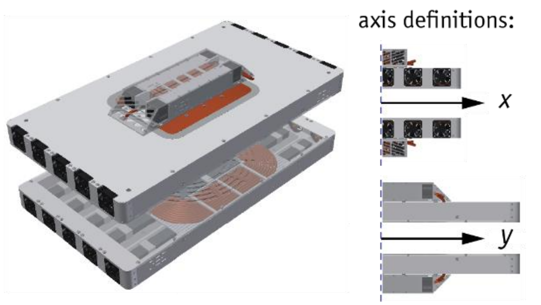

► Core Losses in Double-D Coil Design

■ Double-D has Higher Flux Density in Central Cores

- High Core Losses in Coil Center due to High Ampère-Turns
- Additional Core Elements Required to Reduce Flux Density
- No Additional Eddy-Current Shield on Top/Bottom Needed

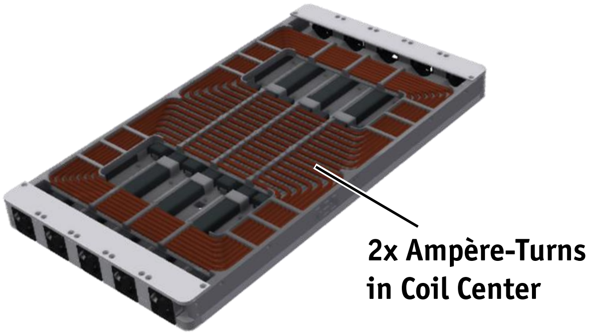

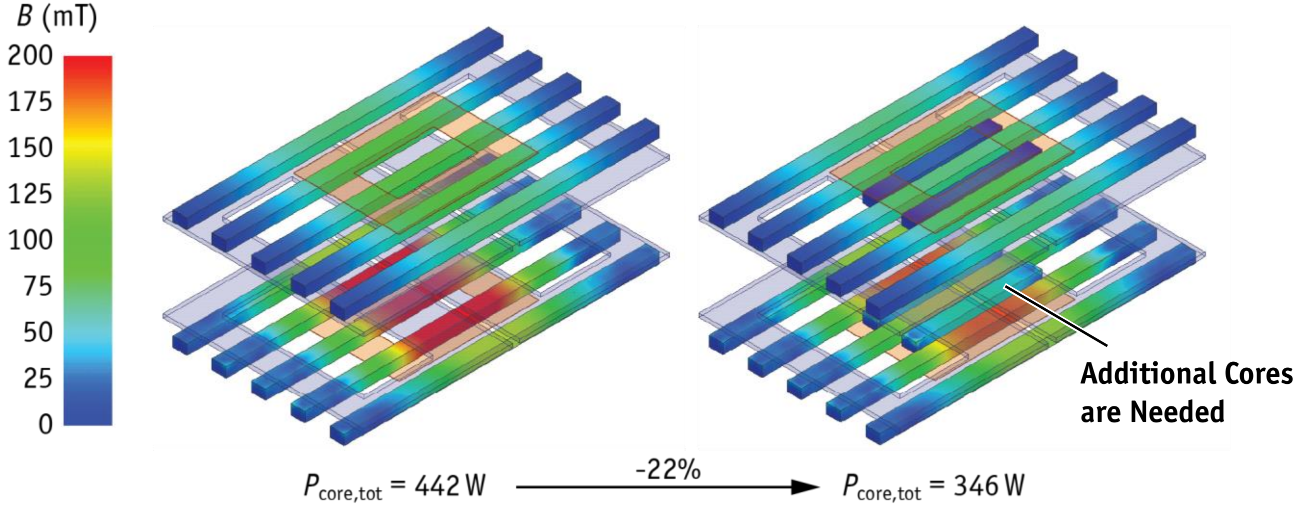

▲ FEM Simulation Results without (left) and with (right) additional cores for flux density / core loss reduction in coil center

► Pareto Fronts for Rectangular and Double-D Coil (1)

- **Rectangular Coil Designs are Lighter and Reach Higher Efficiency**
  - Main Reason are High Core Losses in Central Part of Double-D Transmitter & Receiver Coil

- **Double-D Coil Designs have Lower Stray Field Compared to Rectangular Designs**
  - Main Reason is Integration of Return Path for Flux in Main Coil Structure

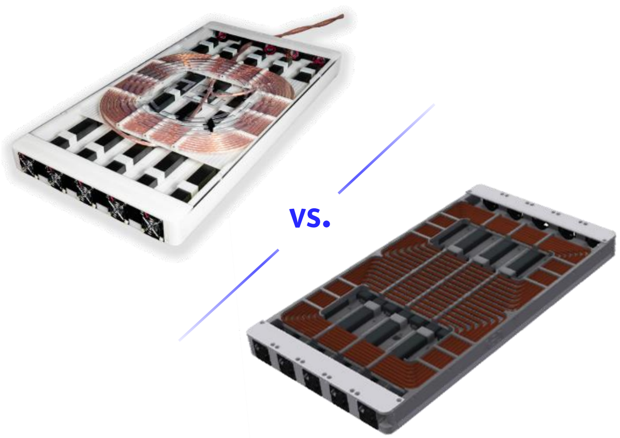

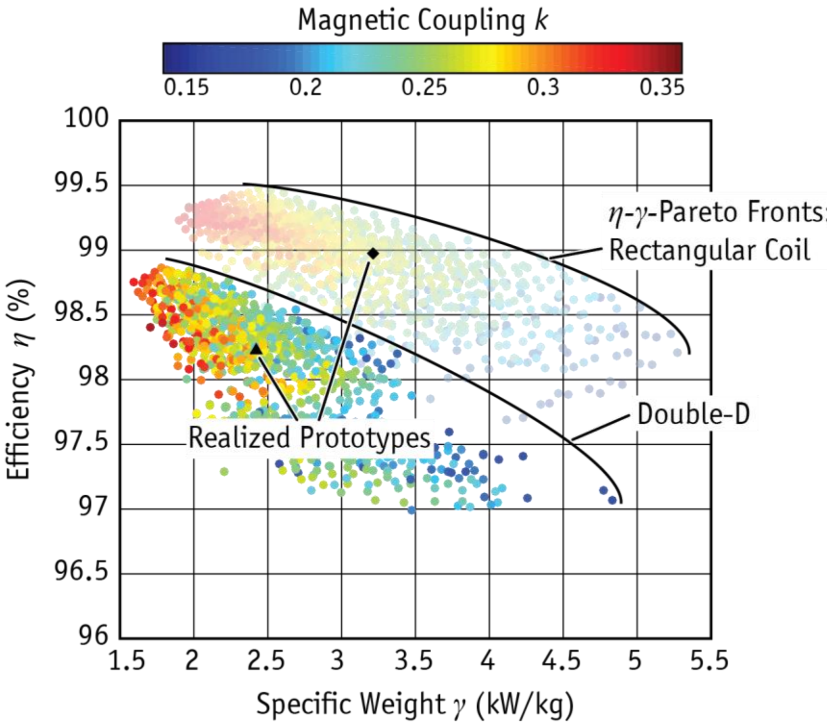

▲ **Results of 3360 3D-FEM Simulations**

► Pareto Fronts for Rectangular and Double-D Coil (2)

■ **Rectangular Coil Designs are Lighter and Reach Higher Efficiency**
- Main Reason are High Core Losses in Central Part of Double-D Transmitter & Receiver Coil

■ **Double-D Coil Designs have Lower Stray Field Compared to Rectangular Designs**
- Main Reason is Integration of Return Path for Flux in Main Coil Structure

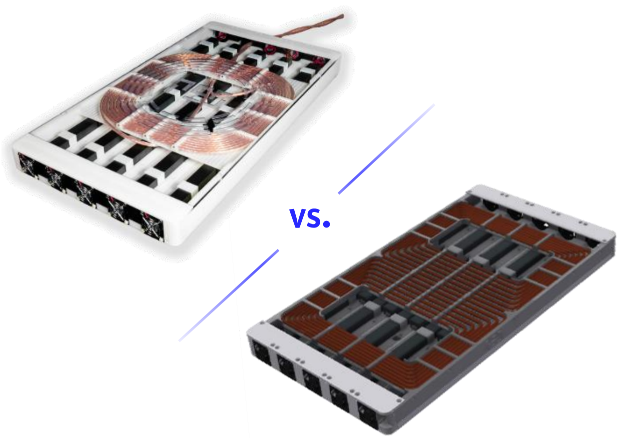

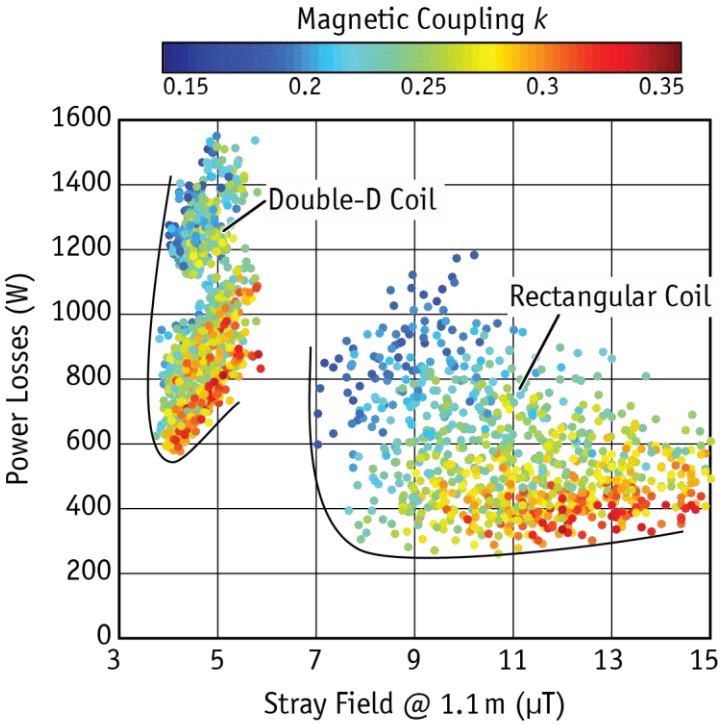

▲ **Results of 3360 3D-FEM Simulations**

► Comparison: Power Losses of the Selected Prototypes

- **Double-D has Higher Core Losses in Central Core Elements due to High Core Flux Density**
  - But does not Require Additional Eddy-Current Shield that is used in Rectangular Design
  - Power Losses in Remaining Parts are Comparable, Since Coupling is almost Equal

→ Calculated Efficiency of Rectangular and Double-D Coil is very Similar
→ Additional Cores were needed for Double-D → Higher Weight: +1.2 kg / +5%

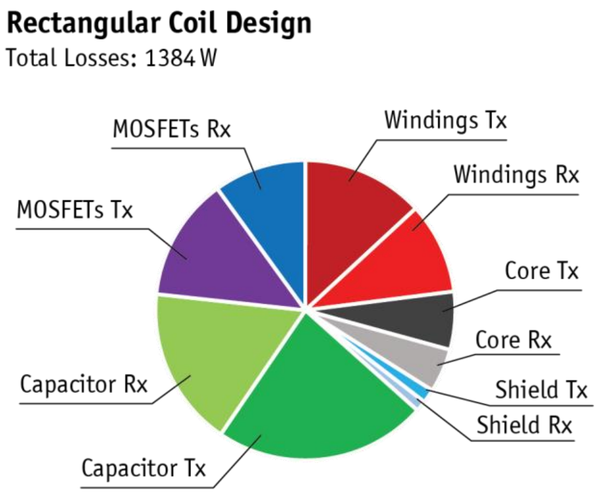

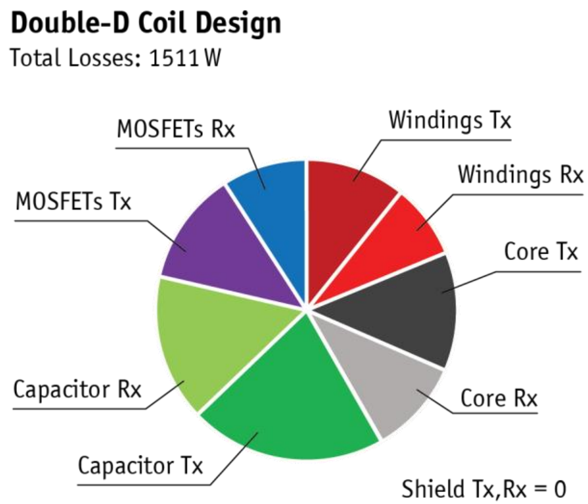

▶ Comparison: Stray Field of the Selected Prototypes

■ Magnetic Stray Field in at Specified Reference Position

- Note: Coils are Designed for Same Operating Frequency

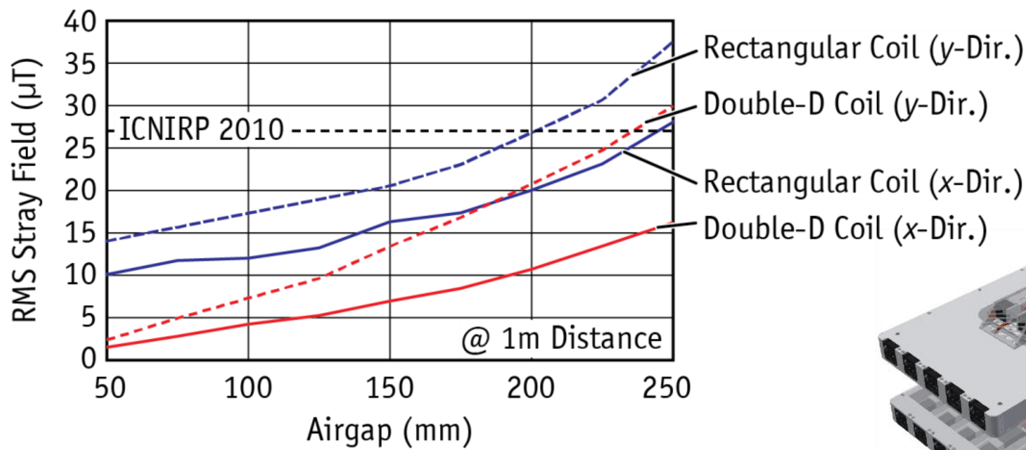

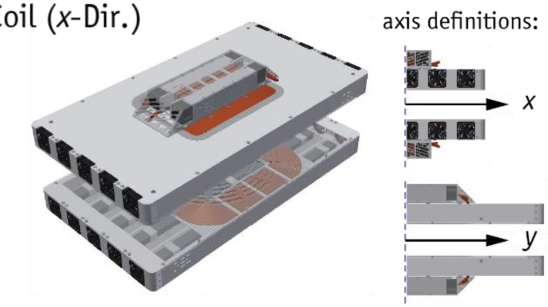

■ Intuitive Explanation:

- Structural Integration of Return Path for Flux

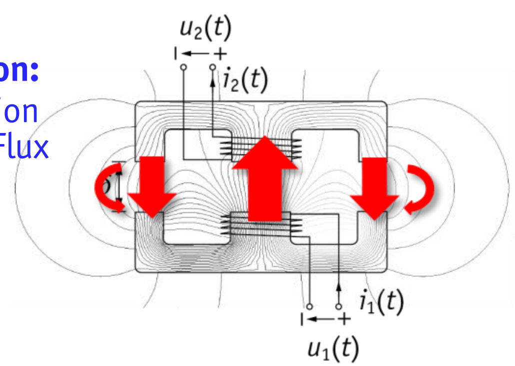

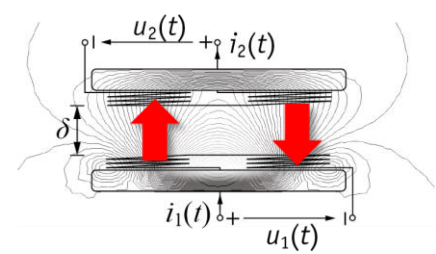

Technological Limitations of IPT Systems for EV

► Limiting Factor 1: High-Frequency Design

■ Litz Wires

- High Manufacturing Cost of Litz Wire
- Difficult Handling and Reliability of very Thin Strands under Mechanical Stress
- Decreasing Copper Filling-Factor

■ Power Electronics

- Low-*ESR* / High-Power Resonant Capacitors
- Low-Loss (Wide Bandgap) Semiconductors
- Fast Switching for Low (ZVS) Losses

■ Converter & Coil Parasitics

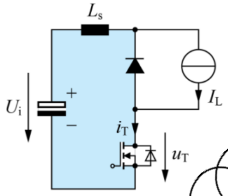

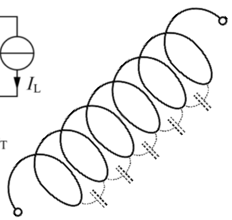

- Stray Inductance of Layout & Device Packages
- Coil Self-Capacitance (→ Include in Models)
- Sensitive Tuning of Resonant Circuit

▶ Limiting Factor 2: High-Frequency EMI

■ **Magnetic Stray Fields at High Power Levels**
- Inherently Required for Inductive Power Transfer, can be Reduced by Increasing Frequency
- Magnetic Field Standards are Limiting Factor in Design (e.g. ICNRIP 1998, 2010)

■ **Radiated Electric Field Interference with other Electronic Systems in EV (e.g. Radio Comm.)**
- High Series Resonant Voltages with SS-Comp. (can be Limited by Splitting Capacitance)
- Wide Bandgap SiC/GaN Semiconductors show high dV/dt even with ZVS

→ Possibly dV/dt-Filter Needed to Limit EMI
→ Additional Filter Components Required
→ Additional Losses in Filter Reduce Efficiency

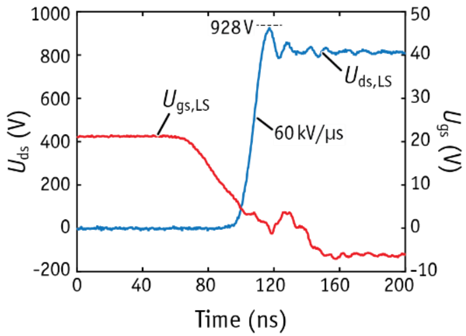

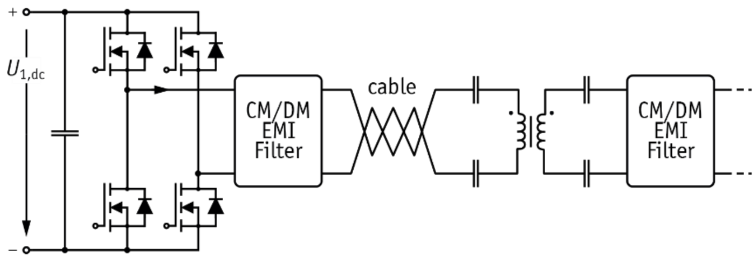

► Limiting Factor 3: Thermal Management

■ **Limited Cooling Possibilities for EV Charging Coils**
- No Metal Heatsink for Cooling Possible due to Eddy Current
- Limited Lifetime of Rotating Parts in Forced-Air Cooling Fans
- Engine Cooling Water has Operating Temperature 80-90°C

■ **Limited Efficiency & Power Capability of Compact IPT Systems**
- Small IPT Coils have Lower Coupling and Reduced Efficiency
- Limited Surface Area for Passive Heat Dissipation

→ Charging Power IPT System with Natural Convection Cooling is Limited to 3-5 kW

→ Cooling Technology Results in
… a Minimum Coil Size
… a Power Density Maximum

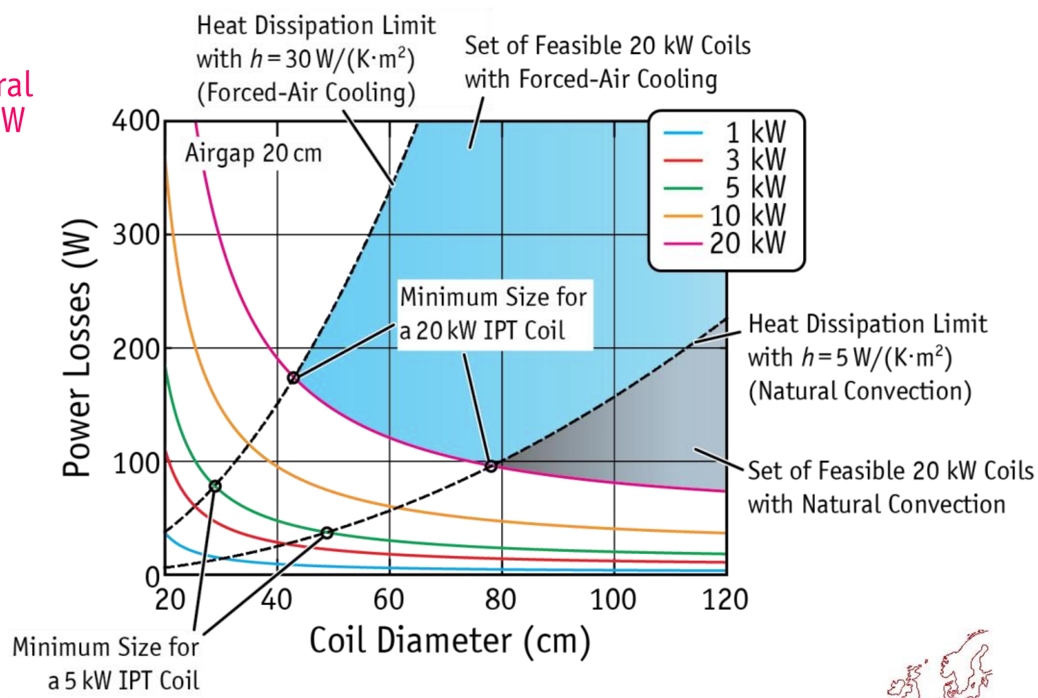

■ **Key Assumptions:**
- 10-Turn Air Coils without Core
- Airgap 20 cm for EV Charging
- Quality Factor Q = 300
- Identical Tx- & Rx-Coils

► Limiting Factor 4: Material Effort & Cost

- **High Charging Power Requires Large Coils for Low Losses & Sufficient Heat Dissipation**
  - Large Material Effort & Cost Compared to Conductive Charging Solutions
  - Material Effort can be Reduced Significantly with Active Cooling Concepts

- **Nearly No Benefit from Technology Progress Possible (Semiconductors, Digital Control, etc.)**
  - Increase of Freq. Blocked by Standards (SAE J2954) and Materials (Ferrite, Copper, Polypropylene)

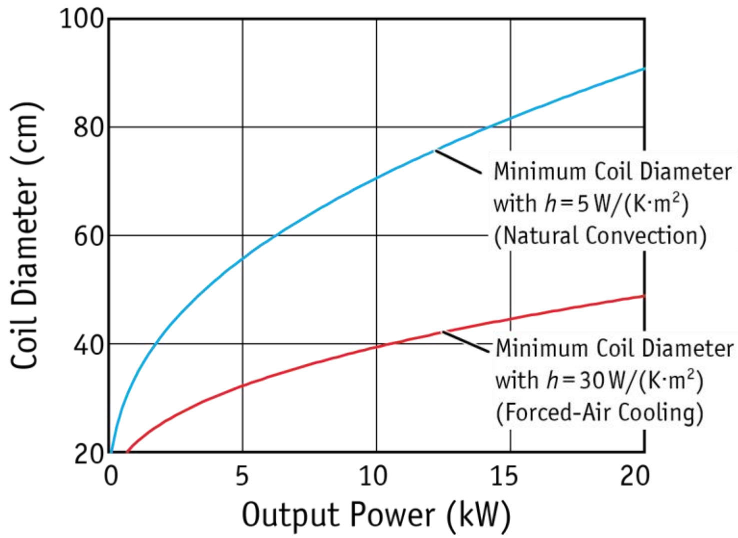

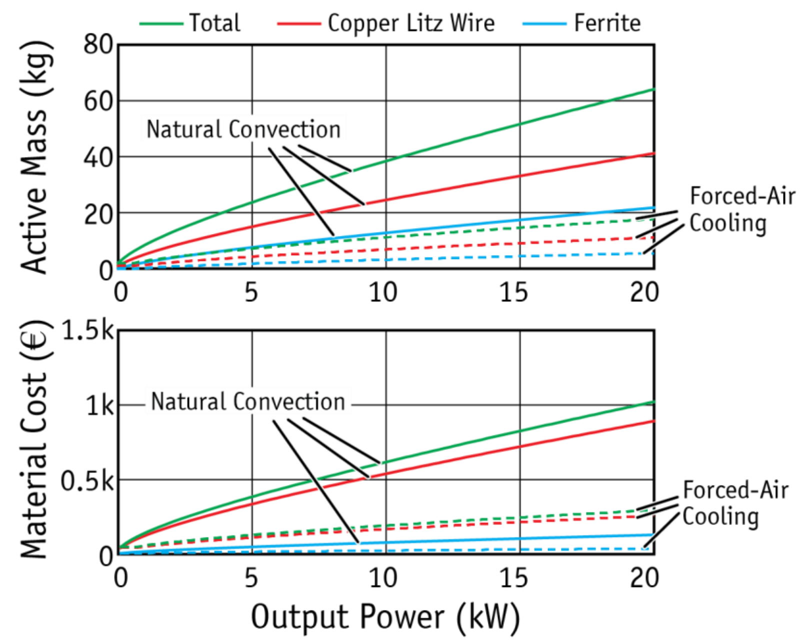

Key Assumptions:
- Dissipation of 50% Losses in Receiver Coil, 30% thereof via Exposed Bottom Coil Surface
- Thickness of IPT Receiver Coil is approx. 15 mm; Equal Ferrite and Copper Volumes (cf. Transformer)
- Price of Ferrite: 5.5 €/kg; Price Model of 0.2 mm Copper Litz Wire from Fit to Manufacturer Data

Power Electronics Concept for 50 kW

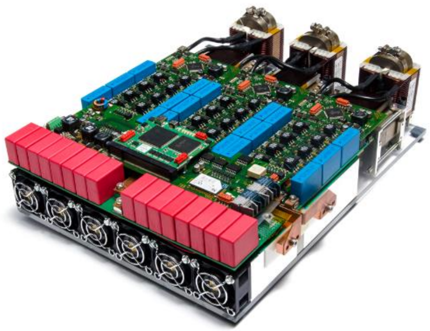

System Topology
IPT Coil Interface
3-Φ PFC Rectifiers

▶ Main System Components

■ **IPT Transmission Coils**
- Magnetic Design (using FEM)
- Shielding of Stray Field

■ **Receiver-Side Power Electronics**
- (Synchronous) Rectification
- Battery Current Regulation

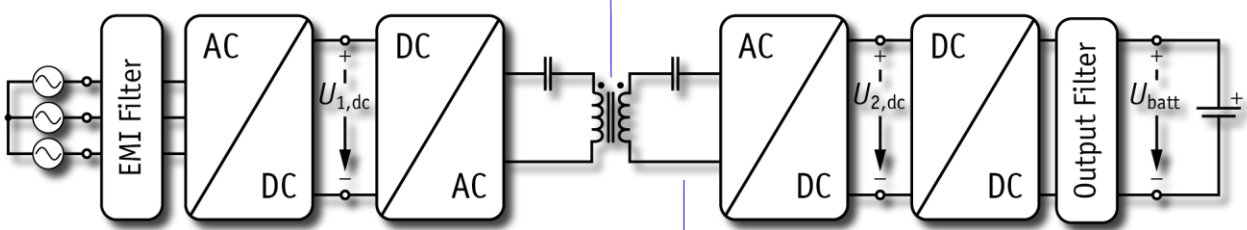

■ **Transmitter-Side Power Electronics**
- 1/3-Φ Mains Interface
- High-Frequency Inverter Stage

■ **Resonant Compensation**
- Requirements for Capacitor
- Optimal Component Selection

▶ IPT Test Bench for 50 kW with Energy Feedback

- **Test Setup for High-Power IPT Operation up to 50 kW**
  - Direct DC-to-DC Power Loss Measurements at DC Power-Supply for High Measurement Accuracy
  - Enables Experimental Evaluation of Different Control Options at Nominal Power
  - Experimental Evaluation and Comparison of Different Coil Designs

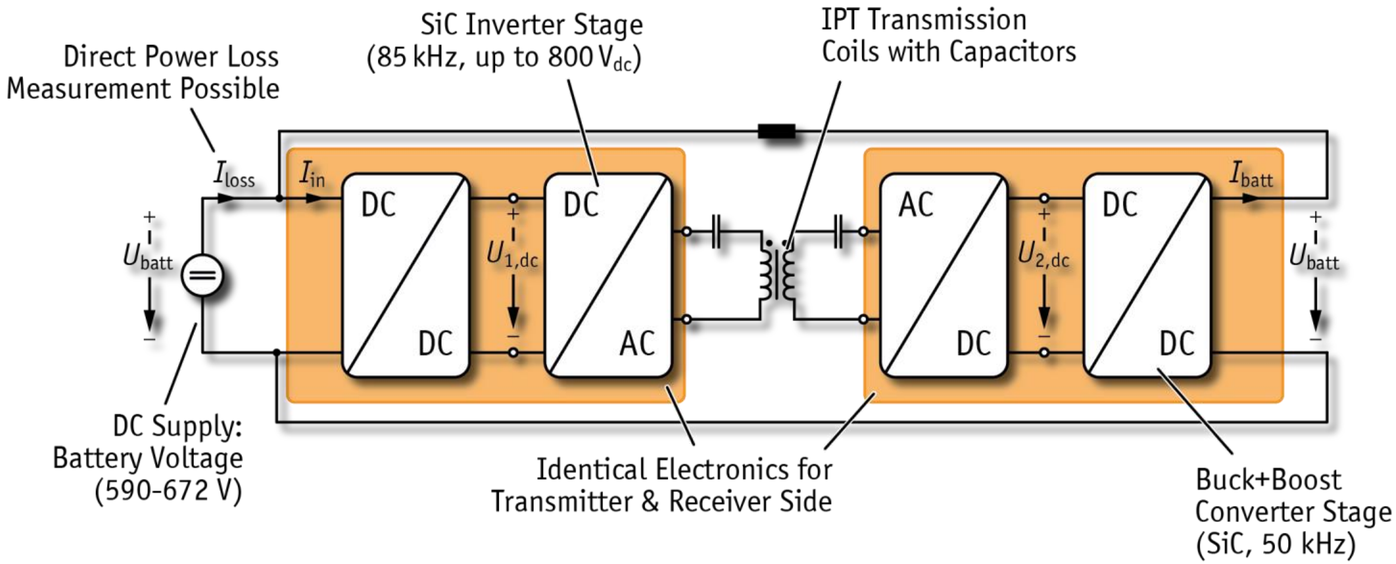

► Design Concept for 50 kW Prototype System

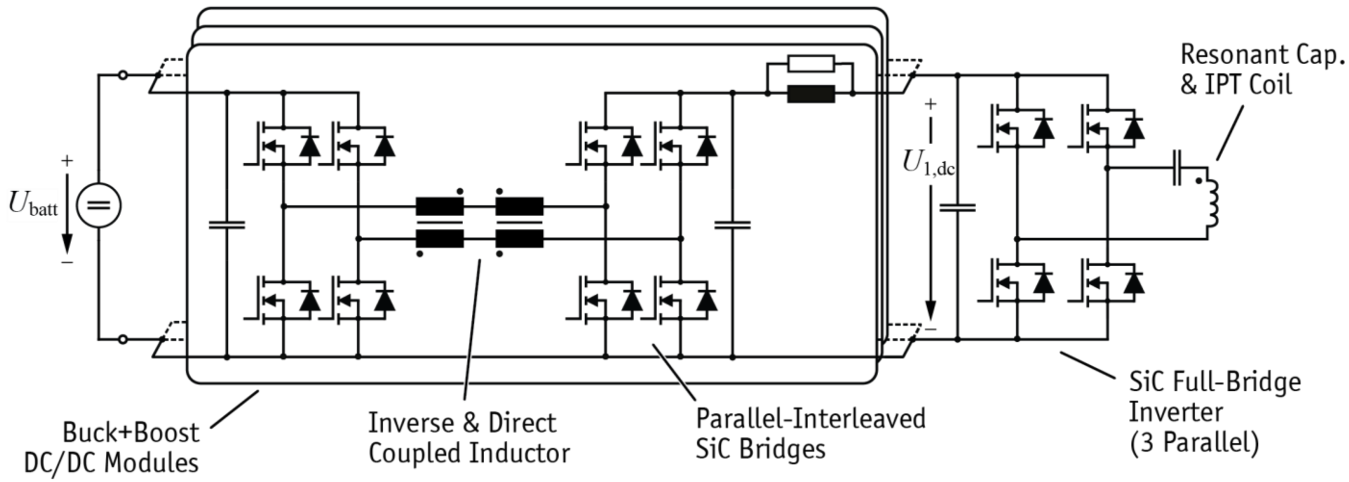

- **Ripple Cancellation by Parallel Interleaving**
  - 3 x 20 kW DC/DC-Converter Modules
  - Each Module has 2 Interleaved and Magnetically Coupled Stages

- **Modular Design allows Disabling Stages at Low Output Power**
  → Fully Benefit from High Partial-Load Efficient Concept of IPT Transmission

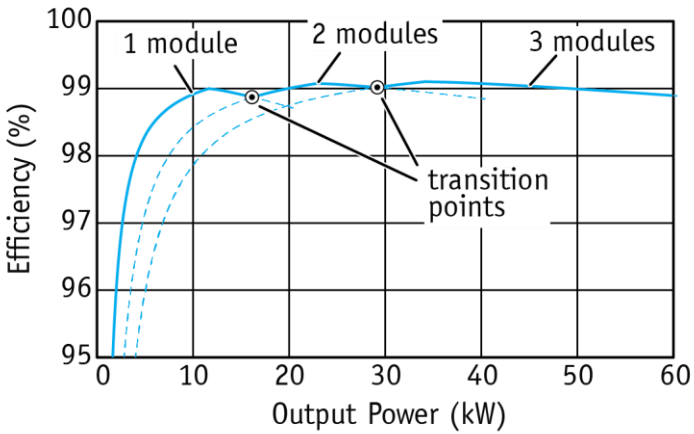

Modular Buck+Boost Type DC/DC Stage

▶ Interleaved DC/DC-Converter with Coupled Inductors (2)

■ **Explicit Separation of Common-Mode & Differential Mode Inductance**

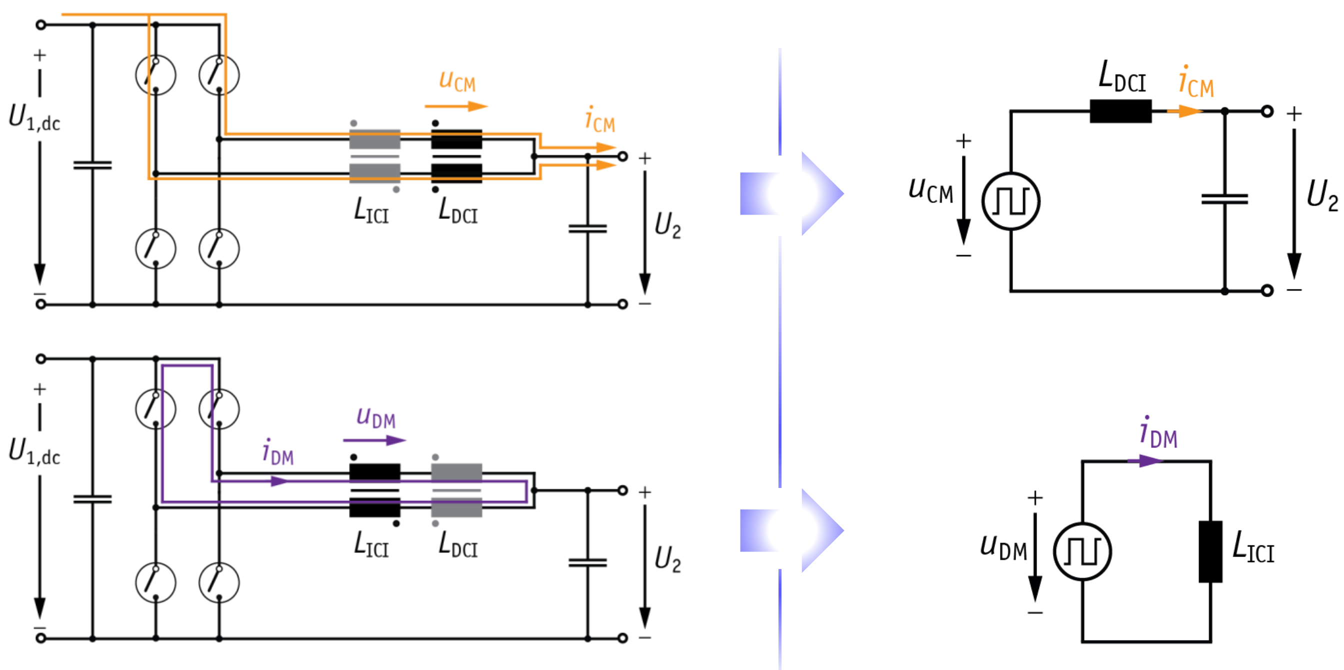

■ Common-Mode Flux Cancels in ICI → Only DCI Inductance Effective for $i_{CM} = 0.5 \cdot (i_1 + i_2)$
■ Differential-Mode Flux Cancels in DCI → Only ICI Inductance Effective for $i_{DM} = 0.5 \cdot (i_1 - i_2)$

→ Allows Separate Design of CM/DM Current Ripple Amplitudes

▶ Measured CM/DM Current Ripples (1)

■ **180°-Interleaved Switching in Buck-Mode with Duty-Cycle $D = 25\%$**

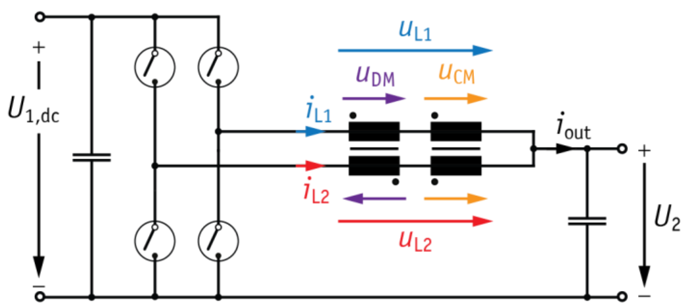

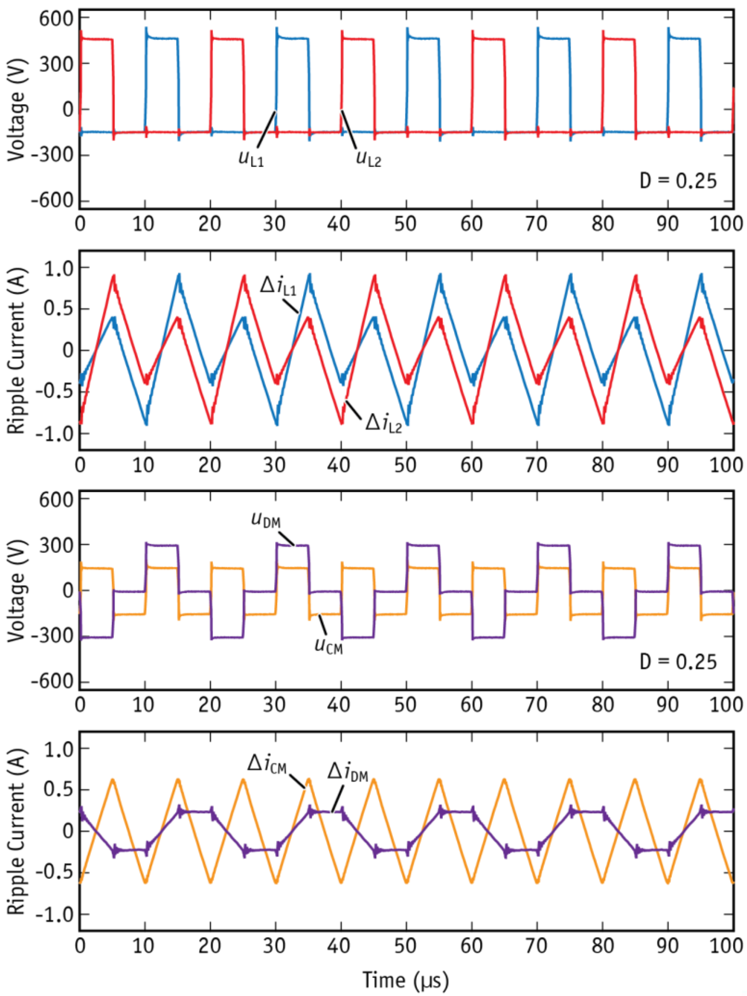

■ **CM/DM Equivalent Circuit Diagrams**

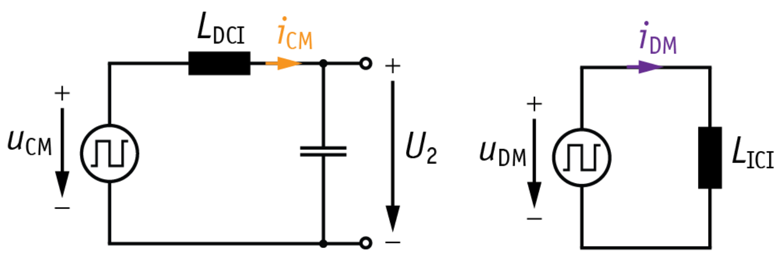

▶ Measured CM/DM Current Ripples (2)

■ **180°-Interleaved Switching in Buck-Mode with Duty-Cycle D=50%**

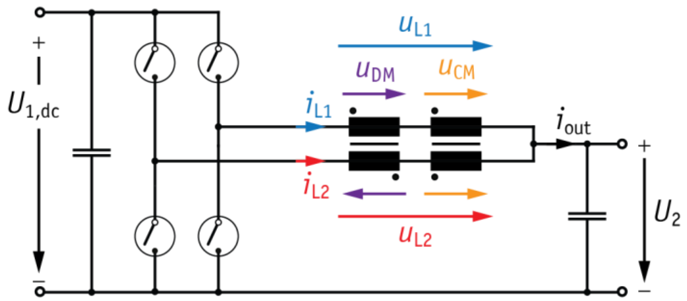

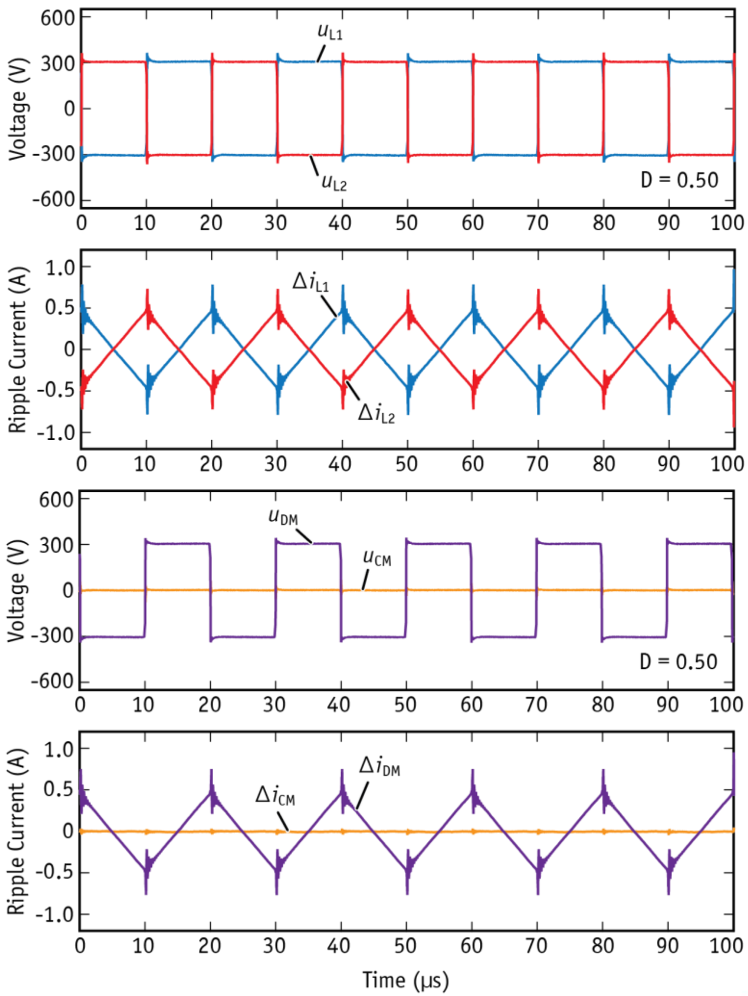

■ **CM/DM Equivalent Circuit Diagrams**

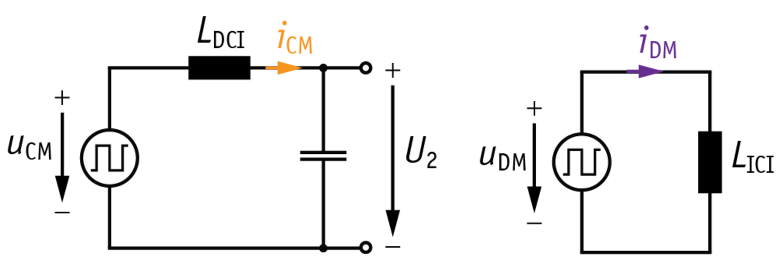

► Separation of CM/DM Current Ripples (1)

- Common-Mode Flux Cancels in ICI → Only DCI Inductance Effective for iCM = 0.5·(i1 + i2)
- Differential-Mode Flux Cancels in DCI → Only ICI Inductance Effective for iDM = 0.5·(i1 - i2)

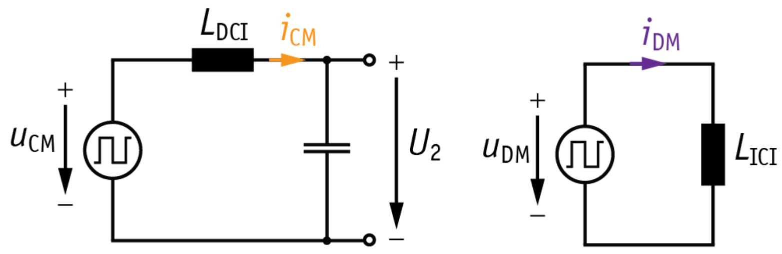

- Significant Ripple Reduction Compared to Two Uncoupled, Interleaved Converter Stages
- Reduced Total Magnetics Volume for Equal Output Current Ripple

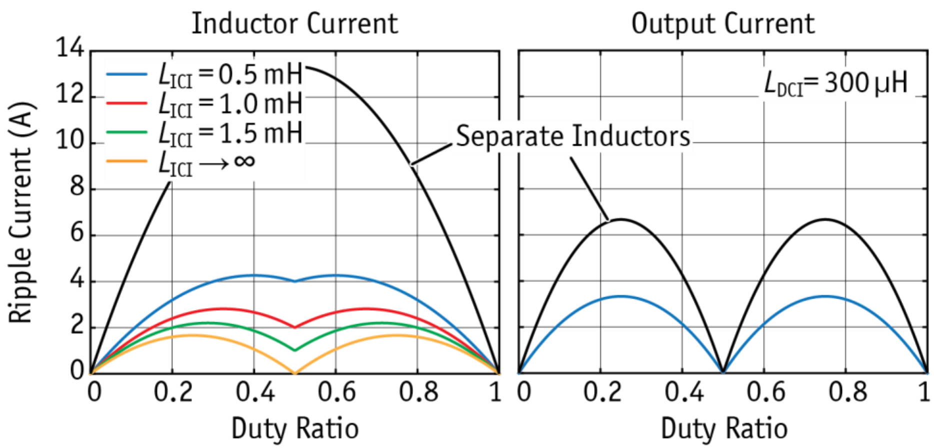

▲ Calculated Inductor/Output Current Ripple

► Separation of CM/DM Current Ripples (2)

■ **Direct Coupled Inductor**
- Flux due to Common-Mode Voltage
- DC-Flux → Energy Storage
- Reduction of Current-Ripple Requires Stored Magnetic Energy

■ **Inverse Coupled Inductor**
- Flux due to Differential-Mode Voltage
- No DC-Flux → No Stored Energy
- Reduction of Current-Ripple does not Require Energy Storage

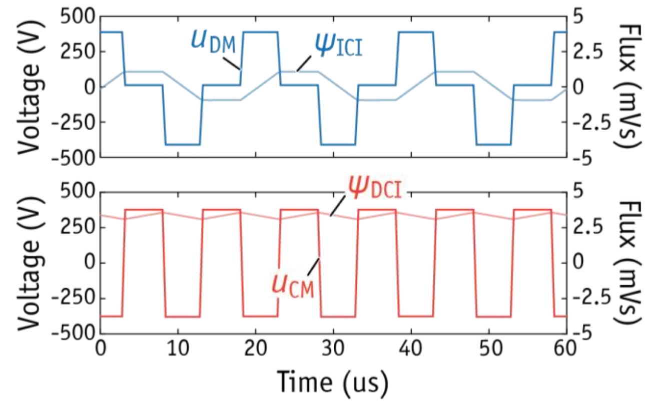

▲ **Calculated Core Flux Waveforms**

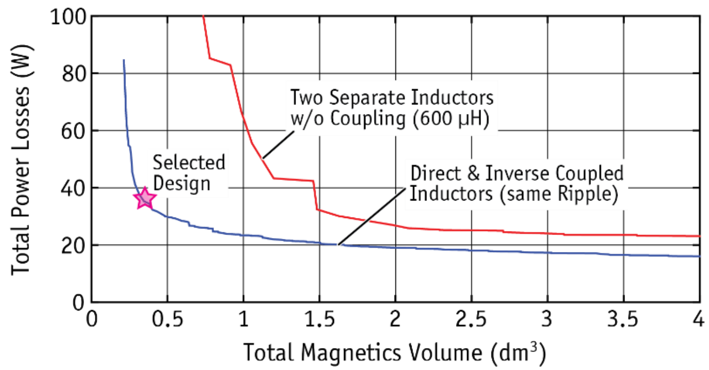

▲ **Calculated Volume Couled vs. Un-Coupled**

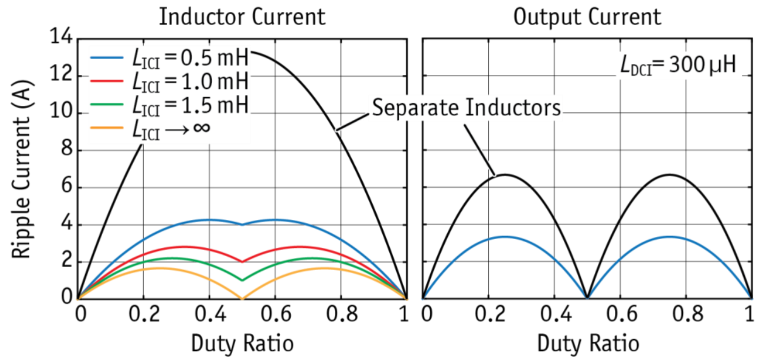

▲ **Calculated Inductor/Output Current Ripple**

► Compact Realization of the Magnetic Components

- **Flat-Wire Helical Winding**
  - Highest Copper Filling Factor

- **Tape Wound Iron Cores**
  - DCI: Amorphous Iron Core with Gap (Flux has DC+AC Components)
  - ICI: Nano-Crystalline Core w/o Gap (Flux has only AC Components)

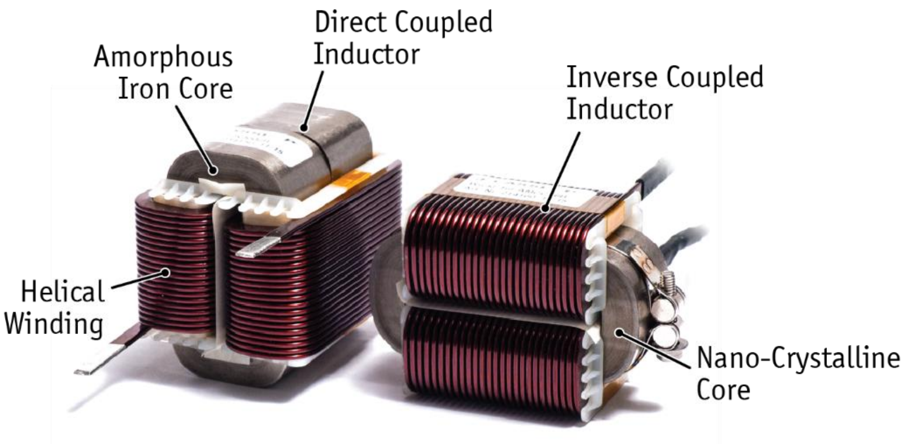

▲ **Realized Inductor Prototypes**

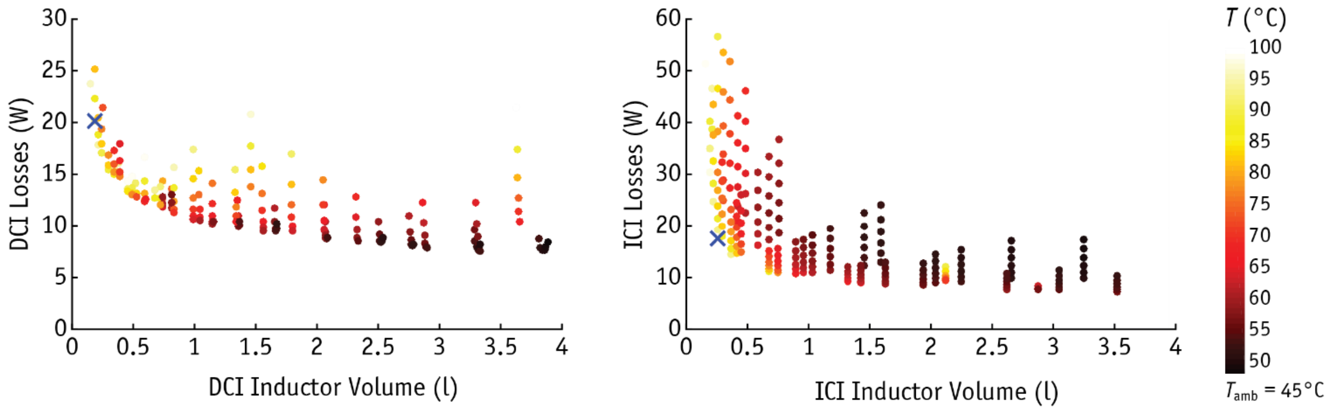

▲ **Inductor Optimization Results**

► DC/DC Module: Efficiency Measurement Results

- **Back-to-Back Operation of two Identical DC/DC Modules to Circulate 20 kW Power**
  - Direct Power Loss Measurement is More Accurate than Taking $P_{loss} = P_{in} - P_{out}$
  - DC Voltage & Current (>30 A) Measurement with Precision Shunt Resistors and Multimeters

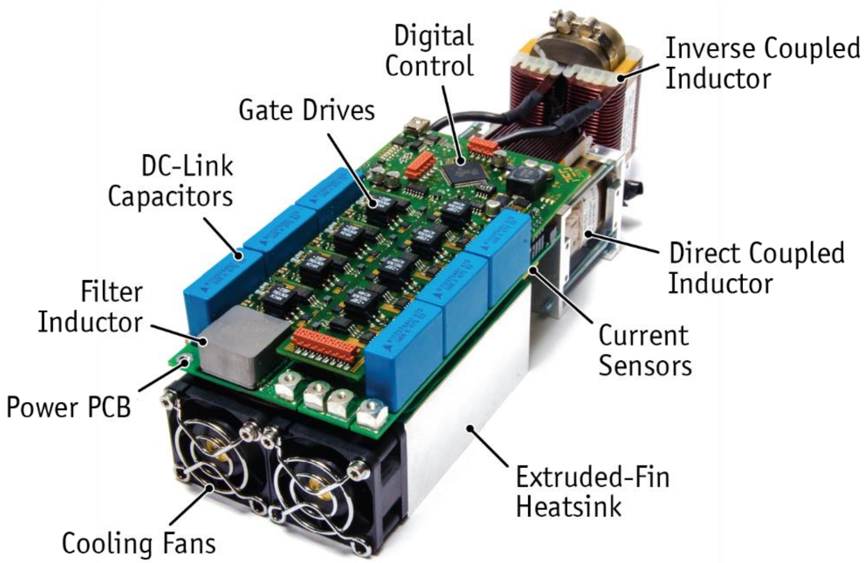

▲ **Buck+Boost Type DC/DC-Converter Module (20 kW, 50 kHz, 11.5 kW/l)**

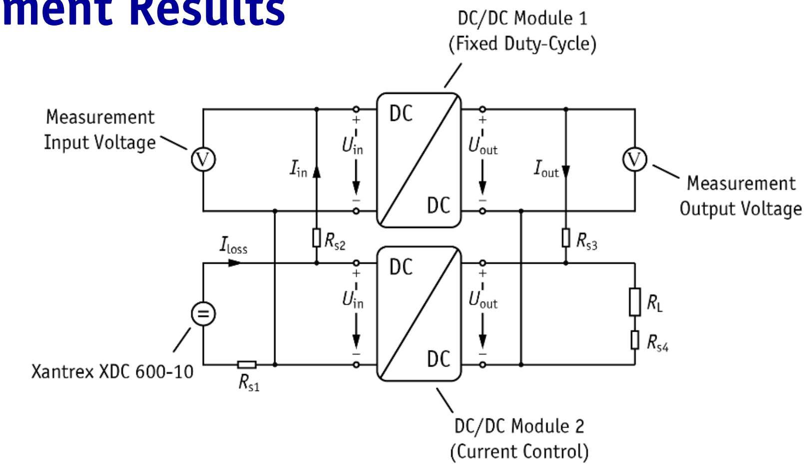

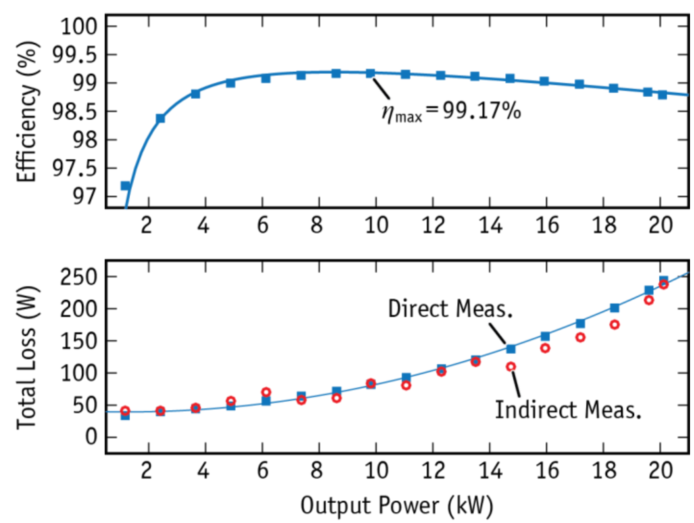

▲ **Efficiency Measurement Results**

ZVS Full-Bridge Inverter Stage

► SiC MOSFET ZVS Full-Bridge Inverter Stage

- **60 kW Inverter Stage: SiC ZVS Full-Bridge @ 800 V, 100 A_{rms}**
  - Tree Discrete 25 mΩ SiC-MOSFET Devices in Parallel Connection for Low $R_{ds(on)}$ (Available Half-Bridge Modules have Higher Commutation & Gate Loop Inductance)
  - Single Gate-Driver for Three Parallel Devices for Minimum Realization Complexity

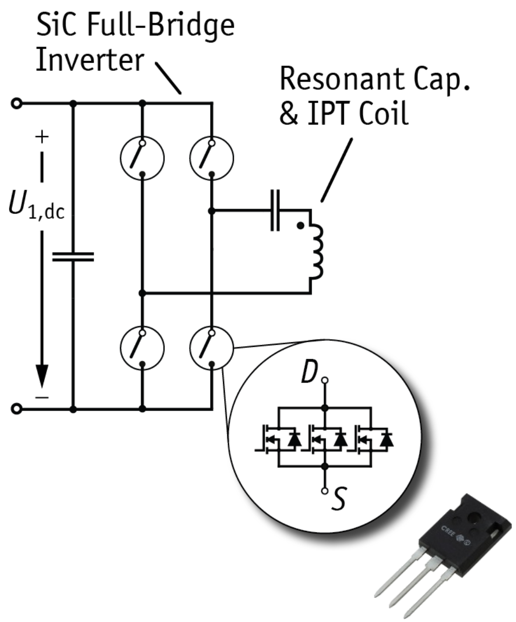

▲ **Bridge Topology with 3 SiC MOSFET Devices Connected in Parallel**

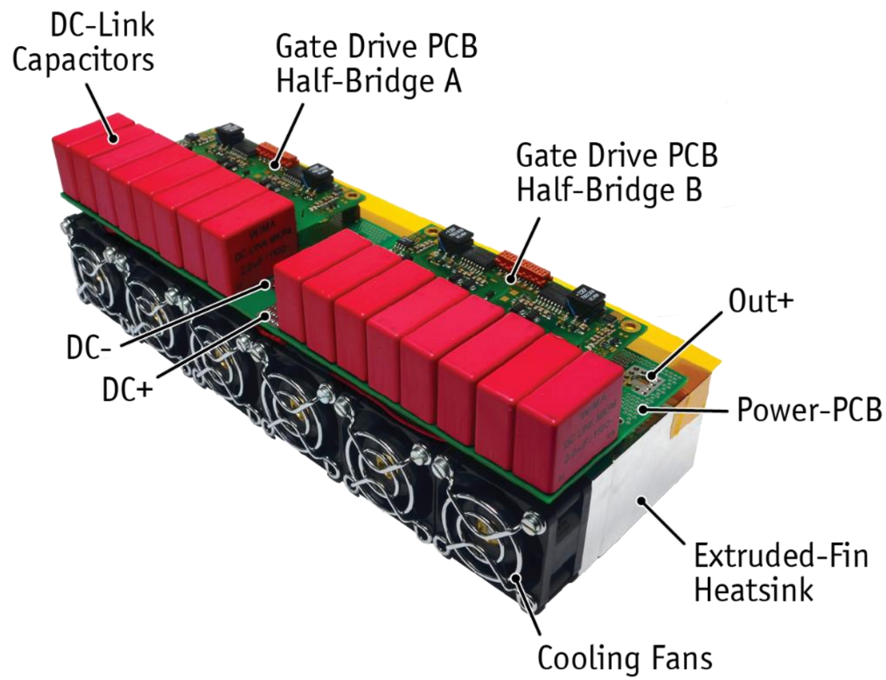

▲ **SiC ZVS Full-Bridge Inverter Stage (60 kW, 85 kHz, 40 kW/l)**

► Gate-Drive Concept for Parallel-Connected Devices (1)

■ SiC Half-Bridge Gate-Driver for Three Parallel Devices

- One Driver IC for all Three Parallel MOSFET Devices, Separate Gate Resistors for each Device
- Ensure Synchronous Turn-On w/o Gate-Oscillation

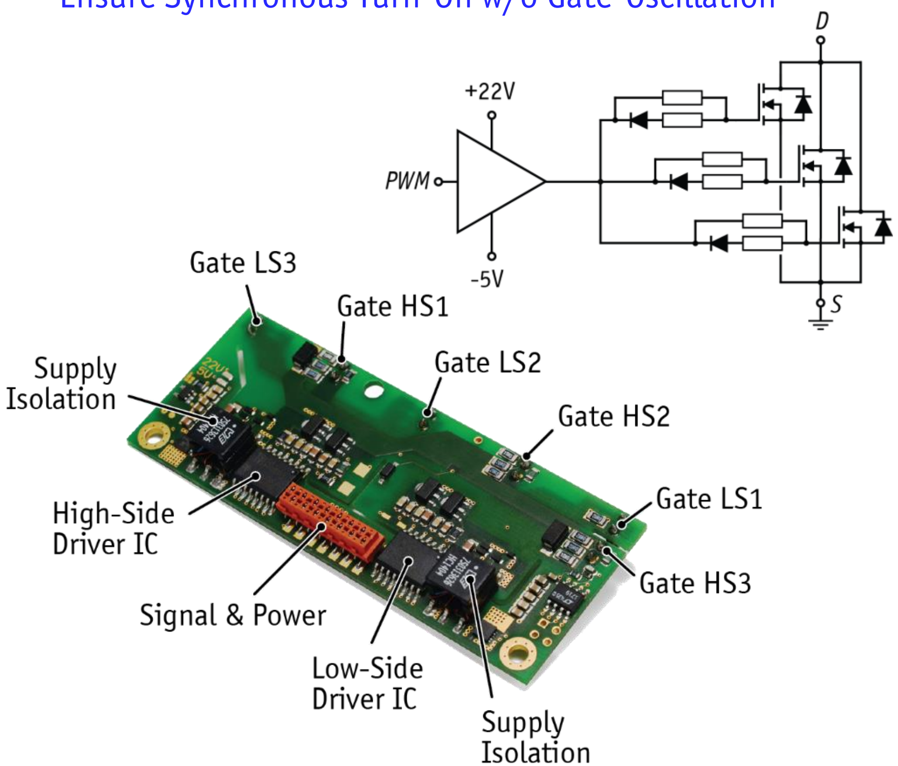

▲ **Half-Bridge Gate Driver PCB for Three MOSFETs in Parallel for each Switch**

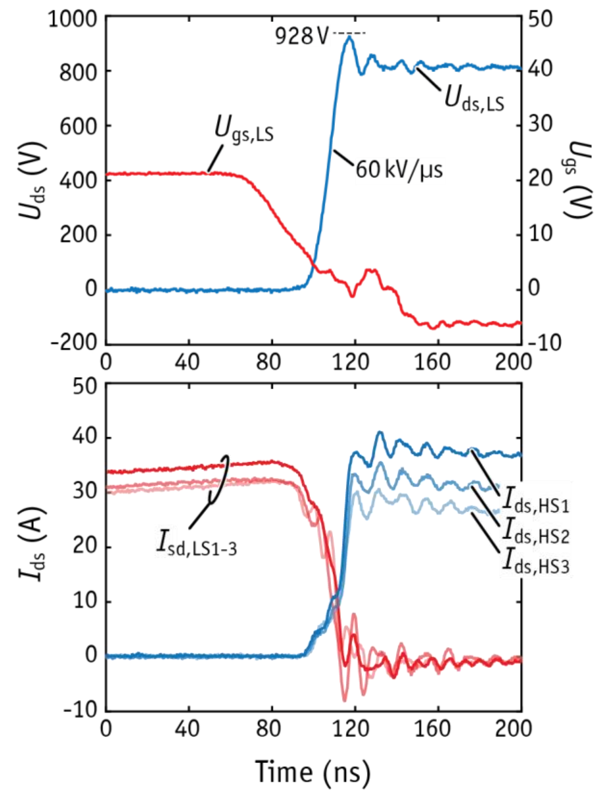

▲ **Individual Device Currents During Half-Bridge Switching Transition**

► Gate-Drive Concept for Parallel-Connected Devices (2)

■ SiC Half-Bridge Gate-Driver for Three Parallel Devices

- One Driver IC for all Three Parallel MOSFET Devices, Separate Gate Resistors for each Device
- Ensure Synchronous Turn-On w/o Gate-Oscillation

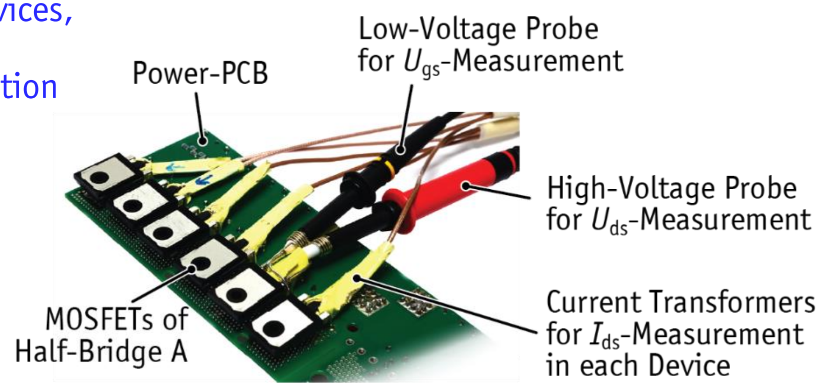

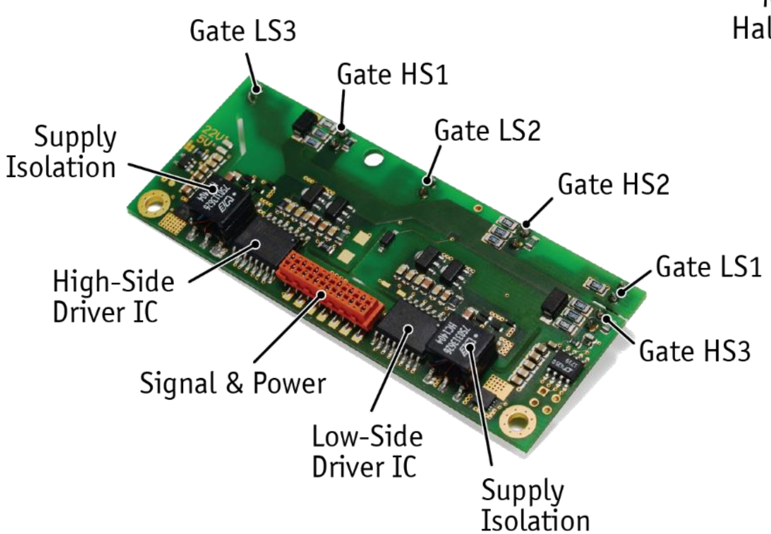

▲ **Half-Bridge Gate Driver PCB for Three MOSFETs in Parallel for each Switch**

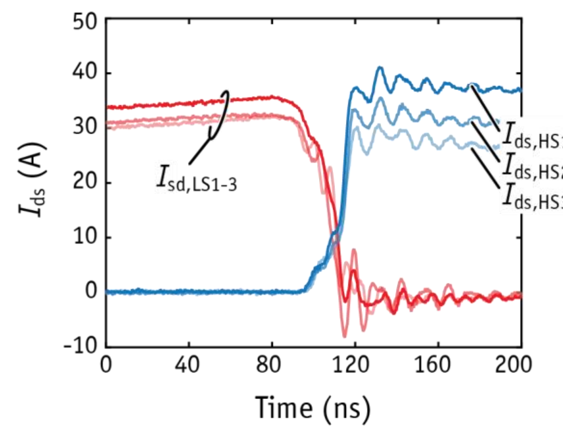

▲ **Individual Device Currents During Half-Bridge Switching Transition**

► Power-PCB Layout for Symmetrical Current Distribution

■ Layout of Power-PCB is Critical for Symmetrical Device Current Distribution

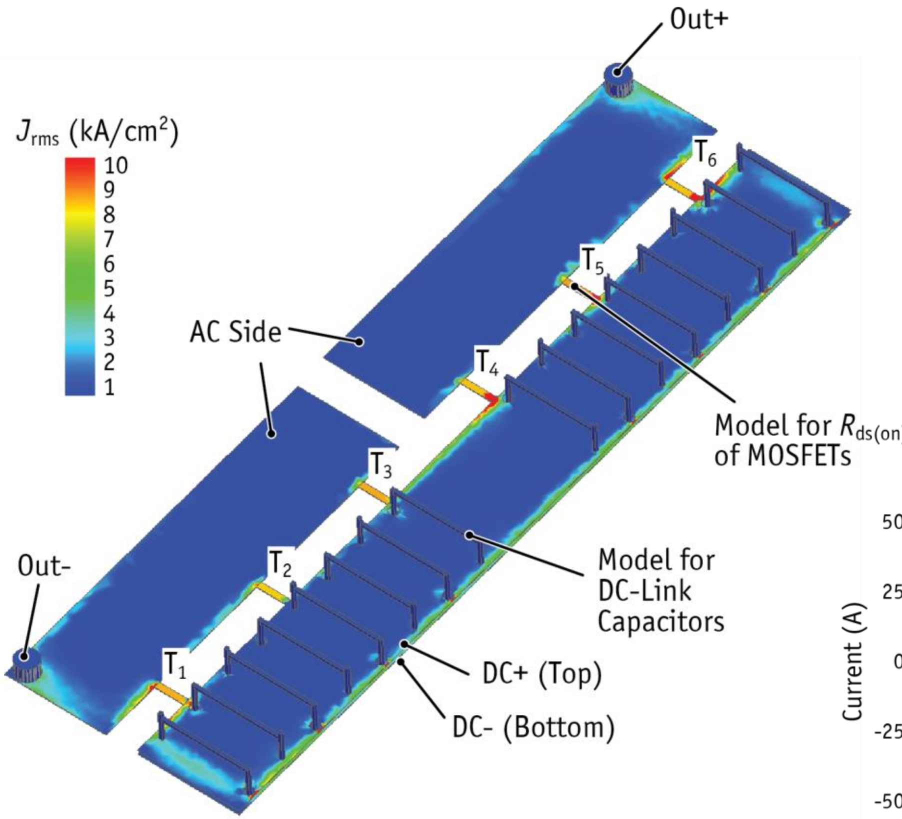

▲ 3D-FEM Simulation of Power-PCB Layout

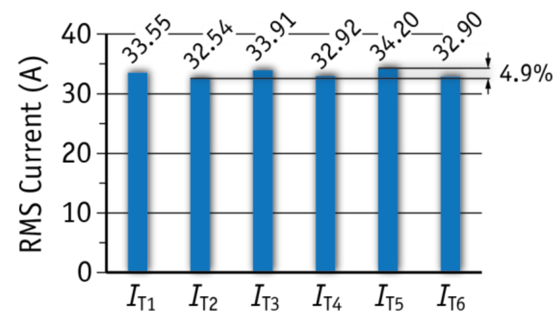

▲ FEM Calculated Device Currents

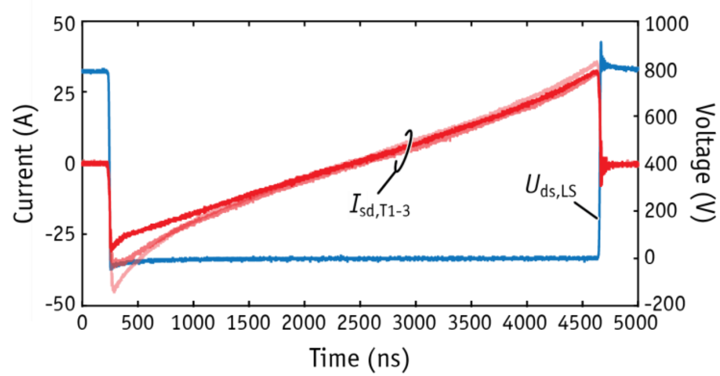

▲ Measured Individual Device Currents

► 60 kW SiC Power Converter

- **Efficiency 98%, Power Density 9.2 kW/l, Forced-Air Cooled**

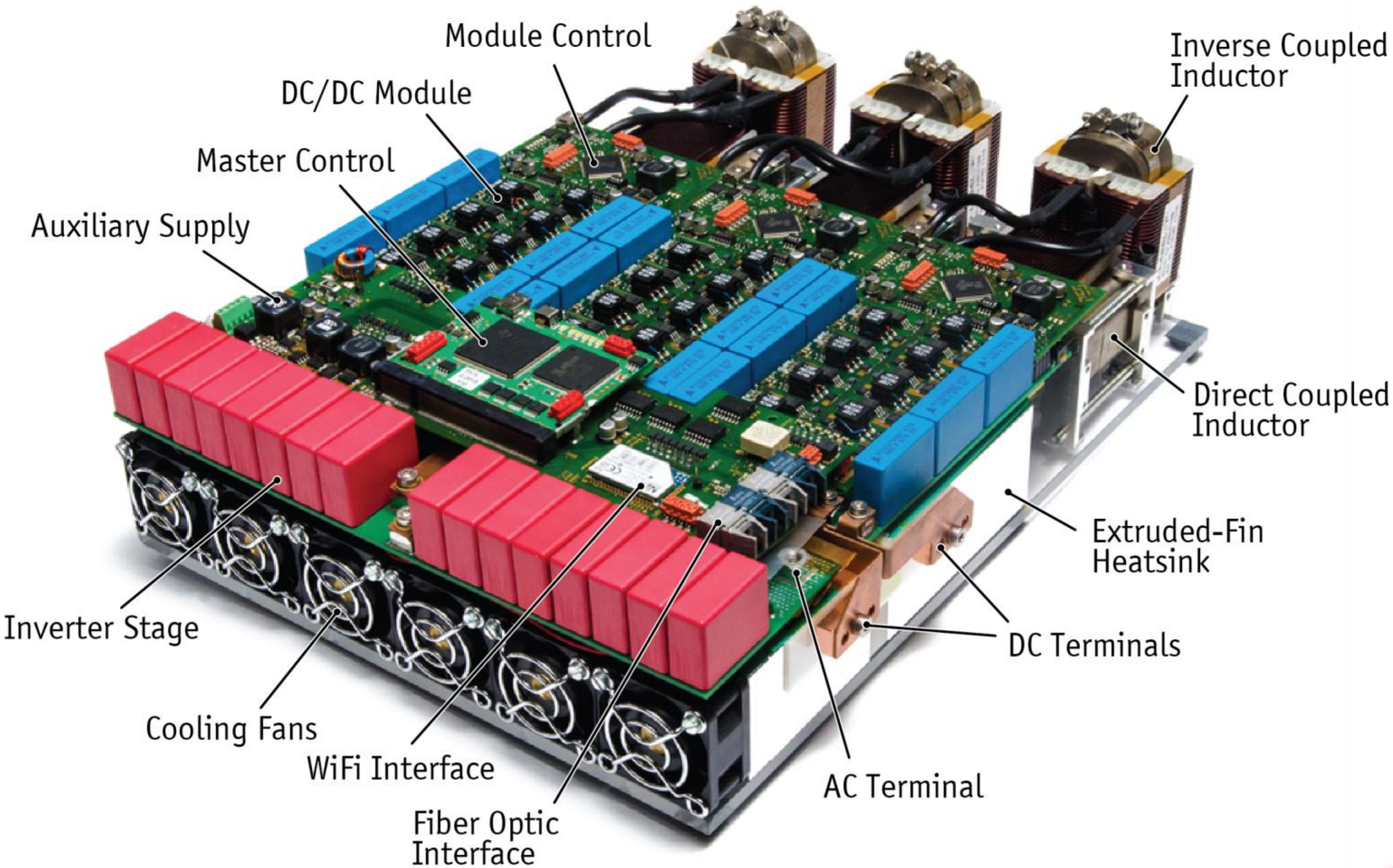

3-Φ PFC Rectifier Systems

J. W. Kolar, T. Friedli, *The Essence of Three-Phase PFC Rectifier Systems - Part I*, IEEE Transactions on Power Electronics, Vol. 28, No. 1, pp. 176-198, January 2013.

T. Friedli, M. Hartmann, J. W. Kolar, *The Essence of Three-Phase PFC Rectifier Systems - Part II*, IEEE Transactions on Power Electronics, Vol. 29, No. 2, February 2014.

3-Φ AC/DC Power Conversion

■ **Basis Requirement for EV Charging / IPT Front End Converter Stages**

- **Wide Input/Output Voltage Range – Voltage Adaption**
- **Mains Side Sinusoidal Current Shaping / Power Factor Correction**

- **Boost Type**
- **Buck Type**

V_B .... Output Voltage
$V_{N,ll,rms}$ ... RMS Value of Mains Line-to-Line Voltage

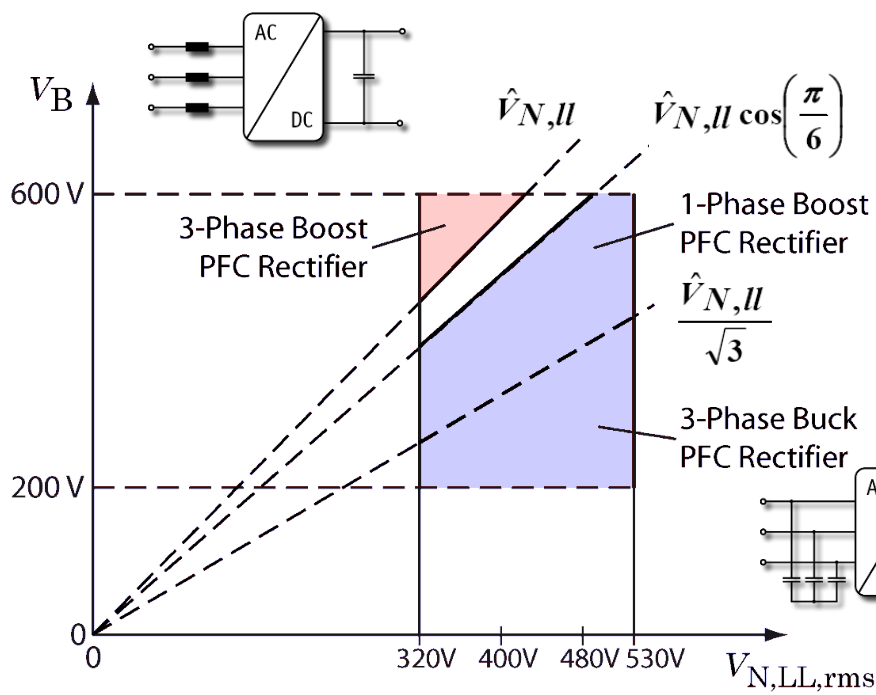

► Classification of General Unidirectional 3-Φ Rectifier Systems

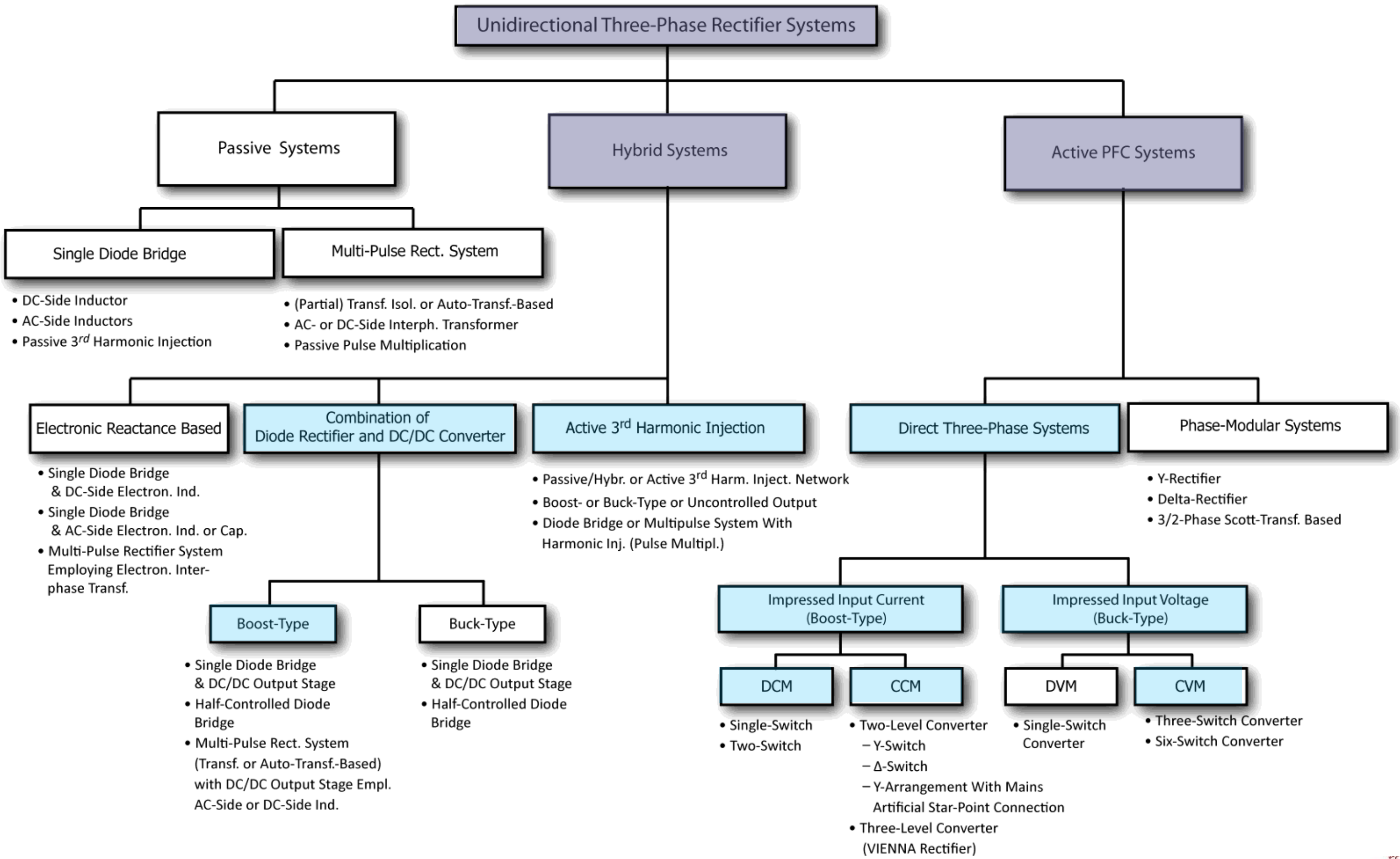

▶ Classification of Unidirectional Rectifier Systems

- **Passive Rectifier Systems**
  - Line Commutated Diode Bridge/Thyristor Bridge - Full/Half Controlled
  - Low Frequency Output Capacitor for DC Voltage Smoothing
  - Only Low Frequency Passive Components Employed for Current Shaping, No Active Current Control
  - No Active Output Voltage Control

- **Hybrid Rectifier Systems**
  - Low Frequency and Switching Frequency Passive Components and/or
  - Mains Commutation (Diode/Thyristor Bridge - Full/Half Controlled) and/or Forced Commutation
  - Partly Only Current Shaping/Control and/or Only Output Voltage Control
  - Partly Featuring Purely Sinusoidal Mains Current

- **Active Rectifier Systems**
  - Controlled Output Voltage
  - Controlled (Sinusoidal) Input Current
  - Only Forced Commutations / Switching Frequ. Passive Components

■ **Phase-Modular Systems**
  - Phase Rectifier Modules of Identical Structure
  - Phase Modules connected in Star or in Delta
  - Formation of Three Independent Controlled DC Output Voltages

■ **Direct Three-Phase Syst.**
  - Only One Common Output Voltage for All Phases
  - Symmetrical Structure of the Phase Legs
  - Phase (and/or Bridge-)Legs Connected either in Star or Delta

Evaluation of Boost-Type Systems

Boost-Type PFC Rectifiers

- 3rd Harmonic Inj. Type
- Diode Bridge Conduction Modulation

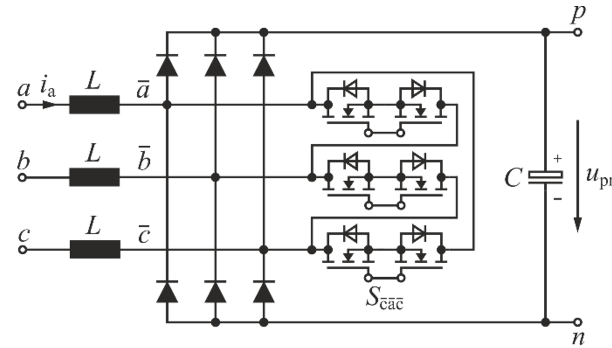

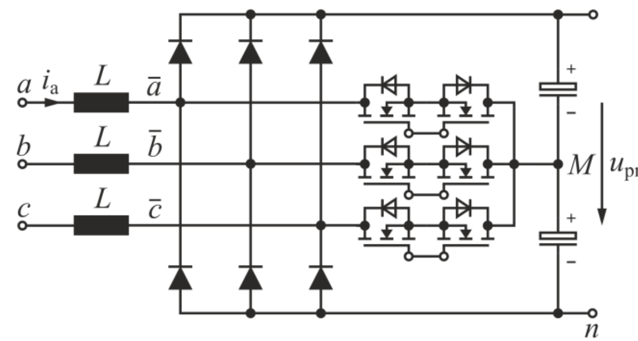

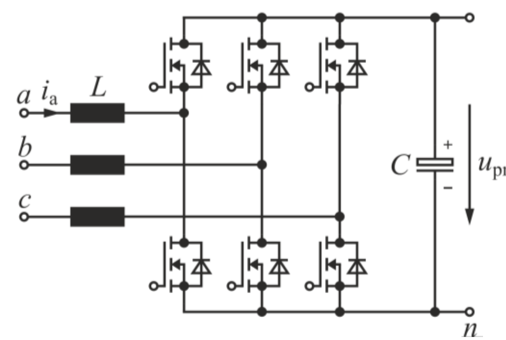

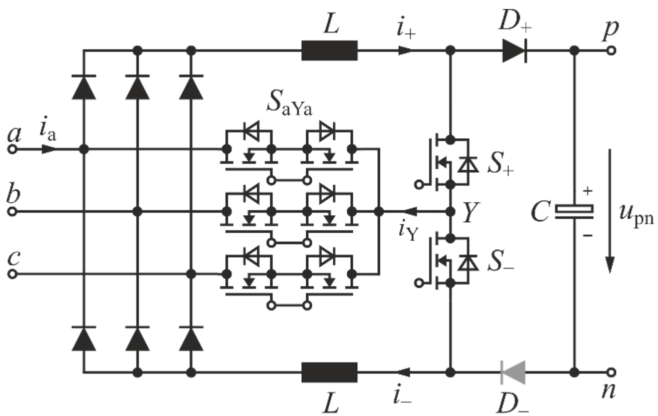

Vienna Rectifier vs. Six-Switch Rectifier

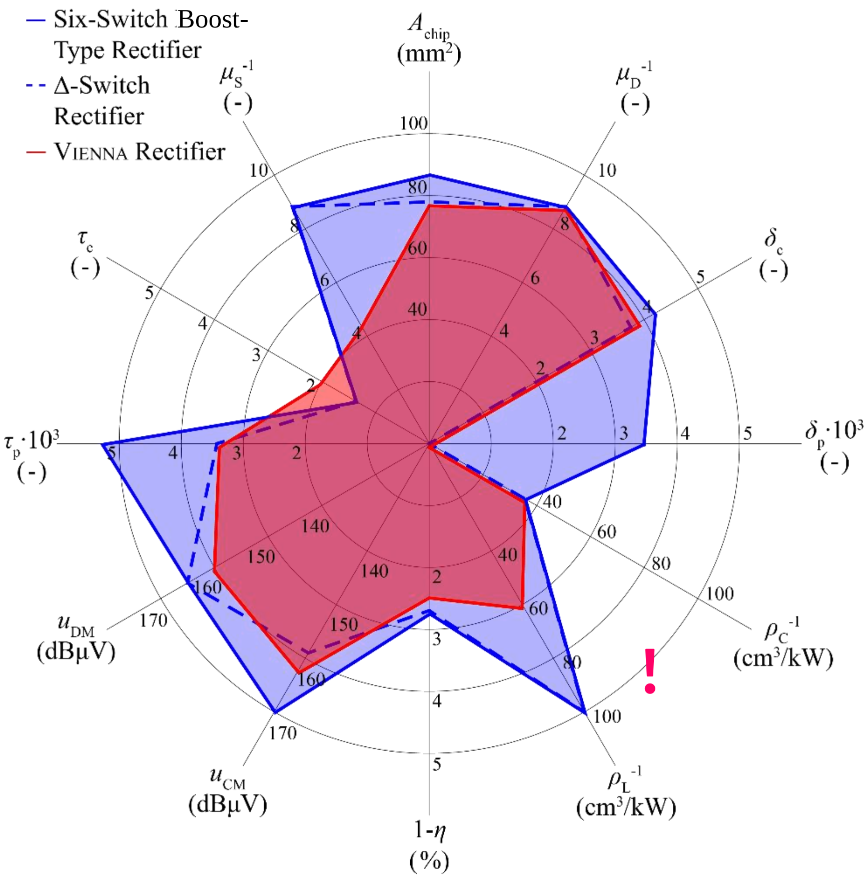

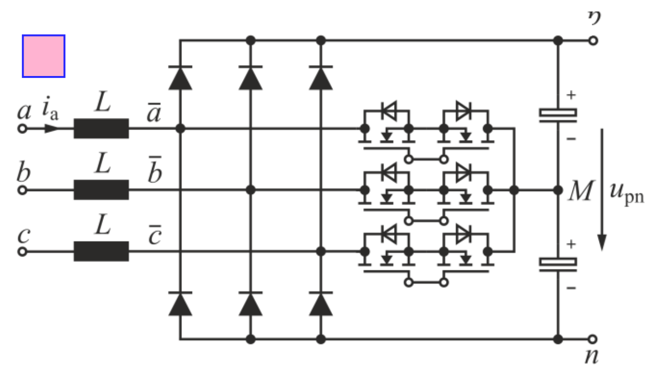

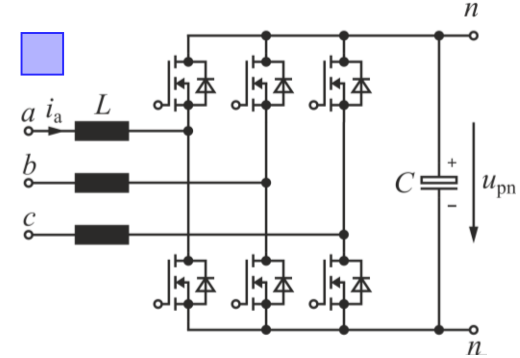

Comparison of Buck-Type Systems

Buck-Type PFC Rectifiers

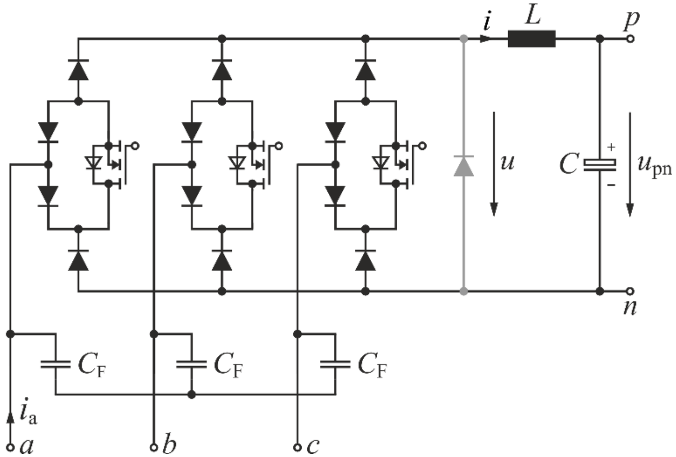

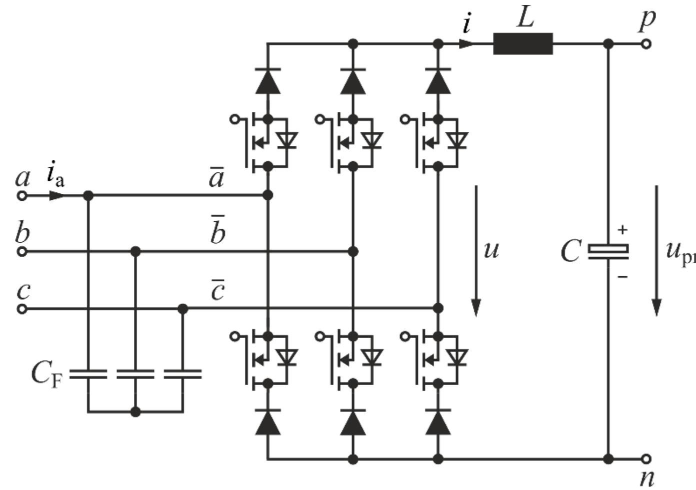

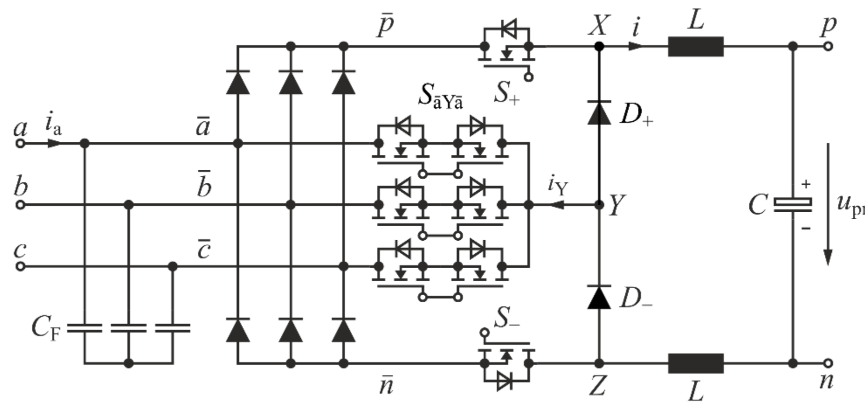

- 3rd Harmonic Inj. Type
- Diode Bridge Cond. Modulation

SWISS Rectifier vs. Six-Switch Rectifier

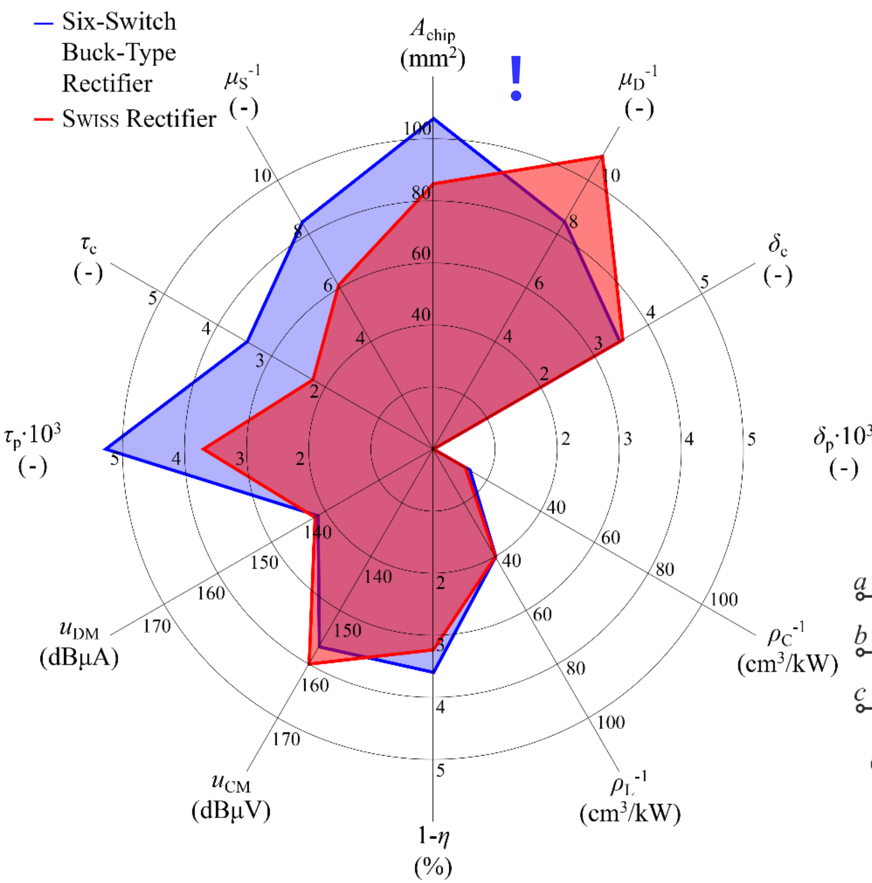

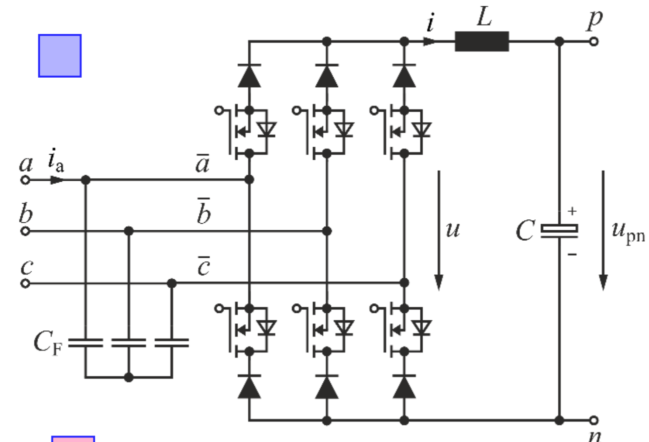

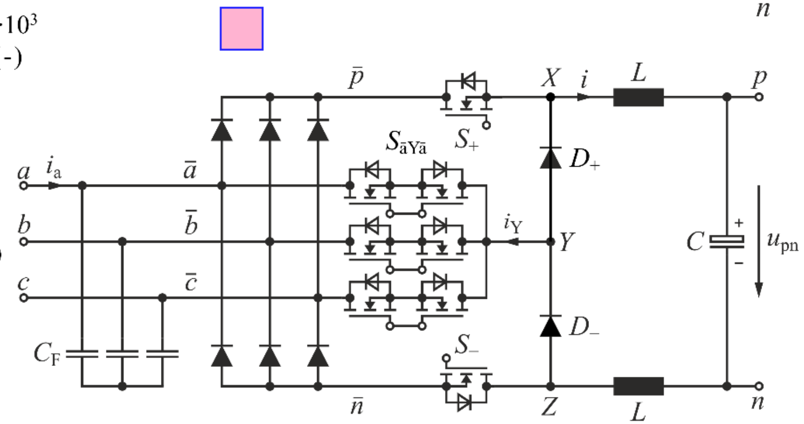

Summary: Unidirectional PFC Rectifier Systems

▶ Block Shaped Input Current Rectifier Systems

- \+ **Controlled Output Voltage**
- \+ **Low Complexity**
- \+ **High Semicond. Utilization**
- \+ **Total Power Factor $\lambda \approx 0.95$**
- − **$THD_I \approx 30\%$**

Boost-Type

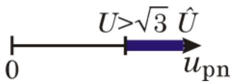

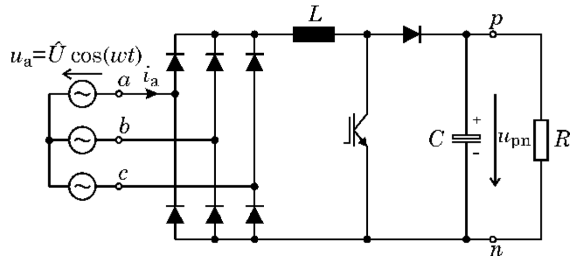

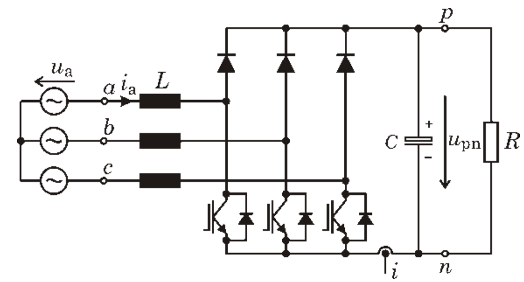

Buck-Type

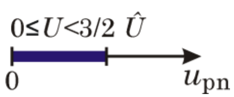

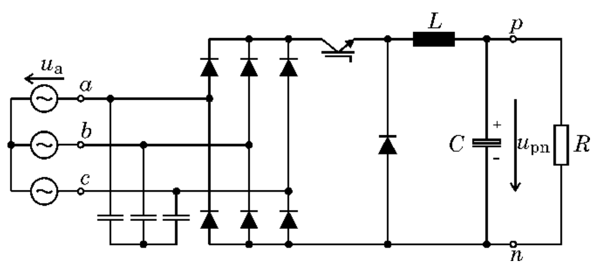

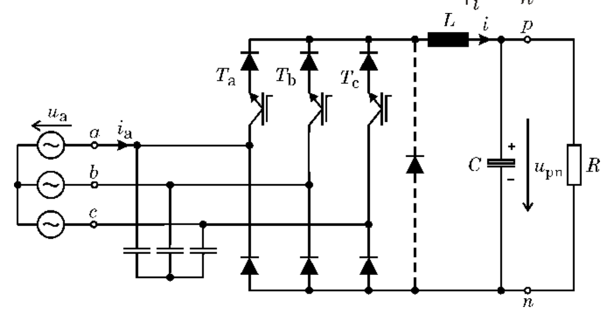

Buck+Boost-Type

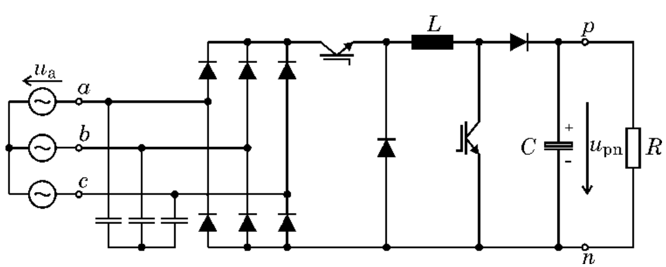

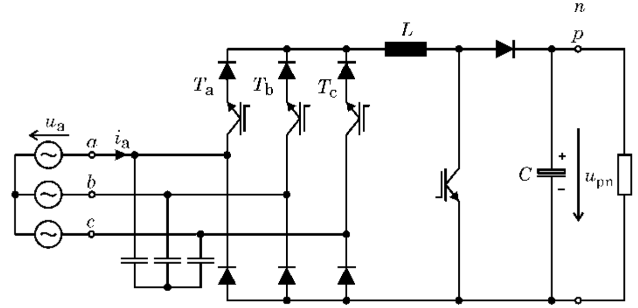

▶ Sinusoidal Input Current Rectifier Systems (1)

+ Controlled Output Voltage
+ Relatively Low Control Complexity
+ Tolerates Mains Phase Loss

– 2-Level Characteristic
– Power Semiconductors Stressed with Full Output Voltage

Boost-Type

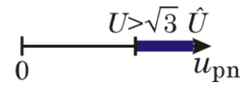

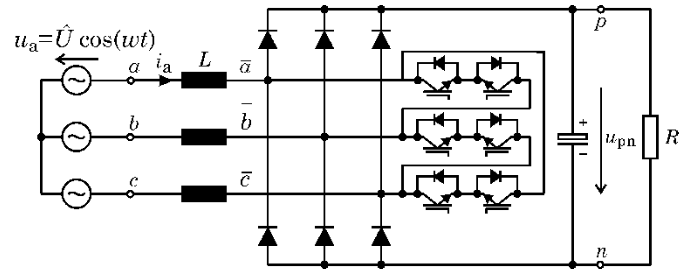

+ Controlled Output Voltage
+ 3-Level Characteristic
+ Tolerates Mains Phase Loss
+ Power Semicond. Stressed with Half Output Voltage

– Higher Control Complexity

Boost-Type

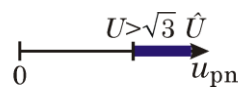

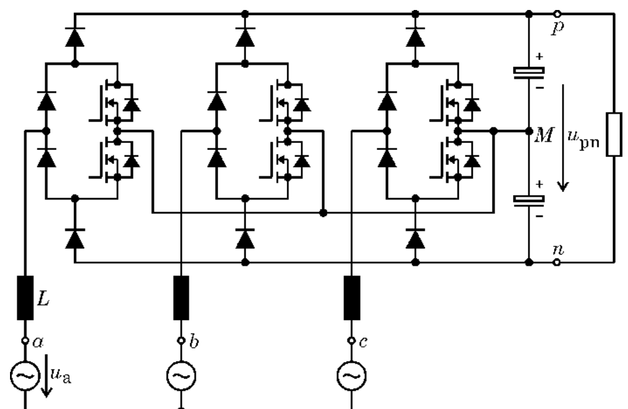

+ Low Current Stress on Power Semicond.
+ In Principal No DC-Link Cap. Required
+ Control Shows Low Complexity

– Sinusoidal Mains Current Only for Const. Power Load
– Power Semicond. Stressed with Full Output Voltage
– Does Not Tolerate Loss of a Mains Phase

Unregulated Output

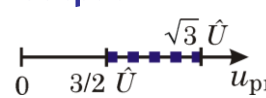

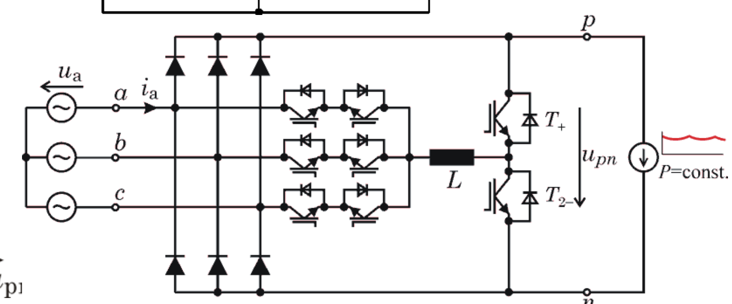

▶ Sinusoidal Input Current Rectifier Systems (2)

Buck-Type

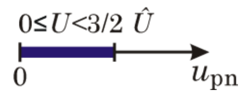

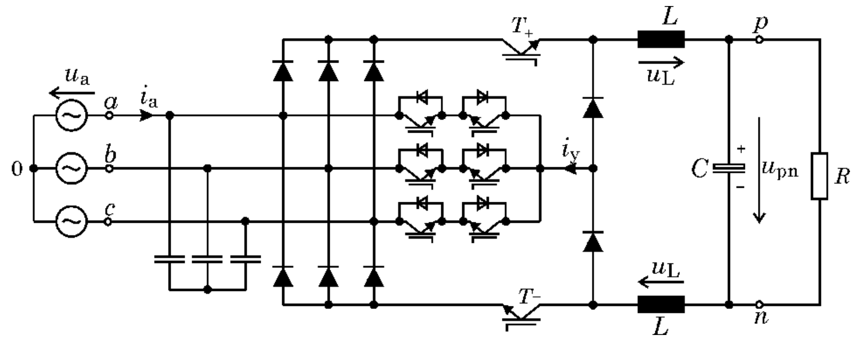

\+ Allows to Generate Low Output Voltages
\+ Short Circuit Current Limiting Capability

– Power Semicond. Stressed with LL-Voltages
– AC-Side Filter Capacitors / Fundamental Reactive Power Consumption

Buck+Boost-Type

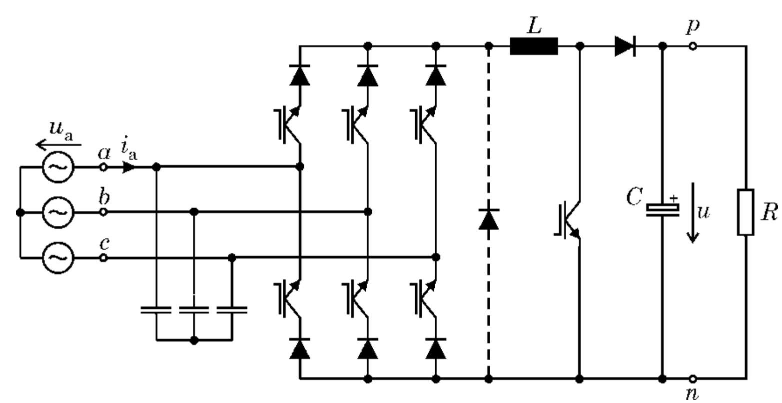

\+ See Buck-Type Converter
\+ Wide Output Voltage Range
\+ Tolerates Mains Phase Loss, i.e. Sinusoidal Mains Current also for 2-Phase Operation

– See Buck-Type Converter (6-Switch Version of Buck Stage Enables Compensation of AC-Side Filter Cap. Reactive Power)

Conclusions & Outlook

Summary of Key Results
Advantageous Applications
Key Challenge

Σ Inductive Power Transfer for EV Charging

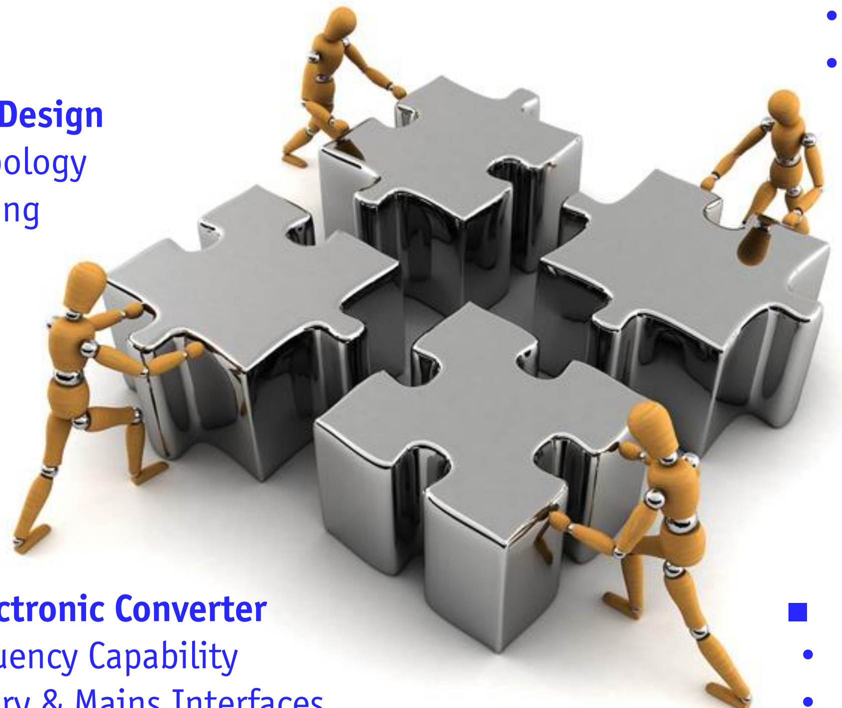

- **Coil Design & Optimization**
  - Magnetic Modeling & Design
  - Multi-Objective Optimization
- **Resonant Circuit Design**
  - Compensation Topology
  - Impedance Matching
- **Power Electronic Converter**
  - High Frequency Capability
  - Coil, Battery & Mains Interfaces
- **Modulation & Control Scheme**
  - Active Load Matching
  - High Partial-Load Efficiency

► Key Figures of Designed Transmission Systems

■ 5 kW Prototype System

• Output Power	5 kW @ 400 V, 100 kHz
• DC/DC-Efficiency	96.5% @ 52 mm (measured)
• Coil Dimensions	210 mm x 30 mm
• Weight Coil + Cap.	2.3 kg
• Spec. Weight	2.2 kW/kg
• Area-Rel. Power Dens.	1.47 kW/dm^2
• Power Density	4.8 kW/dm^3
• Spec. Copper Weight	43 g/kW
• Spec. Ferrite Weight	112 g/kW

■ 50 kW Prototype System

• Output Power	50 kW @ 800 V, 85 kHz
• DC/DC-Efficiency	96.5% (calculated)
• Coil Dimensions	41 x 76 x 6 cm
• Weight Coil + Cap.	24.6 kg
• Spec. Weight	2.0 kW/kg
• Area-Rel. Power Dens.	1.6 kW/dm^2
• Power Density	2.7 kW/dm^3
• Spec. Copper Weight	52 g/kW
• Spec. Ferrite Weight	160 g/kW
• Spec. SiC-Chip Area	9.4 mm^2/kW

Inductive Power Transfer for

Stationary EV Charging

- **Domestic EV Charging form Household Supply**
  - Lower Power Level Simplifies Design

- **Stationary EV Charging for Public Transportation**
  - Simplified Quick-Charging at Bus Stops
  - Reduced Battery Volume/Weight/Cost
  - Reduced Number of Fleet Vehicles

→ **Reduced Operating Costs!**

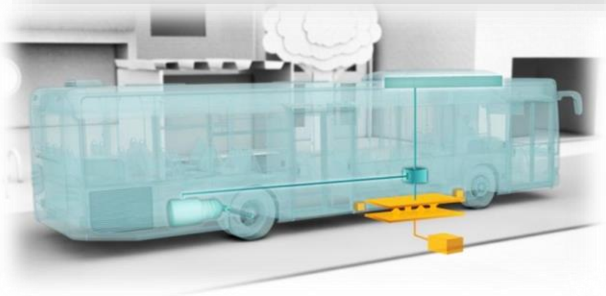

Evatran PLUGLESS, http://pluglesspower.com (6.11.2014).
Bombardier PRIMOVE, http://primove.bombardier.com.

Inductive Power Transfer for EV Charging

Technical Limits

- **Magnetic & Electric Stray Fields at High Power Levels**
  - Magnetic Field Standards (e.g. ICNRIP 1998, 2010)
  - Electric Field Emissions due to High Resonant Voltages and Steep dV/dt of Power Switches
- **Limited Efficiency of Compact Systems**
  - Desired Small IPT Coils have Low Coupling and Reduced Efficiency → Physical Limit!
- **Limited Power Capability with Passive Cooling**
  - Active Cooling Typically Not Available in EVs
  - Limited Convection Cooling w/o Metal Heatsink

→ Charging Power Limited to Approx. 3-5 kW for Natural Convection Cooling

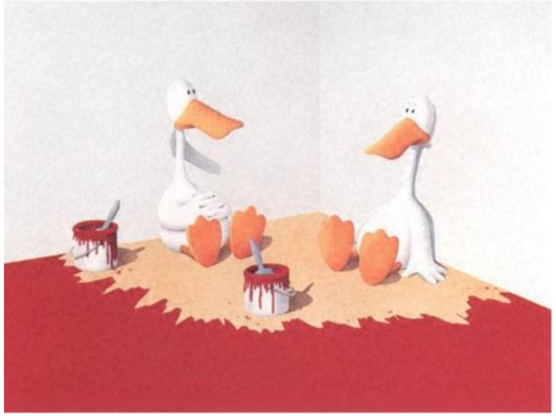

▲ **Very Limited Room for Improvement**

Inductive Power Transfer

Potential Application Areas

- **Transportation Vehicles Industrial Environments**
  - Conveyor Vehicles at Industrial Sites / Airports / Hospitals
  - Reduced Battery Volume & Weight → Lower Cost
- **Power Supply to Moving Vehicles in Clean Rooms**
  - No Slip-Contacts Required → Reduced Particle Generation
- **Applications with High Insulation Requirements**
  - Auxiliary Supply with High Insulation Strength, e.g. for Gate Drives, Modular Multi-Level, …

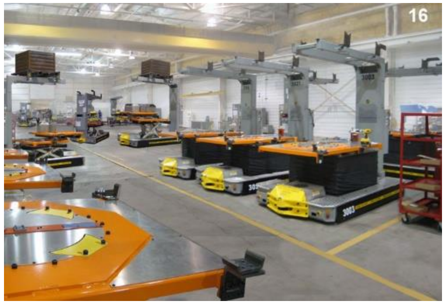

Inductive Power Transfer

Applications ... the Hype Cycle

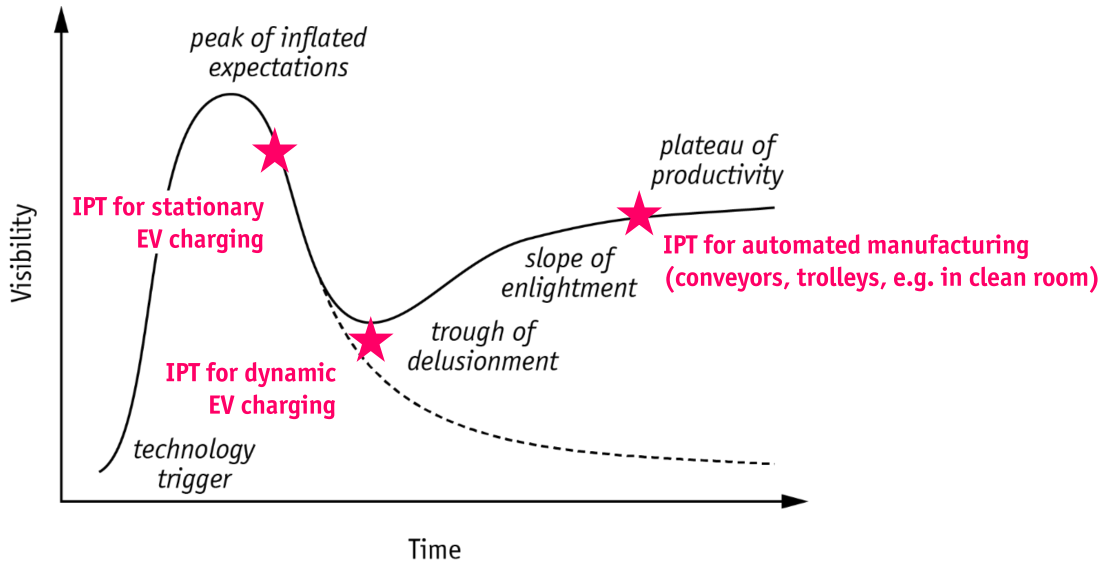

Thank You!

Questions?

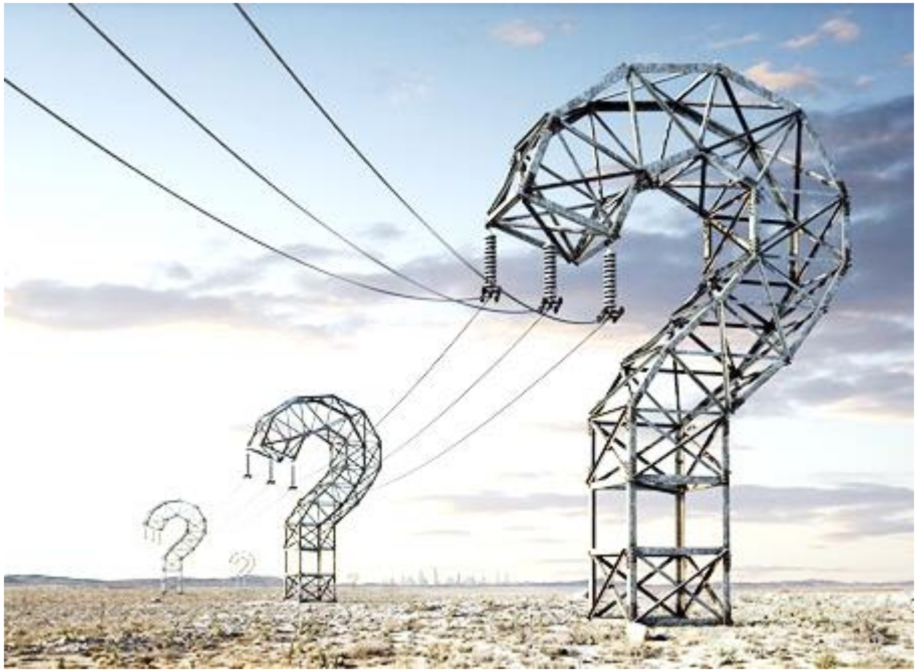

► Further Information

- **Appendix 1:** Comments on Dynamic IPT Charging
- **Appendix 2:** 3-Φ PFC Rectifier Systems

- **List of Key Publications** (click title to view online)

- **R. Bosshard, J. W. Kolar, J. W. Mühlethaler, I. Stevanovic, B. Wunsch, F. Canales,** "Modeling and η-α-Pareto optimization of inductive power transfer coils for electric vehicles," *IEEE J. Emerg. Sel. Topics Power Electron.*, vol. 3, no. 1., pp.50-64, March 2015.
- **R. Bosshard, J. W. Kolar, B. Wunsch,** "Control Method for Inductive Power Transfer with High Partial-Load Efficiency and Resonance Tracking," Proc. Int. Power Electron. Conf. - ECCE Asia (IPEC 2014), May 2014.
- **R. Bosshard, J. W. Kolar, B. Wunsch,** "Accurate Finite-Element Modeling and Experimental Verification of Inductive Power Transfer Coil Design," Proc. 29th Appl. Power Electron. Conf. and Expo. (APEC 2014), March 2014.
- **R. Bosshard, J. Mühlethaler, J. W. Kolar, I. Stevanovic,** "Optimized Magnetic Design for Inductive Power Transfer Coils," Proc. 28th Appl. Power Electron. Conf. and Expo. (APEC 2013), March 2013.
- **R. Bosshard, U. Badstübner, J. W. Kolar, I. Stevanovic,** "Comparative Evaluation of Control Methods for Inductive Power Transfer," Proc. Int. Conf. on Renewable Energy Research and Appl. (ICRERA 2012), November 2012.
- **R. Bosshard, J. Mühlethaler, J. W. Kolar, I. Stevanovic,** "The η-α-Pareto Front of Inductive Power Transfer Coils," Proc. Annu. Conf. IEEE Ind. Electron. Soc. (IECON 2012), October 2012.

- **J. W. Kolar, T. Friedli,** "The Essence of Three-Phase PFC Rectifier Systems - Part I," *IEEE Trans. Power Electron.*, vol. 28, no. 1, pp. 176-198, January 2013.
- **T. Friedli, M. Hartmann, J. W. Kolar,** "The Essence of Three-Phase PFC Rectifier Systems - Part II", *IEEE Trans. Power Electron.*, vol. 29, no. 2, February 2014.

- **Contact Information**

- Roman Bosshard: bosshard@lem.ee.ethz.ch
- Johann W. Kolar: kolar@lem.ee.ethz.ch

Appendix 1:
Comments on Dynamic IPT Charging

Inductive Power Transfer for

Dynamic EV Charging

James Provost for IEEE Spectrum

Simplified Calculation

- **20 km of Highway @ avg. 25 kW[1], 120 km/h**
  - 20/120 h x 25 kW = 4.2 kWh used
- **200 m IPT-Lane per 20 km of Highway**
  - Electrification of 1%
- **Speed while Charging 50 km/h**
  - 14 s for Charging of 4.2 kWh

- **1 MW / Vehicle Required Charging Power**
  - High Cost for Medium Voltage Infrastructure
  - Battery that Handles 1 MW?
  - Slowing Down to 50 km/h every 20 km?

- **Stationary: 10 min x 1 MW = 167 kWh → 6.6 h Driving!**

[1] ***T. Bütler and H. Winkler,*** «Energy consumption of battery electric vehicles (BEV),» EMPA, Dübendorf, Switzerland, 2013.

Inductive Power Transfer for

Dynamic EV Charging

- **Large & Expensive Installation vs. Improving Battery Technology**
- **Medium-Voltage Supply & Distribution of Power along 1% of all Highways**
- **Efficiency of Dynamic IPT vs. Increasing Energy Cost?**
- **Possible Applications:**
  - Electrification @ Traffic Lights, Bus Stops, ...
  - Transportation Vehicles @ Industrial Sites

Appendix 2:
3-Φ PFC Rectifier Systems

J. W. Kolar, T. Friedli,
The Essence of Three-Phase PFC Rectifier Systems - Part I, IEEE Transactions on Power Electronics, Vol. 28, No. 1, pp. 176-198, January 2013.

T. Friedli, M. Hartmann, J. W. Kolar,
The Essence of Three-Phase PFC Rectifier Systems - Part II, IEEE Transactions on Power Electronics, Vol. 29, No. 2, February 2014.

Hybrid 3-Φ Boost-Type PFC Rectifier Systems

3rd Harmonic Injection Rectifier

► Classification of Unidirectional Rectifier Systems

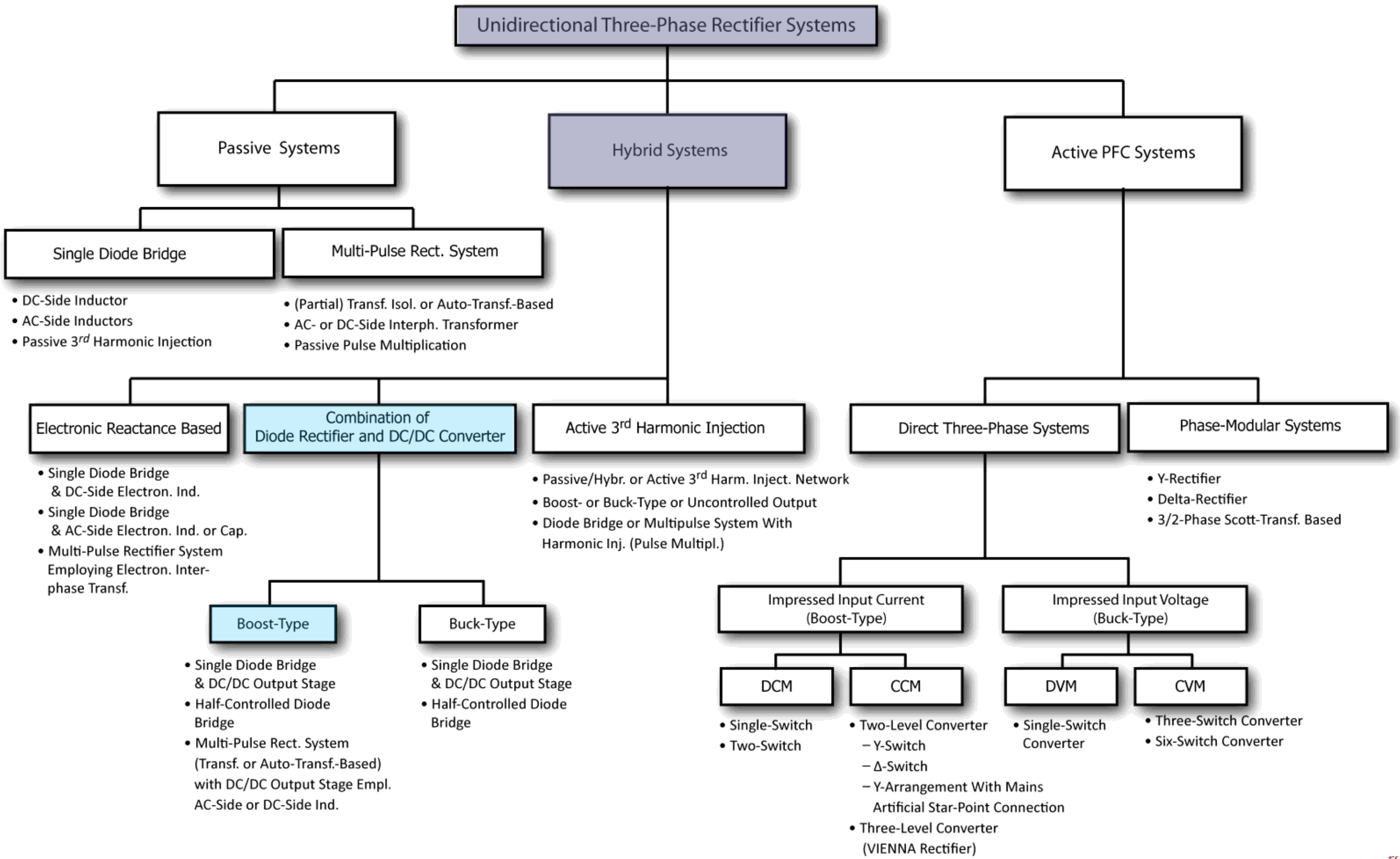

Diode Bridge + DC/DC Boost Converter

- Controllable Output Voltage
- Low-Frequency Mains Current Distortion

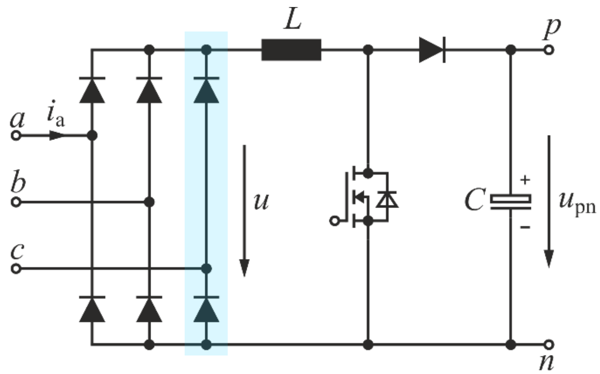

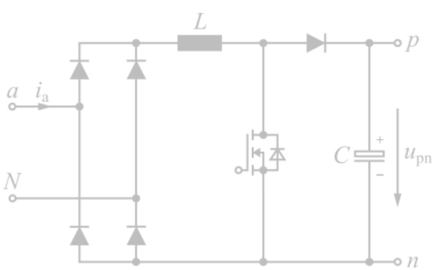

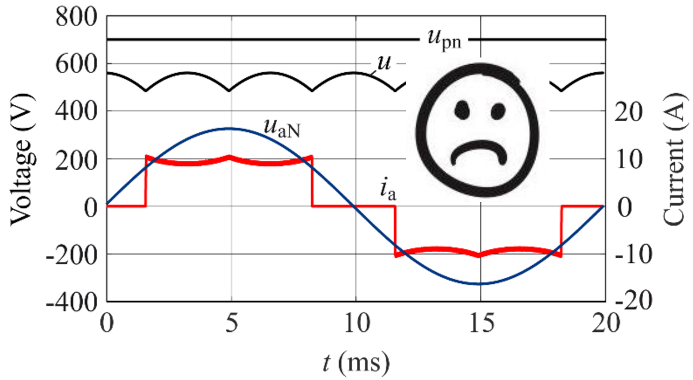

3-Φ DCM (PFC) Boost Rectifier

- Controllable Output Voltage
- Low-Frequency Mains Current Distortion

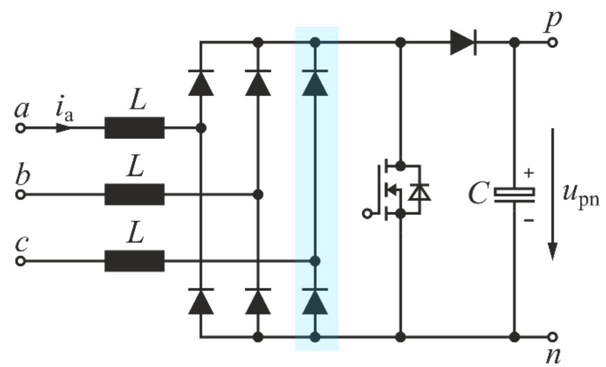

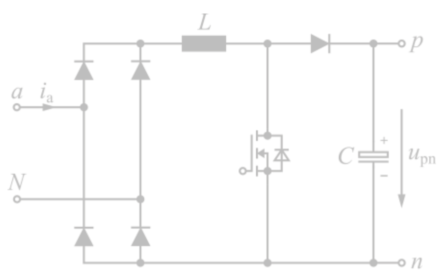

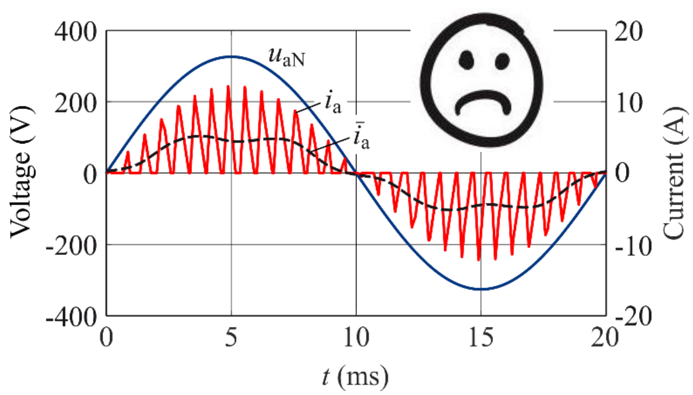

► Classification of Unidirectional Rectifier Systems

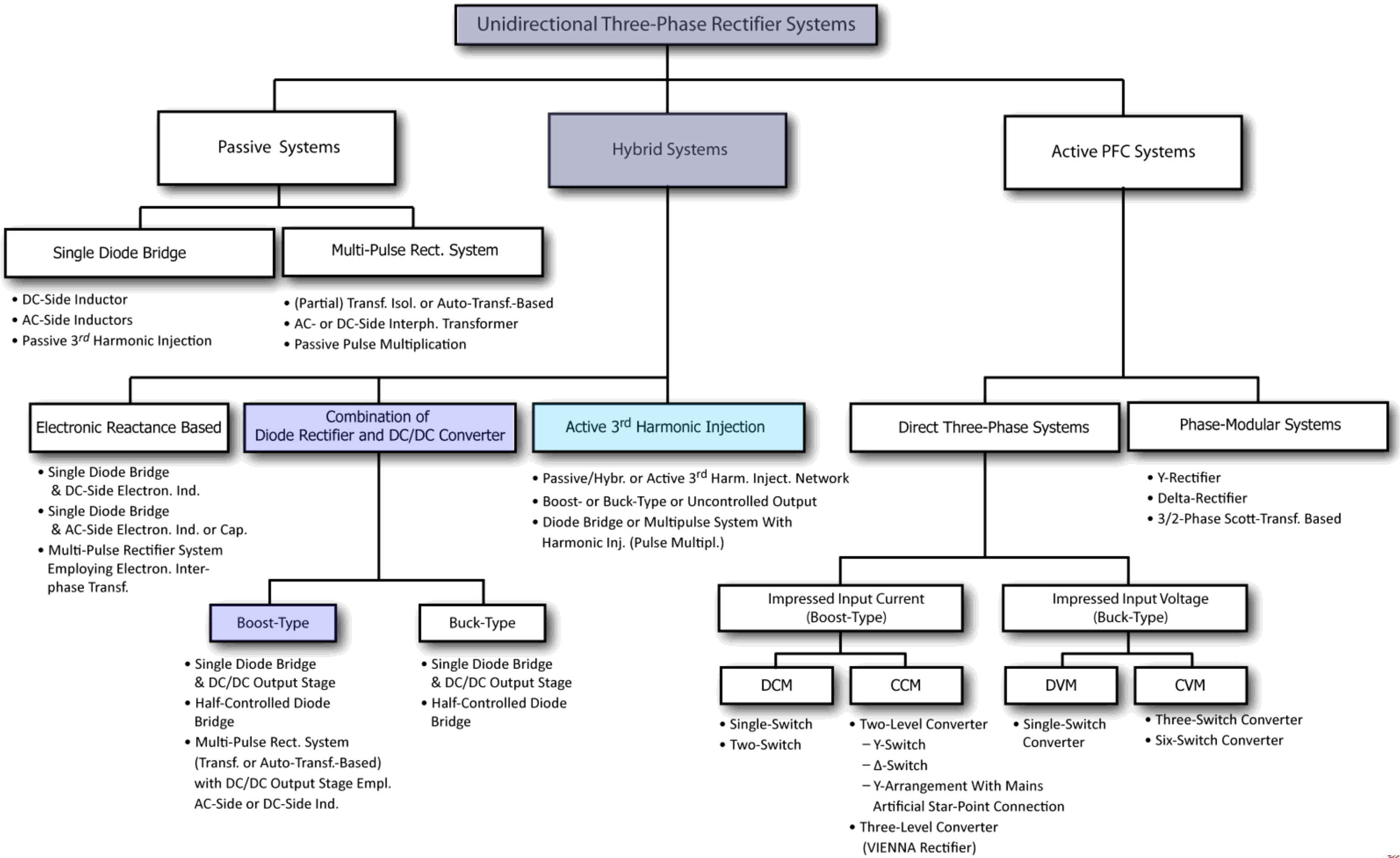

3-Φ Hybrid 3rd Harmonic Inj. PFC Boost-Rectifier

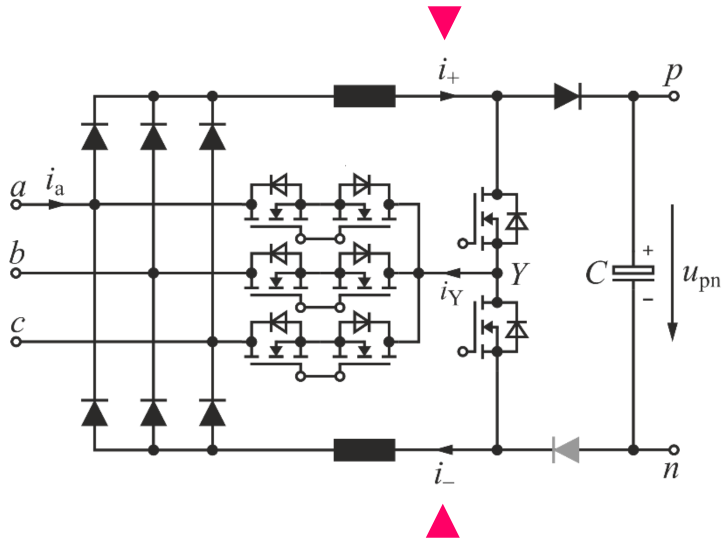

- **Independent Control of *i*+ and *i*-**

3-Φ Hybrid 3rd Harmonic Inj. PFC Boost-Rectifier

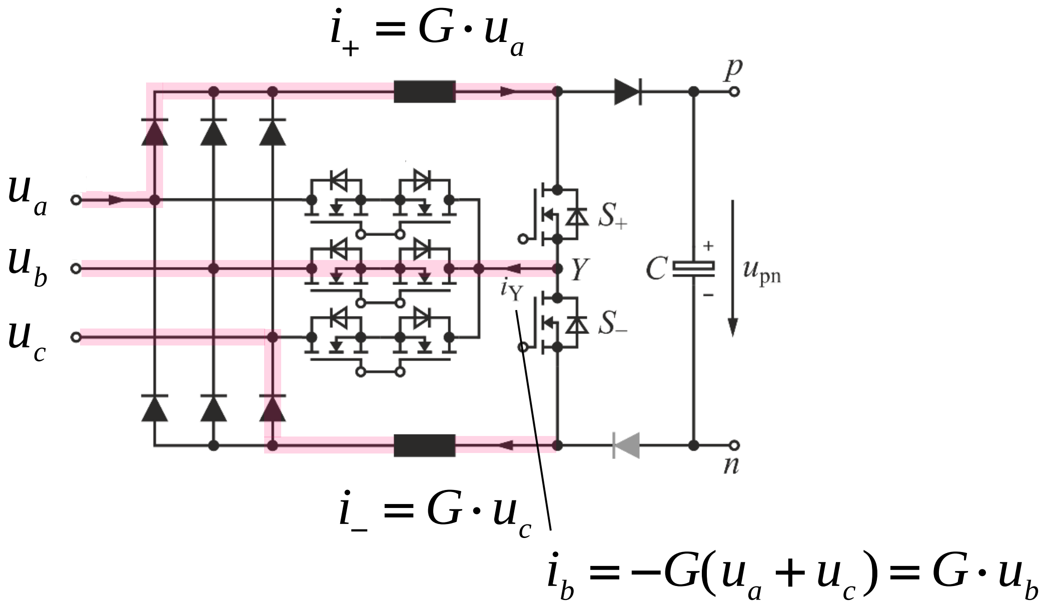

- **Sinusoidal Control of *i*+ and *i*- and i_Y**

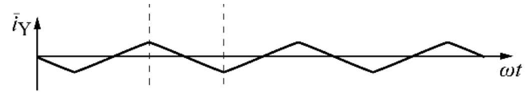

3-Φ Hybrid 3rd Harmonic Inj. PFC Boost-Rectifier

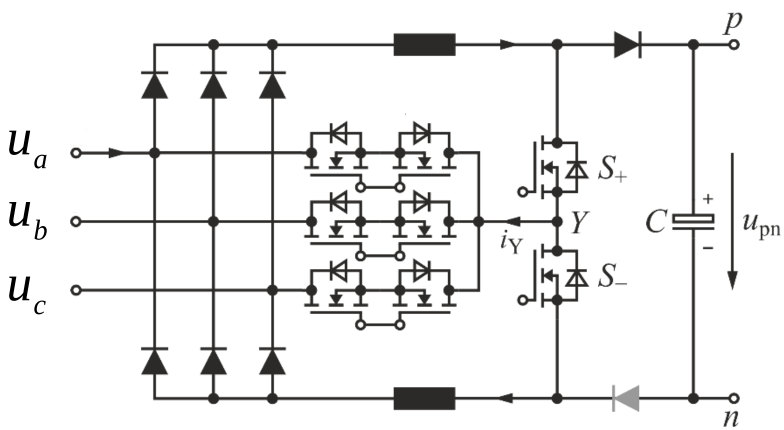

- Sinusoidal Mains Current Control → Limited to Ohmic Mains Behavior
- Output Voltage Control → High Minimum Output Voltage Level

3-Φ Active Filter Type PFC Rectifier

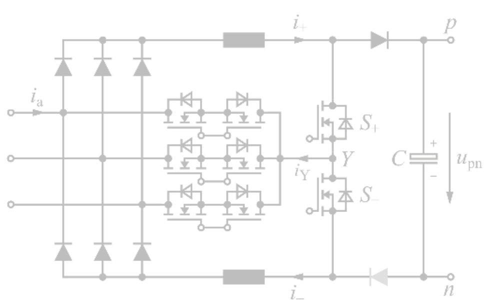

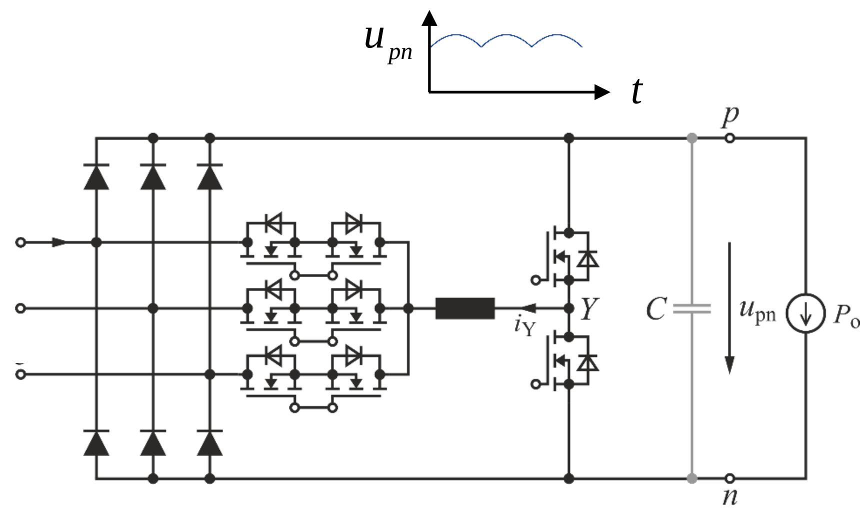

- Sinusoidal Mains Current

→ **Requires Constant Power Load** P_0**= const.**
→ ***NO* (!) *Output Voltage Control***

Active 3-Φ Boost-Type PFC Rectifier Systems

Δ-Switch Rectifier
Vienna-Rectifier
Six-Switch Rectifier

Classification of Unidirectional Rectifier Systems

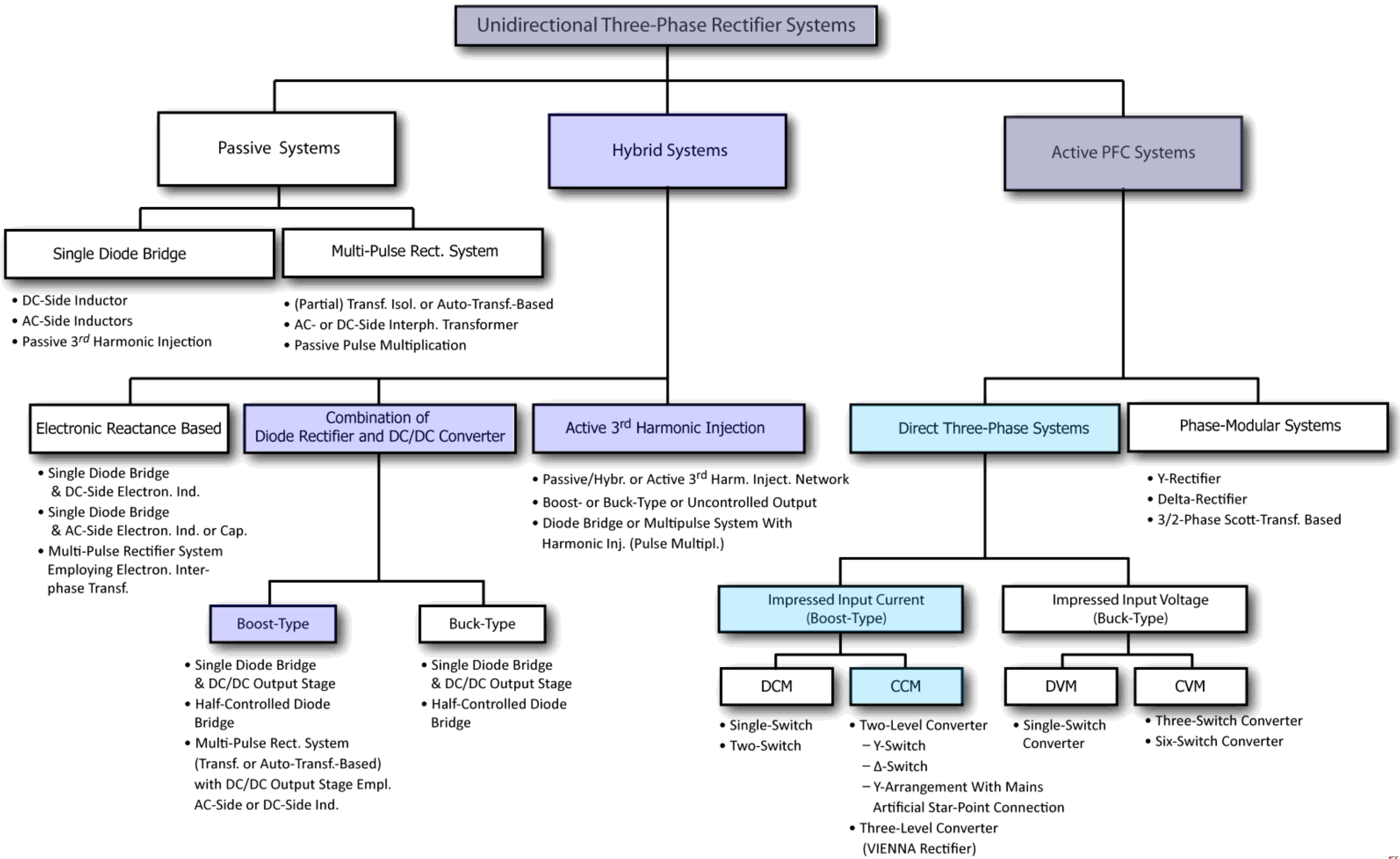

Δ-Switch Rectifier

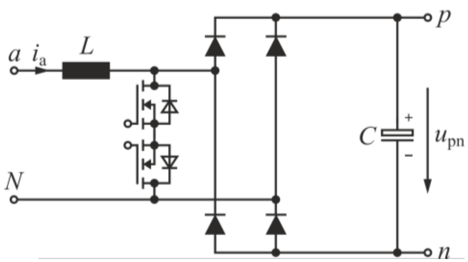

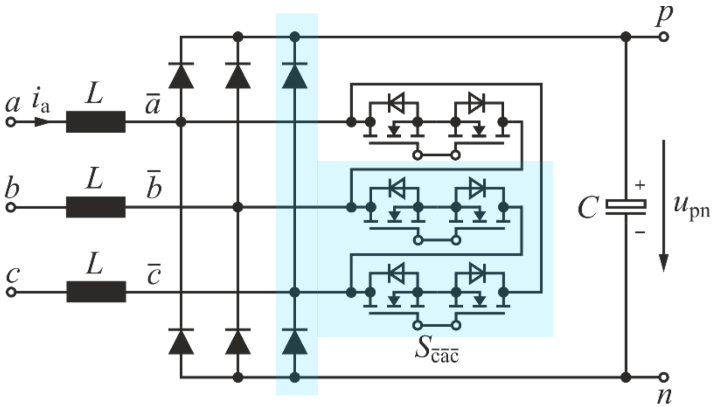

- Modulation of Diode Bridge Input Voltages / Conduction States
- Derivation of 3-Φ Topology → Phase-Symmetry / Bridge-Symmetry

Δ-Switch Rectifier

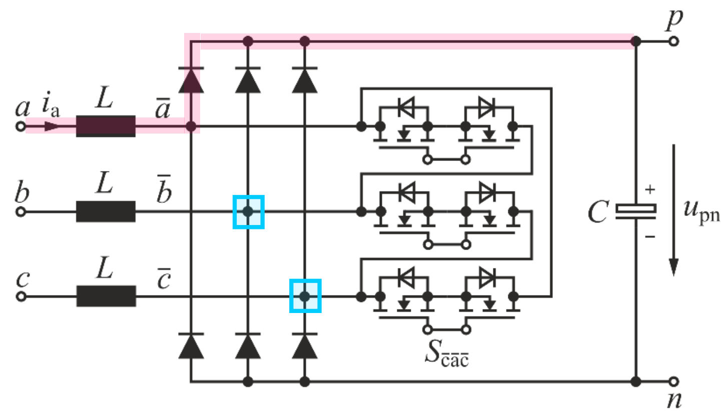

- Output Voltage Control
- Sinusoidal Mains Current Control
- Φ = (-30°,+30°)

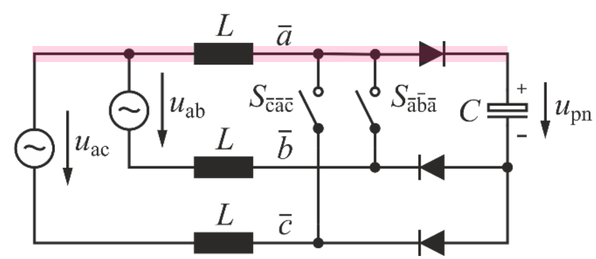

Vienna Rectifier

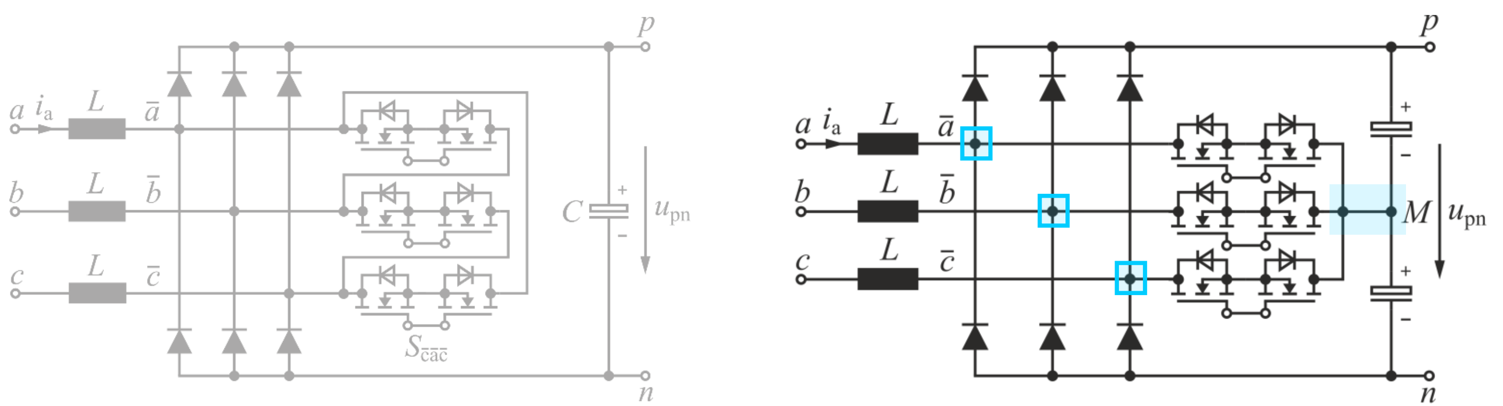

- Replace Δ-Switch by Y-Switch
- Connect Y-Switch to Output Center Point
- Maximum Phase/Bridge Symmetry
- Output Voltage Control
- Sinusoidal Mains Current Control
- Φ = (-30°,+30°)

Vienna Rectifier

▶ Three-Level Characteristic

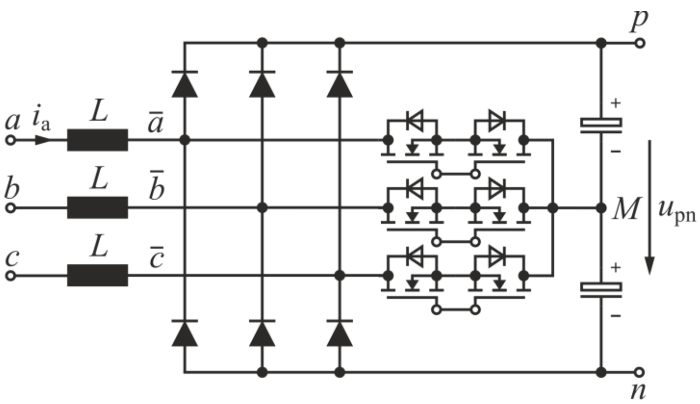

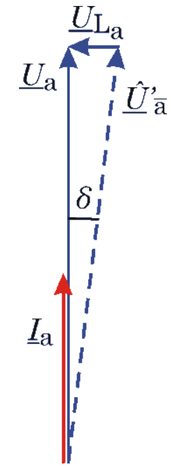

+ Low Input Inductance Requ.
+ Low Switching Losses,
+ Low EMI

– Higher Circuit Complexity
– Control of Output Voltage Center Point Required

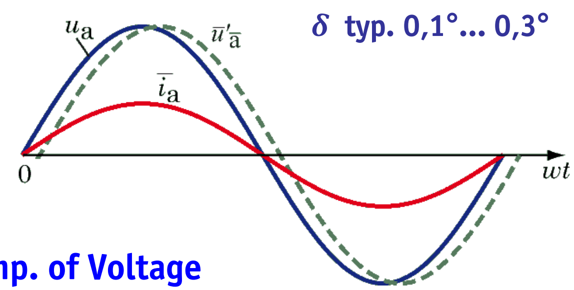

▶ Difference of Mains Voltage (e.g. u_a) and Mains Frequency Comp. of Voltage Formed at Rectifier Bridge Input (e.g. $\bar{u}'_{\bar{a}}$) Impresses Mains Current (e.g. i_a)

Control Structure

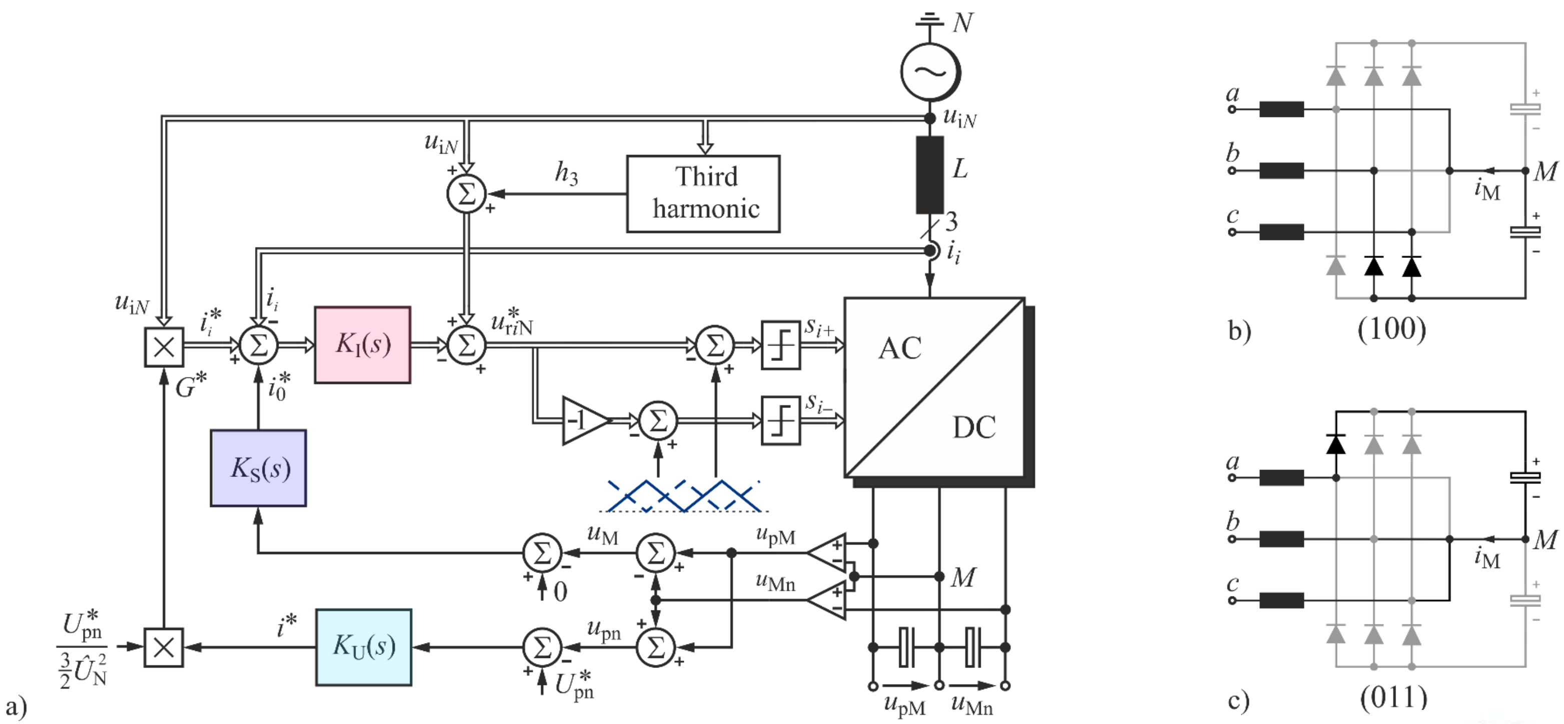

■ **Output Voltage Control & Inner Mains Current Control & *NPP* Control**

Experimental Results

P_0 = 10kW
U_N = 230V
f_N = 800Hz
U_0 = 800V
THD_i = 1.6%

★ 10kW/dm³

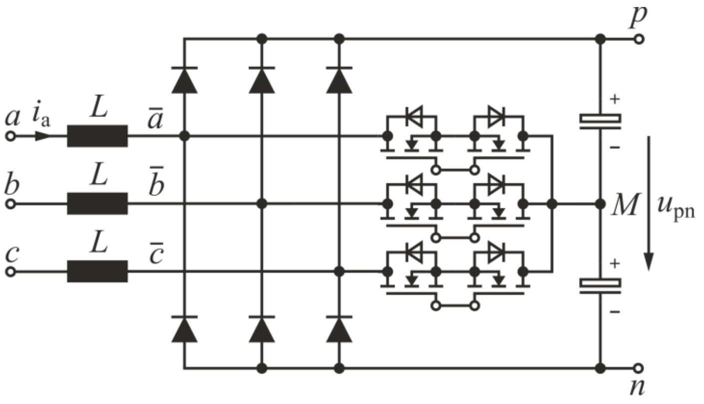

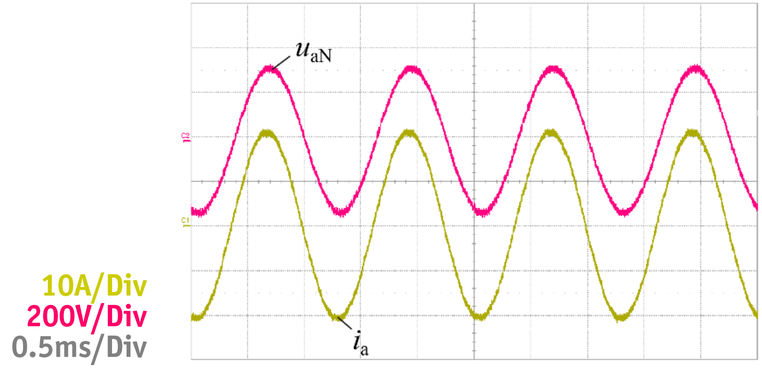

Fully-Controlled (Six-Switch) Bridge Rectifier

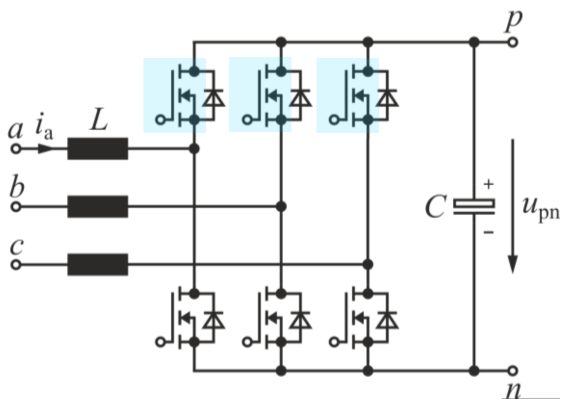

■ **Output Voltage Control**

→ Phase- & *Bridge-Symmetry*
→ *Sinusoidal Mains Current Control*
→ Φ = *(-180°,+180°) – Bidirectional (!)*

3-Φ Buck-Type PFC Rectifier Systems

– Unidirectional
– Bidirectional

Classification of Unidirectional Rectifier Systems

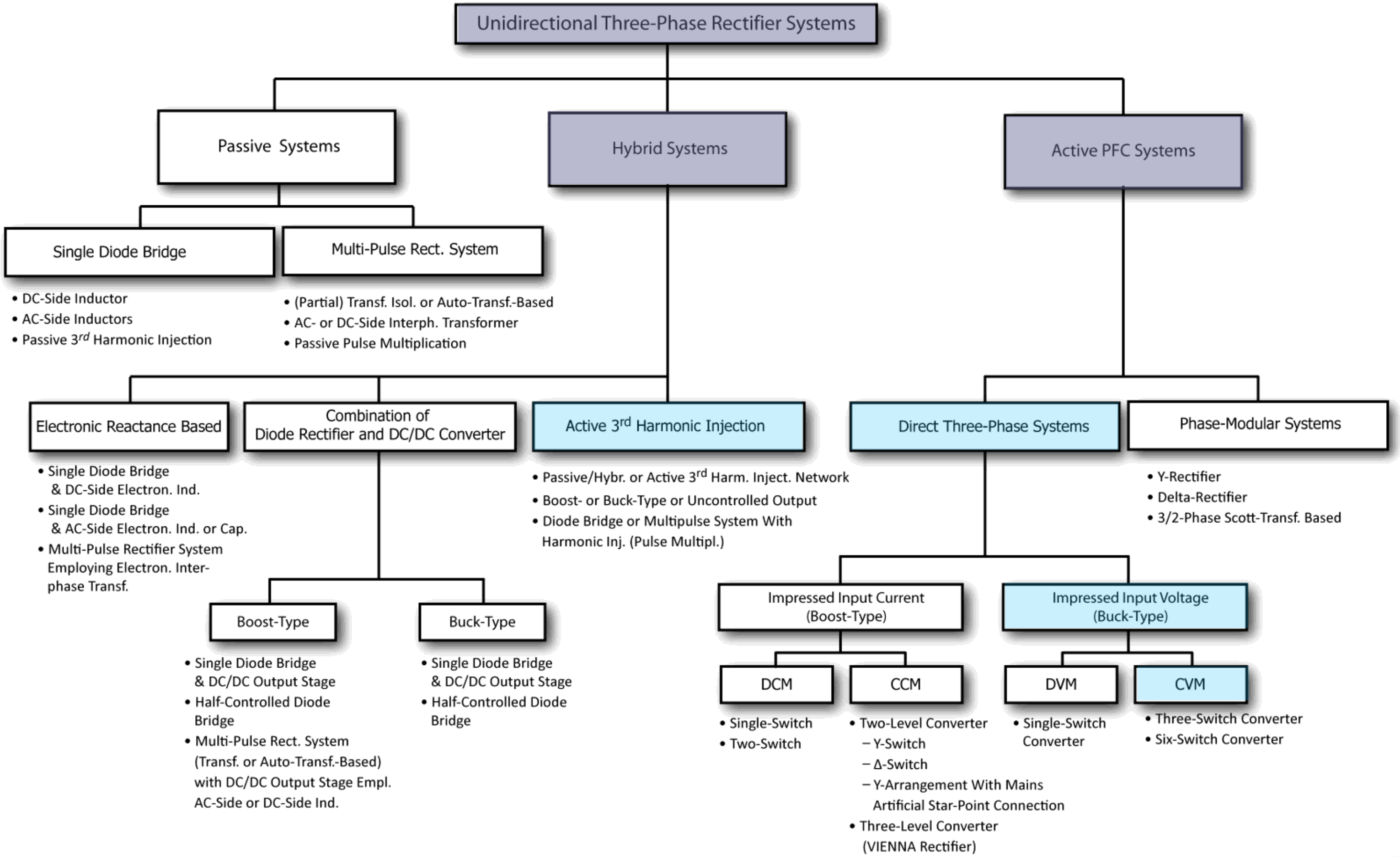

Active 3-Φ Buck-Type PFC Rectifier Systems

Three-Switch Rectifier
Six-Switch Rectifier

Three-Switch PFC Rectifier

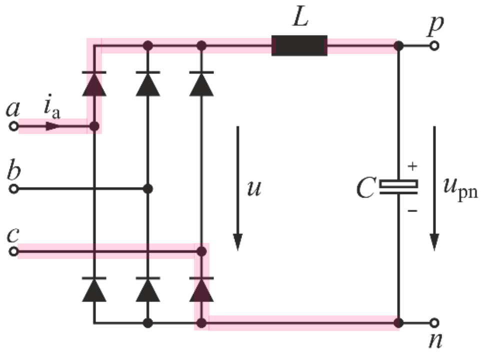

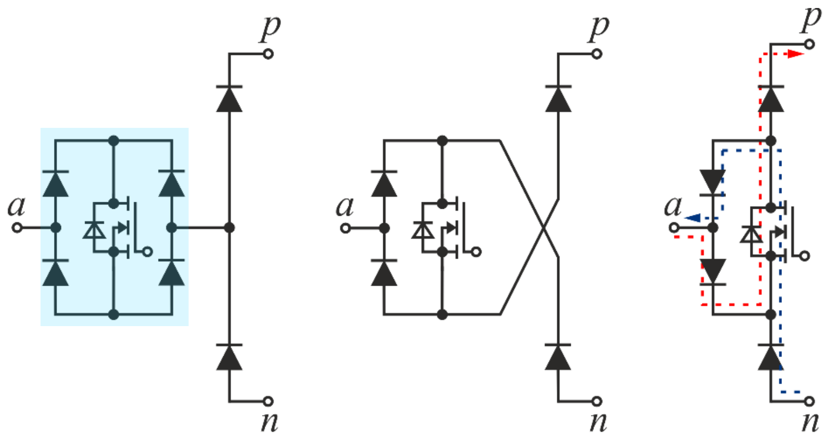

- Derivation of Rectifier Topology

→ Controllability of Conduction State
→ Phase-Symmetry / Bridge-Symmetry

Three-Switch PFC Rectifier

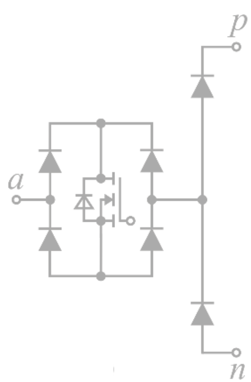

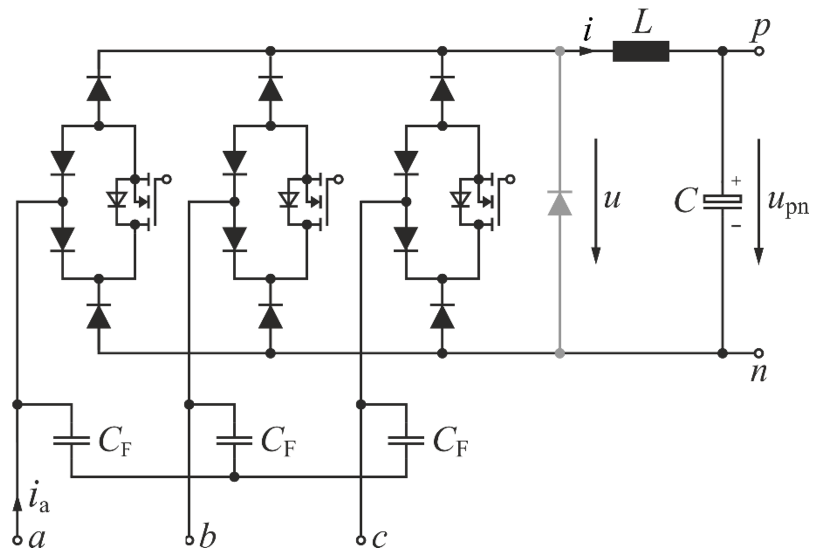

- Output Voltage Control
- Sinusoidal Mains Current Control
- Φ = (-30°,+30°)

→ Relatively High Conduction Losses

Six-Switch PFC Rectifier

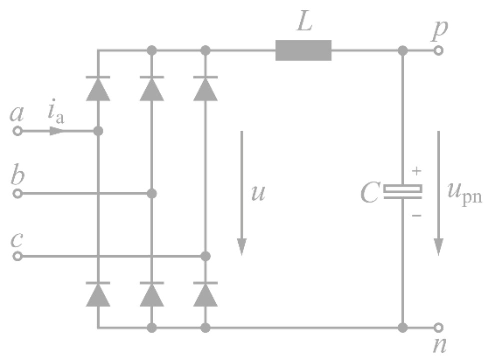

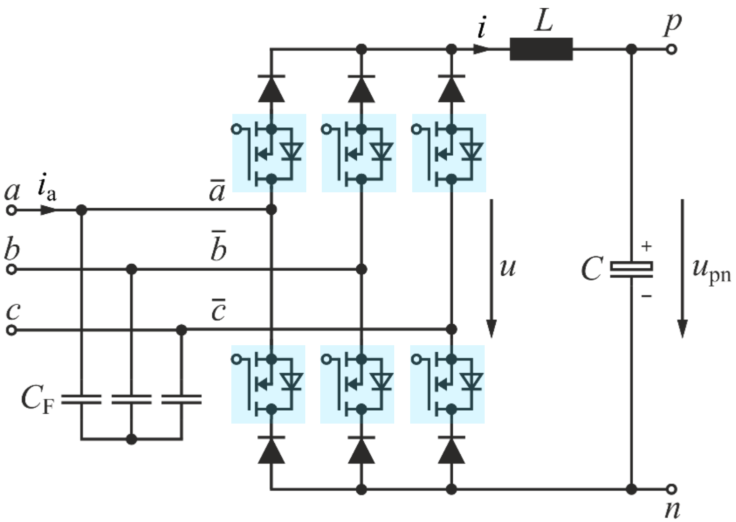

→ Controllability of Conduction State
→ Phase-Symmetry / Bridge-Symmetry

- Output Voltage Control
- Sinusoidal Mains Current Control
- Φ = (-90°,+90°)

▶ Modulation Scheme

- Consider 60°-Wide Segment of the Mains Period; Suitable Switching States Denominated by (s_a, s_b, s_c)

- Clamping to Phase with Highest Absolute Voltage Value, i.e.

- Phase *a* for $\omega t \in \left(-\frac{\pi}{6},+\frac{\pi}{6}\right)$,
- Phase *c* for $\omega t \in \left(+\frac{\pi}{6},+\frac{\pi}{2}\right)$ etc.

- Assumption: $\omega t \in \left(0,+\frac{\pi}{6}\right)$

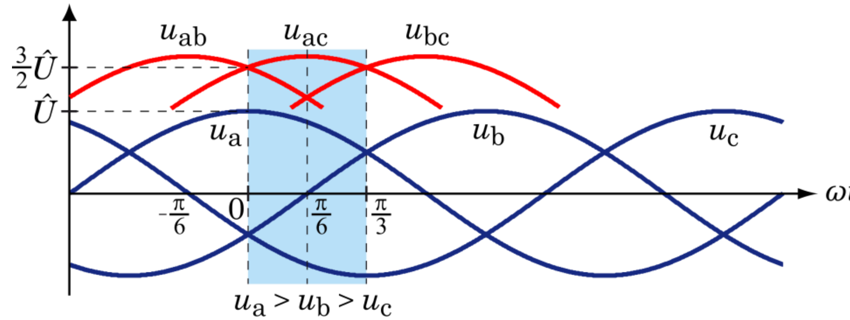

(111)

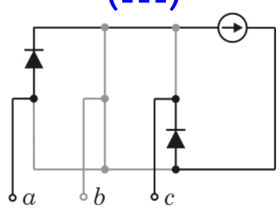

(110)

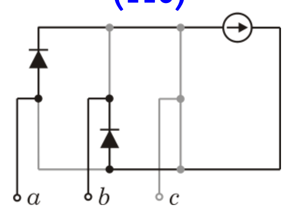

(100)

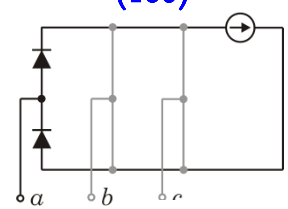

(101)

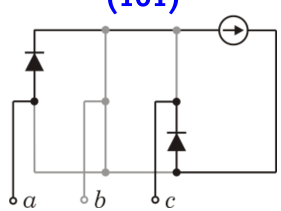

(011)

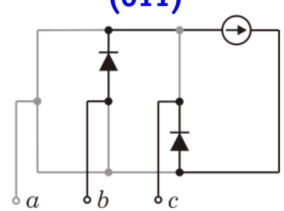

also: (010)
(011)

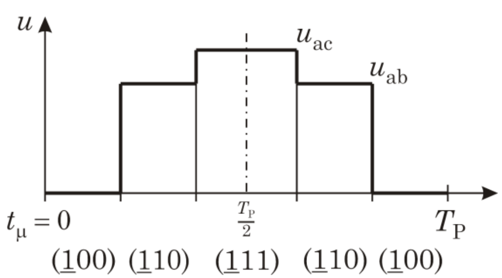

- Clamping and "Staircase-Shaped" Link Voltage in Order to Minimize the Switching Losses

▶ Input Current and Output Voltage Formation

- Assumption: $\omega t \in \left(0, +\dfrac{\pi}{6}\right)$

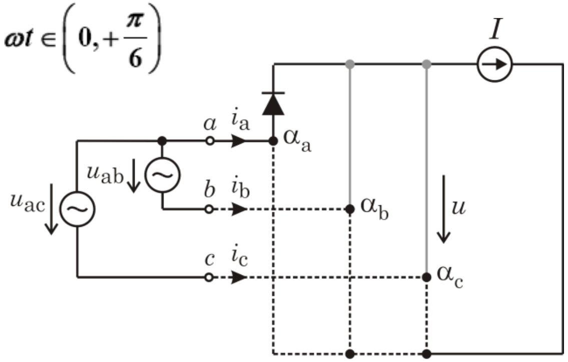

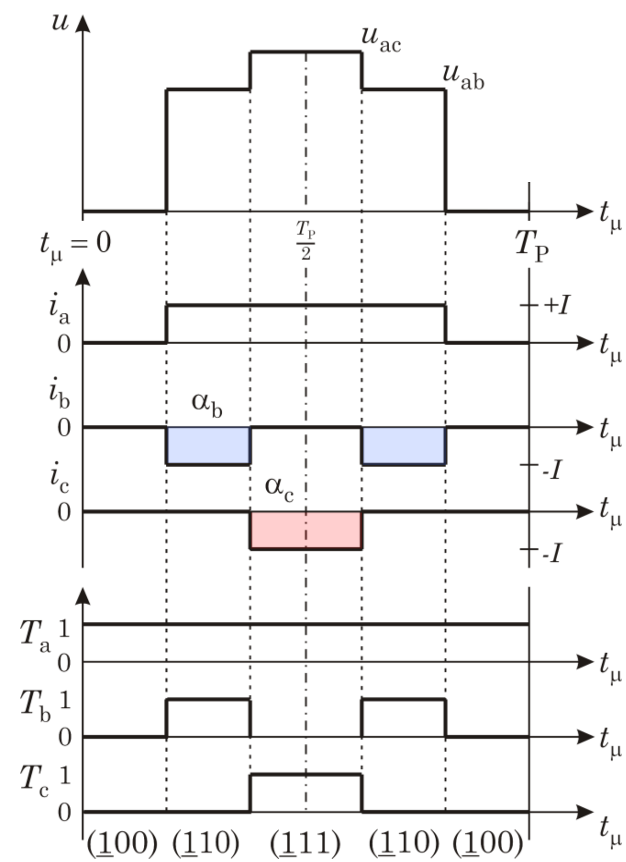

- Output Voltage Formation:

$$\overline{u} = u_{ab} \cdot \alpha_b + u_{ac} \cdot \alpha_c$$

$$P_{link} = P_{input}$$

$$\overline{u} \cdot I = \frac{3}{2} \cdot \hat{U} \cdot \hat{I}^*$$

$$\overline{u} = \frac{3}{2} \cdot \hat{U} \cdot \frac{\hat{I}^*}{I} = \frac{3}{2} \cdot \hat{U} \cdot M$$

- **Output Voltage is Formed by Segments of the Input Line-to-Line Voltages**
- **Output Voltage Shows Const. Local Average Value**

Control Structure

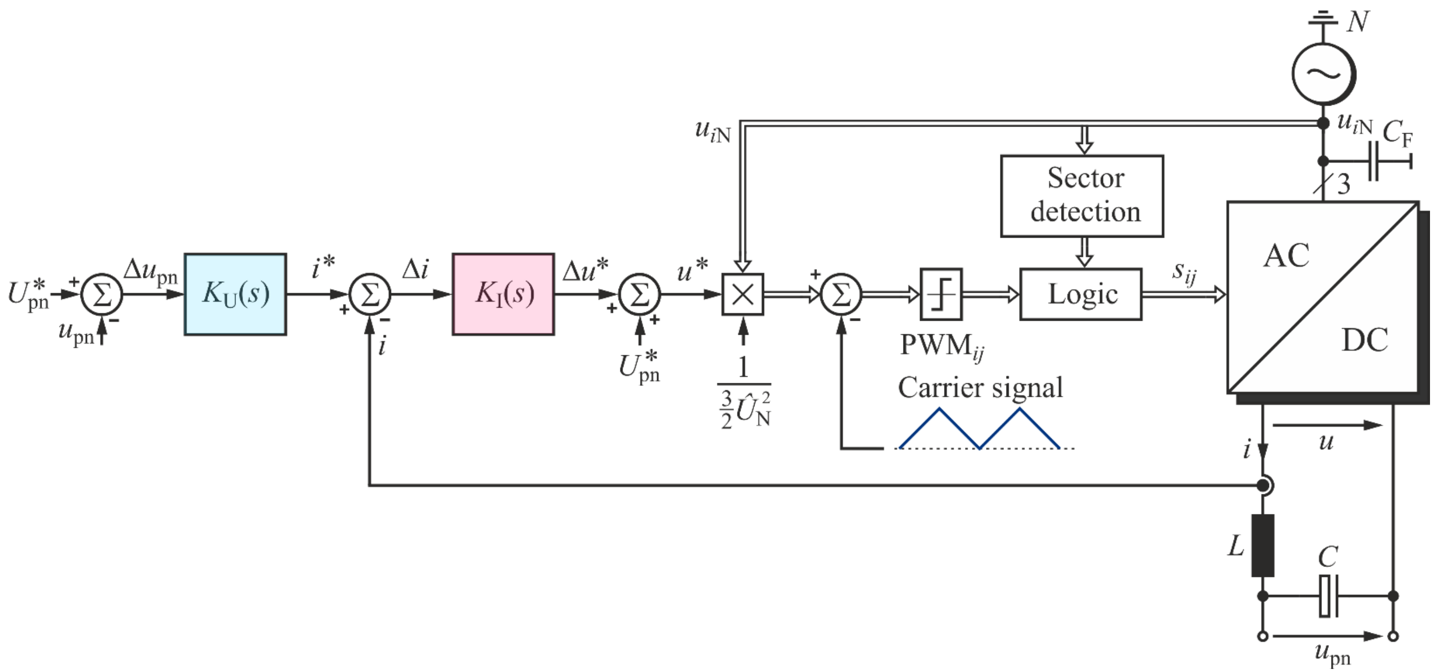

- **Output Voltage Control & Inner Output Current Control**

▶ Experimental Results

■ Ultra-Efficient Demonstrator System

U_{LL} = 3 x 400 V (50 Hz)
P_o = 5 kW
U_o = 400 V
f_s = 18 kHz
L = 2 x 0.65 mH

η = 98.8% (Calorimetric Measurement)

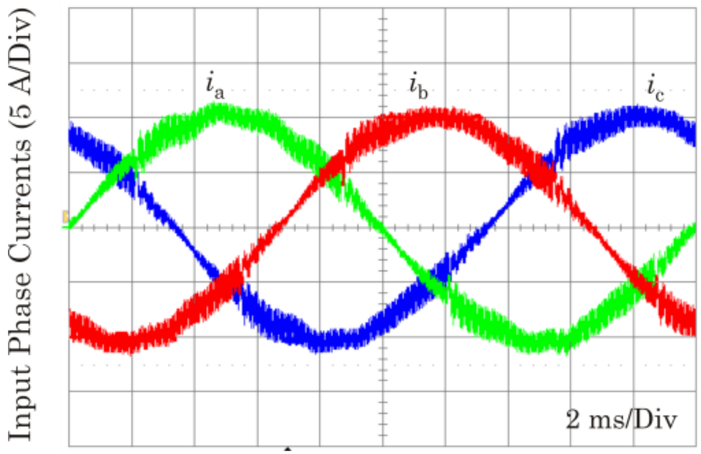

3^{rd} Harmonic Inj. Buck-Type PFC Rectifier Systems

SWISS Rectifier

► Classification of Unidirectional Rectifier Systems

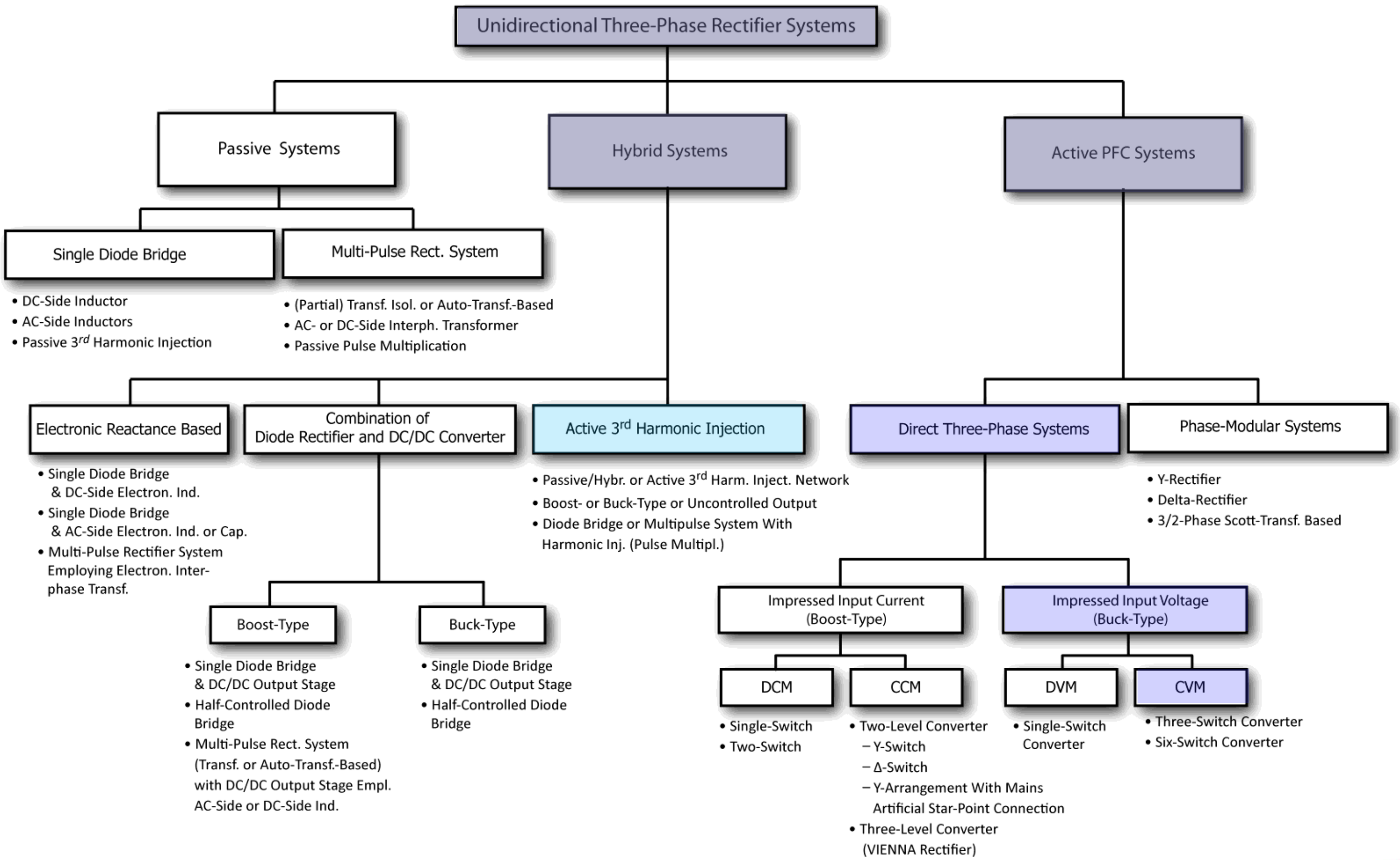

SWISS Rectifier

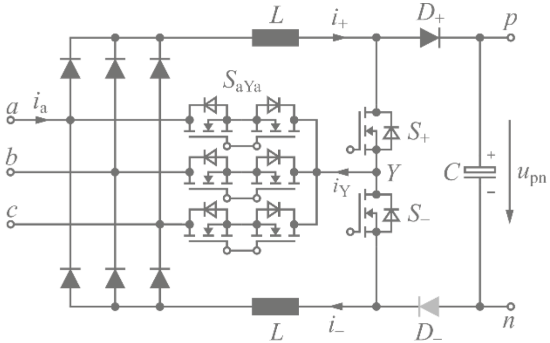

- 3rd Harmonic Inj. Concept

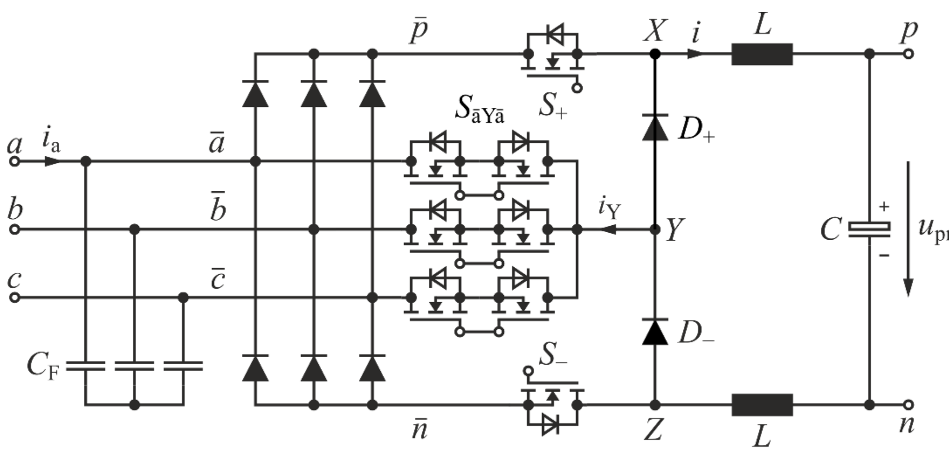

SWISS Rectifier

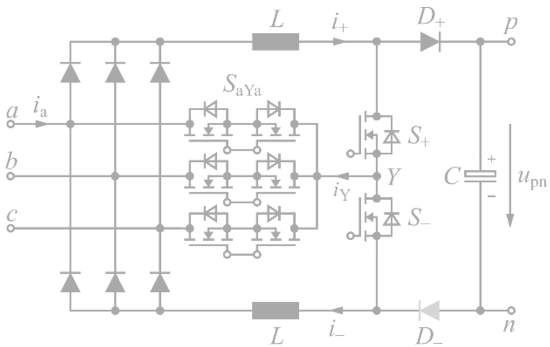

- Output Voltage Control
- Sinusoidal Current Control

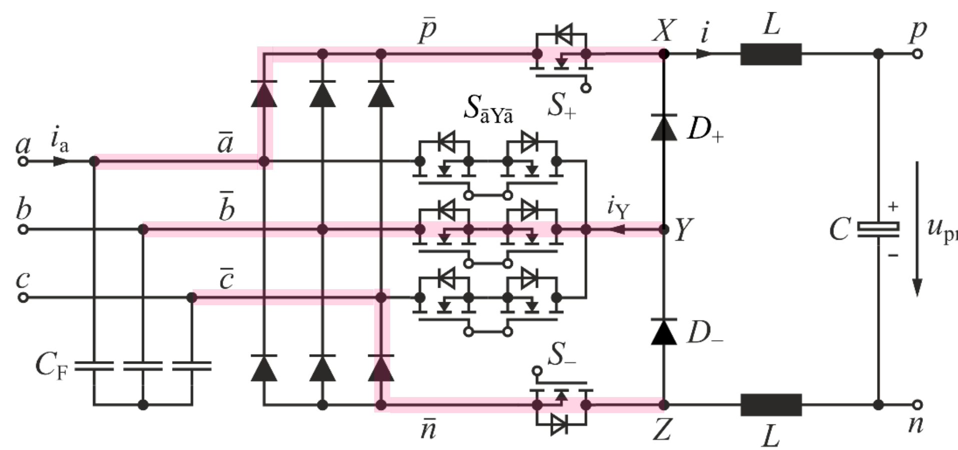

SWISS Rectifier

- Output Voltage Control
- Sinusoidal Current Control

→ Low Complexity

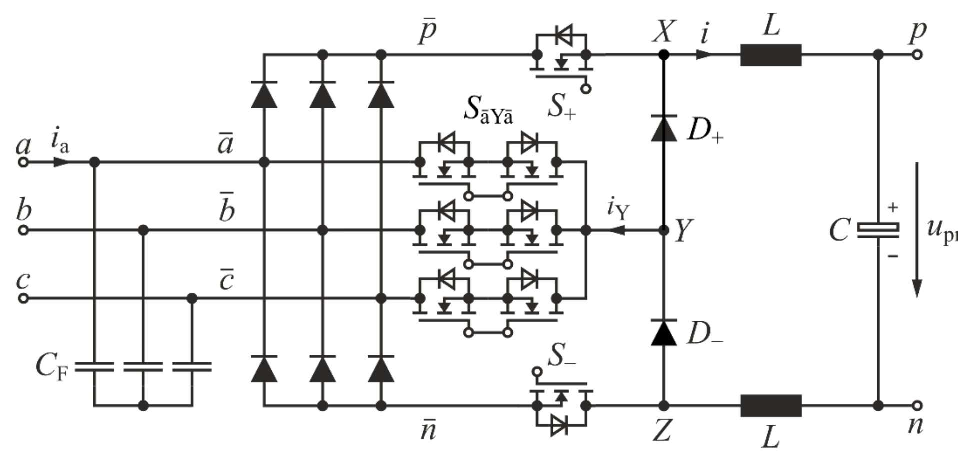

Bidirectional PFC Rectifier Systems

- *Boost-Type Topologies*
- *Buck-Type Topologies*

Boost-Type Topologies

► Classification of Bidirectional Boost-Type Rectifier Systems

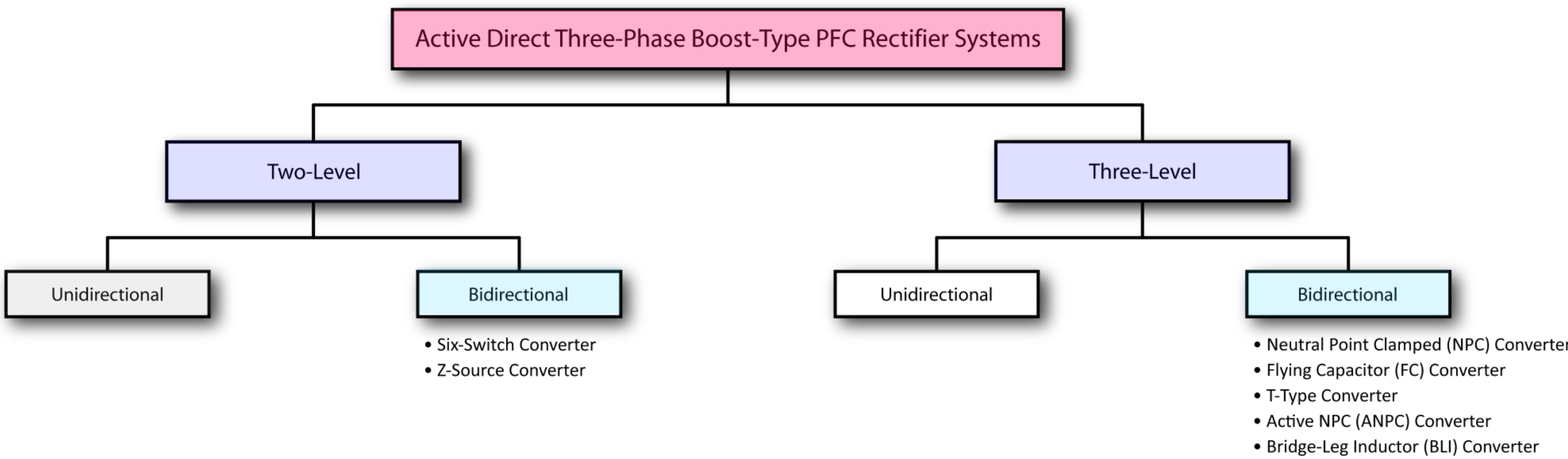

▶ Derivation of Two-Level Boost-Type Topologies

- **Output Operating Range**

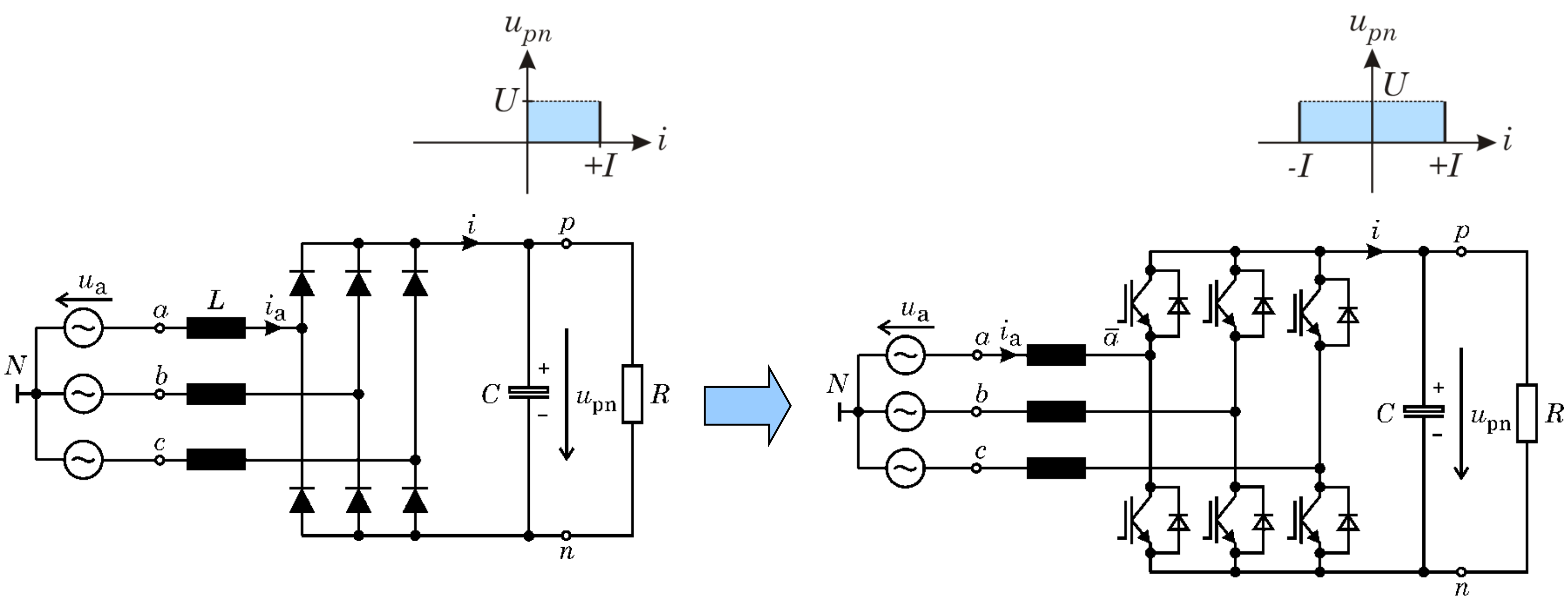

▶ Derivation of Three-Level Boost-Type Topologies

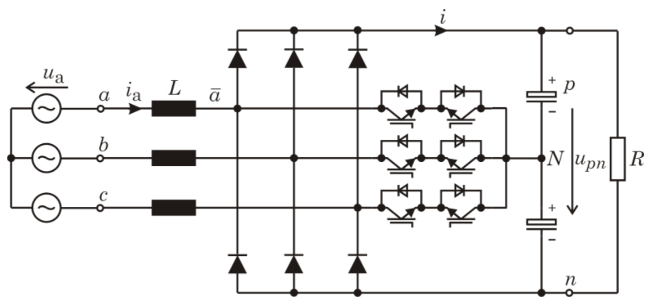

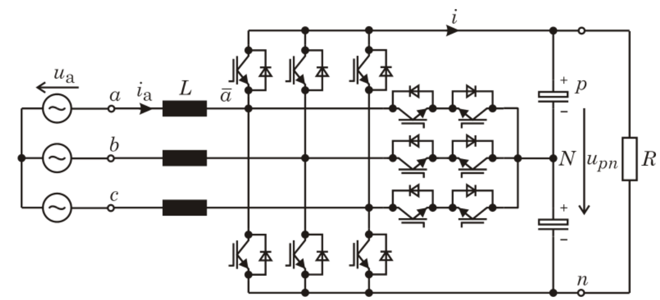

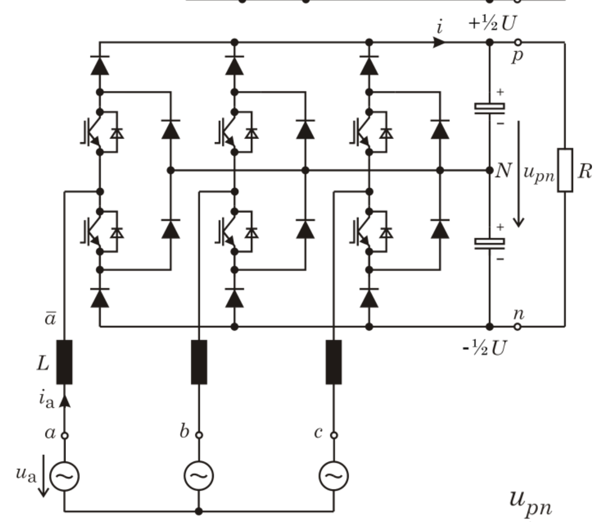

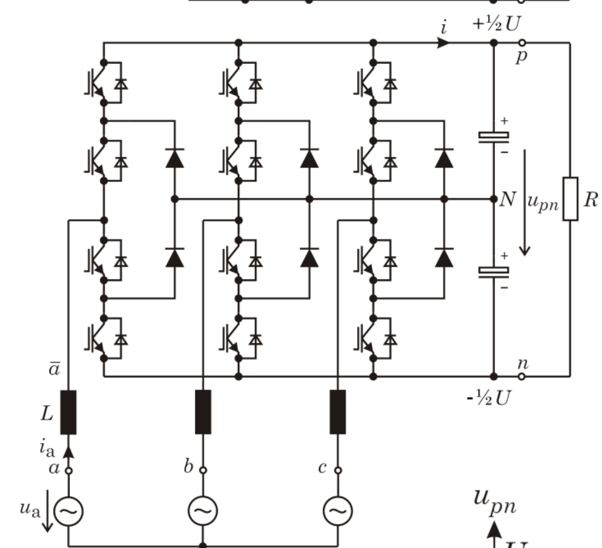

- **Output Operating Range**

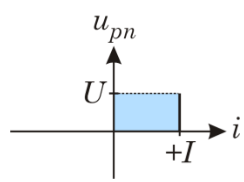

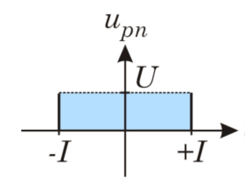

▶ Comparison of Two-Level/Three-Level NPC Boost-Type Rectifier Systems

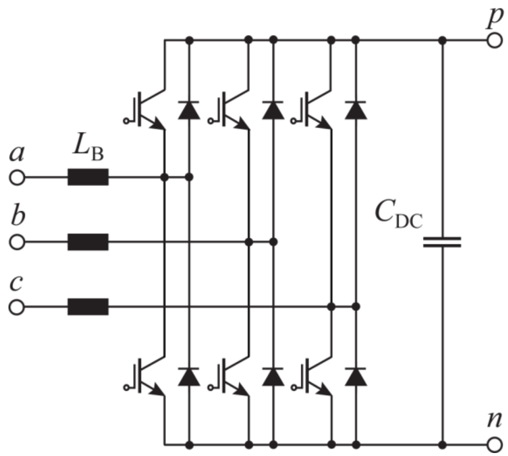

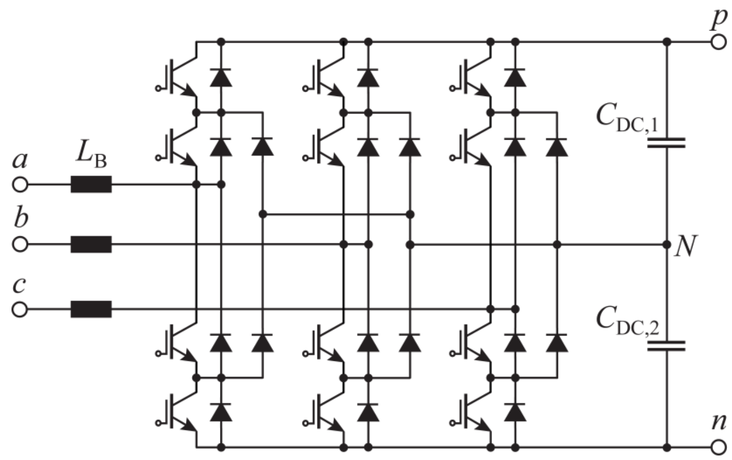

- Two-Level Converter Systems

\+ State-of-the-Art Topology for LV Appl.
\+ Simple, Robust, and Well-Known
\+ Power Modules and Auxiliary Components Available from Several Manufacturers

\- Limited Maximum Switching Frequency
\- Large Volume of Input Inductors

- Two-Level → Three-Level Converter Systems

\+ Reduction of Device Blocking Voltage Stress
\+ Lower Switching Losses
\+ Reduction of Passive Component Volume

– Higher Conduction Losses
– Increased Complexity and Implementation Effort

► T-Type Three-Level Boost-Type Rectifier System

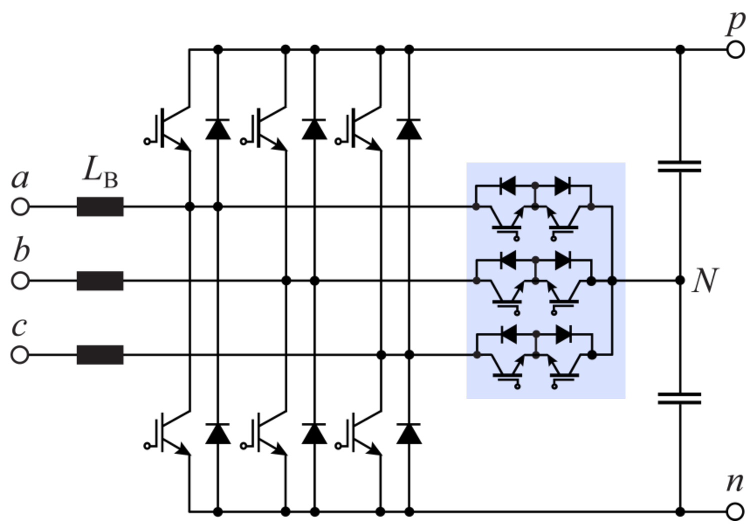

- + Semiconductor Losses for Low Switching Frequencies Lower than for NPC Topologies
- + Can be Implemented with Standard Six-Pack Module

- − Requires Switches for 2 Different Blocking Voltage Levels

► Pros and Cons of Three-Level vs. Two-Level Boost-Type Rectifier Systems

- \+ Losses are Distributed over Many Semicond. Devices; More Even Loading of the Chips → Potential for Chip Area Optimization for Pure Rectifier Operation
- \+ High Efficiency at High Switching Frequency
- \+ Lower Volume of Passive Components

- − More Semiconductors
- − More Gate Drive Units
- − Increased Complexity
- − Capacitor Voltage Balancing Required
- − Increased Cost

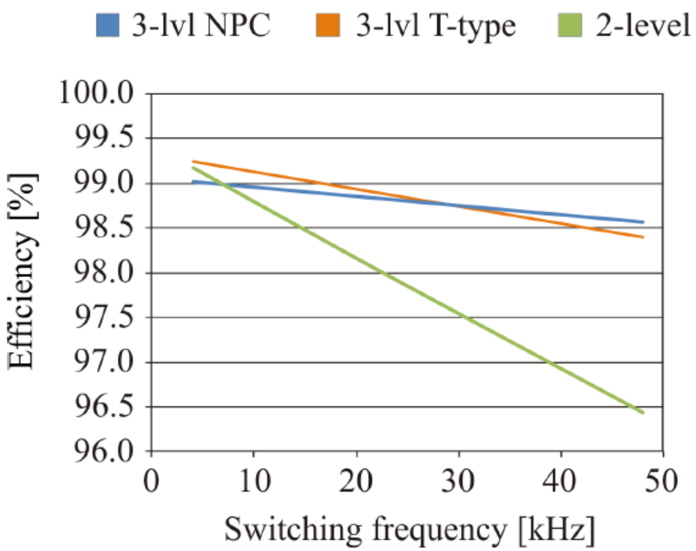

Consideration for 10kVA/400V_{AC} Rectifier Operation; Min. Chip Area, $T_{j,max}$= 125°C

- ● Moderate Increase of the Component Count with the T-Type Topology

► Multi-Level Topologies are Commonly Used for Medium Voltage Applications but Gain Steadily in Importance also for Low-Voltage Renewable Energy Applications

Buck-Type Topologies

▶ Derivation of Unipolar Output Bidirectional Buck-Type Topologies

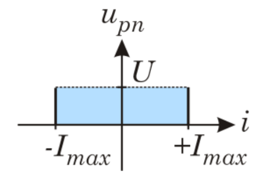

- **Output Operating Range**

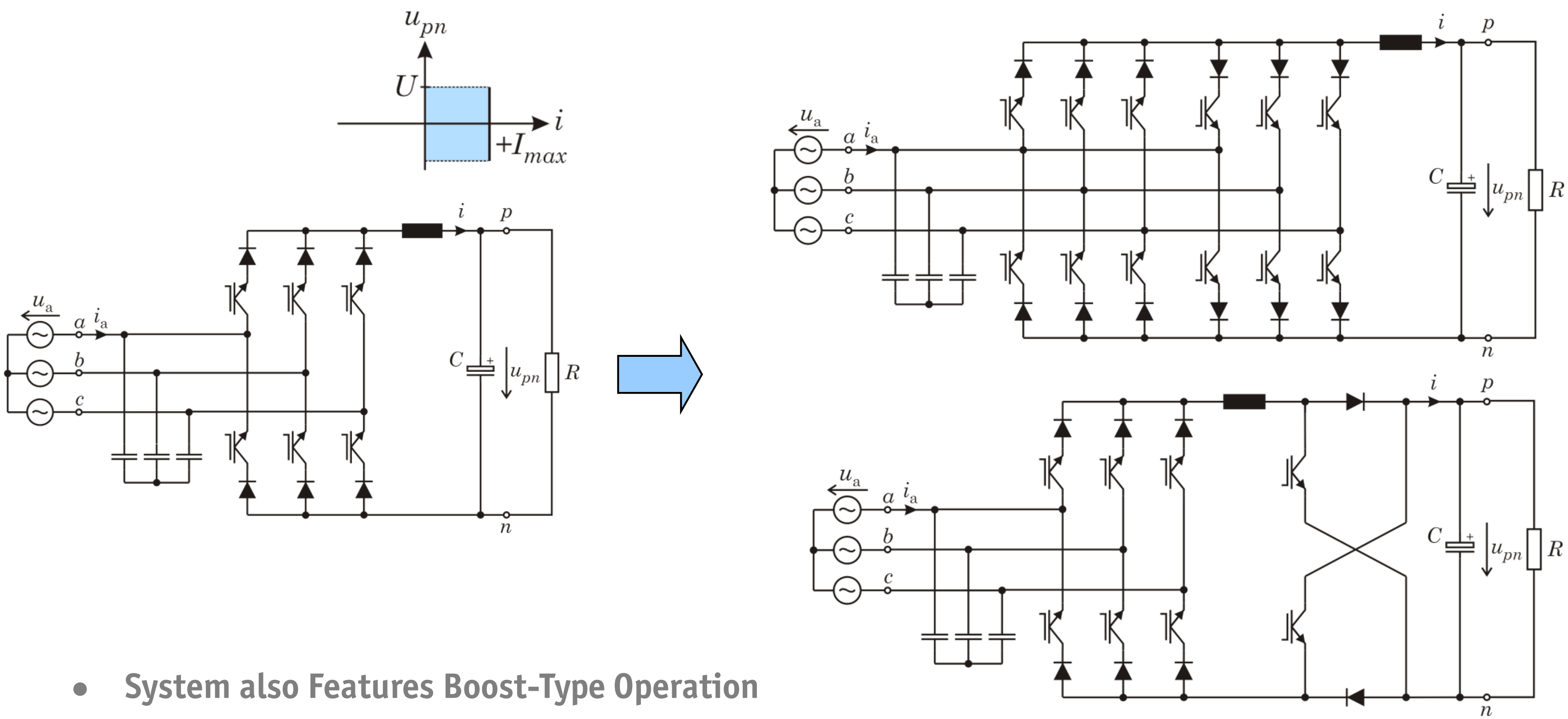

- System also Features Boost-Type Operation

▶ Derivation of Unipolar Output Bidirectional Buck-Type Topologies

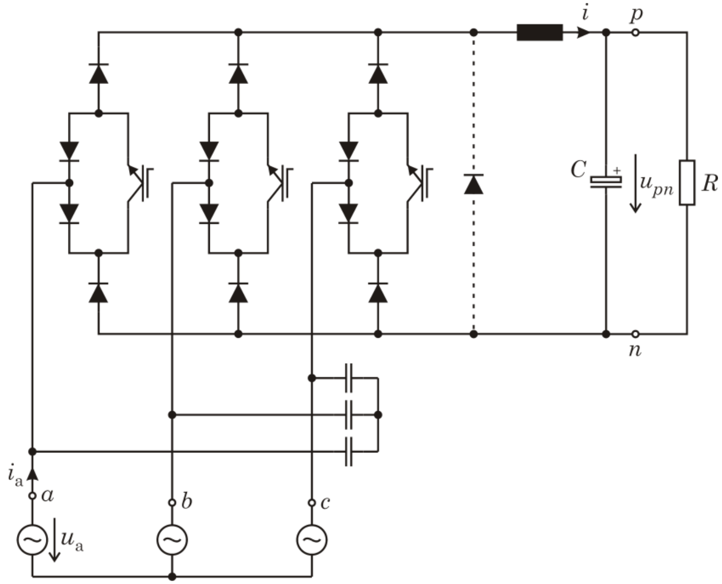

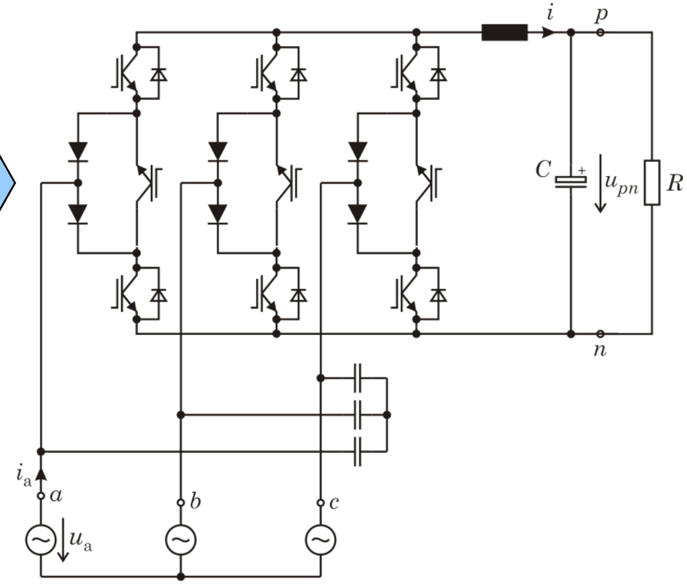

- **Output Operating Range**

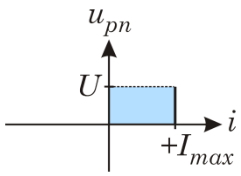

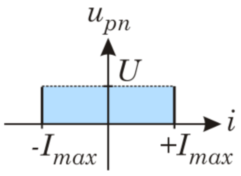

Thank you!

About

Johann W. Kolar (F'10)

received his M.Sc. and Ph.D. degree (summa cum laude / promotio sub auspiciis praesidentis rei publicae) from the University of Technology Vienna, Austria. Since 1984 he has been working as an independent international consultant in close collaboration with the University of Technology Vienna, in the fields of power electronics, industrial electronics and high performance drives. He has proposed numerous novel converter topologies and modulation/control concepts, e.g., the VIENNA Rectifier, the SWISS Rectifier, the Delta-Switch Rectifier, the isolated Y-Matrix AC/DC Converter and the three-phase AC-AC Sparse Matrix Converter. Dr. Kolar has published over 450 scientific papers at main international conferences, over 180 papers in international journals, and 2 book chapters. Furthermore, he has filed more than 110 patents. He was appointed Assoc. Professor and Head of the Power Electronic Systems Laboratory at the Swiss Federal Institute of Technology (ETH) Zurich on Feb. 1, 2001, and was promoted to the rank of Full Prof. in 2004. Since 2001 he has supervised over 60 Ph.D. students and PostDocs.

The focus of his current research is on AC-AC and AC-DC converter topologies with low effects on the mains, e.g. for data centers, More-Electric-Aircraft and distributed renewable energy systems, and on Solid-State Transformers for Smart Microgrid Systems. Further main research areas are the realization of ultra-compact and ultra-efficient converter modules employing latest power semiconductor technology (SiC and GaN), micro power electronics and/or Power Supplies on Chip, multi-domain/scale modeling/simulation and multi-objective optimization, physical model-based lifetime prediction, pulsed power, and ultra-high speed and bearingless motors. He has been appointed an IEEE Distinguished Lecturer by the IEEE Power Electronics Society in 2011.

He received 9 IEEE Transactions Prize Paper Awards, 8 IEEE Conference Prize Paper Awards, the PCIM Europe Conference Prize Paper Award 2013 and the SEMIKRON Innovation Award 2014. Furthermore, he received the ETH Zurich Golden Owl Award 2011 for Excellence in Teaching and an Erskine Fellowship from the University of Canterbury, New Zealand, in 2003.

He initiated and/or is the founder/co-founder of 4 spin-off companies targeting ultra-high speed drives, multi-domain/level simulation, ultra-compact/efficient converter systems and pulsed power/electronic energy processing. In 2006, the European Power Supplies Manufacturers Association (EPSMA) awarded the Power Electronics Systems Laboratory of ETH Zurich as the leading academic research institution in Power Electronics in Europe.

Dr. Kolar is a Fellow of the IEEE and a Member of the IEEJ and of International Steering Committees and Technical Program Committees of numerous international conferences in the field (e.g. Director of the Power Quality Branch of the International Conference on Power Conversion and Intelligent Motion). He is the founding Chairman of the IEEE PELS Austria and Switzerland Chapter and Chairman of the Education Chapter of the EPE Association. From 1997 through 2000 he has been serving as an Associate Editor of the IEEE Transactions on Industrial Electronics and from 2001 through 2013 as an Associate Editor of the IEEE Transactions on Power Electronics. Since 2002 he also is an Associate Editor of the Journal of Power Electronics of the Korean Institute of Power Electronics and a member of the Editorial Advisory Board of the IEEJ Transactions on Electrical and Electronic Engineering.

About

Roman Bosshard (S'10)

received the M.Sc. degree from the Swiss Federal Institute of Technology (ETH) Zurich, Switzerland, in 2011. During his studies, he focused on power electronics, electrical drive systems, and control of mechatronic systems. As part of his M.Sc. degree, he participated in a development project at ABB Switzerland as an intern, working on a motor controller for traction converters in urban transportation applications. In his Master Thesis, he developed a sensorless current and speed controller for a ultrahigh-speed electrical drive system with CELEROTON, an ETH Spin-off founded by former Ph.D. students of the Power Electronic Systems Laboratory at ETH Zurich.

In 2011, he joined the Power Electronic Systems Laboratory at the Swiss Federal Institute of Technology (ETH) Zurich, where he is currently pursuing the Ph.D. degree. His main research area is inductive power transfer systems for electric vehicle battery charging, where he published five papers at international IEEE conferences and one paper in the IEEE Journal of Emerging and Selected Topics in Power Electronics.